

Biotechnologically important biotransformations by CYP106A2 and CYP109E1 from *Bacillus megaterium*

Kumulative Dissertation
zur Erlangung des Grades
des Doktors der Naturwissenschaften
der Naturwissenschaftlich-Technischen Fakultät
der Universität des Saarlandes

von

Natalia Putkaradze

Saarbrücken

2018

Tag des Kolloquiums: **08.08.2018**

Dekan: **Prof. Dr. Guido Kickelbick**

Berichterstatter: **Prof. Dr. Rita Bernhardt**

Prof. Dr. Gert-Wieland Kohring

Vorsitz: **Prof. Dr. Uli Müller**

Akad. Mitarbeiter: **Dr. Yutaka Suzuki**

With love to my brother Giorgi Putkaradze!

Contents

Acknowledgements	v
Abbreviations	vi
Abbreviations of amino acids	vii
Abstract	1
Zusammenfassung.....	2
Scientific contributions	3
1. Introduction.....	5
1.1 Cytochrome P450 monooxygenases.....	5
1.1.1 Nomenclature and reaction types	5
1.1.2 Electron transfer and catalytic cycle	7
1.1.3 Structure and spectroscopic features.....	10
1.1.4 Substrate diversity.....	11
1.1.5 Biotechnological importance and applications	13
1.2 Prokaryotic cytochrome P450s	14
1.2.1 CYP106A2	16
1.2.2 CYP109E1	17
1.2.3 <i>Bacillus megaterium</i> as expression host for P450 systems	18
1.3 Aims.....	19
2. Scientific articles.....	21
2.1 Putkaradze et al. 2017a.....	21
2.2 Abdulkughni et al. 2017.....	32
2.3 Putkaradze et al. 2017b	43
2.4 Milhim et al. 2016.....	74
3. Discussion and outlook	88
3.1 Production of glucocorticoid drug derivatives	89
3.2 CYP109E1 as versatile biocatalyst	92
3.3 Towards engineering of CYP109E1 for pravastatin production.....	96
3.4 Conclusions.....	99
4. References.....	101
5. Appendix	117
5.1 Supplemental methods.....	117
5.2 Supplemental data	118

Acknowledgements

First and foremost, I wish to express my deepest gratitude to Prof. Dr. Rita Bernhardt for providing me the opportunity to work in the Biochemistry Lab at Saarland University, for her guidance, continuous support, valuable suggestions and encouragement.

I would like to express my thanks to Prof. Dr. Gert-Wieland Kohring for being the second supervisor. Special thanks to Dr. Frank Hannemann for his support and useful discussions. Thanks to Dr. Josef Zapp for the NMR measurement and analysis. I am grateful to Dr. Michael C. Hutter for CYP106A2 modeling experiments. I am particularly thankful to Dr. Daniela Schmitz and Dr. Flora Marta Kiss for their enthusiasm and contribution to my first publication. I want to thank Dr. Martin Litzenburger for the useful discussions and evaluation the NMR data. Special thanks to Gabi Schon, who was always there to help in all administrative aspect. Many thanks go to Birgit Heider-Lips and Antje Eiden-Plach for their great support in and outside the lab. Thanks to Dr. Mohammed Milhim for the scientific discussions and Ammar Abdulmughni for the productive collaboration.

I would also like to thank my former and current colleagues for creating a perfect atmosphere in the lab and for the pleasant time together: Tanja Sagadin, Dr. Simone Brixius-Anderko, Adrian Gerber, Benjamin Stenger, Dr. Lina Schiffer, Dr. Alexander Schifrin, Dr. Jens Neunzig, Dr. Yogan Khatri, Dr. Fredy Kern, Dr. Azzam Mosa, Julia Nikolaus, Lisa König and Philip Hartz.

I want to thank my friends for keeping me company outside the work. Special thanks to Ghamdan for his help, support and enjoyable discussions.

My deepest and very loving thank to Giorgi, for loving me, motivating and always being with me. And also for proof-reading this Thesis.

Last but not least, I want to thank my parents Lela and Demuri the most, for their love and invaluable contributions in my life. Many thanks to Lika, to the best sister in the world. My deepest and extremely painful thanks to my brother Giorgi for being the best brother for 25 years and priceless support to me. Gukuna, I miss you every second of my life!

Abbreviations

AdR	adrenodoxin reductase
Adx	adrenodoxin
Arh1	adrenodoxin reductase homolog 1
ATCC	American Type Culture Collection
BmCPR	cytochrome P450 reductase from <i>B. megaterium</i>
Cpd 0	compound 0
Cpd I	compound I
Cpd II	compound II
CPR	cytochrome P450 reductase
DOC	11-deoxycorticosterone
ER	endoplasmic reticulum
FdR	ferredoxin reductase
Fdx	ferredoxin
FMN	flavin mononucleotide
GRAS	generally recognized as safe
HPLC	high performance liquid chromatography
HTS	high-throughput screening
KBA	11-keto- β -boswellic acid
k_{cat}	turnover number
K_d	dissociation constant
K_M	Michaelis-Menten constant
MD	molecular dynamics
MW	molecular weight
NAD(P)H	nicotinamide adenine dinucleotide (phosphate)
NMR	nuclear magnetic resonance
PCR	polymerase chain reaction
PHB	poly-3-hydroxybutyrate
RSS	11-deoxycortisol
SRS	substrate recognition site
UV/Vis	ultraviolet/visible
RMSD	root mean square deviation

Abbreviations of amino acids

A	alanine
C	cysteine
D	aspartic acid
E	glutamic acid
F	phenylalanine
G	glycine
H	histidine
I	isoleucine
K	lysine
L	leucine
M	methionine
N	asparagine
P	proline
Q	glutamine
R	arginine
S	serine
T	threonine
V	valine
W	tryptophan
Y	tyrosine

Abstract

Cytochrome P450s are natural catalysts capable of performing many chemically challenging reactions under mild conditions with high regio- and stereo-selectivity. Biotransformations of various biotechnologically and pharmaceutically important compounds with two P450s from *Bacillus megaterium*, CYP106A2 and CYP109E1, were studied within this work. The investigated compounds include steroidal drugs, sterols, statins, flavorings and odorants. The reactions were characterized through binding titrations, *in vitro* conversions using the bovine adrenal redox chain, and whole-cell biotransformations with P450-based systems in *B. megaterium*. The results showed the 15 β hydroxylase activity of CYP106A2 towards glucocorticoid drugs, prednisone and dexamethasone. Applying different CYP106A2-based whole-cell systems, the production of the 15 β -hydroxylated drugs and new drug derivatives was demonstrated. Furthermore, the substrate range of CYP109E1 was expanded with 13 compounds. Selective transformations of new substrates were accomplished by CYP109E1 *in vitro* as well as *in vivo* and biotechnologically attractive reactions were identified. Among them, the conversion of compactin to pravastatin was further investigated with CYP109E1 mutants, identifying a variant with 2.5 times greater productivity. Furthermore, CYP109E1 was shown to produce valuable oxysterols and a whole-cell biocatalyst was established in *E. coli* showing 3.3-fold higher activity than the *B. megaterium* system.

Zusammenfassung

Cytochrome P450 sind natürlich vorkommende Biokatalysatoren, die eine Vielzahl chemisch anspruchsvoller Reaktionen unter milden Bedingungen mit einer hohen Regio- und Stereoselektivität durchführen. Die Biotransformation von biotechnologisch und pharmazeutisch wichtigen Verbindungen (steroidale Medikamente, Sterole, Statine, Aroma- und Geruchsstoffe) wurde mit den Enzymen CYP106A2 und CYP109E1 aus *Bacillus megaterium* untersucht. Die Charakterisierung dieser Reaktionen erfolgte mittels Bindungsstudien, *in vitro* Umsätzen unter Verwendung der bovinen adrenalen Redox-Kette und Ganzzell-Biokatalyse in *B. megaterium*. CYP106A2 zeigte eine 15 β -Hydroxylase-Aktivität gegenüber den Glucocorticoid Arzneimitteln, Prednison und Dexamethason. Unter Einsatz verschiedener *B. megaterium* Stämme konnte die Produktion von 15 β -hydroxy-Steroiden sowie neuer Arzneimittelerivate erreicht werden. Des Weiteren wurde das Substratspektrum von CYP109E1 um 13 Verbindungen erweitert. Durch die selektiven *in vitro* und *in vivo* Umsätze dieser neuen Substrate mittels CYP109E1 konnten biotechnologisch interessante Reaktionen gefunden werden. Der Umsatz von Compactin zu Pravastatin wurde dabei näher untersucht, wobei eine CYP109E1 Mutante eine 2,5-fach höhere Produktivität zeigte. Zudem konnte CYP109E1 zur Produktion wertvoller Oxysterole eingesetzt werden. Mit Hilfe eines neuen Ganzzell-Systems in *E. coli* konnte deren Ausbeute im Vergleich zu dem *B. megaterium* System um das 3,3-fache gesteigert werden.

.

Scientific contributions

Part of the results presented in this work is published in the publications listed below and reproduced in the chapter 2 with permission of Elsevier, Journal of Biotechnology (Putkaradze et al. 2017a, Abdulkughni et al. 2017, Milhim et al. 2016), and Springer Science and Business Media, Applied Microbiology and Biotechnology (Putkaradze et al. 2017b).

Putkaradze et al. 2017a

Biotransformation of prednisone and dexamethasone by cytochrome P450 based systems - Identification of new potential drug candidates*

The author, together with Dr. Flora Marta Kiss, carried out the experiments, analyzed and interpreted the data and drafted the manuscript.

* Preliminary results of this work have been obtained during my Master's Thesis

Abdulkughni et al. 2017

Characterization of cytochrome P450 CYP109E1 from *Bacillus megaterium* as a novel vitamin D₃ hydroxylase

The author performed preparative whole-cell conversions and isolated two vitamin D₃ metabolites for NMR analysis.

Putkaradze et al. 2017b

CYP109E1 is a novel versatile statin and terpene oxidase from *Bacillus megaterium*

The author participated in designing the project, carried out the experiments, analyzed and interpreted the results, and drafted the manuscript.

Milhim et al. 2016

Identification of a new plasmid-encoded cytochrome P450 CYP107DY1 from *Bacillus megaterium* with a catalytic activity towards mevastatin

The author participated in conducting the *in vitro* experiments, in addition to participating in the interpretation and discussion of the results.

1. Introduction

1.1 Cytochrome P450 monooxygenases

Cytochrome P450s (P450s) are important heme-containing proteins that are ubiquitously distributed in nature. They build one of the most diverse and largest superfamily of metalloenzymes and are involved in many metabolic and synthetic processes (Sligar, 1999). For example, in mammals P450s synthesize steroid hormones, fat-soluble vitamins, bile acids and metabolize drugs as well as xenobiotics (Bernhardt, 2006). In plants they contribute in the pathways of secondary metabolism: in coloration, in lignification, in the synthesis of defense chemicals, and in degradation of herbicides (Guengerich, 2001; Werck-Reichhart and Feyereisen, 2000). In microbes P450s are involved in the synthesis of bioactive compounds as well as in the degradation and utilization of animal and plant metabolites (Kelly and Kelly, 2013; Müller et al., 1984).

The research on P450s started 60 years ago when Klingenberg and Garfinkel independently reported about a presence of unknown pigments in rat and pig liver microsomes having an intense absorption band at 450 nm in the reduced carbon monoxide bound complex (Garfinkel, 1958; Klingenberg, 1958). Few years later, this unique spectral property gave the name "P450" (meaning "Pigment 450") to these heme enzymes (cytochromes) (Omura and Sato, 1962, 1964). Very soon thereafter these special proteins have been found in other tissues, organs and organisms (Cardini and Jurtschuk, 1968; Estabrook et al., 1963; Katagiri et al., 1968; Lebeault et al., 1971; Ruhmann-Wennhold et al., 1970), and nowadays, there are already over 41000 identified genes from hundreds of species in the P450 database (Nelson, 2018).

1.1.1 Nomenclature and reaction types

The rapidly increasing number of identified P450s lead to inconsistent naming by different working groups such as "P-450_{BM-3}", "P-450_{CAM}" or "P450_{SCC}"/"20,22 desmolase", showing the necessity of a universal nomenclature already in the 1980s. Consequently, a standardized P450 nomenclature based on the similarity of amino acid sequences was introduced and (slightly modified) is still being used (Nebert et al., 1987). The enzymes with more than 40% sequence identity are grouped in the same family expressed with a number, whereas the ones with more than 55% similarity belong to the same subfamily indicated by a letter of the alphabet. A digit after the subfamily letter is given to enzymes consecutively. For example, CYP109E1 is the first P450 enzyme from the 109th family and E subfamily (Figure 1).

CYP109E1

family
 subfamily
 individual enzyme

Figure 1. Systematic nomenclature of P450s on the example of CYP109E1

P450s belong to a large subclass of enzymes called external monooxygenases also known as mixed-function oxidases (oxygenase and oxidase). Thus, they catalyze the scission of atmospheric dioxygen and the insertion of one oxygen atom into organic molecules as well as the reduction of the second oxygen atom to water. For the catalysis, they require two electrons from an external donor which in most cases is NAD(P)H (Figure 2) (Bernhardt, 2006; Fasan, 2012; Hannemann et al., 2007).

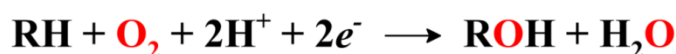


Figure 2. General reaction catalyzed by P450s

Hydrocarbon hydroxylation is the most common reaction catalyzed by P450 enzymes. Further reaction types occurring through P450-mediated catalysis include epoxidation, N-hydroxylation, N-, O-, S-dealkylation, C–C bond cleavage, aromatization, lactonization, oxidative deamination, oxidative phenol coupling and others (Sono et al., 1996). Table 1 provides several P450-catalyzed reaction types with selected examples such as aliphatic hydroxylation of vitamin D₃ into 25-hydroxyvitamin D₃, testosterone ring aromatization forming estradiol, cholesterol side chain cleavage forming the general steroid hormone precursor pregnenolone, and 14α-demethylation of lanosterol leading to sterol synthesis (by mammalian CYP27A1, CYP19A1, CYP11A1 and CYP51A1, respectively). The aromatic ring epoxidation example shows a "bad behavior" of hepatic microsomal CYP1A1 contributing to the metabolic activation of the carcinogen benzo(a)pyrene. Other examples such as oxidation of castasterone to plant hormone brassinolide (a Baeyer-Villiger oxidation) by plant CYP85A2, epoxidation of epothilone D to the anticancer agent epothilone B by bacterial CYP167A1 and degradation of harmful naphthalene (aromatic ring hydroxylation), a "good behavior" of bacterial CYP101A1, are also listed. Although showing a tiny fraction of P450-catalyzing biotransformations, the examples from Table 1 emphasize the importance and versatility of these enzymes in nature. Based on their metabolic functions the numerous members of P450 superfamily can be divided into P450s involved in catabolic processes and P450s contributing to anabolic reactions. Both groups are highly important for medicine, health, environment and industry.

Table 1. P450-catalyzed reaction types and some important examples

Reaction type	Example	P450	Reference
Aliphatic hydroxylation	vitamin D ₃ -> 25-hydroxyvitamin D ₃	CYP27A1	(Cali and Russell, 1991)
Aromatic hydroxylation	naphthalene ->1- naphthol	CYP101A1	(England et al., 1998)
Epoxidation	epothilone D -> epothilone B	CYP167A1	(Ogura et al., 2004)
Aromatic epoxidation	benzo(a)pyrene -> benzo(a)pyrene-7,8-epoxide	CYP1A1	(Moorthy et al., 2015)
Aromatization	testosterone -> estradiol	CYP19A1	(Kellis and Vickery, 1987)
Demethylation	lanosterol -> sterols	CYP51A1	(Lepesheva and Waterman, 2004)
C-C bond cleavage	cholesterol -> pregnenolone	CYP11A1	(Matteson et al., 1984)
Baeyer-Villiger oxidation	castasterone -> brassinolide	CYP85A2	(Kim et al., 2005)

1.1.2 Electron transfer and catalytic cycle

The vast majority of P450s is not able to obtain necessary electrons from NAD(P)H directly (Ewen et al., 2012). For this, they require electron-transporting proteins, called redox partners. P450 enzyme systems are classified according to the composition of these proteins (Hannemann et al., 2007). The majority of prokaryotic and eukaryotic mitochondrial P450s belong the class I. They occur as three-component systems consisting of a P450, a FAD-containing reductase (FdR), and a ferredoxin (Fdx) of different cluster types among which [2Fe-2S] is most common (Matsubara and Saeki, 1992). In class I systems of prokaryotes the proteins are exclusively cytosolic and soluble (Figure 3a), whereas in systems of eukaryotes only Fdx is a soluble protein of the mitochondrial matrix (Figure 3b). The two other components of mitochondrial systems, P450 and FdR, are bound and associated to the inner mitochondrial membrane, respectively (Hannemann et al., 2007). In these systems, the soluble Fdx is proposed as an electron “shuttle” between FdR and P450s and has been shown to be required in excess over FdR for sufficient activity of CYP11A1 and CYP11B1, two important mitochondrial class I systems (Bernhardt, 2006; Lambeth et al., 1979).

Most of the eukaryotic P450s belong to microsomal class II systems. These two-component systems comprise proteins integrated in the endoplasmic reticulum (ER) membrane: P450 and cytochrome P450 reductase (CPR) (Figure 3c). The correct orientation of these two proteins in the membrane is a necessary prerequisite for the catalytic activity and is controlled by the orientational matrix of phospholipids (Ruckpaul and Bernhardt, 1984). Besides the common class II systems, other systems from the same class are also reported, in which cytochrome *b*5 alone or together with cytochrome *b*5

reductase provides the second electron (Correia and Mannering, 1973; Hannemann et al., 2007). Apart from being an electron transporter, cytochrome *b*5 can act as an effector on hepatic P450 (Hlavica, 1984). In addition to the most abundant class I and class II systems, other one-, two- and multi-component systems have also been reported (classes III-X), for example, the self-sufficient CYP102A1 from *Bacillus megaterium* (*B. megaterium*) (naturally fused with its redox partner) and CYP176A1 from *Citrobacter braakii* having flavodoxin instead of ferredoxin as a component of its P450 system (Hannemann et al., 2007; Hawkes et al., 2002; Narhi and Fulco, 1987).

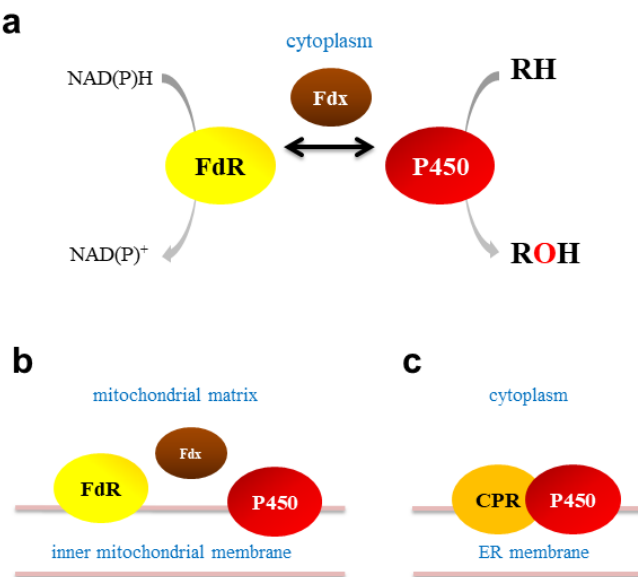


Figure 3. Class I bacterial (a) and mitochondrial (b) as well as class II microsomal (c) systems. Figure adapted from Hannemann et al. (2007)

As mentioned before, P450s need two electrons derived from NAD(P)H via redox partner(s) to react with atmospheric dioxygen and to insert one oxygen atom into a substrate. Direct reactivity of dioxygen (triplet) with stable organic molecules (singlets) at ambient temperatures is a spin-forbidden process in chemistry (Sono et al., 1996). P450 enzymes utilize heme-ligated iron for the activation of molecular oxygen and perform a multistep catalytic cycle leading to an oxygenated product (Figure 4). The resting enzyme is in the ferric state (1) and usually has a water molecule as sixth axial ligand (Sligar, 1999). Substrate binding displaces the water (2) and changes the heme iron spin state and redox potential. The redox potential of the heme increases to a value higher than that of the redox protein, and this difference thermodynamically enables the first electron transfer (Ortiz de Montellano, 2010; Sligar, 1999). The enzyme is in the ferrous state (3) after electron transfer and goes in the ferric superoxy state (4) after dioxygen binding. This is followed by a second electron transfer, yielding the ferric peroxy anion (5), which is subsequently protonated, resulting in the ferric hydroperoxy state called compound 0 (Cpd 0) (6). This intermediate is not stable and is further

protonated resulting in the highly reactive ferryl intermediate called compound I (Cpd I) (7), which initiates hydrogen abstraction from a C-H bond resulting in formation of the compound II (Cpd II) (8). This metal bound hydroxide rapidly "rebounds" to the substrate radical, forms oxygenated product (9) and returns the enzyme in the ferric state (1) (Groves et al., 1978; Huang and Groves, 2017; Rittle and Green, 2010).

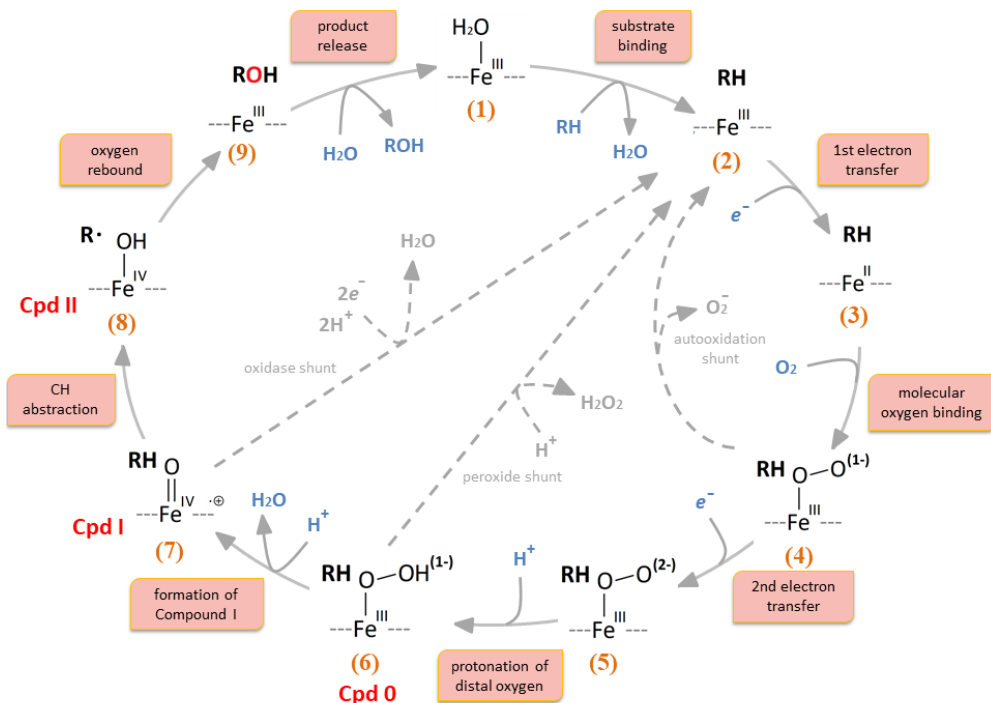


Figure 4. Scheme of the catalytic cycle of P450s. Figure adapted from Yashimoto and Auchus (2016) and Denisov et al. (2005)

It is noteworthy that in many P450s at least three unproductive pathways, called “shunt” reactions, can occur at different steps of the catalytic cycle: autooxidation shunt, peroxide shunt and oxidase shunt (Denisov et al., 2005). In these cases, a P450 consumes electrons and from the ferric superoxy (4), the ferric hydroperoxy (6), or the ferryl (7) state returns to the ferric resting state (2) without forming the oxygenated product. As a consequence, the bound oxygen is released as superoxide anion (O_2^-) after the first electron transfer, as hydrogen peroxide (H_2O_2) after two-electron reduction, or as water after four-electron reduction (Figure 4) (Denisov and Sligar, 2015). On the other hand, a number of P450s such as CYP152A1 from *Bacillus subtilis* (*B. subtilis*) and CYP191A1 from *Mycobacterium smegmatis* are able to directly use peroxides for substrate oxidation without the need for NAD(P)H regeneration, redox partners, or molecular oxygen activation via the catalytic cycle (Bernhardt, 2006; Jo et al., 2017; Matsunaga et al., 2002; Sakaki, 2012).

1.1.3 Structure and spectroscopic features

Despite the functional diversity and low sequence identity (in some cases <15%), all P450s possess a quite conservative unique protein fold and have one invariant amino acid, cysteine, as the fifth or proximal ligand of the heme prosthetic group (Munro et al., 2002; Peterson and Graham, 1998). The structural core of these proteins is conserved, whereas the regions responsible for substrate recognition and binding as well as redox partner binding are variable. The P450 core consists of helices D, E, J, L, I, K, two sets of β sheets and a coil structure called "meander" (Figure 5a) (Peterson and Graham, 1998; Werck-Reichhart and Feyereisen, 2000). The I helix contains a highly conserved threonine with an acidic residue, whereas the K helix includes a fully conserved E-X-X-R motif. Furthermore, there is a characteristic sequence F-X-X-G-X-R-X-C-X-G with the absolutely conserved cysteine residue on the proximal face of the heme just prior to the L helix (Werck-Reichhart and Feyereisen, 2000).

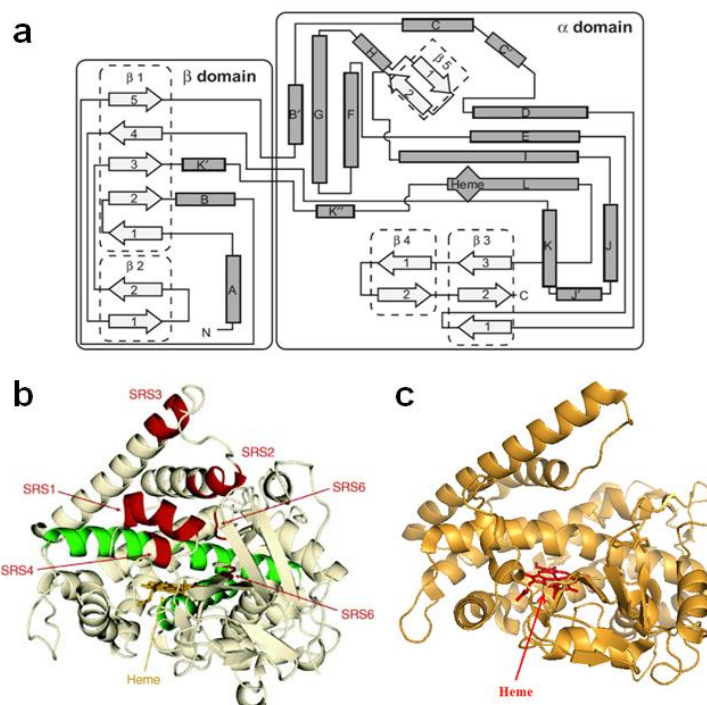


Figure 5. Secondary and tertiary structures of P450s. Topology diagram of the secondary structural elements on the example of CYP102A1 (a). Figure adapted from Werck-Reichhart and Feyereisen (2000). Tertiary structure model of P450s with six SRSs on the example of CYP102A1 (b). Figure adapted from Urlacher and Eiben (2006). Tertiary structure model of CYP109E1 (c). The model was generated using PyMOL (DeLano Scientific, CA, USA) and substrate-free crystal structure of CYP109E1 (PDB ID: 5L90) (Józwik et al., 2016)

The conserved rigid architecture of P450s near the heme is essential to provide a suitable electrostatic environment around the cysteine-iron ligation for the maintenance of the redox potential in a

physiologically reasonable range (Poulos and Johnson, 2015). In addition, the highly conserved part of the I helix near the heme is thought to be involved in specific positioning and stabilization of waters, which is crucial for proper proton delivery and oxygen activation (Denisov and Sligar, 2015). As it was already mentioned, the regions related to the substrate specificity are not consistent and it is not surprising that they vary the most. For example, the B' helix can occur in orientations differing by 90° (Poulos and Johnson, 2015). There are six known regions in the P450 structure related to substrate recognition (SRSs) identified by Gotoh for CYP101A1 and its natural substrate camphor (Figure 5b): SRS1 (BC loop and B' helix), SRS2 (part of the F helix), SRS3 (part of the G helix), SRS4 (part of the I helix), SRS5 (the K helix with β 2 region) and SRS6 (β 4 hairpin structure) (Gotoh, 1992). Due to the characteristic fold of these enzymes (Figure 5b and c), the equivalent structural regions in different P450s are considered to be SRSs.

It is important to note that the heme of P450s, a non-covalently bound iron protoporphyrin IX, is very sensitive to changes in its ligands as well as in its redox state and enables spectroscopic monitoring of chemical transformations and transitions (Urlacher and Eiben, 2006; Yoshimoto and Auchus, 2016). The UV/Vis spectrum of the heme prosthetic group in the low-spin state shows a red-shifted Soret band at approximately 380–420 nm as well as two other minor characteristic α (560 nm) and β (525 nm) peaks (Bernhardt, 2006; Ruckpaul and Bernhardt, 1984). Binding of carbon monoxide to the reduced P450 shifts the Soret band to 450 nm, which is a characteristic feature of an active P450 and is used to determine the concentration of a purified enzyme (Omura and Sato, 1964). The binding of a cognate substrate to the active site increases the redox potential and changes the spin state from low-spin ($S=1/2$) to high-spin ($S=5/2$) ferric state (Denisov et al., 2005). The spin state transition upon substrate binding shifts the Soret band from about 420 nm to approximately 390 nm (type I difference spectrum), whereas an inhibitor binding shifts the maximum to approximately 425 nm (type II difference spectrum) (Jefcoate, 1978). Optical difference spectroscopy is a powerful technique for binding titrations in order to identify dissociation constants of P450 ligands and can be also used for high-throughput screening (HTS) of potential P450 substrates (Khatri et al., 2016; Schmitz et al., 2012).

1.1.4 Substrate diversity

P450 substrates comprise a plethora of hydrophobic chemical structures with diverse functionalities such as physiological substances, synthetic pharmaceuticals, aroma compounds and environmental pollutants. According to the physiological role of particular P450s, some of them have a very strict substrate and reaction spectrum, while the others have broader catalytic activity and selectivity. For example, human 25-hydroxyvitamin D₃ 1 α -hydroxylase, CYP27B1, shows high substrate specificity,

converting exclusively terminally hydroxylated vitamin D₃ derivatives (Tang et al., 2013), whereas human hepatic CYP3A4 possesses the longest list of substrates, metabolizing approximately 50% of existing drugs (Guengerich, 1999).

Steroids and steroid alcohols, such as cholesterol, are important substrates of different P450s. In mammals, several P450s are involved in multistep pathways of steroidogenesis (producing glucocorticoids, mineralocorticoids and sex hormones): mitochondrial CYP11A1 (cholesterol side-chain cleavage), CYP11B1 (steroid 11 β -hydroxylase), CYP11B2 (aldosterone synthase), as well as microsomal CYP17A1 (steroid 17 α -hydroxylase/17,20-lyase), CYP19A1 (aromatase), and CYP21A2 (steroid 21-hydroxylase) (Bureik and Bernhardt, 2007). There are three other P450s acting directly on cholesterol: microsomal CYP46A1 (24(S)-hydroxylase), CYP7A1 (7 α -hydroxylase), and mitochondrial CYP27A1 (27-hydroxylase) (Pikuleva, 2006). Several P450s contribute to the activation and deactivation of an essential seco-steroid, vitamin D, such as mitochondrial CYP27A1 (25-hydroxylase of vitamin D), CYP27B1 (1 α -hydroxylase of 25-hydroxy vitamin D), CYP24A1 (24-hydroxylase of 25-hydroxy vitamin D and 1 α ,25-dihydroxy vitamin D), and microsomal CYP2R1 (25-hydroxylase of vitamin D) (Schuster, 2011). Various microbial P450s also accept steroids as their substrates and perform selective hydroxylations at different sites of steroid (gonane) nucleus. Some of them are capable of a terminal oxidation of the side chain (Bureik and Bernhardt, 2007; Donova and Egorova, 2012; Sakaki et al., 2011). Besides the physiological steroidal compounds, bacterial P450s can also metabolize synthetic steroids, such as the glucocorticoid drugs prednisone and dexamethasone.

Plant and fungal natural products are common P450 substrates. It is not surprising since numerous P450s are involved in biosynthetic pathways. One of the important examples is plant CYP71AV1 from *Artemisia annua*, which is able to hydroxylate the sesquiterpene amorpha-4,11-diene to the antimalarial drug precursor artemisic acid (Teoh et al., 2006). Several plant P450s contribute to the synthesis of a phytochemical anticancer drug, a taxol diterpenoid, paclitaxel, such as CYP725A4 capable of 5 α -hydroxylation of an intermediate, taxa-4(5),11(12)-diene (Hefner et al., 1996). Flavonoids, plant polyphenols with mainly antioxidant properties, represent an interesting class of P450 substrates and ligands. Besides the plant P450s, which transform various flavonoids in their biosynthetic pathways (producing defence compounds, pigments and odors), there are other P450s, especially in mammals, interacting with these compounds (Hodek et al., 2002). Some flavonoids are substrates of mammalian enzymes, whereas others show therapeutically highly important stimulatory or inhibitory effects on xenobiotic-metabolizing P450s: CYP1A1, CYP1A2, CYP2B1 and CYP3A4 as well as steroidogenic CYP19A1 (aromatase) (He et al., 1998; Hodek et al., 2002; Lu et al., 2012; Zhai et al., 1998). Similar to plants, numerous fungal primary and secondary metabolites are

characterized as P450 substrates (Durairaj et al., 2016). One of the important examples is lovastatin, a powerful statin drug, which is a natural product of *Aspergillus terreus* and is metabolized by hepatic CYP3A4 (Barriuso et al., 2011). Other significant P450 substrates include diverse drugs, fatty acids, alkanes and polycyclic aromatic hydrocarbons (PAHs).

In general, the number of P450s with known physiological function is much lower than that with unknown natural role, including eight orphan P450 enzymes encoded by the human genome (Nebert et al., 2013). Identification of physiological substrates of many known and newly discovered P450s is mostly unsolved (Werck-Reichhart and Feyereisen, 2000), despite being extremely important for human health and relevant to biotechnology. Up to now, many human P450-mediated diseases have been identified (Pikuleva and Waterman, 2013). Some of these enzymes are also known to be involved in different reactions such as steroidogenic P450s that are capable of converting drugs (Schiffer et al., 2016a, 2016b). Therefore, a good understanding of P450 functions is required for successful drug design. The knowledge of their physiological role can also provide novel strategies to current therapies for the treatment of diseases caused by resistant pathogenic strains such as *Mycobacterium tuberculosis* (*M. tuberculosis*), whose genome encodes 20 P450s. Among them, CYP121A1 was found to be crucial for bacterial growth and now represents a therapeutic target (Ortiz de Montellano, 2018).

1.1.5 Biotechnological importance and applications

Regio- and stereo-selective oxyfunctionalization of non-active C-H bonds in organic molecules is very important for synthetic applications (Wong, 1998). Controlled oxidation of such bonds is, however, difficult to perform by chemical methods due to the C-H bond strength, the presence of several C-H bonds with similar bond energies in organic molecules, and the overoxidation reactions (Fasan, 2012; Lewis et al., 2011). P450s are able to attack chemically inert bonds and functionalize molecules often with high regio- and stereo-selectivity. Moreover, in contrast to chemical processes, these natural catalysts do not require several reaction steps or many reagents, and perform catalytic reactions under mild conditions (Girhard et al., 2015). Due to several advantages over organic synthesis, P450 enzymes, especially from prokaryotes, are attractive for biotechnology as potential producers of valuable compounds. As mentioned before, soluble bacterial P450s are robust enzymes, and are easier to overproduce and purify, in contrast to the membrane-bound ones from eukaryotes (Virus and Bernhardt, 2008). Although the physiological substrates are mostly not known, they are able to convert diverse biotechnologically and pharmaceutically important compounds, producing drugs, human drug metabolites, vitamins, flavors and fragrances (Sakaki, 2012). A fascinating example of industrial application of a prokaryotic P450 is 6'-hydroxylation of a lead statin

compound, compactin, into the cholesterol-lowering drug pravastatin by CYP105A3 (Sakaki, 2012; Watanabe et al., 1995). Other biotechnologically highly relevant bacterial P450-based reactions include 25-hydroxylation and $1\alpha,25$ -dihydroxylation of vitamin D₃ by several P450s such as CYP105A1 from *S. griseolus* (Sugimoto et al., 2008). In addition to known high-value compounds, bacterial P450 enzymes can also produce novel oxyfunctionalized chemical structures which appear to be promising for application in different fields. This follows from the fact that introduction of one hydroxyl group often strongly changes the properties of the compound, such as its solubility and biological activity (Donova and Egorova, 2012; Sakaki, 2012).

In spite of implementing many valuable reactions, practical application of P450 enzymes is still limited (Julsing et al., 2008, Bernhardt and Urlacher, 2014). The limiting factors are the multi-component nature of these biocatalysts, inefficient electron transfer inside non-natural P450 systems, requirement of the expensive cofactor NAD(P)H in stoichiometric amounts, low catalytic activity of P450s, and low solubility of substrates in water (Bernhardt and Urlacher, 2014). On the one hand, there are open questions related to the biocatalysis such as electron transfer mechanism in P450 systems, however, on the other hand, several strategies have been reported in order to overcome the aforementioned restrictions. For example, protein engineering methods can be applied to improve the catalytic activity of P450 (Wong, 1998). For sufficient electron supply, redox proteins can be replaced by electrodes as it was shown for bacterial and mammalian systems CYP101A1, CYP102A1, CYP17A1 and CYP2E1 (Estabrook et al., 1996; Sadeghi et al., 2011; Shumyantseva et al., 2005). Sufficient supply of NAD(P)H can be ensured by its regeneration using whole-cell systems, which are also generally favored for biotechnological purposes over isolated enzymes (Straathof et al., 2002). Common limitations of using P450-based whole-cell systems are complicated substrate transport into cells as well as substrate and product toxicity (Bernhardt and Urlacher, 2014). These important issues need to be thoroughly investigated for a particular P450 system in order to develop novel attractive systems for biotechnological processes. For example, limited substrate transport into the cell can be overcome using membrane permeabilizing agents (Janocha and Bernhardt, 2013), crude cell extracts (Zehentgruber et al., 2010) or by implementation of suitable host organism with uptake capability of a particular substrate (Bleif et al., 2012).

1.2 Prokaryotic cytochrome P450s

With about 3000 members, the prokaryotic P450s represent a much smaller group compared to over 35000 representatives of eukaryotes (Nelson, 2018). They are classified within CYP101-CYP299 and CYP1001-CYP1407 families with an exception of CYP51. The vast majority of them originates from bacteria, and only three families CYP109, CYP147 and CYP197 are shared with bacterial and

archaeal P450 enzymes (Nelson, 2018). Despite their relatively low number, bacterial P450s have several advantages over eukaryotic counterparts, thus being essential for P450 research. They are soluble proteins lacking the hydrophobic membrane anchor, most of them exhibit higher stability and activity than eukaryotic P450s and, therefore, they are easier to handle and crystallize (Munro et al., 2002; Urlacher and Eiben, 2006). It is not surprising that the most studied P450s, CYP101A1 (P450_{CAM}) and CYP102A1 (BM3), have bacterial origin. The first crystal structures were derived from these two P450s (Poulos et al., 1985, 1987; Ravichandran et al., 1993). In general, the huge part of structural and mechanistic knowledge on P450 enzymes is derived from these two bacterial proteins. To date, over 100 crystal structures of CYP102A1 have been reported (Janocha et al., 2016).

Table 2 shows a short overview of important prokaryotic P450s and their known catalytic activities. Although many of them have been investigated since many years, the knowledge about their physiological function and natural redox partners is still missing in most cases. The selected examples include P450s from *Amycolatopsis orientalis* (*A. orientalis*), contributing to the vancomycin biosynthetic pathway and performing one of the unusual P450 reactions, oxidative phenol coupling, from *N. aromaticivorans* metabolizing aromatic hydrocarbons, as well as remarkable representatives from *S. cellulosum*, *B. subtilis*, *Pseudomonas putida* (*P. putida*) and *Streptomyces* sp. Other important examples comprise P450s originating from *M. tuberculosis*, highly interesting ones for therapeutic purposes (Souter et al., 2000), and from *B. megaterium* that are of considerable biotechnological importance (Schmitz et al., 2018; Whitehouse et al., 2012).

There are five identified and partially characterized P450s from three different families of *B. megaterium* up to date: CYP102A1, CYP106A1, CYP106A2, CYP109E1 and CYP109A2 (Table 2). CYP102A1 and CYP106A2 have been identified about forty years ago and are still extensively studied (Berg et al., 1976, Narhi and Fulco, 1982). CYP102A1 from ATCC14581 is a fatty acid hydroxylase and an extraordinary member of the P450 superfamily, having a self-sufficient flavocytochrome nature as well as the highest coupling efficiencies and catalytic turnover (>3000 min⁻¹) among all known P450s (Furuya and Kino, 2010; Narhi and Fulco, 1982; Whitehouse et al., 2012). This enzyme has been a subject of numerous protein engineering studies. Its diverse mutants are able to accept a variety of other substrates such as drugs, terpenes and gaseous alkanes (Whitehouse et al., 2012). CYP106A2 is a highly interesting steroid hydroxylase that is important for this work, and together with CYP109E1 will be discussed in detail below. CYP109E1, CYP109A2 and CYP106A1 from DSM319 are relatively new members of the *B. megaterium* subfamily, identified after the genome sequencing of the strain (Brill, 2013; Eppinger et al., 2011).

Table 2. Selected examples of P450s from prokaryotic organisms with known characteristics

Organism	Activity	Reference
<i>Amycolatopsis orientalis</i>	CYP105AS1 – compactin hydroxylase CYP105EBH – epothilone B hydroxylase CYP165A1/B1/C1 – oxidative phenol coupling (vancomycin biosynthesis)	(Basch and Chiang, 2007; Bischoff et al., 2005; McLean et al., 2015; Urlacher, 2010)
<i>Bacillus megaterium</i>	CYP102A1 – fatty acid hydroxylase CYP106A1/A2 – steroid hydroxylase CYP109E1/A2 – vitamin D ₃ hydroxylase	(Berg and Rafter, 1981; Brill, 2013; Narhi and Fulco, 1982)
<i>Bacillus subtilis</i>	CYP109B1 – fatty acid/terpene oxidase CYP102A2/3 – fatty acid hydroxylase P450 Biol – biotin synthesis	(Girhard et al., 2010; Green et al., 2001; Gustafsson et al., 2004)
<i>Mycobacterium tuberculosis</i>	CYP51B1 – sterol 14α-demethylase CYP121A1 – intramolecular C-C bond formation CYP124A1/125A1/142A1 – cholesterol / cholest-4-en-3-one oxidase	(Belin et al., 2009; Horiuchi et al., 1998; Johnston et al., 2010; McLean et al., 2009; Ouellet et al., 2010)
<i>Novosphingobium aromaticivorans</i>	CYP101B1/108D1 – aromatic hydrocarbon hydroxylase; CYP101B1 – norisoprenoid oxidase	(Bell and Wong, 2007; Bell et al., 2012; Hall and Bell, 2014)
<i>Pseudomonas putida</i>	CYP101A1 – camphor 5-hydroxylase CYP111A1 – linalool 8-hydroxylase	(Katagiri et al., 1968; Ullah et al., 1990)
<i>Sorangium cellulosum</i>	CYP109C1/C2/D1 – fatty acid hydroxylase CYP167A1 – epothilone D oxidase CYP260A1 – steroid 1α-hydroxylase CYP260A1/CYP264B1 – sesquiterpene oxidase CYP260B1/CYP267B1 – norisoprenoid oxidase CYP267A1/B1 – drug metabolizer	(Kern et al., 2015, 2016; Khatri et al., 2010, 2013; Litzenburger and Bernhardt, 2016; Ringle, 2013; Schifrin et al., 2015)
<i>Streptomyces species</i>	CYP105A3 – compactin hydroxylase CYP105A1 – vitamin D ₃ hydroxylase	(Sugimoto et al., 2008; Watanabe et al., 1995)

1.2.1 CYP106A2

CYP106A2 from *B. megaterium* ATCC13368 is a bacterial steroid hydroxylase, identified in the late 1970s (Berg et al., 1975, 1976, 1979). The enzyme was cloned, sequenced and heterologously expressed in *E. coli* as well as in *B. subtilis* (Rauschenbach et al., 1993). The first substrate identified for CYP106A2 was progesterone, which was mainly converted to 15β-hydroxyprogesterone. Various other 3-oxo-Δ⁴ steroids, such as 11-deoxycortisol (RSS) and testosterone, were also found to be 15β-hydroxylated by CYP106A2. Therefore, this enzyme was characterized as the first bacterial steroid 15β-hydroxylase (Berg et al., 1976; Kiss et al., 2015). Furthermore, other hydroxylation positions were identified with related substrates, such as 6β, 7β, 9α and 11α in the gonane and 7β in ursane skeleton. Interestingly, 12α and 12β, 7β and 11α hydroxylation positions were identified for abietane

and dammarane terpenoid cores, respectively (for review see: Schmitz et al., 2018). Due to its versatility and high regio-and stereo-specificity, the enzyme has been intensively studied for four decades. HTS methods, using more than 16000 synthetic compounds and 500 bioactive natural products, identified various compounds as novel substrates for CYP106A2 such as the pentacyclic triterpene 11-keto- β -boswellic acid (KBA) (Bleif et al., 2012), the triterpenoid dipterocarpol (Schmitz et al., 2012), the diterpene resin acid abietic acid (Bleif et al., 2011) and several other compounds with biotechnological or pharmaceutical importance (Schmitz et al., 2018). Despite the number of identified substrates of CYP106A2, the information about the physiological role of this P450 and its natural substrate(s) is still missing (Schmitz et al., 2012). In contrast, the natural redox partners of CYP106A2, a NADPH-dependent FMN-containing flavoprotein (megaredoxin reductase) as well as an iron-sulfur protein (megaredoxin) have been described, although, they have not been cloned yet (Berg et al., 1976; Bureik and Bernhardt, 2007). It has been shown that the activity of CYP106A2 can be reconstituted using an adrenal protein pair, adrenodoxin (Adx) and adrenodoxin reductase (AdR) and redox systems from *B. subtilis* and *P. putida* (Agematu et al., 2006; Rauschenbach et al., 1993; Simgen et al., 2000; Virus and Bernhardt, 2008). In addition, the electron transfer protein etp1 from *Schizosaccharomyces pombe* (*S. pombe*) was found to interact with CYP106A2 effectively (Bureik et al., 2002).

Effective protein engineering work on CYP106A2 was done using directed evolution as well as rational design strategies to increase the catalytic activity and change the regio-selectivity of progesterone hydroxylation from 15 β to pharmaceutically important 11 α , 9 α and 6 β positions. A study on two generations of directed evolution using fluorescence-based HTS methods revealed mutants with 4- and 1.4-fold improved k_{cat}/K_M for hydroxylation towards RSS and progesterone, respectively (Virus and Bernhardt, 2008). Great shifts of regio-selectivity from 15 β to 11 α and 9 α of CYP106A2 towards progesterone was achieved by mutants created through saturation and site-directed mutagenesis based on a CYP106A2 homology model (Lisurek et al., 2008; Nguyen et al., 2012; Nikolaus et al., 2017). The X-ray structure of CYP106A2 was recently solved, showing a mainly hydrophobic active site and several side chains capable of forming hydrogen bonds and salt bridges with its substrates (Janocha et al., 2016). Furthermore, a single mutant based on docking of progesterone to the active site of CYP106A2, showed an increase of 6 β -hydroxylation activity of progesterone from 8.7 (wild type) to 82.7% (Nikolaus et al., 2017).

1.2.2 CYP109E1

CYP109E1 is a recently identified P450, encoded by the genome of *B. megaterium* strain DSM319 (Brill, 2013). In contrast to CYP106A2, only little is known about this P450. Testosterone induced a

type I spectral shift and has been converted to mainly 16 β -hydroxytestosterone by this enzyme. Thus, CYP109E1 was characterized as the first bacterial wild type steroid 16 β -hydroxylase (Józwik et al., 2016). Three other compounds, vitamin D₃, nootkatone and isolongifolen-9-one, were further identified as its substrates (Brill, 2013). It was shown that vitamin D₃ was converted by CYP109E1 into 6 products, whereas the enzyme was selective towards two sesquiterpene substrates.

CYP109E1 was successfully heterologously expressed in *E. coli*, purified and crystallized in substrate-free as well as ligand- and substrate-bound forms (Józwik et al., 2016). Interestingly, among the tested 13 steroids, only testosterone showed considerable *in vitro* turnover by CYP109E1 using bovine AdR and truncated Adx₄₋₁₀₈ as redox proteins. Although some of the screened steroidal compounds were able to induce a type I shift of the heme iron, they were not converted by CYP109E1 or the conversion was negligible. The active site pocket of the substrate-free CYP109E1 was found to be constructed by mainly hydrophobic amino acids, whereas the residues near the substrate entrance channel are mostly polar and charged. The structural environment of the active site is similar to the six SRSs identified for CYP101A1 (Gotoh, 1992): the BC loop (SRS1), part of F (SRS2) and G (SRS3) helices, the middle region of the I helix (SRS4), the region between the K helix and β 5 strand (SRS5) and the β 9-10 turn (SRS6) (Józwik et al., 2016). The substrate/ligand binding narrows the active site pocket and causes large orientational changes of the FG loop and helices F and G (Józwik et al., 2016). The I helix at residues 242-246 widens locally, allowing steroids to go closer to the heme. Additionally, water molecules were found at the interface of helices I and E. It is believed that they, together with residues A242, G243, T246-248, build a hydrogen-bonded proton delivery pathway (Denisov and Sligar, 2015; Józwik et al., 2016). Based on the results of structural modeling, several single alanine mutants have been created to check the importance of identified residues for testosterone binding and hydroxylation. The loss of the catalytic activity caused by V169A and I241A substitutions indicated their importance for productive binding of testosterone. The mutant of the highly conserved threonine at position 246 showed drastically decreased activity, supporting the hypothesis that this residue contributes in proton delivery and oxygen activation (Józwik et al., 2016).

1.2.3 *Bacillus megaterium* as expression host for P450 systems

The Gram-positive rod-shaped soil bacterium *B. megaterium* gained popularity in the field of biotechnology due to its GRAS nature, ability to grow on different cheap media, high capacity for production of important substances, e.g. heterologous proteins and due to enzymes encoded by its genome such as the very successful representative of the P450 superfamily, CYP102A1 and the steroid hydroxylases, CYP106A1/A2 (Brill, 2013; Bunk et al., 2010; Kiss et al., 2015a; Rygus and Hillen, 1992; Vary et al., 2007; Whitehouse et al., 2012). Moreover, *B. megaterium* is found to be a

suitable host for the coexpression of both endogenous and mammalian P450s and their redox partners. The resulting P450 whole-cell systems based on the MS941 strain, were found to be suitable biocatalysts for cost-effective production of various important compounds in several studies by our group (Bleif et al., 2012; Brill et al., 2014; Ehrhardt et al., 2016a, 2016b; Gerber et al., 2015; Kiss et al., 2015b). For example, whole-cell systems overexpressing CYP106A1 or CYP106A2 produced pharmaceutically important metabolites of KBA, cyproterone acetate as well as various hydroxysteroids (Bleif et al., 2012; Brill et al., 2014; Kiss et al., 2015a). Interestingly, the activity of the mammalian mitochondrial P450 systems containing CYP11A1 and CYP27A1 supported by adrenal redox chain (AdR, Adx) was successfully reproduced in *B. megaterium*, showing effective side-chain cleavage and 27-hydroxylation of cholesterol, respectively (Ehrhardt et al., 2016a; Gerber et al., 2015). The established whole-cell systems of mammalian P450s in *B. megaterium* showed efficient bioconversions, and thus emphasized the high potential of this bacterium in P450-based biocatalysis. Since bacterial P450 systems are soluble and generally easier to express, endogenous P450-based systems are expected to be even more promising for biotechnological applications. The CYP106A2-based *B. megaterium* system has been successfully scaled up at a 400 mL scale for cyproterone acetate conversion, yielding 0.43 g/L product, 15 β -hydroxycyproterone acetate using a bench-top bioreactor (Kiss et al., 2015b). It is important to note, that in this whole-cell system only CYP106A2 was overexpressed and its activity was successfully supported by redox partners endogenously synthesized in the MS941 strain. Although several redox proteins of this strain have been identified such as Fdxs and BmCPR (Brill et al., 2014; Milhim et al., 2016b), the natural partners for endogenous P450s remain unknown. Moreover, the physiological substrates of the P450s have not been identified yet, thus the potential of this bacterium for the production of oxyfunctionalized molecules is not fully discovered.

1.3 Aims

The current work aims to study the catalysis of various biotechnologically and pharmaceutically important compounds by two functionally different P450 enzymes from *B. megaterium*, CYP106A2 and CYP109E1.

CYP106A2 is one of the few characterized bacterial steroid hydroxylases showing high potential for biotechnological applications. Prednisone and dexamethasone, synthetic steroidal anti-inflammatory and immunosuppressive drugs, have been identified previously as substrates of CYP106A2. Since hydroxylation is one of the important reactions for steroid functionalization, the goal is to investigate CYP106A2-mediated biotransformations of prednisone and dexamethasone in order to generate novel steroidal drug candidates or important intermediates for further modification of steroid structure. The

reactions will be investigated *in vitro* with a reconstituted CYP106A2 system as well as with binding titrations in order to identify product patterns, the kinetic parameters (k_{cat} , K_M) and the dissociation constant (K_d). The conversion of the substrates will be further investigated with several CYP106A2-based *B. megaterium* strains. In case of a successful *in vivo* turnover of prednisone and dexamethasone by CYP106A2, preparative whole-cell biotransformations will be performed with subsequent product purification for the structural identification of steroid derivatives via nuclear magnetic resonance (NMR) analysis.

CYP109E1 is a recently identified P450 and there is only little known about its substrates and catalytic functions. Therefore, the aim is to expand the substrate range of CYP109E1 and evaluate its potential for synthetic applications. A focused library of compounds will be screened through monitoring high-spin shifts spectroscopically and *in vitro* conversions. The conversions will be analyzed by high performance liquid chromatography (HPLC) or gas chromatography-mass spectrometry (GC-MS). Biotransformations of the newest substrates, selectively converted *in vitro*, will be investigated using a CYP109E1-based *B. megaterium* whole-cell biocatalyst in order to test the system for the ability to reproduce the *in vitro* conversion and to generate the products on milligram-scale. The reaction products should be isolated for their structural elucidation in order to characterize the new CYP109E1-mediated reactions.

2. Scientific articles

2.1 Putkaradze et al. 2017a

Biotransformation of prednisone and dexamethasone by cytochrome P450 based systems - Identification of new potential drug candidates

Natalia Putkaradze, Flora Marta Kiss, Daniela Schmitz, Josef Zapp, Michael C.Hutter, Rita Bernhardt

2017, Journal of Biotechnology. 242:101-110

DOI: 10.1016/j.biotec.2016.12.011

Reprinted with the permission of Elsevier.



Research Paper

Biotransformation of prednisone and dexamethasone by cytochrome P450 based systems – Identification of new potential drug candidates



Natalia Putkaradze^{a,1}, Flora Marta Kiss^{a,1}, Daniela Schmitz^a, Josef Zapp^b, Michael C. Hutter^c, Rita Bernhardt^{a,*}

^a Institute of Biochemistry, Saarland University, D-66123 Saarbruecken, Germany

^b Institute of Pharmaceutical Biology, Saarland University, D-66123 Saarbruecken, Germany

^c Center for Bioinformatics, Saarland University, D-66123 Saarbruecken, Germany

ARTICLE INFO

Article history:

Received 5 September 2016

Received in revised form 8 December 2016

Accepted 13 December 2016

Available online 14 December 2016

ABSTRACT

Prednisone and dexamethasone are synthetic glucocorticoids widely used as anti-inflammatory and immunosuppressive drugs. Since their hydroxylated derivatives could serve as novel potential drug candidates, our aim was to investigate their biotransformation by the steroid hydroxylase CYP106A2 from *Bacillus megaterium* ATCC13368. *In vitro* we were able to demonstrate highly selective 15β-hydroxylation of the steroids with a reconstituted CYP106A2 system. The reactions were thoroughly characterized, determining the kinetic parameters and the equilibrium dissociation constant. The observed lower conversion rate in the case of dexamethasone hydroxylation was clarified by quantum chemical calculations, which suggest a rearrangement of the intermediately formed radical species. To identify the obtained conversion products with NMR, CYP106A2-based *Bacillus megaterium* whole-cell systems were applied resulting in an altered product pattern for prednisone, yet no significant change for dexamethasone conversion compared to *in vitro*. Even the MS941 control strain performed a highly selective biotransformation of prednisone producing the known metabolite 20β-dihydrocortisone. The identified novel prednisone derivatives 15β, 17, 20β, 21-tetrahydroxy-preg-4-en-3,11-dione and 15β, 17, 20β, 21-tetrahydroxy-preg-1,4-dien-3,11-dione as well as the 15β-hydroxylated variants of both drugs are promising candidates for drug-design and development approaches.

© 2016 Elsevier B.V. All rights reserved.

1. Introduction

Cytochromes P450 (P450s) comprise one of the largest and oldest enzyme families, being present in almost every life form. Today the P450 database (<http://drnelson.uthsc.edu/CytochromeP450.html>; status of April 2016) lists more than 35,000 representatives, reflecting the central role of these enzymes in nature. P450s are external monooxygenases, catalyzing the scission of molecular oxygen and the following monooxygenation of an aliphatic or aromatic substrate (Ortiz de Montellano, 2010). Furthermore, P450s encompass a broad range of reactions such as hydroxylation, dehalogenation, *N*-oxidation, *N*-, *O*-, *S*-dealkylation, and C–C bond cleavage (Bernhardt, 2006; Bernhardt and Urlacher, 2014). Unusual P450 reactions including cyclopropanation via the carbene

transfer (Coelho et al., 2013) and intramolecular C–H amination are also described (McIntosh et al., 2013). Besides the wide range of catalyzed reactions, their broad substrate spectrum is also remarkable. P450s perform the oxyfunctionalization of a variety of complex substrates such as alkaloids, polyketides, terpenes and steroids (Bernhardt, 2006). The appeal of P450s rests upon their unique ability to perform reactions under mild conditions, including atmospheric pressure and temperatures ranging from 20 to 37 °C (Urlacher and Girhard, 2012).

Glucocorticoids (GCs) are a class of steroid hormones that regulate the glucose metabolism via interaction with the intracellular glucocorticoid receptor. GCs are so-called stress hormones and, as such, they exhibit potent anti-inflammatory and immunosuppressive effects. Besides their fundamental anti-inflammatory activities, they display a plethora of pleiotropic effects on multiple signaling pathways (Rhen and Cidlowski, 2005). The steroid mode of action can be regulated by the introduction of a functional group, in particular, an oxyfunctionalization in specific orientation and position, attached to the steroid core. The GC activity requires a 17-hydroxylated, 21-carbon steroid with an activating

* Corresponding author at: Institute of Biochemistry, Campus B2.2, Saarland University, D-66123 Saarbruecken, Germany.

E-mail address: ritabern@mx.uni-saarland.de (R. Bernhardt).

¹ These authors contributed equally to this work.

hydroxylation at position 11β , also shown to be crucial for anti-inflammatory activity. The 11β -hydroxylation regulates the GC activity via higher affinity towards the intracellular GC receptor. When the 11 -hydroxyl group is converted to a keto group, it is not able to bind and activate the GC and the mineralocorticoid (MC) receptor. The enzyme responsible for the pivotal reaction, activating glucocorticoids is the 11β -hydroxysteroid-dehydrogenase type 1 (HSD1) (Chapman et al., 2013b). The reverse reaction, inactivating glucocorticoids is catalyzed by the tissue-specific 11β -hydroxysteroid-dehydrogenase type 2 (HSD2), whose role is to convert endogenous GCs into their inactive keto forms (Chapman et al., 2013a). Both cortisone and 11 -dehydrocorticosterone have a substantially reduced affinity towards the GC receptor compared to cortisol and corticosterone (Chapman et al., 2013a; Hunter and Bailey, 2015). This protective mechanism is essential in aldosterone target tissues, such as the liver, lungs, colon and kidneys, to prevent unfavourable activation of the MC receptor, and in the placenta to control foetal exposure to maternal GCs (Brown et al., 1996; Chapman et al., 2013a).

The main targets of GC drugs are inflammatory and autoimmune diseases, such as Crohn's disease, ulcerative colitis, psoriasis, rheumatic and allergic disorders, lupus and many more. However, due to their long-term application and complex actions, GCs show various side effects including hypogonadism, hypertension, bone necrosis, acne, development disorders, Cushing's syndrome and changes in behaviour (Rhen and Cidlowski, 2005). In certain cases long-term GC therapy can not be avoided, consequently, synthetic GCs have been developed to overcome some of these side effects, especially those triggered by the transactivation of the MC receptor. This transactivation can be reduced by derivatization at position C-16 on the steroid core, like 16α -methylation (present in dexamethasone) and 16β -methylation (present in betamethasone). Both methylations decrease MC transactivation by selectively increasing the GC receptor activation (Diederich et al., 2004). On the contrary, a 9α -fluorination (present in dexamethasone) increases both, receptor transactivation along with a reduced oxidation via HSD2. The $\Delta 1$ -dehydro derivatization, however, increases HSD2 activity, resulting in an enhanced inactivation of the GC receptor (Diederich et al., 2004).

In this work, we aimed to convert the synthetic GCs prednisone and dexamethasone in order to produce novel hydroxylated derivatives of both drugs. The opportunity to selectively introduce hydroxyl groups into prednisone and dexamethasone opens up the possibility to observe new effects of these substances. In addition, such hydroxysteroids could have the potential to be used in subsequent studies developing them into newly functionalized drugs with altered specificity and pharmacokinetics. Our primary goal included the efficient hydroxylation of both steroids using a P450 based biotransformation system. To achieve this, we used CYP106A2 from *Bacillus megaterium* (*B. megaterium*) ATCC13368 as biocatalyst. This enzyme has been extensively studied in our group, and researchers have been investigating its steroid hydroxylating capacity since the late 1970s (Berg et al., 1976; Berg and Rafter, 1981; Rauschenbach et al., 1993; Lisurek et al., 2004; Virus et al., 2006; Zehentgruber et al., 2010; Kiss et al., 2015a). The conversion of prednisone and dexamethasone has been proved in our previous studies, however, the respective hydroxylation positions have not yet been determined (Schmitz et al., 2014; Kiss et al., 2015a). With the goal of detailed characterization of these CYP106A2-based reactions, substrate binding as well as reconstituted *in vitro* assays were performed. To understand the binding and kinetic behaviour of the P450 with the substrates, computational methods were applied. The conversion of both glucocorticoids was further investigated *in vivo* using different CYP106A2-based *B. megaterium* whole-cell systems. These preparative scale conversions enabled us to obtain sufficient amounts of reaction products for structural elucidation

via NMR. Interestingly, the main product of all dexamethasone conversions was identified as 15β -hydroxydexamethasone whereas prednisone was converted with *B. megaterium* strains ATCC13368 and MS941 into different and novel hydroxyprednisone derivatives besides 15β -hydroxyprednisone. The former strain gave a product with rehydrated C-1 and subsequent loss of the $\Delta 1$ -dehydro moiety, the latter one with a reduced keto group at position 20β .

2. Materials and methods

2.1. Chemicals and solvents

Prednisone and dexamethasone were purchased from Sigma-Aldrich (St. Louis, Missouri, USA). 17 , 20β , 21 -trihydroxy-preg-4-en-3,11-dione (20β -dihydrocortisone, Q3960-000) was purchased from Steraloids (Newport, RI, USA). All solvents and other chemicals were of highest purity available and were obtained from standard sources.

2.2. Protein expression and purification

CYP106A2 and its bovine redox partners, the truncated form of adrenodoxine (Adx₄₋₁₀₈) and adrenodoxine reductase (AdR) were expressed and purified as described before (Uhlmann et al., 1992; Sagara et al., 1993; Simgen et al., 2000; Lisurek et al., 2004).

2.3. Spectroscopic substrate binding assay

The binding behaviour of dexamethasone and prednisone to CYP106A2 was investigated by difference spectroscopy, using tandem quartz cuvettes as described before. (Jefcoate, 1978; Schenkman and Jansson, 1998). The titration of the CYP106A2 enzyme solution with the corresponding steroid substrate dissolved in DMSO was performed according to Schmitz et al. (Schmitz et al., 2014). The spectrum was recorded from 350 to 500 nm during each titration step, encompassing a concentration range of 0–500 μ M for dexamethasone and 700 μ M for prednisone. The equilibrium dissociation constant (K_d) was calculated by plotting the peak-to-through differences against the total substrate concentration. The mean values of three independent titration sets were fitted with OriginPro 9.0G software, using hyperbolic regression (OriginLab, Massachusetts, USA).

2.4. In vitro turnover and catalytic activity

The *in vitro* substrate turnover was performed with a reconstituted system, containing CYP106A2, bovine Adx₄₋₁₀₈ and AdR, in a molar ratio of 1:20:2. For the continuous electron supply, an NADPH regeneration system was used [glucose-6-phosphate-dehydrogenase (1 U), glucose-6-phosphate (5 mM) and MgCl₂ (1 mM)]. All reactions were carried out in 250 μ L total volume at 30 °C in 50 mM potassium phosphate buffer (with 10% glycerol, pH 7.4).

The kinetic parameters were estimated with a substrate concentration range from 0 to 500 μ M using 0.5 μ M of P450, 10 μ M of Adx and 1 μ M of AdR. The reactions were started by adding 0.2 mM NADPH and quenched after 2 min for prednisone and after 10 min for dexamethasone by adding one reaction volume of ethyl acetate. Steroids were extracted twice with ethyl acetate. The organic phases were combined, evaporated to dryness and resuspended in acetonitrile/water (20:80) for high performance liquid chromatography (HPLC) analysis. The product amounts were determined from the conversion ratio using area under-peak of product and substrate from the HPLC chromatograms. The kinetic constants were calculated by plotting the product formation rates against the corresponding substrate concentrations and fitting the data using

the Michaelis-Menten fit with the OriginPro 9.0G software. The values represent the mean of three independent reactions.

2.5. *Bacillus megaterium* strains and cultivation

The *B. megaterium* ATCC13368 strain (ATCC_wt) was provided by Dr. R. Rauschenbach (Bayer HealthCare AG, Berlin, Germany). The *B. megaterium* MS941 strain (MS941_wt) (Wittchen and Meinhardt, 1995) was donated by Prof. Dr. D. Jahn (Institute of Microbiology, TU Braunschweig, Germany). Besides the wild type strains, two previously established recombinant systems were applied, overexpressing either only the CYP106A2, or the enzyme in combination with its heterologous redox partners, adrenodoxine (Adx) and adrenodoxine reductase (AdR), using the expression vectors pSMF2.1_C and pSMF2.1_CAA transformed into *B. megaterium* MS941 to give MS941_C and MS941_CAA, respectively (Bleif et al., 2011).

The *B. megaterium* cells were cultivated in complex TB medium (24 g/L yeast extract, 12 g/L soytone, 0.5% glycerol (v/v), 2.31 g/L KH₂PO₄ and 12.5 g/L K₂HPO₄, pH 7.4) at 30 °C and 150 rpm. The cultures were grown in baffled shake flasks (300 mL or 2 L) and for the recombinant strains (with any of the pSMF2.1 plasmids) the medium was additionally supplemented with tetracycline to a final concentration of 10 mg/L.

2.6. Whole-cell turnover and product isolation

Pre-cultures were prepared by inoculating 50 mL complex medium with the deep-frozen glycerol stock of the corresponding strain and incubated overnight at 30 °C, 150 rpm. Subsequently, the main cultures were inoculated using the overnight-cultures (1% of the main culture volume) and cultivated until an OD₅₇₈ of 0.4 was reached. The expression of CYP106A2 (MS941_C) and its heterologous redox partners (MS941_CAA) was initiated by adding 5 g/L xylose solution. The protein expression was conducted for 24 h, after which the cultures were harvested (4000 x g, 4 °C) and the cell pellet was washed and resuspended in 100 mM potassium phosphate buffer (with 10% glycerol, pH 7.4) to an end cell-suspension concentration of 50 g wet cell weight (w/w)/L. All whole-cell biotransformations were performed with resting cells in 50 mL buffer using 300 mL baffled shake flasks at 30 °C, 150 rpm. The substrates were added to a final concentration of 200 μM, dissolved in ethanol, with the ethanol concentration not exceeding 5% of the culture volume. To monitor the conversions, 500 μL samples were taken at indicated time points and extracted twice with ethyl acetate. The organic phases were combined and evaporated to dryness for the subsequent analysis by reverse-phase HPLC.

In case of product isolation, the whole reaction volume was extracted twice with one volume of ethyl acetate, the organic phases were dried over anhydrous MgSO₄ and concentrated to dryness in a rotavapor (Büchi R-114). The yellowish residue was dissolved in the HPLC mobile phase and filtered through a sterile syringe filter (Rotilabo syringe filter, 0.22 μm, Carl Roth GmbH, Karlsruhe, Germany). The purification of the product was completed by preparative HPLC, according to its retention time. The collected fractions were evaporated to dryness and analyzed by NMR spectroscopy.

2.7. HPLC analysis

The HPLC analysis was performed on a Jasco system, consisting of a Pu-980 HPLC pump, an AS-950 sampler, an UV-975 UV/Vis detector, and a LG-980-02 gradient unit (Jasco, Gross-Umstadt, Germany). A reversed-phase ec MN Nucleodur C18 (3 μm, 4.0 × 125 mm) column (Macherey-Nagel, Betlehem, PA, USA) was used and kept at an oven temperature of 40 °C. A gradient of

pure acetonitrile (B) and water with 20% acetonitrile (A) (from 0 to 80% of B) was used as the mobile phase, with a flow rate of 1 mL/min. The UV detection of the substrates and products was accomplished at 240 nm. The product isolation was achieved using preparative reversed-phase HPLC [ec MN Nucleodur C18 VP (5 μm, 8.0 × 250 mm), Macherey-Nagel, Betlehem, PA, USA] with a flow rate of 2.5 mL/min. The results are shown as conversion%, calculated from the product area under peak divided by the sum of the substrate and product areas.

2.8. NMR characterization of the main metabolites

All NMR spectra were recorded in CD₃OD at 298 K. The spectra were obtained on a Bruker DRX 500 equipped with a 5 mm BBO probe head or on Bruker Avance III 700 MHz equipped with a 5 mm TCI cryo probe. The chemical shifts were relative to CH₃OD at δ 3.30 (¹H NMR) and CD₃OD at δ 49.00 (¹³C NMR) respectively using the standard δ notation in parts per million. The 1D NMR (¹H and ¹³C NMR, DEPT135) and the 2D NMR spectra (gs-HH-COSY, gs-NOESY, gs-HSQCED, and gs-HMBC) were recorded using the BRUKER pulse program library. All assignments were based on extensive NMR spectral evidence.

2.8.1. 15β-hydroxyprednisone (P1), cortisone (P6), and 15β-hydroxydexamethasone (D1)

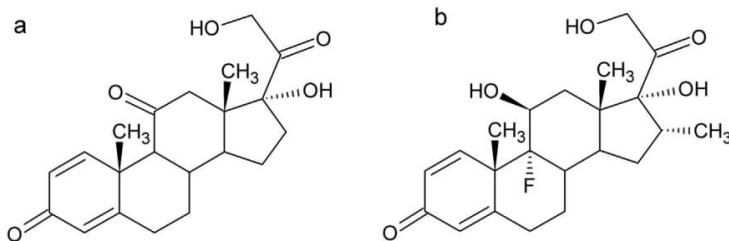
The ¹H and ¹³C NMR spectra of 15β-hydroxyprednisone (P1), Cortisone (P6), and 15β-hydroxydexamethasone (D1) were identical to those of authentic samples and the corresponding data matched with those previously published (Kirk et al., 1990; Kiss et al., 2015a,b).

2.8.2. 15β, 17, 21-trihydroxy-preg-4-en-3,11,20-trione (P2)

In contrast to prednisone the NMR data of its conversion product P2 lacked resonances for the double bond between C-1 and C-2. Instead, signals for two additional methylenes appeared in the ¹³C NMR and DEPT spectra (δ_C 35.66, C-1, and 34.45, C-2) and the resonance of carbonyl C-3 (δ_C 202.45) was shifted downfield by nearly 15 ppm. Resonances at δ_H 4.42 and δ_C 69.36 gave hint to an supplemental hydroxyl group in the molecule. It was located at C-15 since its proton signal correlated with those of H-16a (δ_H 2.21) and H-16b (δ_H 2.75) in the HHCOSY. The ddd coupling pattern of H-15, with coupling constants of *J* = 7.5, 5.3 and 2.3 Hz matched perfectly with those of other 15β-hydroxy steroids isolated in our group (Kiss et al., 2015a,b). ¹H NMR (CD₃OD, 500 MHz): δ 0.80 (s, 3xH-18), 1.35 (m, H-7a), 1.45 (s, 3xH-19), 1.70 (td, *J* = 14.3 and 4.0 Hz, H-1a), 1.99 (d, *J* = 12.2 Hz, H-12a), 2.15 (m, H-9), 2.21 (dd, *J* = 15.8 and 7.5 Hz, H-16a), 2.33 (m, H-7b), 2.34 (m, H-6a), 2.35 (m, 2H, H-8 and H-14), 2.39 (m, H-2a), 2.50 (m, H-2b), 2.55 (m, H-6b), 2.73 (ddd, *J* = 14.3, 5.0 and 3.2 Hz, H-1b), 2.75 (dd, *J* = 15.8 and 2.3 Hz, H-16b), 2.96 (d, *J* = 12.2 Hz, H-12b), 4.20 (d, *J* = 19.5 Hz, H-21a), 4.42 (ddd, *J* = 7.5, 5.3 and 2.3 Hz, H-15), 4.60 (d, *J* = 19.5 Hz, H-21b), 5.72 s (H-4). ¹³C NMR (CD₃OD, 125 MHz): δ 17.55 (CH₃, C-19), 18.67 (CH₃, C-18), 32.87 (CH₂, C-7), 33.43 (CH₂, C-6), 34.01 (CH, C-8), 34.45 (CH₂, C-2), 35.66 (CH₂, C-1), 39.75 (C, C-10), 47.80 (CH₂, C-16), 51.66 (C, C-13), 52.14 (CH₂, C-12), 54.88 (CH, C-14), 63.46 (CH, C-9), 67.77 (CH₂, C-21), 69.36 (CH, C-15), 89.12 (C, C-17), 124.77 (CH, C-4), 172.97 (C, C-5), 202.45 (C, C-3), 211.68 (C, C-11), 212.10 (C, C-20).

2.8.3. 20β-dihydrocortisone (17, 20β, 21-trihydroxy-preg-4-en-3,11-dione, P3)

The NMR spectra of P3 revealed a hydrogenation of the double bond at C-1 (δ_C 35.69) and C-2 (δ_C 34.46) and a reduction of carbonyl C-20 to a secondary alcohol (δ_C 76.01; δ_H 3.70, dd, *J* = 7.3 and 3.1 Hz). Therefore, P3 was found to be a 20-dihydrocortisone. The configuration of the new stereocenter at C-20 followed directly by comparison of its NMR data with those of an authentic sample of the

**Scheme 1.** Structure of prednisone (a) and dexamethasone (b).

20 β -isomer, which fitted perfectly to each other. ^1H NMR (CD_3OD , 500 MHz): δ 0.82 (s, 3xH-18), 1.29 (m, H-7a), 1.34 (m, H-15a), 1.44 (s, 3xH-19), 1.63 (m, H-16a), 1.69 (td, J =14.0 and 4.4 Hz, H-1a), 1.87 (m, H-15b), 1.89 (m, H-16b), 1.99 (m, H-8), 2.00 (m, H-6a), 2.06 (m, H-9), 2.23 (dd, J =17.0, 4.4, 3.1 and 1.0 Hz, H-2a), 2.30 (m, H-14), 2.32 (ddd, J =14.8, 4.0 and 2.0 Hz, H-6b), 2.48 (d, J =12.7 Hz, H-12a), 2.50 (m, 2H, H-2b and H-7b), 2.71 (ddd, J =14.0, 5.2 and 3.2 Hz, H-1b), 2.75 (d, J =12.7 Hz, H-12b), 3.59 (dd, J =11.5 and 7.3 Hz, H-21a), 3.63 (dd, J =11.5 and 3.1 Hz, H-21b), 3.70 (dd, 7.3 and 3.1 Hz, H-20), 5.71 d (2.0 Hz, H-4). ^{13}C NMR (CD_3OD , 125 MHz): δ 15.87 (CH₃, C-18), 17.64 (CH₃, C-19), 24.46 (CH₂, C-15), 33.50 (CH₂, C-6), 33.69 (CH₂, C-7), 34.46 (CH₂, C-2), 34.85 (CH₂, C-16), 35.69 (CH₂, C-1), 38.24 (CH, C-8), 39.59 (C, C-10), 49.77 (CH, C-14), 52.82 (C, C-13), 53.18 (CH₂, C-12), 63.59 (CH, C-9), 65.07 (CH₂, C-21), 76.01 (CH, C-20), 85.19 (C, C-17), 124.68 (CH, C-4), 173.13 (C, C-5), 202.48 (C, C-3), 214.06 (C, C-11).

2.8.4. 15 β , 17, 20 β , 21-tetrahydroxy-preg-4-en-3,11-dione (P4)

P4 and P5 could not be separated by HPLC. However, each molecules-specific NMR data could be obtained by conducting 2D NMR measurements. The data of P4 were close to those of P3 but showed additional signals for a secondary hydroxyl group with resonances at δ_{C} 69.57 and δ_{H} 4.37 (dd, J =7.5, 5.5 and 2.0 Hz). They very much resembled those of C-15 and H-15 β found for P2. 2D NMR measurements supported these findings and led to the structure of 15 β , 17, 20 β , 21-tetrahydroxy-preg-4-en-3,11-dione for P4. ^1H NMR (CD_3OD , 700 MHz): δ 1.04 (s, 3xH-18), 1.33 (m, H-7a), 1.46 (s, 3xH-19), 1.69 (m, H-1a), 1.86 (m, H-16a), 2.11 (d, J =11.3 Hz, H-9), 2.19 (m, H-16b), 2.22 (m, H-14), 2.24 (m, H-2a), 2.28 (m, H-7b), 2.33 (m, H-6a), 2.35 (m, H-8), 2.41 (d, J =12.5 Hz, H-12a), 2.52 (m, H-2b), 2.55 (m, H-6b), 2.73 (m, H-1b), 2.74 (d, J =12.5 Hz, H-12b), 3.59 (dd, J =11.5 and 7.3 Hz, H-21a), 3.63 (dd, J =11.5 and 3.1 Hz, H-21b), 3.79 (dd, J =7.3 and 3.1 Hz, H-20), 4.37 (ddd, J =7.5, 5.5 and 2.0 Hz, H-15), 5.72 s (H-4). ^{13}C NMR (CD_3OD , 175 MHz): δ 17.57 (CH₃, C-19), 18.37 (CH₃, C-18), 32.94 (CH₂, C-7), 33.50 (CH₂, C-6), 34.11 (CH, C-8), 34.46 (CH₂, C-2), 35.72 (CH₂, C-1), 39.75 (C, C-10),

47.85 (CH₂, C-16), 52.42 (C, C-13), 53.76 (CH₂, C-12), 53.99 (CH, C-14), 63.54 (CH, C-9), 65.02 (CH₂, C-21), 69.57 (CH, C-15), 75.94 (CH, C-20), 84.84 (C, C-17), 124.69 (CH, C-4), 173.28 (C, C-5), 202.51 (C, C-3), 213.66 (C, C-11).

2.8.5. 15 β , 17, 20 β , 21-tetrahydroxy-preg-1,4-dien-3,11-dione (P5)

The NMR data of P5 were very close to those of P4 and differed only in the resonances of ring A, which in case of P5 still had the double bond between C-1 (δ_{C} 158.53) and C-2 (δ_{C} 127.76). ^1H NMR (CD_3OD , 700 MHz): δ 1.08 (s, 3xH-18), 1.31 (m, H-7a), 1.49 (s, 3xH-19), 1.86 (m, H-16a), 2.12 (d, J =11.2 Hz, H-9), 2.19 (m, H-16b), 2.23 (m, H-14), 2.27 (m, H-7b), 2.43 (d, 12.5 Hz, H-12a), 2.44 (m, H-8), 2.45 (m, H-6a), 2.63 (m, H-6b), 2.73 (d, 12.5 Hz, H-12b), 3.57 (dd, 11.5 and 7.3 Hz, H-21a), 3.62 (dd, 11.5 and 3.1 Hz, H-21b), 3.80 (dd, J =7.3 and 3.1 Hz, H-20), 4.36 (m, H-15), 6.09 (t, J =2.0 Hz, H-4), 6.18 (dd, J =10.2 and 2.0 Hz, H-2a), 7.80 (d, J =10.2 Hz, H-1). ^{13}C NMR (CD_3OD , 175 MHz): δ 18.47 (CH₃, C-18), 19.38 (CH₃, C-19), 33.47 (CH₂, C-6), 33.95 (CH, C-8), 34.21 (CH₂, C-7), 44.34 (C, C-10), 47.99 (CH₂, C-16), 52.54 (C, C-13), 53.40 (CH₂, C-12), 53.78 (CH, C-14), 61.29 (CH, C-9), 65.01 (CH₂, C-21), 69.62 (CH, C-15), 75.93 (CH, C-20), 84.74 (C, C-17), 124.77 (CH, C-4), 127.76 (CH, C-2), 158.53 (CH, C-1), 171.32 (C, C-5), 188.74 (C, C-3), 212.98 (C, C-11).

2.9. Computational methods

For the docking studies AUTODOCK (version 4.2) was used. The receptor was modeled on the basis of chain B taken from the preliminary X-ray structure of CYP106A2 (Huey et al., 2007; Janocha et al., 2016; Morris et al., 1998). Hydrogen atoms and Kollman charges were added using the Windows version 1.5.6r3 of AutoDock Tools (Sanner, 1999).

The atomic charge of the porphyrin iron a was set to +0.400 e, corresponding to Fe(II), and the partial charges of its ligating nitrogen atoms were set to -0.348 e, respectively, to compensate this. A rectangular grid box (46 × 54 × 52 points with a grid

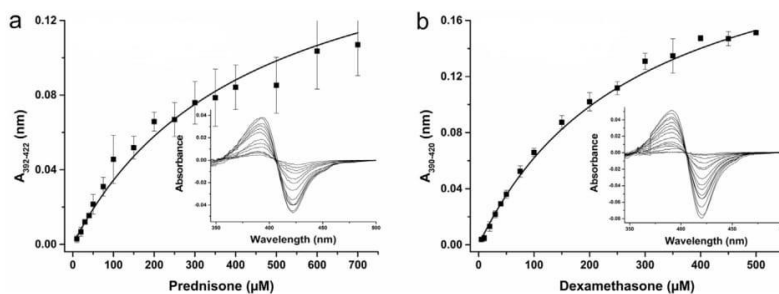


Fig. 1. Type I spectral shifts induced by the binding of prednisone (a) and dexamethasone (b) to CYP106A2. The peak-to-through absorbance differences were plotted against increasing substrate concentrations. The mean values of three independent measurements were fitted by a hyperbolic regression. The K_d values were determined with a regression coefficient (R^2) of 0.99.

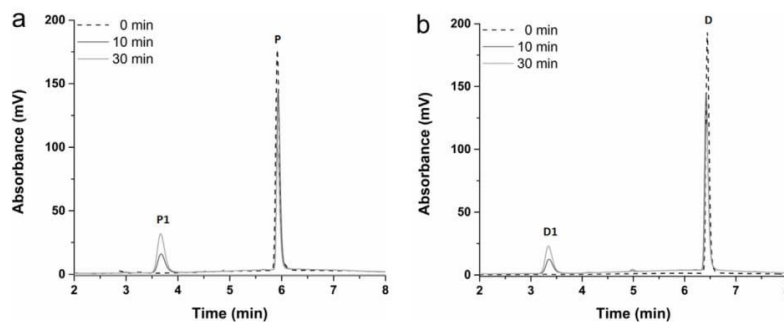


Fig. 2. HPLC chromatograms of the *in vitro* conversions of 200 μ M prednisone (a) and dexamethasone (b) by CYP106A2: P-prednisone, P1—the main product of prednisone, D-dexamethasone, D1—the main product of dexamethasone.

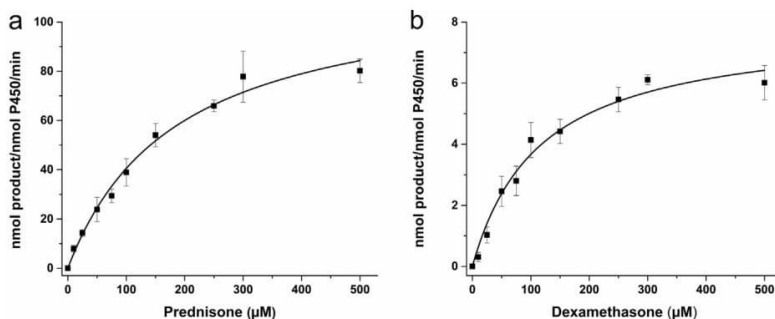


Fig. 3. Determination of the kinetic parameters for prednisone (a) and dexamethasone (b) conversion catalyzed by CYP106A2. The kinetic studies were performed with a reconstituted system containing CYP106A2, bovine Adx₄₋₁₀₈ and AdR as well as an NADPH regeneration system. The reaction velocities were plotted against increasing substrate concentrations. The mean values of three independent measurements were fitted using OriginPro 9.0G software. The k_{cat} and K_M values were determined with a regression coefficient (R^2) of 0.99 for prednisone and 0.98 for dexamethasone.

spacing of 0.375 Å) was centered about 5 Å above the heme iron. The side chains of Thr89 and Thr247 were treated flexible, since they can be involved in hydrogen-bonding with substrates. The structures of dexamethasone and prednisone were prepared manually and energetically minimized applying the MM+ force field as implemented in HYPERCHEM (HYPERCHEM, Version 6, Hypercube Inc., Gainesville, FL, USA). Corresponding Gasteiger-Marsili charges were generated using AutoDock Tools. A total of 200 docking runs were carried out for each ligand applying the Lamarckian genetic algorithm using default parameter settings. Quantum chemical calculations were performed using a modified version of the semi-empirical program package VAMP applying the AM1 Hamiltonian (Rauhut, et al., 1997). The structures of dexamethasone, prednisone and their corresponding radicals were energetically optimized below a gradient norm of 0.1 kcal/mol Å⁻¹. The unpaired electrons of the radicals were specified as doublets by the unrestricted Hartree-Fock formalism. Hydrogen abstraction energies were computed following the approach of Mayeno (Mayeno et al., 2009).

3. Results

3.1. In vitro assays

To characterize the binding of the synthetic glucocorticoids and to determine their binding constants, spin-shift alterations upon substrate binding were monitored by difference spectroscopy. As expected, binding of both steroids resulted in the formation of high-spin heme. In order to calculate the binding affinities for prednisone and dexamethasone, CYP106A2 was titrated with both the steroids until the shift in the absorbance from 417 to 390 was saturated

(Fig. 1). The calculated K_d values are $434 \pm 40 \mu$ M for prednisone and $289 \pm 5 \mu$ M for dexamethasone, respectively.

To gain further information about the reaction of CYP106A2 with the steroids, *in vitro* conversions were performed followed by kinetic studies. Product formation was analyzed using HPLC with UV-detection showing that both substrates were converted into one main product (Fig. 2). CYP106A2 hydroxylated prednisone into product P1 with a k_{cat} of $116 \pm 8 \text{ min}^{-1}$ and a K_M of $185 \pm 27 \mu\text{M}$. The conversion of dexamethasone into the main product D1 was much slower, with a k_{cat} of $7.9 \pm 0.5 \text{ min}^{-1}$ and a K_M of $115 \pm 20 \mu\text{M}$ (Fig. 3).

3.2. Molecular docking and quantum chemical calculations

For both, dexamethasone and prednisone, docked conformations where found that show the heme iron in close proximity from which the 15β -hydroxylation is possible. The corresponding distances are 3.83 Å for dexamethasone (Fig. 4) and somewhat longer for prednisone (4.15 Å). To investigate if there is a substantial difference regarding the hydrogen abstraction energies between the two substrates we performed similar quantum chemical calculations as previously done to explain the differences in the hydroxylation pattern of 11-deoxycorticosterone (Hobler et al., 2012). The predicted activation energies for the abstraction of a hydrogen atom in position 15 for dexamethasone and prednisone are, however, within 0.4 kcal/mol and thus almost identical with respect to the accuracy of the applied method. Therefore, the considerably slower conversion of dexamethasone compared to prednisone must be caused by other factors. We found that the initial radical, which is formed after removing a hydrogen atom in position 15, can undergo

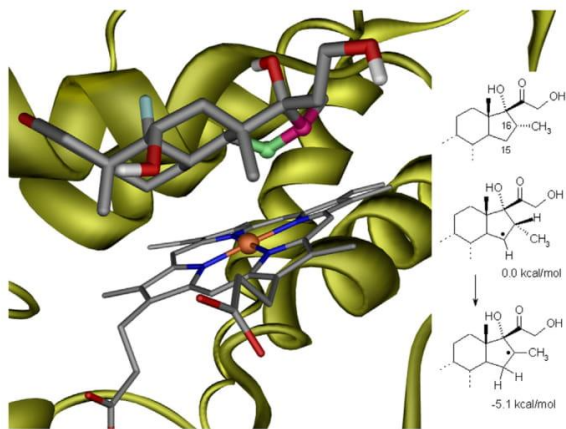


Fig. 4. The energetically most favorable docking conformation of dexamethasone shows position 15 (green) within a distance of 3.83 Å to the heme iron (orange). The radical being formed after hydrogen abstraction in this position can, however, migrate to position 16 (magenta) which is 5.1 kcal/mol more favorable in energy (see inset). This position is, however, further away (5.10 Å) and thus less accessible. Due to the strongly depleted fraction of radical species in position 15, hydroxylation becomes slow as was experimentally observed. (For interpretation of the references to color in this figure legend, the reader is referred to the web version of this article).

rearrangement and migrate to position 16 being lower in energy by 5.1 kcal/mol (Fig. 4). This position is, however, further away from the heme iron and less accessible, which explains why no traceable amounts of 16-hydroxydexamethasone were obtained. Consequently, the rate of hydroxylation is limited by the strongly depleted fraction of radical species in position 15 and thus, less product formation is observed despite the stronger binding of dexamethasone compared to prednisone (Scheme 1).

3.3. In vivo biotransformation

To obtain sufficient amounts of the hydroxylated prednisone and dexamethasone products for structural characterization by NMR, *in vivo* biotransformations were performed. We used four different *B. megaterium* systems to establish dexamethasone and prednisone bioconversions: ATCC_{WT} that naturally encodes CYP106A2 in its genome, MS941_{WT} which does not contain the CYP106A2, but naturally expresses other P450s, MS941.C, which contains the pSMF2.1C plasmid for CYP106A2 expression and MS941.CAA that contains the pSMF2.1CAA plasmid for CYP106A2, AdR and Adx expression under the control of a xylose inducible promoter. The latter two strains were used to compare the effect of endogenous redox partners versus heterologously expressed redox proteins on the resulting product pattern.

The ATCC_{WT} strain converted 98% prednisone already within 8 h (Figs. 5 and 6). HPLC analysis of the bioconversion showed two peaks indicating two reaction products: a hydrophobic minor compound eluting 0.2 min after the substrate (P6), its amount increasing quickly in the first minutes of the conversion, then decreasing parallel to the main products formation (at 3.8 min). The main product was identified as a mixture of two compounds, 15β-hydroxyprednisone (P1) and 15β, 17, 21-trihydroxy-preg-4-en-3,11-dione (P4) and 15β, 17, 20β, 21-tetrahydroxy-preg-1,4-dien-3,11-dione (P5). Two additional side products with retention times around 5.5 min were also observed (Figs. 5 e, g and 6 b). A scheme of all identified conversion products of prednisone is shown in Fig. 7.

The MS941_{WT} system was used as control strain and also tested for the conversion of prednisone and dexamethasone to study the effect of the additional enzymatic activity in the strain on the product formation. This strain generated two reaction products of prednisone, one eluting 0.2 min after the substrate peak and the main product eluting at 5.5 min which was identified as

20β-dihydrocortisone (P3). The main product is most probably a CYP106A2-independent metabolite of a steroid dehydrogenase encoded in the *B. megaterium* genome (Gerber et al., 2016).

The product pattern was the same using MS941.C and MS941.CAA resting cells. In both cases, 100% of the substrate was converted within 24 h. However, when looking at earlier time points, the conversion of prednisone was significantly faster with the MS941.CAA strain, showing already 80% conversion within 4 h compared with the MS941.C strain which transformed only 48% in 4 h and 75% in 8 h (Fig. 6a). The conversion in both cases yielded the more-hydrophobic, so-called intermediate product P6, eluting 0.2 min after the substrate peak which was detected during the conversion by the MS941.WT strain as well. This product was identified as cortisone. The conversion also resulted in the formation of a main product (P1), 15β-hydroxyprednisone, eluting at 3.8 min and a minor product with 2.4 min retention time. The latter one was identified as a mixture of 15β, 17, 20β, 21-tetrahydroxy-preg-4-en-3,11-dione (P4) and 15β, 17, 20β, 21-tetrahydroxy-preg-1,4-dien-3,11-dione (P5). Two additional side products with retention times around 5.5 min were also observed (Figs. 5 e, g and 6 b). A scheme of all identified conversion products of prednisone is shown in Fig. 7.

Dexamethasone was converted into one hydroxylated product by all strains, except for the MS941.WT, which did not show any conversion. The selectivity of dexamethasone conversion was similar in the three cases, in contrast to that of prednisone. The reactions resulted in one main product, which was identified as 15β-hydroxylated dexamethasone (D1) and two to three minor side products whose overall amounts were not sufficient for structure elucidation (Fig. 5b, f and h). Dexamethasone was hydroxylated slower in all three cases than prednisone. After eight hours, only the ATCC_{WT} converted more than 50% of dexamethasone into its hydroxylated product, while the MS941 strains did not even reach 50% conversion within 24 h (Fig. 8a and b). The highest product amount after 24 h was achieved by the ATCC_{WT} strain, converting 88% of the substrate in 24 h, while the MS941 strains converted only 35–40% of dexamethasone within the same time.

4. Discussion

In this work, we investigated the conversion of prednisone and dexamethasone using CYP106A2 in order to obtain novel steroids with hydroxy-functionalized carbon atoms. Hydroxyl groups serve as easy accessible reaction sites and are, therefore, interesting for drug design and development approaches. The major advantage of P450 biocatalysts is that they can selectively hydroxylate aliphatic or aromatic C–H bonds under mild conditions, especially at positions where classical chemistry is only scarcely applicable. Therefore, P450s are considered as potential alternatives for the production of selectively functionalized steroid hormones, among other drugs, for the pharmaceutical industry. In the past two decades, CYP106A2 from *B. megaterium* emerged as a potent steroid hydroxylase. A variety of C19 and C21 steroids were identified as its substrates including synthetic steroids such as prednisone and dexamethasone (Schmitz et al., 2014; Kiss et al., 2015a). Using 3-oxo-Δ⁴-steroids as substrates, CYP106A2 was shown to favor the 15β-position for hydroxylation. However, with 3-hydroxy-Δ⁵-steroids, we recently showed that the enzyme predominantly hydroxylates the 7β-position (Schmitz et al., 2014). Regarding the A-ring configuration of prednisone and dexamethasone, with a keto-ene moiety and an additional double-bond between C1 and C2, the final hydroxylation position of prednisone and dexamethasone was not predictable. However, we expected a predominant 15β-hydroxylation influenced by the keto group at C3.

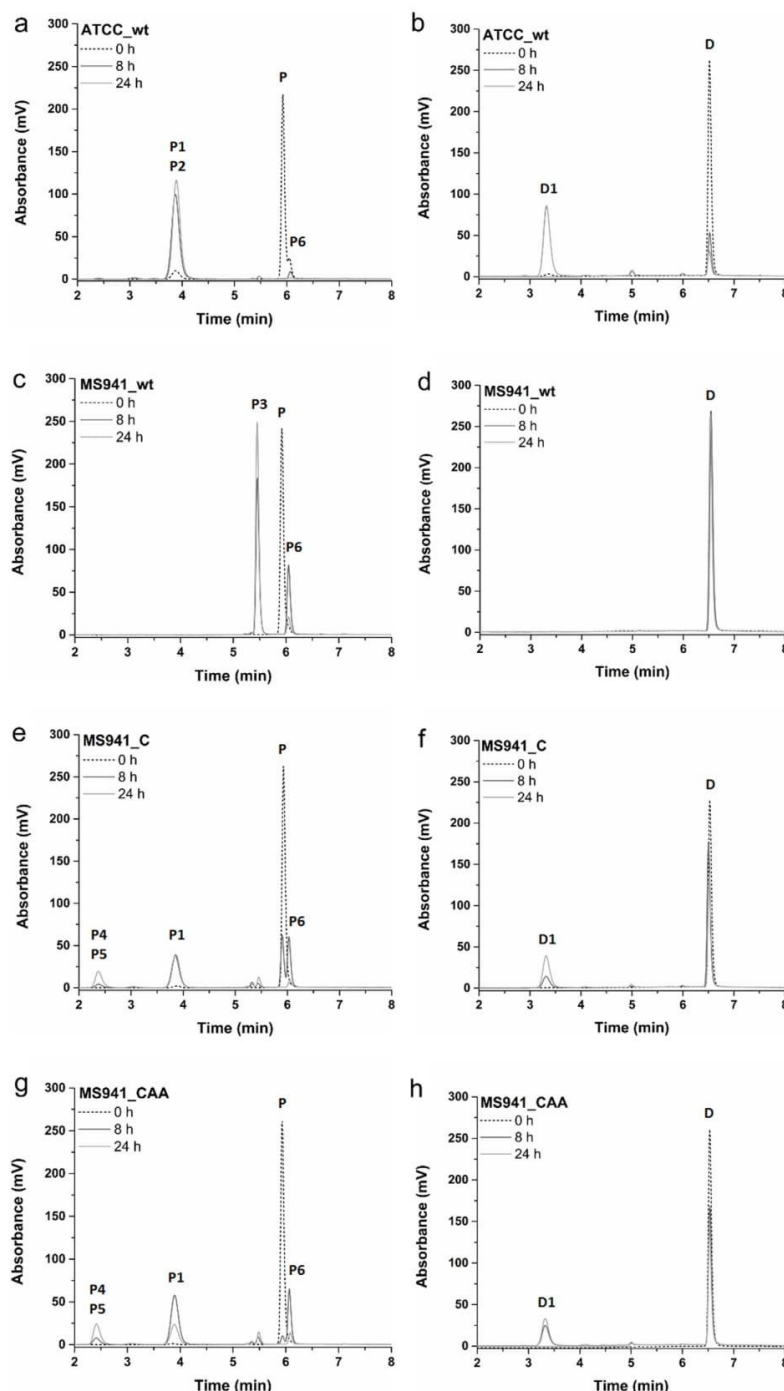


Fig. 5. HPLC chromatograms of the *in vivo* conversion of prednisone (a, c, e, g) and dexamethasone (b, d, f, h) by different *B. megaterium* strains. Conversions were performed with the ATCC_wt strain (a, b), the MS941_wt strain (c, d), with MS941_C (e, f), a recombinant variant overexpressing CYP106A2 and with MS941_CAA (g, h), expressing Adx and AdR besides the P450. The reactions were performed with resting cells, in 100 mM potassium phosphate buffer, pH 7.4 at 30 °C and samples were collected at the indicated time points.

To gain further insight into the prednisone and dexamethasone binding towards CYP106A2, the dissociation constants of both substrates were estimated using difference spectroscopy. The K_d values

(434 μ M for prednisone and 189 μ M for dexamethasone) match those observed in previous studies for other steroids (Kiss et al., 2015a). The reaction kinetics of both substrates showed Michaelis-

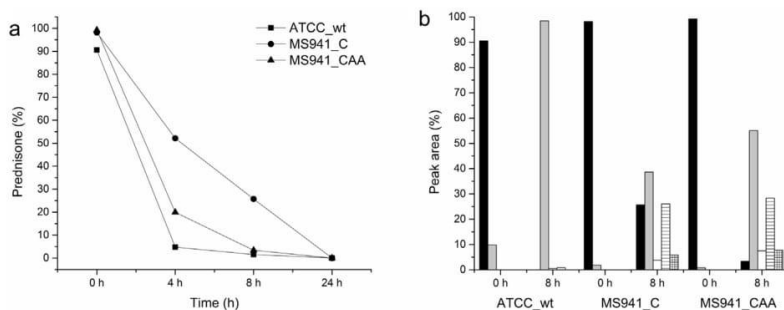


Fig. 6. Prednisone consumption by the ATCC_wt and the recombinant MS941 strains over 4, 8 and 24 h (a). The product distribution following 8 h conversion is shown on the right (b): prednisone (black), main product (grey), minor products (white), intermediate product (lined white), side products (grid white).

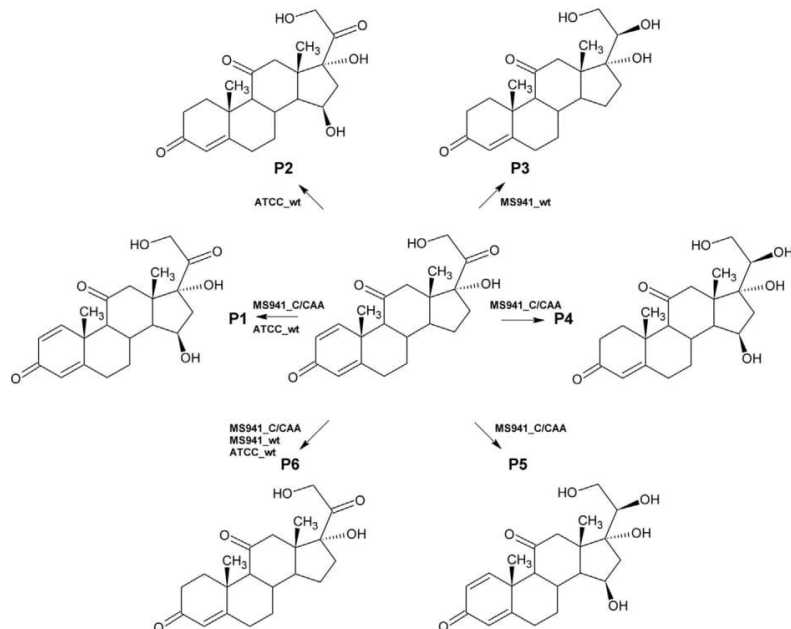


Fig. 7. Chemical structures of all identified conversion products (P1–P6) of prednisone (in the middle). P1: 15 β -hydroxyprednisone, P2: 15 β , 17, 21-trihydroxy-preg-4-en-3,11,20-trione, P3: 20 β -dihydrocortisone, P4: 15 β , 17, 20 β , 21-tetrahydroxy-preg-4-en-3,11-dione, P5: 15 β , 17, 20 β , 21-tetrahydroxy-preg-1,4-dien-3,11-dione, P6: cortisone.

Menten behaviour, with k_{cat} values of 116 min⁻¹ for prednisone, and 7.9 min⁻¹ for dexamethasone. The apparent K_M values were 185 μ M and 115 μ M for prednisone and dexamethasone, respectively. According to the K_d and K_M values, one can assume, that dexamethasone has a higher affinity for the active site resulting in a tighter binding mode, though the hydroxylation velocity proved to be slower than with prednisone.

In order to prepare sufficient amounts of the conversion products for NMR analysis, *in vivo* biotransformations were performed with both steroids. In addition, to explore the biotransformation capacity of the *B. megaterium* based CYP106A2 systems established in our group, we used four different strain variants: ATCC_wt, MS941_wt, MS941_C, and MS941_CAA.

As a first step, we investigated the product pattern and product distribution of prednisone and dexamethasone conversions with the four strains and identified the reaction products (Fig. 7). Performing the conversion of prednisone with the control strain (MS941_wt), we detected two important known glucocorticoids:

cortisone (P6) and 20 β -dihydrocortisone (P3), natural metabolites of the stress hormone cortisol in humans and animals. These compounds were not detected during the *in vitro* conversion of prednisone and, therefore, they were considered to be conversion products of endogenous enzymes expressed by MS941_wt strain. We propose that 20 β -dihydrocortisone is a conversion product of the recently identified 20 β -hydroxysteroid dehydrogenase from *B. megaterium*. This enzyme has already shown the same activity (reduction of ketones at position 20 β) towards other steroid substrates such as 11-deoxycortisol and 17 α -hydroxyprogesterone (Gerber et al., 2016). According to the time-dependent conversions with MS941_wt, we concluded that cortisone is an intermediate product and that the substrate is converted to 20 β -dihydrocortisone within 24 h almost entirely (Fig. 5c). Hereby, we report a highly regio- and stereoselective whole-cell conversion of prednisone resulting in 20 β -dihydrocortisone without side products. To the best of our knowledge, apart from our described method, there is no chemical synthesis known to date being capable

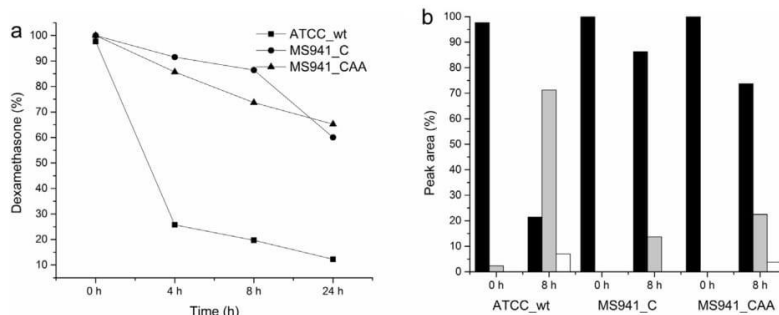


Fig. 8. Dexamethasone consumption by the ATCC_wt and the recombinant MS941 strains over 4, 8 and 24 h (a). The product distribution following 8 h conversion is shown on the right (b): dexamethasone (black), main product (grey), side products (white).

of reducing the ketone in the glucocorticoid structure at position 20 in such a selective manner. In addition, 20 β -dihydrocortisone is a 100-times more expensive compound than prednisone. As a result, a simple, environmentally friendly and cost-effective, highly selective bioconversion of prednisone with the *B. megaterium* whole-cell system might be biotechnologically promising for the production of 20 β -dihydrocortisone. Besides the MS941_wt, all studied strains showed the formation of intermediate cortisone ($t_R = 6.2$ min). Remarkably, the ATCC_wt strain generated 15 β -hydroxylated variants of prednisone and cortisone (P1 and P2) while the recombinant MS941_C and MS941_CAA strains produce 15 β -hydroxyprednisone and two diverse reaction products (P4 and P5). The latter MS941 strains also produced a minor metabolite ($t_R = 5.5$ min), showing matching retention times with the main product of the MS941_wt strain (20 β -dihydrocortisone). The prednisone derivatives, P4 and P5, were produced only by the CYP106A2-based strains MS941_C and MS941_CAA but not by the ATCC_wt strain expressing CYP106A2 enzyme endogenously. This allows us to speculate that the above mentioned compounds are reaction products of the P450 enzyme in combination with other enzymes from *B. megaterium*.

Concerning dexamethasone, all tested strains, except for the MS941.wt (lacking the CYP106A2 gene), showed a successful conversion yielding one main product, which was identified as 15 β -hydroxydexamethasone. The selectivity of dexamethasone conversion was similar with all three strains tested, in contrast to that of prednisone. Besides the main product, two to three side products were also detected via HPLC, however, due to their low yields (<20% of the total conversion) they were not subjected to structure determination. Dexamethasone was hydroxylated slower in all three cases compared with prednisone (Figs. 6 and 8). The fastest hydroxylation was achieved by the ATCC_wt strain with 88% conversion of 200 μ M substrate within 24 h. The recombinant MS941 strains hydroxylated 35–40% of dexamethasone within 24 h. We assume that dexamethasone conversion is limited by the low enzyme activity towards this substrate, which was also confirmed by a lower k_{cat} value estimated *in vitro*. Our computational results based on docking studies and quantum chemical calculations suggest that the observed low enzymatic activity regarding hydroxylation of dexamethasone is due to rearrangement of the radical intermediate in position 15, which migrates to the energetically preferred position 16. Since the latter position is much less accessible, the rate of hydroxylation becomes limited by the remaining fraction of corresponding species in position 15. Therefore, hydroxylation of prednisone is faster despite its lower binding affinity. However, reactions limited either by low CYP106A2 amounts or reactivity can be improved by large scale bioconversion processes in bioreactors (Kiss et al., 2015c) or mutagenesis (Virus et al., 2006; Virus and Bernhardt, 2008).

Comparing the conversions of prednisone and dexamethasone by ATCC_wt and three MS941 strains, we observed significant differences in activity and product pattern. For both substrates, the whole-cell conversion was higher with ATCC_wt than MS941 cells. The presence of other P450s coded by the genome of MS941 cells and the lack of information about the presence of other P450s except for CYP106A2 in ATCC_wt strain did not allow us to quantify and compare the CYP106A2 concentrations in different *B. megaterium* cells used for the biotransformation. However, the ATCC_wt seems to be more effective for the conversion of both substrates and this might be, on the one hand, due to different expression levels of CYP106A2 and its redox partners and, on the other hand, due to differences in the expression of other P450s and redox proteins in various *B. megaterium* cells. In contrast to dexamethasone, prednisone seems to be a substrate of other endogenous enzymes from *B. megaterium* resulting in the formation of cortisone and 15 β , 17, 21-trihydroxy-preg-4-en-3,11,20-trione by ATCC_wt and cortisone, 15 β , 17, 20 β , 21-tetrahydroxy-preg-4-en-3,11-dione and 15 β , 17, 20 β , 21-tetrahydroxy-preg-1,4-dien-3,11-dione by MS941 cells.

In summary, we were able to demonstrate and thoroughly characterize the *in vitro* 15 β -hydroxylation of prednisone and dexamethasone catalyzed by CYP106A2. Using various previously established CYP106A2-based *B. megaterium* systems, the 15 β -hydroxylation of the synthetic GCs was also confirmed *in vivo* on a preparative scale. By further exploring the whole-cell conversions and their resulting products, two new glucocorticoid compounds, 15 β , 17, 20 β , 21-tetrahydroxy-preg-4-en-3,11-dione and 15 β , 17, 20 β , 21-tetrahydroxy-preg-1,4-dien-3,11-dione, were identified. These tetrahydroxylated steroids, as well as 15 β -hydroxyprednisone and 15 β -hydroxydexamethasone represent pharmaceutically interesting compounds, which can be used for further derivatization, since the newly introduced hydroxyl groups are perfect candidates for structural modifications leading to the design and development of novel steroid drugs.

Author contributions

NP and FMK carried out the experiments and together with DS analyzed and interpreted the data and drafted the manuscript. JZ measured the NMR samples and determined structures of the reaction products. MCH performed the docking simulations and quantum chemical calculations. RB designed the project, analyzed and interpreted the results, and assisted in drafting the manuscript.

Acknowledgements

This work was supported by the DAAD (Deutscher Akademischer Austauschdienst) and by the People Programme (Marie Curie

Actions) of the European Union's 7th Framework Programme (FP7/2007–2013), P4FIFTY – FP7 PEOPLE ITN 2011–289217. The authors thank Birgit Heider-Lips for the purification of AdR and Adx4-108 and Dr. Martin Litzenburger for helpful discussions.

References

- Berg, A., Rafter, J.J., 1981. Studies on the substrate specificity and inducibility of cytochrome P-450meg. *Biochem. J.* 196, 781–786.
- Berg, A., Gustafsson, J.A., Ingelman-Sundberg, M., 1976. Characterization of a cytochrome P-450-dependent steroid hydroxylase system present in *Bacillus megaterium*. *J. Biol. Chem.* 251, 2831–2838.
- Bernhardt, R., Urlacher, V.B., 2014. Cytochromes P450 as promising catalysts for biotechnological application: chances and limitations. *Appl. Microbiol. Biotechnol.* 98, 6185–6203.
- Bernhardt, R., 2006. Cytochromes P450 as versatile biocatalysts. *J. Biotechnol.* 124, 128–145.
- Bleif, S., Hannemann, F., Zapp, J., Hartmann, D., Jauch, J., Bernhardt, R., 2011. A new *Bacillus megaterium* whole-cell catalyst for the hydroxylation of the pentacyclic triterpene 11-keto- β -boswellic acid (KBA) based on a recombinant cytochrome P450 system. *Appl. Microbiol. Biotechnol.* 93, 1135–1146.
- Brown, R.W., Diaz, R., Robson, A.C., Kotelevtsev, Y.V., Mullins, J.J., Kaufman, M.H., Seckl, J.R., 1996. The ontogeny of 11 beta-hydroxysteroid dehydrogenase type 2 and mineralocorticoid receptor gene expression reveal intricate control of glucocorticoid action in development. *Endocrinology* 137, 794–797.
- Chapman, K., Holmes, M., Seckl, J., 2013a. 11 β -Hydroxysteroid dehydrogenases: intracellular gate-keepers of tissue glucocorticoid action. *Physiol. Rev.* 93, 1139–1206.
- Chapman, K.E., Coutinho, A.E., Zhang, Z., Kipari, T., Savill, J.S., Seckl, J.R., 2013b. Changing glucocorticoid action: 11 β -hydroxysteroid dehydrogenase type 1 in acute and chronic inflammation. *J. Steroid Biochem. Mol. Biol.* 137, 82–92.
- Coelho, P.S., Brustad, E.M., Kannan, A., Arnold, F.H., 2013. Olefin cyclopropanation via carbene transfer catalyzed by engineered cytochrome P450 enzymes. *Science* 339, 307–310.
- Diederich, S., Scholz, T., Eigendorff, E., Bumke-Vogt, C., Quinkler, M., Exner, P., Pfeiffer, A.F., Oelkers, W., Bähr, V., 2004. Pharmacodynamics and pharmacokinetics of synthetic mineralocorticoids and glucocorticoids: receptor transactivation and preceptor metabolism by 11 β -hydroxysteroid-dehydrogenases. *Horm. Metab. Res.* 36, 423–429.
- Gerber, A., Milhim, M., Hartz, P., Zapp, J., Bernhardt, R., 2016. Genetic engineering of *Bacillus megaterium* for high-yield production of the major teleost progestogens 17 α ,20 β -di- and 17 α ,20 β ,21 α -trihydroxy-4-pregnen-3-one. *Metab. Eng.* 36, 19–27.
- Hobler, A., Kagawa, N., Hutter, M.C., Hartmann, M.F., Wudy, S.A., Hannemann, F., Bernhardt, R., 2012. Human aldosterone synthase: recombinant expression in *E. coli* and purification enables a detailed biochemical analysis of the protein on the molecular level. *J. Steroid Biochem. Mol. Biol.* 132, 57–65.
- Huey, R., Morris, G.M., Olson, A.J., Goodsell, D.S., 2007. A semiempirical free energy force field with charge-based desolvation. *J. Comput. Chem.* 28, 1145–1152.
- Hunter, R.W., Bailey, M.A., 2015. Glucocorticoids and 11 β -hydroxysteroid dehydrogenases: mechanisms for hypertension. *Curr. Opin. Pharmacol.* 21, 105–114.
- Janocha, S., Carius, Y., Hutter, M., Lancaster, C.R.D., Bernhardt, R., 2016. Crystal structure of CYP106A2 in substrate-free and substrate-bound form. *Chembiochem* 17 (9), 852–860.
- Jefcoate, C.R., 1978. Measurement of substrate and inhibitor binding to microsomal cytochrome P-450 by optical-difference spectroscopy. In: FLEISCHER, S., Packer, L. (Eds.), *Methods in Enzymology*. Academic Press, pp. 258–279.
- Kirk, D.N., Toms, H.C., Douglas, C., White, K.A., Smith, K.E., Latif, S., Hubbard, R.W.P., 1990. A survey of the high-field 1H NMR spectra of the steroid hormones, their hydroxylated derivatives, and related compounds. *J. Chem. Soc. Perkin Trans. 2*, 1567.
- Kiss, F.M., Schmitz, D., Zapp, J., Dier, T.K.F., Volmer, D.A., Bernhardt, R., 2015a. Comparison of CYP106A1 and CYP106A2 from *Bacillus megaterium* – identification of a novel 11-oxidase activity. *Appl. Microbiol. Biotechnol.* 99, 8495–8514.
- Kiss, F.M., Khatri, Y., Zapp, J., Bernhardt, R., 2015b. Identification of new substrates for the CYP106A1-mediated 11-oxidation and investigation of the reaction mechanism. *FEBS Lett.* 589, 2320–2326.
- Kiss, F.M., Lundemo, M.T., Zapp, J., Woodley, J.M., Bernhardt, R., 2015c. Process development for the production of 15 β -hydroxycoproterone acetate using *Bacillus megaterium* expressing CYP106A2 as whole-cell biocatalyst. *Microbiol. Cell Fact.* 14, 28.
- Lisurek, M., Kang, M.-J., Hartmann, R.W., Bernhardt, R., 2004. Identification of monohydroxy progesterones produced by CYP106A2 using comparative HPLC and electrospray ionisation collision-induced dissociation mass spectrometry. *Biochem. Biophys. Res. Commun.* 319, 677–682.
- Mayeno, A.N., Robinson, J.L., Yang, R.S.H., Reisfeld, B., 2009. Predicting activation enthalpies of cytochrome-P450-mediated hydrogen abstractions. 2. Comparison of semiempirical PM3 SAM1, and AM1 with a density functional theory method. *J. Chem. Inf. Model.* 49, 1692–1703.
- McIntosh, J.A., Coelho, P.S., Farwell, C.C., Wang, Z.J., Lewis, J.C., Brown, T.R., Arnold, F.H., 2013. Enantioselective intramolecular CH amination catalyzed by engineered cytochrome P450 enzymes in vitro and in vivo. *Angew. Chem.* 125, 9479–9482.
- Morris, G.M., Goodsell, D.S., Halliday, R.S., Huey, R., Hart, W.E., Belew, R.K., Olson, A.J., 1998. Automated docking using a Lamarckian genetic algorithm and an empirical binding free energy function. *J. Comput. Chem.* 19, 1639–1662.
- Ortiz de Montellano, P.R., 2010. Hydrocarbon hydroxylation by cytochrome P450 enzymes. *Chem. Rev.* 110, 932–948.
- Rauhut, G., Alex, A., Chandrasekhar, J., Steinke, T., Sauer, W., Beck, B., Hutter, M., Gedeck, P., Clark, T., 1997. VAMP Version 6.5. Oxford Molecular, Erlangen, Germany.
- Rauschenbach, R., Isernhagen, M., Noeske-Jungblut, C., Boidol, W., Siewert, G., 1993. Cloning sequencing and expression of the gene for cytochrome P450meg, the steroid-15 β -monooxygenase from *Bacillus megaterium* ATCC 13368. *Mol. Genet. MGG* 241, 170–176.
- Rhen, T., Cidlowski, J.A., 2005. Antiinflammatory action of glucocorticoids – new mechanisms for old drugs. *N. Engl. J. Med.* 353, 1711–1723.
- Sagara, Y., Wada, A., Takata, Y., Waterman, M.R., Sekimizu, K., Horiochi, T., 1993. Direct expression of adrenodoxin reductase in *Escherichia coli* and the functional characterization. *Biol. Pharm. Bull.* 16, 627–630.
- Sanner, M.F., 1999. Python: a programming language for software integration and development. *J. Mol. Graph. Model.* 17, 57–61.
- Schenkman, J.B., Jansson, I., 1998. Spectral analyses of cytochromes P450. In: Phillips, J., Shepard, E. (Eds.), *Cytochrome P450 Protocols*. Humana Press, pp. 25–34.
- Schmitz, D., Zapp, J., Bernhardt, R., 2014. Steroid conversion with CYP106A2 – production of pharmaceutically interesting DHEA metabolites. *Microb. Cell Fact.* 13, 81.
- Simgen, B., Contzen, J., Schwarzer, R., Bernhardt, R., Jung, C., 2000. Substrate binding to 15 β -hydroxylase (CYP106A2) probed by FT infrared spectroscopic studies of the iron ligand CO stretch vibration. *Biochem. Biophys. Res. Commun.* 269, 737–742.
- Uhlmann, H., Beckert, V., Schwarz, D., Bernhardt, R., 1992. Expression of bovine adrenodoxin in *E. coli* and site-directed mutagenesis of 2 FE-2S/cluster ligands. *Biochem. Biophys. Res. Commun.* 188, 1131–1138.
- Urlacher, V.B., Girhard, M., 2012. Cytochrome P450 monooxygenases: an update on perspectives for synthetic application. *Trends Biotechnol.* 30, 26–36.
- Virus, C., Bernhardt, R., 2008. Molecular evolution of a steroid hydroxylating cytochrome P450 using a versatile steroid detection system for screening. *Lipids* 43, 1133–1141.
- Virus, C., Lisurek, M., Simgen, B., Hannemann, F., Bernhardt, R., 2006. Function and engineering of the 15 β -hydroxylase CYP106A2. *Biochem. Soc. Trans.* 34, 1215–1218.
- Wittchen, K.D., Meinhardt, F., 1995. Inactivation of the major extracellular protease from *Bacillus megaterium* DSM319 by gene replacement. *Appl. Microbiol. Biotechnol.* 42, 871–877.
- Zehentgruber, D., Hannemann, F., Bleif, S., Bernhardt, R., Lütz, S., 2010. Towards preparative scale steroid hydroxylation with cytochrome P450 monooxygenase CYP106A2. *Chembiochem* 11, 713–721.

2.2 Abdulmughni et al. 2017

Characterization of cytochrome P450 CYP109E1 from *Bacillus megaterium* as a novel vitamin D₃ hydroxylase

Ammar Abdulmughni, Ilona K. Józwik, Natalia Putkaradze, Elisa Brill, Josef Zapp, Andy-Mark W.H.Thunnissen, Frank Hannemann, Rita Bernhardt

2017, Journal of Biotechnology. 243:38-47

DOI: 10.1016/j.biotec.2016.12.023

Reprinted with the permission of Elsevier.



Characterization of cytochrome P450 CYP109E1 from *Bacillus megaterium* as a novel vitamin D₃ hydroxylase



Ammar Abdulmughni^a, Ilona K. Józwik^b, Natalia Putkaradze^a, Elisa Brill^a, Josef Zapp^c, Andy-Mark W.H. Thunnissen^b, Frank Hannemann^{a,*}, Rita Bernhardt^{a,*}

^a Department of Biochemistry, Campus B2.2, 66123, Saarland University, Saarbrücken, Germany

^b Laboratory of Biophysical Chemistry, Groningen Biomolecular Sciences and Biotechnology Institute, University of Groningen, Nijenborgh 7, 9747 AG, Groningen, The Netherlands

^c Pharmaceutical Biology, Campus C2.2, 66123, Saarland University, Saarbrücken, Germany

ARTICLE INFO

Article history:

Received 22 September 2016

Received in revised form

26 December 2016

Accepted 28 December 2016

Available online 30 December 2016

Keywords:

Bacillus megaterium

CYP109E1

Whole-cell conversion

Vitamin D₃

25-Hydroxy-vitamin D₃

Site-directed mutagenesis

ABSTRACT

In this study the ability of CYP109E1 from *Bacillus megaterium* to metabolize vitamin D₃ (VD₃) was investigated. In an *in vitro* system using bovine adrenodoxin reductase (AdR) and adrenodoxin (Adx₄₋₁₀₈), VD₃ was converted by CYP109E1 into several products. Furthermore, a whole-cell system in *B. megaterium* MS941 was established. The new system showed a conversion of 95% after 24 h. By NMR analysis it was found that CYP109E1 catalyzes hydroxylation of VD₃ at carbons C-24 and C-25, resulting in the formation of 24(S)-hydroxyvitamin D₃ (24S(OH)VD₃), 25-hydroxyvitamin D₃ (25(OH)VD₃) and 24S,25-dihydroxyvitamin D₃ (24S,25(OH)₂VD₃). Through time dependent whole-cell conversion of VD₃, we identified that the formation of 24S,25(OH)₂VD₃ by CYP109E1 is derived from VD₃ via the intermediate 24S(OH)VD₃. Moreover, using docking analysis and site-directed mutagenesis, we identified important active site residues capable of determining substrate specificity and regio-selectivity. HPLC analysis of the whole-cell conversion with the I85A-mutant revealed an increased selectivity towards 25-hydroxylation of VD₃ compared with the wild type activity, resulting in an approximately 2-fold increase of 25(OH)VD₃ production (45 mg l⁻¹ day⁻¹) compared to wild type (24.5 mg l⁻¹ day⁻¹).

© 2017 Elsevier B.V. All rights reserved.

1. Introduction

Cytochromes P450 (P450s) are heme-containing enzymes found in all domains of life (Nelson, 2011). They are involved in many metabolic processes, including the biosynthesis of steroids and fatty acids, the metabolism of drugs and the detoxification of xenobiotics (Bernhardt, 2006). P450 monooxygenases are gaining importance as enzymes for industrial biotechnology since they have the ability to introduce oxygen into non-activated C–H bonds of various compounds in a regio- and stereo-selective manner under mild conditions (Bernhardt and Urlacher, 2014; Urlacher and Girhard, 2012).

Vitamin D₃ (VD₃) is a fat-soluble prohormone, which is synthesized in the presence of ultraviolet radiation from the precursor 7-dehydrocholesterol (Holick et al., 1979; Kametani and Furuyama, 1987). The activation of VD₃ is achieved by different P450s: the mitochondrial CYP27A1 mediates hydroxylation of VD₃ at carbon

25, producing 25-hydroxyvitamin D₃ (25(OH)VD₃), which is then further hydroxylated by CYP27B1 resulting in the most active form of VD₃, i.e., 1 α ,25-dihydroxyvitamin D₃ (1 α -25(OH)₂VD₃) (Prosser and Jones, 2004; Schuster, 2011). It was found that other P450s such as the microsomal CYP2R1, CYP3A4 and CYP2J3 can also hydroxylate VD₃ at C-25 (Cheng et al., 2014; Gupta et al., 2004).

The active form of VD₃, 1 α -25(OH)₂VD₃, is involved in the regulation of the calcium and phosphate metabolism, amongst other physiological processes (Sakaki et al., 2005; Demay, 2006; Jurutka et al., 2007). However, sufficient levels of the precursor 25(OH)VD₃ are required for the regulatory action of 1 α -25(OH)₂VD₃ (Di Rosa et al., 2011). Moreover, 25(OH)VD₃ represents the most abundant VD₃ circulating metabolite and, therefore, is used clinically as an indicator for the VD₃ status of patients (Hollis, 2005).

During the last years there has been a growing interest in the biotransformation of VD₃ to its active metabolites, 25(OH)VD₃ and 1 α -25(OH)₂VD₃. Thereby, recent research activity focused on microbial P450s (Sakaki et al., 2011). However, only few bacterial P450s are known to produce these active metabolites such as CYP105A1 from *S. griseolus* (Sasaki et al., 1991) and CYP107 (Vdh) from *P. autotrophica* (Fujii et al., 2009). Therefore, the identification

* Corresponding authors.

E-mail addresses: f.hannemann@mx.uni-saarland.de (F. Hannemann), ritabern@mx.uni-saarland.de (R. Bernhardt).

of new microbial P450s with 1- α and/or 25-hydroxylation activity towards VD₃ is of great interest.

Recently, CYP109E1 from *Bacillus megaterium* DSM319 was identified and characterized in our group (Józwik et al., 2016). It was shown that CYP109E1 has a 16 β -hydroxylation activity towards testosterone. In addition, the X-ray crystal structures of CYP109E1 were solved for substrate-free protein and in complexes with testosterone or corticosterone. In the absence of bound steroids, CYP109E1 contains a large, open active site pocket at the distal side of the heme. The testosterone-bound CYP109E1 structure shows a different conformation, in which the active site pocket is more narrow (closed state of CYP109E1) (Józwik et al., 2016), which likely reflects the protein's functionally relevant state and therefore was applied in this study for vitamin D₃ docking calculations.

In this study, the substrate specificity of CYP109E1 was investigated for VD₃. Herein, for the first time we present the results demonstrating that CYP109E1 from *B. megaterium* exhibits hydroxylation activity towards VD₃. In addition, whole-cell conversion of VD₃ was carried out using *B. megaterium*. Furthermore, site-directed mutagenesis based on docking simulations of CYP109E1 and VD₃ was performed in order to optimize the regio-selectivity of CYP109E1 towards 25-hydroxylation. The effect of the mutations on the conversion of VD₃ was examined in the whole-cell system.

2. Materials and methods

2.1. Chemicals

VD₃, 25(OH)VD₃, 1 α -25(OH)₂VD₃, (2-hydroxypropyl)- β -cyclodextrin and saponin (from quillaja bark) were purchased from Sigma-Aldrich Chemie GmbH (Steinheim, Germany). Isopropyl β -D-1-thiogalactopyranoside (IPTG) and 5-aminolevulinic acid were purchased from Carbolution chemicals (Saarbruecken, Germany). Bacterial media were purchased from Becton Dickinson (Heidelberg, Germany). All other chemicals were from standard sources and of highest purity available.

2.2. Bacterial strains and plasmids

Cloning experiments were carried out with *E. coli* Top10 (Invitrogen, San Diego, USA). The *E. coli* strain C43 (DE3) for the heterologous protein expression was purchased from Lucigen Corporation (Wisconsin, USA). Whole-cell conversions were carried out using *B. megaterium* MS941 (Wittchen and Meinhardt, 1995; Stammen et al., 2010). pET17b (Merck Bioscience, Bad Soden, Germany) and pSMF2.1 (Bleif et al., 2012) were used for expression purposes in *E. coli* and *B. megaterium*, respectively.

2.3. Cloning of CYP109E1

The coding region for CYP109E1 (GenBank GeneID 9119265) was amplified by polymerase chain reaction (PCR) using genomic DNA of *B. megaterium* MS941 as template. The coding region of CYP109E1 was cloned into the *Spel* and *Kpn*I restriction sites of pSMF2.1, yielding pSMF2.1.CYP109E1. The gene of CYP109E1 with a hexahistidine tag at the C-terminus was cloned into *Nde*I and *Kpn*I restriction sites of pET17b, yielding pET17b.CYP109E1.

2.4. Site-directed mutagenesis

The mutants of CYP109E1 were generated by the QuikChange site-directed mutagenesis method using the plasmid pSMF2.1.CYP109E1 as template and Phusion DNA polymerase (Thermo Fisher Scientific GmbH, Dreieich, Germany). The PCR primers (MWG-Biotech AG, Ebersberg, Germany) were designed

Table 1
Oligonucleotides used in PCR to generate CYP109E1 mutants.

Primer name	oligonucleotides
I85A-for	5'-ACGAGCCTAGCTAATATTGATCCGCTAAG-3'
I85A-rev	5'-CTTAGCGGATCAATTAGCTAGGCTCGT-3'
I168A-for	5'-TCGGATATTGCGGTAGCCGGTCTCTTAATAACGAACGT-3'
I168A-rev	5'-ACGTTCTGTTATTAGAAAGGACCGCTACGGCAATATCCG-3'
V169A-for	5'-GATATTATCGCAGCGGTCTCTTAATAACGAACGT-3'
V169A-rev	5'-ACGTTCTGTTATTAGAAAGGACCGCTCGGATAATATC-3'
K187A-for	5'-CTTCAGCAAGAGGCAATGAAAGCAAATGATGAGC-3'
K187A-rev	5'-GCTCATCATTTGCTTCATIGCTCTGCTGGAG-3'
I241A-for	5'-CTATTTGCTACTGGCTGCTGGAAACGAAACACCAC-3'
I241A-rev	5'-GTGGTTGTTCTGCTTCCAGCAGCCAGTAGCAAATAG-3'

to introduce point mutation at the desired positions. The oligonucleotide primers for mutagenesis are shown in Table 1. The reactions were performed in a 50 μ l volume using a gradient cycler (PTC-200 DNA Engine cycler). 20 cycles were carried out as follows: initial denaturation at 95 °C for 30 s, denaturation at 95 °C for 30 s, annealing at 58 °C for 30 s and extension at 72 °C for 4 min. Correct generation of the desired mutations was confirmed by DNA sequencing, carried out by Eurofins-MWG (Ebersberg, Germany).

2.5. Heterologous expression in *E. coli* and purification

To express CYP109E1 and its mutants, *E. coli* C43 (DE3) cells were transformed with the corresponding expression plasmids (pET17b.CYP109E1) and cultured overnight in Luria-Bertani (LB) medium containing ampicillin (100 μ g ml⁻¹) at 37 °C and 140 rpm. The seed culture was used to inoculate a 200 ml Terrific Broth (TB) medium containing ampicillin 100 μ g ml⁻¹ (1:100 dilution) in a 2-l baffled flask. The main culture was grown at 37 °C and 140 rpm. When the OD₆₀₀ reached 0.5, the expression was induced with 1 mM IPTG. 0.5 mM delta-aminolevulinic acid served as heme precursor. The cultures were shifted to 30 °C and 120 rpm for 24 h. The *E. coli* cells were harvested by centrifugation at 4500 rpm for 30 min, and the cell pellets were stored at -20 °C until purification. All purification steps were performed at 4 °C. The cell pellets were resuspended in 50 mM potassium phosphate buffer (pH 7.4) containing 300 mM NaCl and 20% glycerol. Phenylmethylsulphonyl fluoride (PMSF) was added to a final concentration of 1 mM and the suspension was sonicated with a T13-sonotrode for 15 min with an amplitude of 12% and consisted of repeated intervals of 15 s pulse and 15 s pause. Cell free extract was obtained by ultracentrifugation at 30,000 rpm for 30 min. The supernatant was applied to an immobilized metal ion affinity chromatography column (TALON, Takara Bio Europe, Saint-Germain-en-Laye, France) that had been equilibrated with 50 mM potassium phosphate buffer (pH 7.4) containing 300 mM NaCl and 20% glycerol. The column was washed with 5 column volumes of 50 mM potassium phosphate buffer (pH 7.4) containing 300 mM NaCl, 20 mM imidazole and 20% glycerol. The tagged protein was eluted with 50 mM potassium phosphate buffer (pH 7.4) containing 300 mM NaCl, 150 mM imidazole and 20% glycerol. The bovine Adx₄₋₁₀₈ and AdR were expressed and purified as described elsewhere (Sagara et al., 1993; Uhlmann et al., 1994).

2.6. Carbon monoxide (CO) difference spectroscopy

The reduced CO difference spectra of P450 were measured with a double-beam spectrophotometer (UV-2101PC, Shimadzu, Japan). The concentration of P450 was estimated using a molar extinction coefficient of $\epsilon_{450-490} = 91 \text{ mM}^{-1} \text{ cm}^{-1}$ referred to the method of Omura and Sato (1964).

2.7. In vitro conversion of VD₃

A reconstituted *in vitro* system containing CYP109E1 (1 μ M), AdR (3 μ M), Adx₄₋₁₀₈ (20 μ M), MgCl₂ (1 mM), and a cofactor regenerating system with glucose-6-phosphate (5 mM) and glucose-6-phosphate dehydrogenase (1 U) was used in a final volume of 250 μ l in potassium phosphate buffer (20 mM, pH 7.4). The substrate was dissolved in 2-hydroxypropyl- β -cyclodextrin (2.25% w/v) and added to a final concentration of 200 μ M. The reaction was started by addition of 0.5 mM NADPH. After 1 h at 30 °C the reaction was stopped and extracted twice with 2 vol of ethyl acetate. The organic phases were combined, evaporated to dryness and prepared for analysis by high-performance liquid chromatography (HPLC).

2.8. Whole-cell conversion of VD₃

The whole-cell conversions were performed in *B. megaterium* MS941. The cells were transformed with the corresponding pSMF2.1.CYP109E1 plasmid using the polyethylene glycol-mediated protoplast transformation method (Barg et al., 2005). The seed culture was prepared with LB medium (10 μ g/ml tetracycline). The main culture (50 ml TB medium, 10 μ g/ml tetracycline) was inoculated with 500 μ l of seed culture (dilution 1:100) in 300 ml baffled flasks and incubated at 37 °C, 140 rpm. The culture was grown to OD₅₇₈ of 0.4 and recombinant gene expression was induced with xylose (5 mg/ml). The culture was grown further at 30 °C for 24 h with shaking at 140 rpm.

For whole-cell conversion experiments, VD₃ was dissolved in 45% 2-hydroxypropyl- β -cyclodextrin and 4% Quillaja Saponin as membrane solubilizing agent. After 24 h of protein expression, 2.5 ml of the substrate solution were added to the 50 ml culture. A final substrate concentration of 200 μ M was used for all conversion experiments. Afterwards, the conversion was performed for the indicated time at 30 °C and 120 rpm in 300 ml baffled flasks. 500 μ l samples of the cultures were taken after defined time periods, extracted and prepared for HPLC analysis.

Large scale whole-cell conversions for purification of VD₃ metabolites were performed in 21 baffled flasks using 250 ml of main culture. Cultivation of bacteria as well as the whole-cell conversion and extraction were accomplished as mentioned above. After extraction, organic phases were dried using solvent evaporator and stored at –20 °C under protection from UV light until product purification by HPLC.

2.9. High-performance liquid chromatography (HPLC)

The HPLC was carried out on a Jasco system (Pu-980 HPLC pump, AS-950 sampler, UV-975 UV/visible detector, LG-980-02 gradient unit; Jasco, Gross-Umstadt, Germany) equipped with a Nucleodur 100-5 C18 column (125 × 4 mm; Macherey-Nagel, Düren, Germany). The column temperature was adjusted to 40 °C. The samples were dissolved in 200 μ l acetonitrile. The flow rate was 1 ml/min with a linear gradient of 60–100% aqueous acetonitrile for 15 min followed by 100% acetonitrile for 15 min. The UV detection of the substrate and products was accomplished at 265 nm. The absorption properties of the products did not differ from the substrate and, therefore, the product formation was calculated from the relative peak area (area%) of the HPLC chromatograms, dividing each respective product peak area by the sum of all peak areas.

2.10. Product purification

Purification of the products was carried out with reversed-phase HPLC using a preparative column VP 250/8 NUCLEODUR 100-5 C18ec (Macherey-Nagel, Düren, Germany). First, the dried

extract was dissolved in an acetonitrile/water mixture and filtered through the Rotilabo syringe filters (0.22 μ m, Carl Roth GmbH, Karlsruhe, Germany). For purification of product P2, a linear gradient of 80–100% acetonitrile aqueous solution as a mobile phase for 17 min was applied (UV detection: 265 nm; flow rate: 3.5–4 ml/min; column temperature: 40 °C). Products P4 and P5 were purified isocratically using a 65% acetonitrile aqueous solution as a mobile phase for 40 min (UV detection: 265 nm; flow rate: 2.5 ml/min; column temperature: 40 °C). Collected product fractions were combined, evaporated to dryness and analyzed by NMR characterization.

2.11. NMR characterization of the metabolites

The NMR spectra were recorded in CDCl₃ with a Bruker Avance 500 NMR spectrometer at 298 K. The chemical shifts were relative to CHCl₃ at δ 7.26 (¹H NMR) and CDCl₃ at δ 77.00 (¹³C NMR) using the standard δ notation in parts per million. The 1D NMR (¹H and ¹³C NMR) and the 2D NMR spectra (gs-HH-COSY and gs-HSQCED) were recorded using the BRUKER pulse program library.

2.12. Molecular docking

Vitamin D₃ (ligand) was docked into the active site of CYP109E1 (receptor) in its closed conformation (PDB: 5L94, CYP109E1-TES) with the use of Autodock Vina 1.1.2 (Trott and Olson, 2010). The testosterone molecule and all waters were removed, and the resulting model was used as a template for the docking experiments. Coordinates for the ligand were taken from an available crystal structure (PDB: 3VRM); six bonds were kept rotatable as confirmed by manual inspection in AutoDockTools 1.5.6. Hydrogens and Gasteiger charges were also added in AutoDockTools 1.5.6. The protein was kept rigid during docking. The simulation cell was limited to a grid box centered at the heme iron with sides adjusted to cover the whole distal heme pocket (x:28 Å, y:34 Å, z:48 Å). Docking simulations were done in triplicate and twenty docking poses were generated for each simulation. The binding poses were analyzed according to lowest binding energies and distances of the target carbon atom (C-25) to the heme iron. Ligand binding residues were identified by analysis done with LigPlot+ (Laskowski and Swindells, 2011) and further visualized with ViewDock tool in UCSF Chimera (Pettersen et al., 2004).

3. Results

3.1. Bioconversion of vitamin D₃ by CYP109E1

CYP109E1 from *B. megaterium* was previously cloned and characterized in our laboratory (Józwik et al., 2016). In order to identify new substrates for this enzyme, screening of a focused library consisting of different steroids was carried out. Hereby, VD₃ was identified as new substrate for CYP109E1. In an *in vitro* reconstituted system containing CYP109E1, AdR and Adx₄₋₁₀₈, about 90% of 200 μ M VD₃ was converted within 1 h into 7 products with the following distribution: 3%, 15%, 8%, 22%, 42%, 5% and 5% of product 1 to product 7 (P1-P7), respectively (Fig. 1A). Over time, it was observed that the increase in the formation of P2 is related to a corresponding decrease of P5. Therefore, we assumed that P5 is converted by CYP109E1 into P2. Through comparison of the retention time (t_R) of the detected products with that of available authentic standards, P1 (t_R = 4.8 min) and P4 (t_R = 11.6 min) were identified as 1 α -25(OH)₂VD₃ and 25(OH)VD₃, respectively (data not shown).

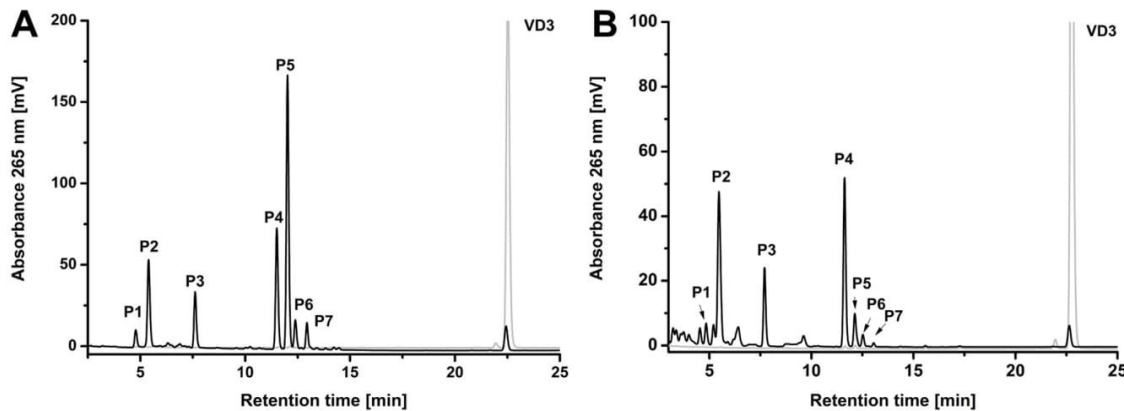


Fig. 1. HPLC chromatogram of the CYP109E1 catalyzed VD₃ conversion. (A) *in vitro* VD₃ conversion, using bovine Adx4-108 (20 μ M) and AdR (3 μ M) and CYP109E1 (1 μ M). The reaction was carried out in a final volume of 250 μ l at 30 °C for 1 h. (B) CYP109E1-dependent whole-cell conversion of VD₃ in *B. megaterium* MS941. The reaction was carried out in 50 ml TB medium for 24 h at 30 °C. Substrate was added at a final concentration of 200 μ M. The peaks of detected products and substrate are labeled with (P1–P7) and VD₃, respectively. The authentic standard of 200 μ M VD₃ (grey) was detected with the same HPLC method.

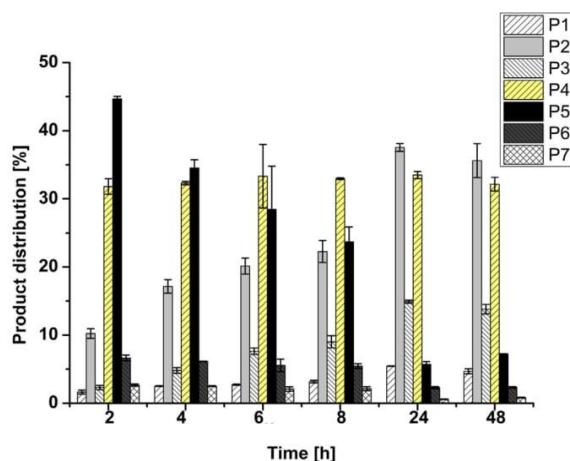


Fig. 2. Product distribution of VD₃ whole-cell conversion in *B. megaterium*. Reactions were carried out in 50 ml TB medium for 48 h at 30 °C. Samples of the cultures were taken after defined time points (2, 4, 6, 8, 24 and 48 h) and analyzed by HPLC as described in "Materials and methods". Labeling of the products (P1–P7) corresponds to that in Fig. 1. The vertical bars indicate the standard deviation values of the mean from two independent experiments.

3.2. Whole-cell conversion of VD₃ in *B. megaterium*

After successful *in vitro* conversion of VD₃, a whole-cell conversion system was established. Fig. 1B shows an HPLC profile of VD₃ whole-cell conversion in *B. megaterium* demonstrating a similar pattern as for the *in vitro* conversion. After 24 h, 95% conversion of 200 μ M substrate was achieved (Fig. 2). The product distribution after 24 h conversion was as follows: 6%, 37%, 14%, 33%, 6%, 2% and 2% for products P1–P7, respectively.

For further characterization, we analyzed the time course of product formation during whole-cell conversions, which showed that the product distribution changed over time (Fig. 2). In the first 2 h of the reaction, P5 was found to be the main product with 44% of total share ($40 \text{ mg l}^{-1} \text{ day}^{-1}$). Afterwards, P5 constituted only 5% of total share ($4.3 \text{ mg l}^{-1} \text{ day}^{-1}$). Accompanied by the decrease of P5, an increase of P2 was observed (Fig. 2). The results obtained thus indicate that P2 formation is dependent on the action of CYP109E1

on P5. Therefore, we hypothesized that CYP109E1 has the potency to hydroxylate VD₃ at different positions. To further test, this we decided to identify the main products by nuclear magnetic resonance (NMR) spectroscopy.

3.3. Large scale conversion of VD₃ and product identification

In order to obtain sufficient amounts of VD₃ metabolites for further characterization by NMR spectroscopy, whole-cell conversions with a total culture volume of 750 ml were performed. Three products were obtained with sufficient purity and amounts (5–25 mg) for structural characterization via NMR spectroscopy.

In contrast to vitamin D₃, its conversion product P4 showed resonances of an additional tertiary hydroxyl group in the ¹³C NMR spectrum (δ_{C} 71.15) and the resonances of the methyl groups C-26 and C-27 appeared both as singlets (δ_{H} 1.19 s, 6H) in the ¹H NMR spectrum. This clearly indicated hydroxylation at position C-25 and led to the structure of 25(OH)VD₃ for P4. The data were in accordance with those reported in literature (Helmer et al., 1985; Mzhiritskii et al., 1996):

¹H NMR (CDCl₃, 500 MHz): δ 0.52 (s, 3xH-18), 0.92 (d, J =6.5 Hz, 3xH-21), 1.02 (m, H-22a), 1.06 (m, H-22b), 1.19 (s, 6H, 3xH-26 and 3xH-27), 1.20 (m, H-23a), 1.24 (m, H-16a), 1.28 (m, H-17), 1.29 (m, H-12a), 1.36 (m, H-24a), 1.39 (m, H-23b), 1.45 (m, 2H, H-11a and H-24b), 1.51 (m, H-20), 1.52 (m, 2H, H-11b and H-15a), 1.60 (m, H-2a), 1.63 (m, H-15b), 1.69 (m, H-9a), 1.86 (m, H-16b), 1.94 (m, H-14), 1.96 (m, H-2b), 1.98 (m, H-12b), 2.16 (dd, J =13.5, 8.5 and 5.0 Hz, H-1a), 2.26 (dd, J =13.0 and 7.5 Hz, H-4a), 2.38 (ddd, J =13.5, 7.5 and 4.6 Hz, H-1b), 2.55 (dd, J =13.0 and 4.0 Hz, H-4b), 2.82 (m, H-9b), 3.92 (m, H-3), 4.80 (d, J =2.5 Hz, H-19a), 5.03 (m, H-19b), 6.01 (d, 11.3 Hz, H-7), 6.21 (d, 11.3 Hz, H-6). ¹³C NMR (CDCl₃, 125 MHz): δ 11.99 (CH₃, C-18), 18.81 (CH₃, C-21), 20.82 (CH₂, C-23), 22.24 (CH₂, C-11), 23.56 (CH₂, C-15), 27.67 (CH₂, C-16), 29.07 (CH₂, C-9), 29.29 (CH₃, C-26), 29.34 (CH₃, C-27), 31.92 (CH₂, C-1), 35.16 (CH₂, C-2), 36.10 (CH₂, C-22), 36.40 (CH, C-20), 40.53 (CH₂, C-12), 44.39 (CH₂, C-24), 45.85 (C, C-13), 45.92 (CH₂, C-4), 56.33 (CH, C-14), 56.53 (CH, C-17), 69.21 (CH, C-3), 71.15 (C, C-25), 112.40 (CH₂, C-19), 117.51 (CH, C-7), 122.45 (CH, C-6), 135.00 (C, C-5), 142.89 (C, C-8), 145.09 (C, C-10).

The NMR spectra of P5 revealed an additional secondary hydroxyl group (δ_{H} 3.34 m, δ_{C} 77.41 CH). Its position at C-24 was obvious by vicinal correlations of its proton to the isopropyl proton H-25 (δ_{H} 1.69 m) in the HHCOSY and to the methyls C-26 (16.69,

CH_3) and C-27 18.93, CH_3) in the HMBC. Comparison of the data with those of an authentic sample (Xi et al., 2014) supported these findings. Especially the chemical shifts of C-1 to C-19 fitted perfectly to each other, whereas the resonances for the side chain slightly differed. This might originate from a different stereochemistry at C-24 in our sample and its epimer from literature. Unfortunately the authors gave no hint to the stereochemistry at C-24 and our sample decomposed within one day in solution. Therefore, the assignment of the absolute configuration at C-24 could not be solved by subsequent NMR measurements, such as Mosher's method. But as was found for closely related 24-hydroxylated steroids the 24(R)- and 24(S)-isomers showed characteristic differences in the ^{13}C NMR (Koizumi et al., 1979). Applying these observations to our problem led to the identification of the 24(S)-form for our molecule and to the 24(R)-form for the epimer reported by Xi et al. (2014):

NMR (CDCl_3 , 500 MHz): δ 0.57 (s, 3xH-18), 0.92 (d, $J=6.9\text{ Hz}$, 3xH-26), 0.95 (d, $J=6.9\text{ Hz}$, 3xH-27), 0.97 (d, $J=6.5\text{ Hz}$, 3xH-21), 1.08 (m, H-22a), 1.28 (m, H-23a), 1.33 (m, H-16a and H-17), 1.34 (m, H-12a), 1.43 (m, H-20), 1.51 (m, H-11a), 1.56 (m, H-15a), 1.58 (m, H-23b), 1.59 (m, H-11b), 1.64 (m, H-22b), 1.68 (m, H-2a), 1.69 (m, H-25), 1.70 (m, H-15b), 1.72 (m, H-9a), 1.93 (m, H-16b), 1.96 (m, H-2b), 2.01 (m, H-14), 2.03 (m, H-12b), 2.20 (dd, $J=13.5, 8.5$ and 5.0 Hz , H-1a), 2.30 (dd, $J=13.0$ and 7.5 Hz , H-4a), 2.42 (ddd, $J=13.5, 7.8$ and 4.6 Hz , H-1b), 2.60 (dd, $J=13.0$ and 4.0 Hz , H-4b), 2.86 (m, H-9b), 3.34 (m, H-24), 3.97 (m, H-3), 4.86 (d, $J=2.5\text{ Hz}$, H-19a), 5.07 (dt, $J=2.5$ and 1.3 Hz , H-19b), 6.06 (d, 11.3 Hz, H-7), 6.26 (d, 11.3 Hz, H-6). ^{13}C NMR (CDCl_3 , 125 MHz): δ 12.00 (CH₃, C-18), 16.69 (CH₃, C-26), 18.93 (CH₃, C-27), 19.05 (CH₃, C-21), 22.23 (CH₂, C-11), 23.55 (CH₂, C-15), 27.62 (CH₂, C-16), 28.99 (CH₂, C-9), 30.74 (CH₂, C-23), 31.91 (CH₂, C-1), 32.16 (CH₂, C-22), 33.15 (CH, C-25), 35.14 (CH₂, C-2), 36.29 (CH, C-20), 40.50 (CH₂, C-12), 45.84 (C, C-13), 45.90 (CH₂, C-4), 56.30 (CH, C-14), 56.37 (CH, C-17), 69.20 (CH, C-3), 77.41 (CH, C-24), 112.44 (CH₂, C-19), 117.51 (CH, C-7), 122.43 (CH, C-6), 135.07 (C, C-5), 142.21 (C, C-8), 145.05 (C, C-10).

P2 was found to be a dihydroxylated conversion product of vitamin D₃. The NMR spectra revealed resonances for a supplementary secondary (δ_{C} 79.55 CH) and a tertiary (δ_{C} 73.15C) hydroxyl function. 2D NMR HHCOSY, HSQCED and HMBC measurements revealed their positions as immediate neighbours at C-24 and C-25. According to P5, C-24 in P2 was expected to be in (S)-configuration. However, we wanted to prove this assumption in an independent manner. Both epimers were known from literature but no comparative NMR studies were available. Therefore, we performed a comparison of the NMR data of their synthetic precursors, the 24(R)- and 24(S)-forms of de-A,B-cholesta-8,24,25-triol (Pérez Sestelo et al., 2002). Analysis of the ^{13}C NMR data for the side chain of P2 and comparison with those of the C-24 epimeric de-A,B-cholestanes gave a clear and unambiguous evidence for 24S,25(OH)₂VD₃ as structure for P2:

NMR (CDCl_3 , 500 MHz): δ 0.55 (s, 3xH-18), 0.95 (d, $J=6.5\text{ Hz}$, 3xH-21), 1.04 (m, H-22a), 1.14 (m, H-23a), 1.17 (s, 3xH-26), 1.22 (s, 3xH-27), 1.28 (m, H-17), 1.29 (m, H-16a), 1.31 (m, H-12a), 1.41 (m, H-20), 1.49 (m, 2H, H-11a and H-11b), 1.54 (m, H-15a), 1.57 (m, H-23b), 1.68 (m, H-2a and H-15b), 1.69 (m, H-9a), 1.77 (m, H-22b), 1.89 (m, H-16b), 1.94 (m, H-2b), 1.98 (m, H-14), 2.00 (m, H-12b), 2.21 (m, H-1a), 2.30 (dd, $J=13.0$ and 7.5 Hz , H-4a), 2.41 (ddd, $J=13.5, 7.8$ and 4.6 Hz , H-1b), 2.58 (dd, $J=13.0$ and 4.0 Hz , H-4b), 2.83 (m, H-9b), 3.29 (d, $J=10.1$ and 2.0 Hz , H-24), 3.94 (m, H-3), 5.05 (dt, $J=2.5$ and 1.3 Hz , H-19b), 4.82 (d, $J=2.5\text{ Hz}$, H-19a), 6.03 (d, 11.3 Hz, H-7), 6.23 (d, 11.3 Hz, H-6). ^{13}C NMR (CDCl_3 , 125 MHz): δ 12.00 (CH₃, C-18), 18.94 (CH₃, C-21), 22.23 (CH₂, C-11), 23.17 (CH₃, C-26), 23.54 (CH₂, C-15), 26.51 (CH₃, C-27), 27.61 (CH₂, C-16), 28.34 (CH₂, C-23), 28.99 (CH₂, C-9), 31.95 (CH₂, C-1), 33.22 (CH₂, C-22), 35.19 (CH₂, C-2), 36.26 (CH, C-20), 40.51 (CH₂, C-12), 45.83 (C, C-13), 45.94 (CH₂, C-4), 56.28 (CH, C-14), 56.39 (CH, C-17), 69.20 (CH, C-3), 73.17 (C, C-

25), 79.55 (CH, C-24), 112.42 (CH₂, C-19), 117.56 (CH, C-7), 122.33 (CH, C-6), 135.21 (C, C-5), 142.08 (C, C-8), 145.09 (C, C-10).

These results confirmed our assumption, that CYP109E1 can hydroxylate VD₃ at different positions. As shown above, the ratio of P2 (24S,25(OH)₂VD₃) increased inversely proportional to the ratio of P5 (24S(OH)VD₃) over time, indicating that CYP109E1 has 25-hydroxylation activity towards VD₃ as well as 24S(OH)VD₃. The reaction pathway of VD₃ conversion by CYP109E1 is shown in Fig. 3.

3.4. Molecular docking of VD₃ to CYP109E1

Unfortunately soaking/co-crystallization trials to obtain the structure of the CYP109E1-VD₃ complex proved unsuccessful, therefore docking of the VD₃ molecule was performed to identify potential substrate-binding residues. A structural comparison of CYP109E1 to other P450s converting VD₃ found in the PDB, revealed that the closed conformer of CYP109E1 (PDB: 5L94) is highly similar to the closed state observed for CYP107 (Vdh) crystallized in complex with VD₃ (PDB: 3A50, Yasutake et al., 2010, r.m.s.d. of 1.23 Å for 347 Cα atoms). Therefore, the closed conformation of CYP109E1 likely reflects the functionally relevant conformational state of the protein and was chosen in this study for the substrate docking calculations. Among the calculated VD₃ conformations, the one showing a suitable distance of the C-25 atom to the heme iron and the lowest predicted free energy of binding was chosen for further analysis. The docked pose places the aliphatic side chain of VD₃ close to the heme iron, productively for 25-hydroxylation (C-25-Fe distance of 3.7 Å), and is well in agreement with the crystallographically observed VD₃ binding mode in CYP107 (Vdh) (C-25-Fe distance of 4.6 Å). The only hydrophilic group (3β-OH group at the A-ring) of VD₃ is solvent exposed, predicted not to interact with any of the protein side chains; the rest of the VD₃ molecule interacts with hydrophobic residues lining the active site pocket, similarly as in Vdh. Since VD₃ hydroxylation is of outstanding importance for sustainable biotransformation process of the production of active VD₃, we were interested to improve the yield of 25(OH)VD₃. Four amino acids predicted to interact with VD₃ were mutated to alanine to determine their roles in CYP109E1 activity and selectivity towards VD₃: I85 (BC-loop, substrate recognition site 1, SRS1), I168 and V69 (F-helix, SRS2) and I241 (I-helix, SRS4). Additionally, one more residue was chosen for mutagenesis, K187 (SRS3), since its mutation to alanine in CYP109E1 was previously shown to cause a slight decrease in testosterone conversion activity. Thus we considered the possibility that this flexible residue, located at the top of the active site (G helix), might also take part in VD₃ binding (Fig. 4).

3.5. Conversion of VD₃ by CYP109E1 mutants

To investigate the effect of selected mutations on activity and regio-selectivity of CYP109E1 towards VD₃ directly in the whole-cell system, *B. megaterium* cells were transformed with the plasmid pSMF2.1.CYP109E1 containing the corresponding CYP109E1 mutations. The results clearly showed that all CYP109E1 mutants still maintained VD₃ hydroxylation activity. However, activity or/and selectivity of CYP109E1 was affected by the amino acid replacements (Fig. 5).

While the K187A mutant showed the same conversion ratio (97%) as compared with wild type, the activity of CYP109E1 was changed by selected mutations (Fig. 6). All other mutants showed decreased activity in the first 8 h of the reaction. However, the activity in case of I85A, I168A, V169A and I241A mutants was increased afterwards. After 24 h conversion, the I168A mutant exhibited a comparable conversion (96%) as the wild type and the I85A mutant showed a maximum conversion of 87%. On the other hand, a significant decrease of the activity was observed in case of V169A and

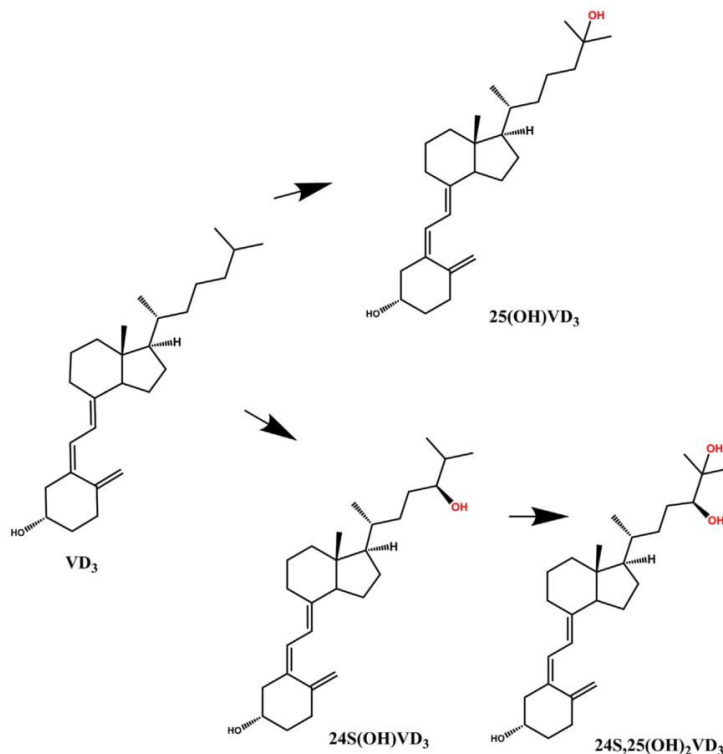


Fig. 3. Reaction pathway of VD₃ by CYP109E1 from *B. megaterium*.

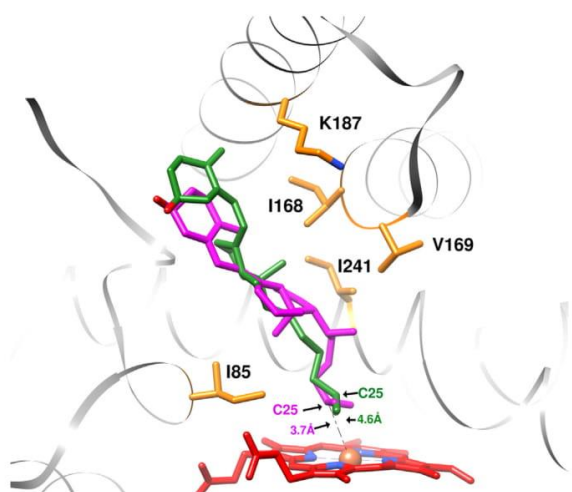


Fig. 4. Docking model of VD₃ in the active site of CYP109E1. The suitable conformation of VD₃ for 25-hydroxylation is shown (in magenta), and compared to the crystallographically observed VD₃ binding mode in CYP107 (Vdh) (in green). Heme is in red coloured sticks. Amino acids selected for site-directed mutagenesis are shown in orange sticks. (For interpretation of the references to color in this figure legend, the reader is referred to the web version of this article.)

I241A mutants, displaying only 76% and 54% conversion, respectively.

Additionally, the effect of the point mutations on the regioselectivity of CYP109E1-dependent VD₃ conversion was studied (Table 2). Compared to wild type, the formation of 24S(OH)VD₃

was decreased over time in case of the I85A and I168A mutants, which, as a consequence, led to reduced amounts of the derived product 24S,25(OH)₂VD₃. On the other hand, the 25-hydroxylation activity towards VD₃ was strongly preferred in the reactions catalyzed by the I85A and I168A mutants resulting in 63% and 49% of total products, respectively (Table 2). Moreover, mutant I85A displayed a significant reduction in the number of products. Consequently, an increase of the absolute 25(OH)VD₃ production was observed with these mutants, compared to the wild type (Fig. 7). These results indicate that the side chains of amino acids I85 and I168 are essential for determining the regio-selectivity of CYP109E1 towards VD₃. Compared to wild type, the regio-selectivity of the K187A mutant was also slightly changed towards 25-hydroxylation (Table 2). Furthermore, it was observed that the 24S,25(OH)₂VD₃ production decreased in the whole-cell conversion with the K187A mutant, compared to wild type. In contrast to the decrease in the 24S,25(OH)₂VD₃ production, an accumulation of 24S(OH)VD₃ was observed, suggesting that the K187A mutant has less specificity towards 24S(OH)VD₃, compared to wild type.

Furthermore, significant changes of the specificity and regioselectivity of CYP109E1 were determined in whole-cell conversions with the V169A and I241A mutants. Compared to the wild type, it was observed that reactions of variant V169A showed a decreased 25-hydroxylation activity of 24S(OH)VD₃, whereas the 25-hydroxylation of VD₃ was enhanced (Table 2). In addition, no formation of P1, P3 and P7 was observed with this mutant. In whole-cell conversions with the V169A mutant, the product distribution was as follows: 24S(OH)VD₃ (40%), 25(OH)VD₃ (47%), 24S,25(OH)₂VD₃ (3%) and P6 (10%). It was further observed that the substitution of I241 to alanine shifts the regio-selectivity of CYP109E1 towards 24-hydroxylation (60% of total products). In

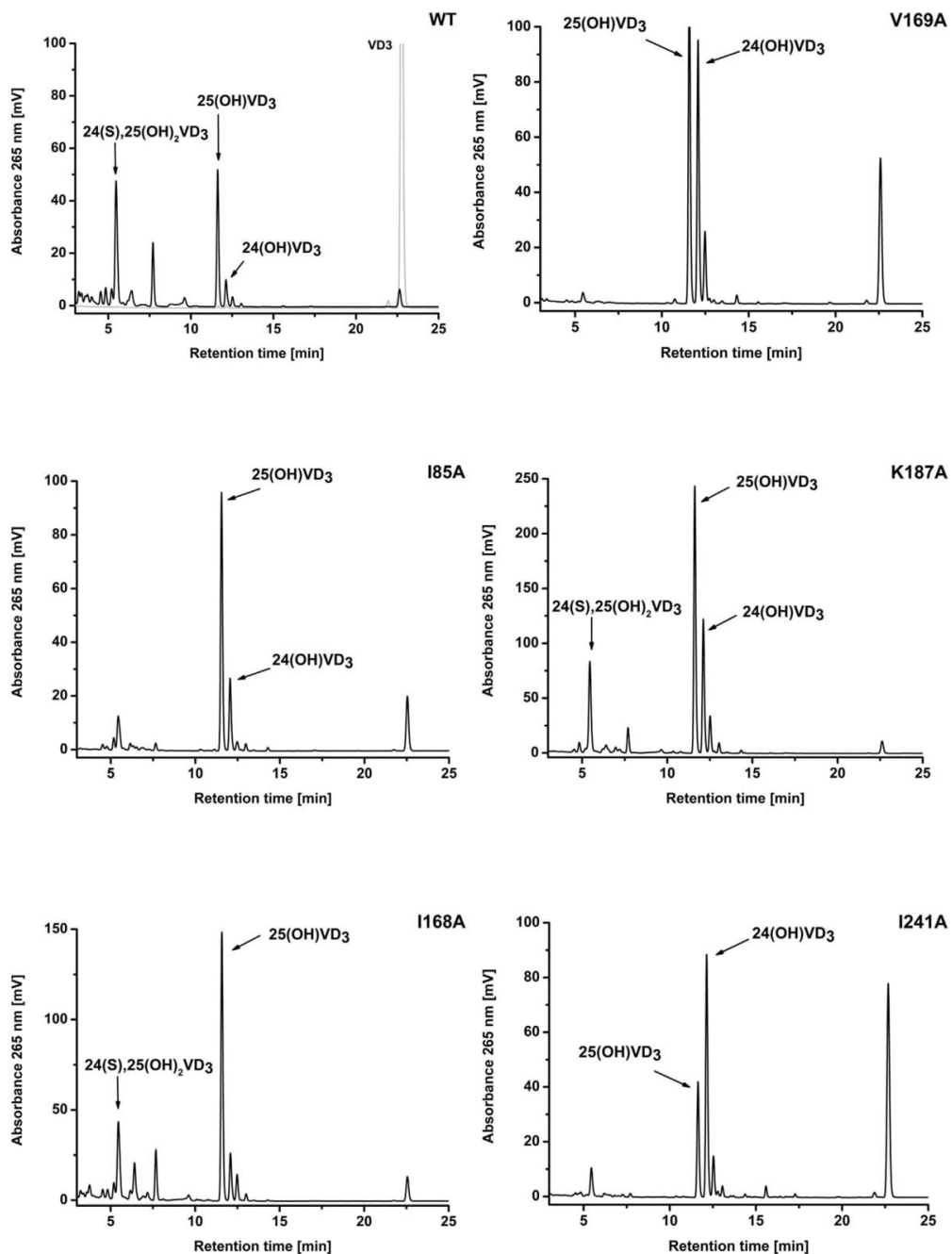


Fig. 5. HPLC chromatograms of VD₃ whole-cell conversions by *B. megaterium* expressing different variants of CYP109E1. The reactions were carried out in 50 ml TB medium for 24 h at 30 °C. The substrate was added at a final concentration of 200 μM. The authentic standard of 200 μM VD₃ (grey) was detected with the same HPLC method.

contrast, a decrease of 24S,25(OH)₂VD₃ was observed (only 3% of total products) indicating that the 25-hydroxylation activity of this mutant of CYP109E1 towards 24S(OH)VD₃ is dramatically decreased.

4. Discussion

During the past years bioconversion processes, including specific hydroxylations, have gained increasing interest, since chemical synthesis often requires complex procedures and environmentally unfriendly conditions. The ability of P450s to

Table 2Comparison of products distribution of 24 h whole-cell conversions of VD_3 by different variants of CYP109E1.

Enzyme variant	Conversion [%]	Number of products	Major product(s) [%] ^a
Wild type	95	7	24S,25(OH) ₂ VD ₃ (37%) 25(OH)VD ₃ (33%)
I85A	87.3	3	25(OH)VD ₃ (63%)
I168A	94	7	24S,25(OH) ₂ VD ₃ (20%) 25(OH)VD ₃ (49%)
V169A	75.4	3	25(OH)VD ₃ (47%) 24S(OH)VD ₃ (42%)
K187A	96.8	7	25(OH)VD ₃ (45%) 24S(OH)VD ₃ (22%)
I241A	53.8	4	25(OH)VD ₃ (27%) 24S(OH)VD ₃ (58%)

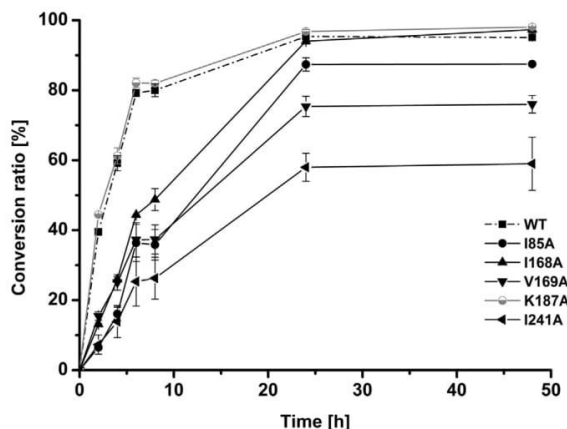
^a Only products with a ratio of $\geq 20\%$ of total products are defined here as major products.

Fig. 6. Effect of selected mutations in CYP109E1 on the conversion of VD_3 . Reactions were performed using *B. megaterium* MS941 in 50 ml TB medium at 30 °C. The substrate was added at a final concentration of 200 μM . Samples of the cultures were taken after defined time points (2, 4, 6, 8, 24 and 48 h) and analyzed by HPLC as described in "Materials and methods". The vertical bars indicate the standard deviation values of the mean from three independent whole-cell experiments.

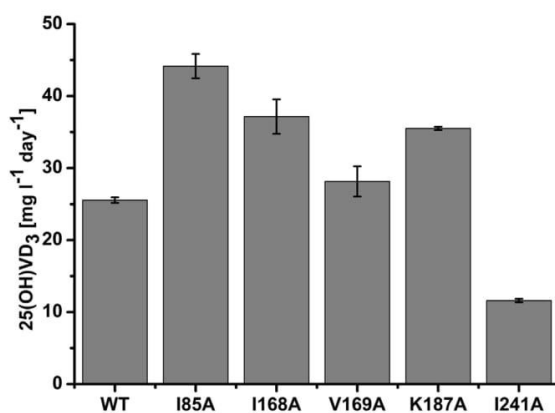


Fig. 7. Production of 25(OH)VD₃ in *B. megaterium* overexpressing different variants of CYP109E1. Reactions were performed in 50 ml TB medium for 24 h at 30 °C. The substrate was added at a final concentration of 200 μM . The amount of 25(OH)VD₃ was measured by HPLC as described in "Materials and methods". The vertical bars indicate the standard deviation values of the mean from three independent whole-cell experiments.

hydroxylate a broad range of compounds makes them suitable as versatile biocatalysts (Bernhardt, 2006; Bernhardt and Urlacher, 2014).

It is known that VD_3 is activated in kidneys and liver by different P450s such as mitochondrial cytochromes CYP27A1 and CYP27B1 as well as the microsomal enzymes CYP2R1, CYP3A4 and CYP2J3. However, low activity and stability of mammalian P450s compared with those of bacterial origin are important factors limiting their industrial applications (Julsing et al., 2008). As a result of such limitation, bacterial P450s constitute an attractive alternative for the industrial production of different valuable products, including VD_3 metabolites. Until now, only a few studies have reported the usage of bacterial P450s for the production of VD_3 metabolites such as CYP105A1 and CYP107 (Vdh) (Sakaki et al., 2011). Therefore, the identification of new bacterial P450s with hydroxylation activity towards VD_3 is of a great interest for the industry. In particular, *B. megaterium* offers a great potential, both as a source and expression host, for such new bacterial P450s. It has been used since many decades for the production of different industrial enzymes (Vary et al., 2007; Korneli et al., 2013). It offers an advantage that replicative plasmids are stable and maintained (Stammen et al., 2010). In addition, *B. megaterium* lacks external alkaline proteases and, therefore, is suitable for heterologous protein expression. Moreover, *B. megaterium* can grow on simple media utilizing a broad spectrum of carbon sources (Vary, 1994).

Therefore, the establishment of *B. megaterium*-based whole cell system using a bacterial P450 as biocatalyst for the production of active VD_3 metabolites, such as 25(OH)VD₃, is an interesting alternative for the industrial production. Recently, *B. megaterium* was used in our laboratory for the conversion of the steroid hormone precursor cholesterol to pregnenolone and for the hydroxylation of 11-keto- β -boswellic acid (KBA) (Gerber et al., 2015; Bleif et al., 2012; Brill et al., 2014). Moreover, a CYP27A1-based whole-cell system was established in *B. megaterium* allowing efficient production of valuable pharmaceuticals such as 27-hydroxycholesterol, 26/27-hydroxy-7-dehydrocholesterol, 25(OH)VD₃ and 25-hydroxy-7-dehydrocholesterol (Ehrhardt et al., 2016).

In this study, we demonstrated for the first time the conversion of VD_3 by a member of the CYP109 family, namely CYP109E1 from *B. megaterium* DSM319. We showed that CYP109E1 can convert VD_3 into different products, in both enzyme-based and whole-cell-based assays. The new whole-cell system converts more than 90% of the added substrate (200 μM) within 24 h supporting its promising potential as VD_3 hydroxylase. The two main products of CYP109E1-dependent conversion of VD_3 were identified by NMR analysis as 25(OH)VD₃ (33%) and 24S, 25(OH)₂VD₃ (37%) with yields of 24.5 $\text{mg l}^{-1} \text{ day}^{-1}$ and 28.6 $\text{mg l}^{-1} \text{ day}^{-1}$, respectively. In addition, the product P5 was identified by NMR analysis as 24S(OH)VD₃. For further characterization of product formation, time-dependent whole-cell conversions were performed. It was

shown that both, 24S(OH)VD₃ (P5) and 25(OH)VD₃ (P4), are initially detected as major products (Fig. 3). Nevertheless, a decrease in the 24S(OH)VD₃ ratio was observed in correlation with the formation of 24S,25(OH)₂VD₃ (P2). In contrast, the ratio of 25(OH)VD₃ was relatively constant over time (30–33% of total products). Thus we conclude that the formation of 24S,25(OH)₂VD₃ from VD₃ proceeds via the intermediate 24S(OH)VD₃. This is to the best of our knowledge a novel reaction pathway of VD₃ leading to 24S,25(OH)₂VD₃ via 24S(OH)VD₃. In addition, these results demonstrate that CYP109E1 has a 25-hydroxylation activity towards VD₃ as well as 24S(OH)VD₃.

It is known that the hydroxylation of VD₃ at C-25 is the first step of the VD₃ activation (Prosser and Jones, 2004; Sakaki et al., 2005; Schuster, 2011). 25(OH)VD₃ is the best indicator of the nutritional status of VD₃ in the circulation (Hollis, 2005). This compound has been gaining importance in recent years as it was shown to be a better therapeutic agent for several diseases than VD₃ itself, due to its direct biological effect and better intestinal absorption (Jean et al., 2008; Leichtmann et al., 1991). It was found that supplementation of 25(OH)VD₃ has a preventive, therapeutic effect against diseases such as hyperglycemia, chronic kidney disease, Crohn's and cholestatic liver disease (Jean et al., 2008; Leichtmann et al., 1991). In addition to applications of this metabolite for human health, it is used as supplement in animal feed (Soares et al., 1995). Whereas specific biological activities for the natural VD₃ metabolite 24R,25(OH)₂VD₃ were identified (Norman et al., 1983; St-Arnaud and Glorieux, 1998; Yamato et al., 1989), so far no functions are known for its unnatural epimer 24S,25(OH)₂VD₃, which was identified here in the CYP109E1-based whole cell conversion of VD₃.

Our aim in the next step of this study was the enhancement of the 25(OH)VD₃ production yield by CYP109E1. Since the crystal structure of a VD₃-bound CYP109E1 complex is not available, the putative substrate-binding residues were predicted with docking simulations. It is anticipated that VD₃ binds with its aliphatic side chain close to the heme iron and the C-25 atom is in a suitable distance for hydroxylation (Fig. 4). High similarity of the CYP109E1-VD₃ model with the experimental CYP107 (Vdh)-VD₃ crystal structure gives credence to the reliability of our docking results. A similar set of hydrophobic residues is predicted to interact with VD₃ in CYP109E1, including I85, I241, I168 and V169, which correspond to I88, I235, L171, and V172 in Vdh (Yasutake et al., 2010). To test their potential role in VD₃ binding and conversion in CYP109E1, these four residues were targeted for mutation to alanines. In addition, residue K187 was chosen for mutagenesis, to test whether this flexible residue may play a role in substrate binding by interacting with the 3β-OH group of VD₃. Previously, it was shown that mutation of this residue to an alanine slightly lowers the conversion rate of testosterone by CYP109E1 (Józwik et al., 2016). However, our results show that considering VD₃ hydroxylation, the mutation of K187 to alanine does not influence CYP109E1 activity (Fig. 6). Thus, residue K187 plays no role in VD₃ binding by CYP109E1, in accordance with the docking results and with the lack of substrate binding interactions by the equivalent residue (K180) in the VD₃-bound crystal structure of Vdh.

Mutagenesis of the other four residues (I85, I168, V169 and I241) ultimately yielded an improved regio-selectivity of CYP109E1 towards VD₃. It has been found that all mutants, except I241A, exhibited a higher selectivity towards 25-hydroxylation than the wild type (Table 2). This enhancement of the regio-selectivity resulted in an increase of the 25(OH)VD₃ production upon whole-cell conversion of VD₃ (Fig. 7). Compared to the wild type, approximately a 2-fold increase of the 25(OH)VD₃ yield was achieved with the I85A mutant, 45 mg l⁻¹ day⁻¹ compared to 24.5 mg l⁻¹ day⁻¹. In the literature, the conversion yield of 25(OH)VD₃ by the most widely investigated P450 for vitamin D₃ hydroxylation, CYP105A1, had been initially very low and was

later significantly improved by protein engineering (Sasaki et al., 1991). The most productive mutant of CYP105A1 (R73A/R84A) is reported to produce 8.3 mg l⁻¹ day⁻¹ of 25(OH)VD₃ (Hayashi et al., 2010; Sakaki et al., 2011). Residue I85 of CYP109E1, as mentioned above, is located in SRS1, in the close vicinity of the heme, and is one of the most investigated residues in P450s. The corresponding position in different P450s was described to interact with the P450s ligands and, therefore, to affect the activity and selectivity of the enzyme (Gricman et al., 2015). The importance of this position was observed in case of CYP102A1 as the substitutions of F87 caused improved selectivity towards propylbenzene and terpene substrates, among others (Gricman et al., 2015; Li et al., 2001; Seifert et al., 2009). In addition, the substitution of S122 to threonine in CYP1A1 (corresponding position to I85 in CYP109E1 and F87 in CYP102A1) improved the 7-methoxy- and 7-ethoxyresorufin O-dealkylase activity (Li et al., 2004).

Furthermore, our results showed that the substitution of V169 or I241 to alanine residues significantly diminished the conversion of the 24S(OH)VD₃ intermediate into 24S,25(OH)₂VD₃, as compared to reactions with the wild type enzyme. The functional importance of V169 and I241 was also previously determined for testosterone conversion by CYP109E1 (Józwik et al., 2016). It was shown that by substituting either residue to an alanine the activity of CYP109E1 towards testosterone is completely abolished. Therefore, we suggest that V169 and I241 of CYP109E1 are substrate specificity-determining residues.

5. Conclusions

This study describes the identification of a new VD₃ hydroxylase from *B. megaterium*, CYP109E1, with 25- and 24-hydroxylation activity. The established *B. megaterium*-based whole-cell system for the conversion of VD₃ has a promising potential for the biotechnological production of the valuable metabolite 25(OH)VD₃.

In addition, further investigations on CYP109E1 were performed in order to increase the production of 25(OH)VD₃. Based on docking studies, site-directed mutagenesis was performed at selected positions in the active site of the enzyme. We were able to demonstrate the importance of selected active site residues for VD₃ conversion. A change of the regio-selectivity and substrate specificity was observed for most of the mutants. A considerable increase of the production of the valuable metabolite 25(OH)VD₃ was achieved with the I85A mutant. In addition, two novel metabolites of VD₃, 24S(OH)VD₃ and 24S,25(OH)₂VD₃, have been identified, whose potential for further drug development needs to be investigated.

Competing interests

The authors declare that they have no competing interest.

Author contributions

AA designed and carried out the experiments, analyzed and interpreted the results and drafted the manuscript. JZ performed the docking simulations and assisted in drafting the manuscript. NP and EB purified the products for NMR analysis. EB carried out the substrate screening. JZ performed the NMR measurements and structure determination of vitamin D₃ metabolites. AT analyzed and interpreted the results, and assisted in drafting the manuscript. FH and RB designed the project, analyzed and interpreted the results, and assisted in drafting the manuscript. All authors read and approved the final manuscript.

Acknowledgments

This work was kindly supported by the German Federation of Industrial Research Associations (AiF/ZIM project FKZ 2214512AJA). The authors would like to thank Birgit Heider-Lips for the purification of AdR and Adx₄₋₁₀₈. Thanks to Mohammed Milhim for proof reading.

References

- Barg, H., Malten, M., Jahn, M., Jahn, D., 2005. Protein and vitamin production in *Bacillus megaterium*. In: Barredo, J.-L. (Ed.), *Microbial Processes and Products, Methods in Biotechnology*. Humana Press, pp. 205–223.
- Bernhardt, R., Urlacher, V.B., 2014. Cytochromes P450 as promising catalysts for biotechnological application: chances and limitations. *Appl. Microbiol. Biotechnol.* 98, 6185–6203.
- Bernhardt, R., 2006. Cytochromes P450 as versatile biocatalysts. *J. Biotechnol.* 124, 128–145.
- Blief, S., Hannemann, F., Zapp, J., Hartmann, D., Jauch, J., Bernhardt, R., 2012. A new *Bacillus megaterium* whole-cell catalyst for the hydroxylation of the pentacyclic triterpene 11-keto-β-boswellic acid (KBA) based on a recombinant cytochrome P450 system. *Appl. Microbiol. Biotechnol.* 93, 1135–1146.
- Brill, E., Hannemann, F., Zapp, J., Brünig, G., Jauch, J., Bernhardt, R., 2014. A new cytochrome P450 system from *Bacillus megaterium* DSM319 for the hydroxylation of 11-keto-β-boswellic acid (KBA). *Appl. Microbiol. Biotechnol.* 98, 1701–1717.
- Cheng, C.Y.S., Slominski, A.T., Tuckey, R.C., 2014. Metabolism of 20-hydroxyvitamin D3 by mouse liver microsomes. *J. Steroid Biochem. Mol. Biol.* 144 (Part B), 286–293.
- Demay, M.B., 2006. Mechanism of vitamin D receptor action. *Ann. N. Y. Acad. Sci.* 1068, 204–213.
- Di Rosa, M., Malaguarnera, M., Nicoletti, F., Malaguarnera, L., 2011. Vitamin D3: a helpful immuno-modulator. *Immunology* 134, 123–139.
- Ehrhardt, M., Gerber, A., Hannemann, F., Bernhardt, R., 2016. Expression of human CYP27A1 in *B. megaterium* for the efficient hydroxylation of cholesterol, vitamin D3 and 7-dehydrocholesterol. *J. Biotechnol.* 218, 34–40.
- Fujii, Y., Kubamoto, H., Nishimura, K., Fujii, T., Yanai, S., Takeda, K., Tamura, N., Arisawa, A., Tamura, T., 2009. Purification, characterization, and directed evolution study of a vitamin D3 hydroxylase from *Pseudonocardia autotrophica*. *Biochem. Biophys. Res. Commun.* 385, 170–175.
- Gerber, A., Kleser, M., Biedendieck, R., Bernhardt, R., Hannemann, F., 2015. Functionalized PHB granules provide the basis for the efficient side-chain cleavage of cholesterol and analogs in recombinant *Bacillus megaterium*. *Microb. Cell Factories* 14.
- Gricman, L., Vogel, C., Pleiss, J., 2015. Identification of universal selectivity-determining positions in cytochrome P450 monooxygenases by systematic sequence-based literature mining. *Proteins Struct. Funct. Bioinf.* 83, 1593–1603.
- Gupta, R.P., Hollis, B.W., Patel, S.B., Patrick, K.S., Bell, N.H., 2004. CYP3A4 is a human microsomal vitamin D 25-hydroxylase. *J. Bone Miner. Res.* 19, 680–688.
- Hayashi, K., Yasuda, K., Sugimoto, H., Ikuhiro, S., Kamakura, M., Kittaka, A., Horst, R.L., Chen, T.C., Ohta, M., Shiro, Y., Sakaki, T., 2010. Three-step hydroxylation of vitamin D3 by a genetically engineered CYP105A1. *FEBS J.* 277, 3999–4009.
- Helmer, B., Schnoes, H.K., DeLuca, H.F., 1985. 1H nuclear magnetic resonance studies of the conformations of vitamin D compounds in various solvents. *Arch. Biochem. Biophys.* 241, 608–615.
- Holick, M.F., Richtand, N.M., McNeill, S.C., Holick, S.A., Frommer, J.E., Henley, J.W., Potts, J.T., 1979. Isolation and identification of previtamin D3 from the skin of rats exposed to ultraviolet irradiation. *Biochemistry (Mosc.)* 18, 1003–1008.
- Hollis, B.W., 2005. Circulating 25-hydroxyvitamin D levels indicative of vitamin D sufficiency: implications for establishing a new effective dietary intake recommendation for vitamin D. *J. Nutr.* 135, 317–322.
- Józwiak, I.K., Kiss, F.M., Gricman, L., Abdumughni, A., Brill, E., Zapp, J., Pleiss, J., Bernhardt, R., Thunissen, A.-M.W.H., 2016. Structural basis of steroid binding and oxidation by the cytochrome P450 CYP109E1 from *Bacillus megaterium*. *FEBS J.* 283, 4128–4148.
- Jean, G., Terrat, J.-C., Vanel, T., Hurot, J.-M., Lorriau, C., Mayor, B., Chazot, C., 2008. Daily oral 25-hydroxycholecalciferol supplementation for vitamin D deficiency in haemodialysis patients: effects on mineral metabolism and bone markers. *Nephrol. Dial. Transplant.* 23, 3670–3676.
- Julsing, M.K., Cornelissen, S., Bühl, B., Schmid, A., 2008. Heme-iron oxygenases: powerful industrial biocatalysts? *Curr. Opin. Chem. Biol.* 12, 177–186.
- Jurutka, P.W., Bartik, L., Whitfield, G.K., Mather, D.R., Barthel, T.K., Gurevich, M., Hsieh, J.-C., Kaczmarśka, M., Haussler, C.A., Haussler, M.R., 2007. Vitamin D receptor: key roles in bone mineral pathophysiology, molecular mechanism of action, and novel nutritional ligands. *J. Bone Miner. Res. Off. J. Am. Soc. Bone Miner. Res.* 22 (Suppl. 2), V2–10.
- Kametani, T., Furuyama, H., 1987. Synthesis of vitamin D3 and related compounds. *Med. Res. Rev.* 7, 147–171.
- Koizumi, N., Fujimoto, Y., Takeshita, T., Ikekawa, N., 1979. Carbon-13 nuclear magnetic resonance of 24-substituted steroids. *Chem. Pharm. Bull. (Tokyo)* 27, 38–42.
- Korneli, C., David, F., Biedendieck, R., Jahn, D., Wittmann, C., 2013. Getting the big beast to work—systems biotechnology of *Bacillus megaterium* for novel high-value proteins. *J. Biotechnol.* 163, 87–96.
- Laskowski, R.A., Swindells, M.B., 2011. LigPlot+: multiple ligand–protein interaction diagrams for drug discovery. *J. Chem. Inf. Model.* 51, 2778–2786.
- Leichtmann, G.A., Bengoa, J.M., Bolt, M.J., Sitrin, M.D., 1991. Intestinal absorption of cholecalciferol and 25-hydroxycholecalciferol in patients with both Crohn's disease and intestinal resection. *Am. J. Clin. Nutr.* 54, 548–552.
- Li, Q.S., Ogawa, J., Schmid, R.D., Shimizu, S., 2001. Residue size at position 87 of cytochrome P450 BM-3 determines its stereoselectivity in propylbenzene and 3-chlorostyrene oxidation. *FEBS Lett.* 508, 249–252.
- Li, J., Erickson, S.S., Sivaneri, M., Besspiata, D., Fisher, C.W., Szklarz, G.D., 2004. The effect of reciprocal active site mutations in human cytochromes P450 1A1 and 1A2 on alkoxyresorufin metabolism. *Arch. Biochem. Biophys.* 424, 33–43.
- Mizhiritskii, M.D., Konstantinovskii, L.E., Vishkautsan, R., 1996. 2D NMR study of solution conformations and complete 1H and 13C chemical shifts assignments of vitamin D metabolites and analogs. *Tetrahedron* 52, 1239–1252.
- Nelson, D.R., 2011. Progress in tracing the evolutionary paths of cytochrome P450. *Biochim. Biophys. Acta* 1814, 14–18. Protein Proteomics, Cytochrome P450: Structure, biodiversity and potential for application.
- Norman, A.W., Leathers, V., Bishop, J.E., 1983. Normal egg hatchability requires the simultaneous administration to the hen of 1 alpha, 25-dihydroxycholecalciferol and 24R,25-dihydroxycholecalciferol. *J. Nutr.* 113, 2505–2515.
- Omura, T., Sato, R., 1964. The carbon monoxide-binding pigment of liver microsomes. *J. Biol. Chem.* 239, 2370–2378.
- Pérez Sestelo, J., Cornella, I., de Uña, O., Mouríño, A., Sarandeses, L.A., 2002. Stereoselective convergent synthesis of 24,25-dihydroxyvitamin D3 metabolites: a practical approach. *Chem. Weinheim Bergstr. Ger.* 8, 2747–2752.
- Pettersen, E.F., Goddard, T.D., Huang, C.C., Couch, G.S., Greenblatt, D.M., Meng, E.C., Ferrin, T.E., 2004. UCSF Chimera—a visualization system for exploratory research and analysis. *J. Comput. Chem.* 25, 1605–1612.
- Prosser, D.E., Jones, G., 2004. Enzymes involved in the activation and inactivation of vitamin D. *Trends Biochem. Sci.* 29, 664–673.
- Sagara, Y., Wada, A., Takata, Y., Waterman, M.R., Sekimizu, K., Horiuchi, T., 1993. Direct expression of adrenodoxin reductase in *Escherichia coli* and the functional characterization. *Biol. Pharm. Bull.* 16, 627–630.
- Sakaki, T., Kagawa, N., Yamamoto, K., Inouye, K., 2005. Metabolism of vitamin D3 by cytochromes P450. *Front. Biosci. J. Virtual Lib.* 10, 119–134.
- Sakaki, T., Sugimoto, H., Hayashi, K., Yasuda, K., Munetsuna, E., Kamakura, M., Ikuhiro, S., Shiro, Y., 2011. Bioconversion of vitamin D to its active form by bacterial or mammalian cytochrome P450. *Biochim. Biophys. Acta BBA – Proteins Proteome.* 1814, 249–256.
- Sasaki, J., Mikami, A., Mizoue, K., Omura, S., 1991. Transformation of 25- and 1 alpha-hydroxyvitamin D3 to 1 alpha, 25-dihydroxyvitamin D3 by using *Streptomyces* sp. strains. *Appl. Environ. Microbiol.* 57, 2841–2846.
- Schuster, I., 2011. Cytochromes P450 are essential players in the vitamin D signaling system. *Biochim. Biophys. Acta* 1814, 186–199.
- Seifert, A., Vomund, S., Grohmann, K., Kriening, S., Urlacher, V.B., Laschat, S., Pleiss, J., 2009. Rational design of a minimal and highly enriched CYP102A1 mutant library with improved regio-, stereo- and chemoselectivity. *Chembiochem.* Eur. J. Chem. Biol. 10, 853–861.
- Soares, J.H., Kerr, J.M., Gray, R.W., 1995. 25-hydroxycholecalciferol in poultry nutrition. *Poult. Sci.* 74, 1919–1934.
- St-Arnaud, R., Glorieux, F.H., 1998. Editorial: 24, 25-dihydroxyvitamin D—active metabolite or inactive catabolite? *Endocrinology* 139, 3371–3374.
- Stammen, S., Müller, B.K., Korneli, C., Biedendieck, R., Gamer, M., Franco-Lara, E., Jahn, D., 2010. High-yield intra- and extracellular protein production using *Bacillus megaterium*. *Appl. Environ. Microbiol.* 76, 4037–4046.
- Trott, O., Olson, A.J., 2010. AutoDock Vina: improving the speed and accuracy of docking with a new scoring function, efficient optimization, and multithreading. *J. Comput. Chem.* 31, 455–461.
- Uhlmann, H., Kraft, R., Bernhardt, R., 1994. C-terminal region of adrenodoxin affects its structural integrity and determines differences in its electron transfer function to cytochrome P-450. *J. Biol. Chem.* 269, 22557–22564.
- Urlacher, V.B., Girhard, M., 2012. Cytochrome P450 monooxygenases: an update on perspectives for synthetic application. *Trends Biotechnol.* 30, 26–36.
- Vary, P.S., Biedendieck, R., Fuerch, T., Meinhardt, F., Rohde, M., Deckwer, W.-D., Jahn, D., 2007. *Bacillus megaterium*—from simple soil bacterium to industrial protein production host. *Appl. Microbiol. Biotechnol.* 76, 957–967.
- Vary, P.S., 1994. Prime time for *Bacillus megaterium*. *Microbiol. Read. Engl.* 140 (Pt. 5), 1001–1013.
- Wittchen, K.D., Meinhardt, F., 1995. Inactivation of the major extracellular protease from *Bacillus megaterium* DSM319 by gene replacement. *Appl. Microbiol. Biotechnol.* 42, 871–877.
- Xi, Z., Zhai, L., Xie, H., Zeng, Z., 2014. Preparation and identification of the related impurities from biotransformed calciferol. *Jingxi-Huangong* 31, 979–982.
- Yamato, H., Matsumoto, T., Fukumoto, S., Ikeda, K., Ishizuka, S., Ogata, E., 1989. Effect of 24,25-dihydroxyvitamin D3 on 1,25-dihydroxyvitamin D3 [1,25-(OH)2D3] metabolism in vitamin D-deficient rats infused with 1,25-(OH)2D3. *Endocrinology* 124, 511–517.
- Yasutake, Y., Fujii, Y., Nishioka, T., Cheon, W.-K., Arisawa, A., Tamura, T., 2010. Structural evidence for enhancement of sequential vitamin D3 hydroxylation activities by directed evolution of cytochrome P450 vitamin D3 hydroxylase. *J. Biol. Chem.* 285, 31193–31201.

2.3 Putkaradze et al. 2017b

CYP109E1 is a novel versatile statin and terpene oxidase from *Bacillus megaterium*

Natalia Putkaradze, Martin Litzenburger, Ammar Abdulmughni, Mohammed Milhim, Elisa Brill, Frank Hannemann, Rita Bernhardt

2017, **Applied Microbiology and Biotechnology.** **101**(23-24):8379-8393

DOI: [10.1007/s00253-017-8552-6](https://doi.org/10.1007/s00253-017-8552-6)

Reprinted with the permission of Springer Science and Business Media.



BIOTECHNOLOGICALLY RELEVANT ENZYMES AND PROTEINS

CYP109E1 is a novel versatile statin and terpene oxidase from *Bacillus megaterium*

Natalia Putkaradze¹ · Martin Litzenburger¹ · Ammar Abdulkumughni¹ ·
 Mohammed Milhim¹ · Elisa Brill¹ · Frank Hannemann¹ · Rita Bernhardt¹

Received: 31 May 2017 / Revised: 22 August 2017 / Accepted: 26 September 2017 / Published online: 11 October 2017
 © Springer-Verlag GmbH Germany 2017

Abstract CYP109E1 is a cytochrome P450 monooxygenase from *Bacillus megaterium* with a hydroxylation activity for testosterone and vitamin D3. This study reports the screening of a focused library of statins, terpene-derived and steroidal compounds to explore the substrate spectrum of this enzyme. Catalytic activity of CYP109E1 towards the statin drug-precursor compactin and the prodrugs lovastatin and simvastatin as well as biotechnologically relevant terpene compounds including ionones, nootkatone, isolongifolen-9-one, damascones, and β -damascenone was found in vitro. The novel substrates induced a type I spin-shift upon binding to P450 and thus permitted to determine dissociation constants. For the identification of conversion products by NMR spectroscopy, a *B. megaterium* whole-cell system was applied. NMR analysis revealed for the first time the ability of CYP109E1 to catalyze an industrially highly important reaction, the production of pravastatin from compactin, as well as regioselective oxidations generating drug metabolites (6' β -hydroxy-lovastatin, 3' α -hydroxy-simvastatin, and 4"-hydroxy-simvastatin) and valuable terpene derivatives (3-hydroxy- α -ionone, 4-hydroxy- β -ionone, 11,12-epoxy-nootkatone, 4(R)-hydroxy-isolongifolen-9-one, 3-hydroxy- α -damascone, 4-hydroxy- β -damascone, and 3,4-epoxy- β -damascone). Besides that, a novel compound, 2-hydroxy- β -damascenone, produced by CYP109E1 was identified. Docking calculations using the crystal structure of

CYP109E1 rationalized the experimentally observed regioselective hydroxylation and identified important amino acid residues for statin and terpene binding.

Keywords *Bacillus megaterium* · CYP109E1 · Biotransformation · Pravastatin · Statins · Terpenes

Introduction

Bacillus megaterium is a gram-positive soil bacterium with industrial importance. The ability of growth on different low-priced media, the absence of alkaline proteases and endotoxins, the stable maintenance of plasmid vectors, and high protein expression capacity make this microorganism an excellent biotechnological production host (Rygus and Hillen 1992; Vary et al. 2007). It is used for the production of industrially important enzymes as well as polyhydroxybutyrate and vitamin B12 (Biedendieck et al. 2010; Korneli et al. 2013; Kulpreet et al. 2009; Malten et al. 2005; Stammen et al. 2010). Besides that, the full genome sequencing of two *B. megaterium* strains (Eppinger et al. 2011) gave rise to the identification of several biotechnologically interesting proteins from this bacterium such as cytochromes P450 (P450s) (Abdulkumughni et al. 2017; Brill et al. 2014; Józwik et al. 2016; Kiss et al. 2015; Milhim et al. 2016).

P450s are heme-containing external monooxygenases. Besides their essential role in steroid hormone biosynthesis and drug metabolism, several more applications of this enzyme class such as bioremediation and implementation of a great variety of chemical reactions are also described (Sono et al. 1996). The broad spectrum of substrates and the ability to perform diverse synthetically challenging reactions under mild conditions provide a high biotechnological potential of these enzymes (Bernhardt 2006; Bernhardt and Urlacher

Electronic supplementary material The online version of this article (<https://doi.org/10.1007/s00253-017-8552-6>) contains supplementary material, which is available to authorized users.

✉ Rita Bernhardt
 ritabern@mx.uni-saarland.de

¹ Institute of Biochemistry, Saarland University,
 66123 Saarbruecken, Germany

2014). P450 family members are widely distributed among different species of life. In contrast to mammalian and plant P450s, microbial ones have the advantages that they are soluble proteins and exhibit higher stability simplifying their handling (Fulco 1991; Urlacher et al. 2004). Three P450s from *B. megaterium*, the self-sufficient fatty acid hydroxylase CYP102A1 (BM3) and two steroid hydroxylases of the CYP106 family, CYP106A1 and CYP106A2, have been extensively studied and described as attractive biocatalysts for potential biotechnological applications (Berg and Rafter 1981; Bleif et al. 2011; Brill et al. 2014; Janocha et al. 2016; Kiss et al. 2015; Putkaradze et al. 2017; Narhi and Fulco 1987; Schmitz et al. 2014; Urlacher et al. 2006; Virus et al. 2006).

CYP109E1 is a new member of *Bacillus* P450s, recently identified by our laboratory, but is not fully characterized so far. The crystal structure of CYP109E1 in substrate-free and substrate-bound state has provided first insights into the structural background of substrate binding and activity of this enzyme (Józwik et al. 2016). Due to the close phylogenetic distance of CYP109E1 to the steroid hydroxylase CYP106A1, its potential as steroidogenic P450 has been investigated. It has been found that CYP109E1 possesses very low or no catalytic activity towards steroid substrates except for testosterone and vitamin D3 (Abdulmughni et al. 2017; Józwik et al. 2016). To extend the substrate range of CYP109E1, a focused library was screened. The library consisted of steroids, statins, and terpenoids reported to be substrates of some *Bacillus* P450s of the 109 family (Furuya et al. 2009; Girhard et al. 2010) (Scheme 1).

Statins are a class of powerful, widely used drugs against cardiovascular diseases. They effectively reduce plasma LDL-cholesterol levels and coronary heart disease risk by inhibiting the key enzyme 3-hydroxy-3-methylglutaryl-coenzyme-A (HMG-CoA) reductase in the mevalonate pathway (Brown 2007; Endo and Hasumi 1993; Lamon-Fava 2013). The first discovered statin, the natural product compactin (mevastatin) undergoes a stereoselective hydroxylation at the position C6' resulting in the formation of pravastatin (6'β-hydroxycompactin). Pravastatin as well as the naturally occurring statin lovastatin and its semi-synthetic derivative simvastatin are efficient drugs. The bioconversion of compactin to pravastatin is one of the successful biotechnological applications of P450-based systems with only few examples of P450s described in the literature capable of performing this reaction (Bernhardt and Urlacher 2014; Matsuoka et al. 1989; McLean et al. 2015; Milhim et al. 2016; Sakaki 2012).

Terpenes and terpenoids are the most diverse class of chemicals occurring mainly in plants. These compounds and their derivatives are important for biotechnology since they are applied in different fields, such as chemical, pharmaceutical, or flavor and fragrance industry (Janocha et al. 2015). The regio- and stereoselective oxyfunctionalization of

terpenes and terpenoids is of high interest but remains to be a challenging task for synthetic chemistry. Microbial P450 enzymes represent an effective alternative to chemical synthesis since they possess the ability to oxidize diverse biotechnologically important terpene and terpenoid compounds in a highly stereo- and regioselective manner. However, only a limited number of microbial P450s have been identified as terpene hydroxylases and epoxidases until now (Janocha et al. 2015). The well-studied and effective bacterial terpene hydroxylating-P450s include CYP101A1, CYP108A1, and CYP111A1 from *Pseudomonas* species having camphor, terpineol, and linalool as their natural substrates, respectively (Katagiri et al. 1968; Peterson et al. 1992; Ullah et al. 1990), as well as enzymes from *Novosphingobium aromaticivorans* such as CYP101B1 (Bell and Wong 2007; Hall and Bell 2014). Two P450s from *B. megaterium* (CYP106 family) have been shown to hydroxylate di- and triterpenes (Bleif et al. 2011; Brill et al. 2014; Schmitz et al. 2014).

Here, we report highly regioselective oxidations of three statins (compactin **1**, lovastatin **2**, and simvastatin **3**) as well as seven terpenes, including α-ionone **4**, β-ionone **5**, nootkatone **6**, isolongifolen-9-one **7**, α-damascone **8**, β-damascone **9**, and β-damascenone **10** by CYP109E1. Reconstituted P450 and *B. megaterium* whole-cell systems were successfully applied for the biotransformation of these substrates. Characterization of the reaction products indicated hydroxylase and epoxidase activity of CYP109E1, producing an important drug, pravastatin, as well as known and novel statin drug metabolites and terpene derivatives.

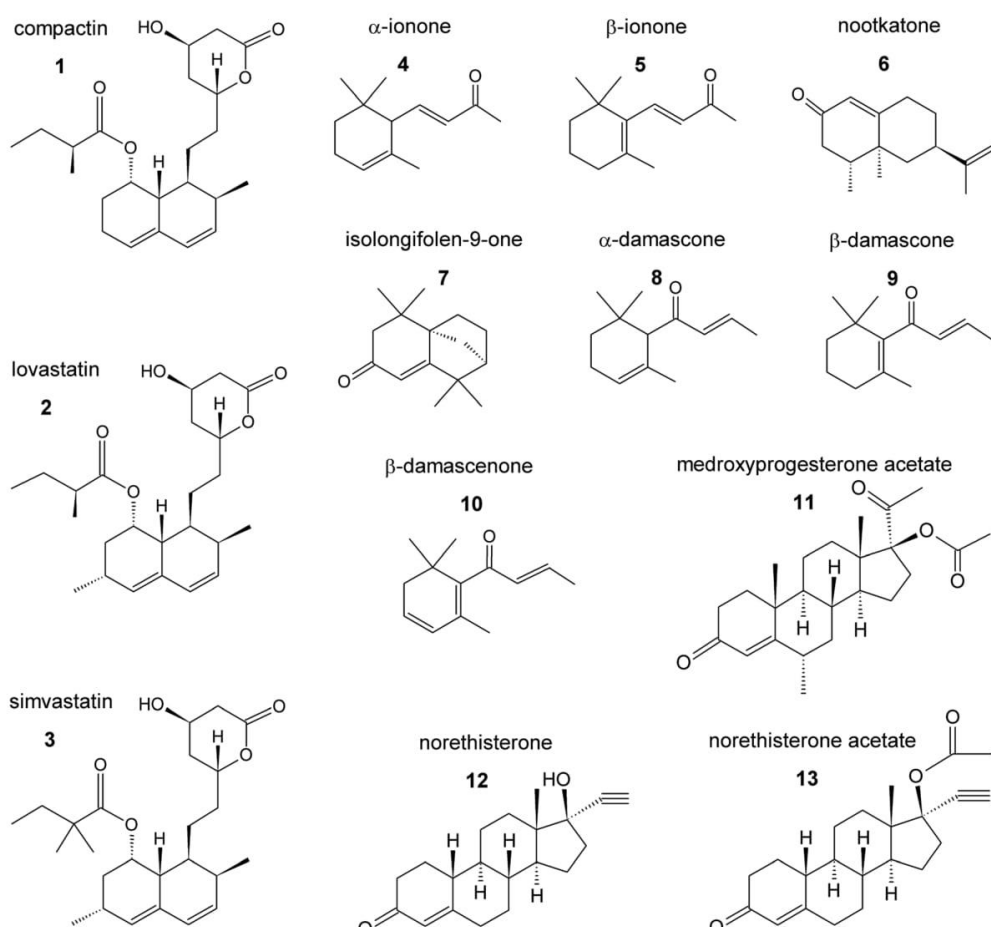
Materials and methods

Reagents and chemicals

Compactin, lovastatin, simvastatin, medroxyprogesterone acetate, norethisterone, and norethisterone acetate were purchased from TCI chemicals (Eschborn, Germany). (+)-Nootkatone, (−)-isolongifolen-9-one, and α- and β-ionone were purchased from Sigma-Aldrich (St. Louis, MI, USA). α-Damascone, β-damascone, and β-damascenone were provided from Bell Flavors & Fragrances (Leipzig, Germany). Bacterial culture media were purchased from Becton, Dickinson and Company (Franklin Lakes, NJ, USA). All other chemicals and solvents were obtained from standard sources and were of the highest purity available.

Strains and plasmids

The *E. coli* C43 (DE3) cells (Lucigen, Middleton, WI, USA) transformed with the plasmid pET17b.CYP109E1 (Abdulmughni et al. 2017) were used for the expression of CYP109E1. *B. megaterium* MS941 cells (Wittchen and



Scheme 1 Chemical structures of compounds investigated with CYP109E1

Meinhardt 1995) transformed either with the plasmid pSMF2.1.CYP109E1 (Abdulmughni et al. 2017) or the control plasmid pSMF2.1 (Bleif et al. 2011) were used for whole-cell conversions.

Enzyme purification and spectral measurements

E. coli cells were cultured overnight in Luria-Bertani (LB) medium containing 100 µg/mL ampicillin at 37 °C and 150 rpm in a rotary shaker. Five milliliters of overnight culture was used to inoculate 500 mL Terrific Broth (TB) medium containing 100 µg/mL ampicillin in a 2-L baffled shake flask, and the culture was incubated at 37 °C and 100 rpm. At OD₆₀₀ of 0.5, the expression of CYP109E1 was induced with 1 mM of isopropyl-thio-β-D-galactopyranoside (IPTG). Simultaneously, 0.5 mM of δ-aminolevulinic acid (δ-ALA) was added to support the heme synthesis. After a 24-h expression, the cells were harvested by centrifugation at 4500×g and stored at –20 °C until purification of the enzyme. The purification of CYP109E1

was carried out using immobilized metal ion affinity chromatography (TALON™ Resin, Clontech) as described elsewhere (Abdulmughni et al. 2017). Fractions containing CYP109E1 were collected, concentrated, and further purified using size exclusion chromatography (Superdex 75 column, GE Healthcare Life Sciences) in 50 mM potassium phosphate buffer (pH 7.4) with a flow rate of 0.1 mL/min. The purified protein fractions were collected, concentrated by ultrafiltration, and stored at –20 °C. The concentration of purified CYP109E1 was estimated by carbon monoxide difference spectroscopy using an extinction coefficient (450–490 nm) of 91 mM⁻¹ cm⁻¹ according to the method of Omura and Sato (1964).

Bovine adrenodoxin reductase (AdR) and a truncated form of bovine adrenodoxin (Adx_{4–108}) were expressed and purified as described elsewhere (Sagara et al. 1993; Uhlmann et al. 1992). Protein concentrations were measured spectroscopically using corresponding molar extinction coefficients as described elsewhere (Lisurek et al. 2004).

Spin-state shift and estimation of dissociation constant (K_d)

Spin-state shifts were investigated using a double beam spectrophotometer (UV-2101PC, Shimadzu, Japan) and two tandem quartz cuvettes. One chamber of each cuvette contained 10 μM CYP109E1 in 50 mM potassium phosphate buffer (pH 7.4), while the other chamber was filled with buffer alone. The substrates were dissolved in DMSO (5 mM stock solutions) and were added into the chamber with CYP109E1 solution of the sample cuvette while an equal amount of each substrate was also added into the buffer containing a chamber of the reference cuvette. Difference spectra were recorded between 350 and 500 nm. Dissociation constant (K_d) was estimated by titrating each substrate (0–200 μM) until saturation. The data were analyzed by plotting the peak-to-trough differences against the substrate concentrations and fitting them (except for lovastatin and simvastatin) with the hyperbolic function $\Delta A = \Delta A_{\max} \times [S] / (K_d + [S])$. Lovastatin and simvastatin exhibited tight binding ($K_d < 5[\text{E}]$), and for these compounds, the data were fitted to the tight binding quadratic equation: $\Delta A = (\Delta A_{\max}/2[\text{E}]) \times \{(K_d + [\text{E}] + [S]) - \{(K_d + [\text{E}] + [S])^2 - 4[\text{E}][S]\}^{1/2}\}$ (Williams and Morrison 1979). ΔA represents the peak-to-trough absorbance difference, $[\text{E}]$ is the enzyme concentration, and $[S]$ is the substrate concentration. The data processing was done with OriginPro 9.0G software (OriginLab, MA, USA). All K_d values represent the mean of three independent measurements with the coefficient of determination (R^2) of 0.99. Spin-state shifts were calculated (to approximately $\pm 5\%$) using the ΔA_{\max} value of each substrate as a percentage of the maximum expected shift for 10 μM enzyme estimated as described by Luthra et al. (2011).

Measurement of CYP109E1 activity in vitro

The catalytic activity of CYP109E1 towards the selected compounds was investigated using a reconstituted in vitro system consisting of 0.5 or 1 μM CYP109E1, bovine AdR, and Adx_{4–108} with a molar ratio of 1:2:20. The reactions were carried out in 250 μL of 50 mM potassium phosphate buffer (pH 7.4) with 10% glycerol. For the sufficient electron supply, a NADPH regeneration system containing glucose-6-phosphate-dehydrogenase (1 U), glucose-6-phosphate (5 mM), and MgCl₂ (1 mM) was used. The in vitro reactions with 100 μM statin **1–3** (20 mM stock solution in DMSO), 200 μM steroid **11–13** (20 mM stock solution in DMSO), and terpene **4–10** (50 mM stock solution in ethanol) compounds were started by addition of 1 mM NADPH in 1.5-mL Eppendorf tubes under mixing at 30 °C and 700 rpm and stopped after 15 min by addition of 250 μL of ethyl acetate or chloroform. The reaction mixtures were extracted twice with 500 μL of the organic solvent. The organic phases

were combined, evaporated to dryness, and stored at –20 °C until analysis via either high-performance liquid chromatography (HPLC) or gas chromatography-mass spectrometry (GC-MS).

Whole-cell conversion with CYP109E1 in *B. megaterium* MS941

The whole-cell conversions were performed in plasmidless *B. megaterium* MS941 strain transformed with pSMF2.1.CYP109E1 shuttle vector by the method of Barg et al. (2005). As a control of the CYP109E1-based whole-cell biotransformation, MS941 cells transformed with the empty vector pSMF2.1 were used. The main cultures were prepared by inoculating 50 mL of complex medium (24 g/L yeast extract, 12 g/L soytone, 0.5% glycerol (v/v), 2.31 g/L KH₂PO₄ and 12.5 g/L K₂HPO₄) with overnight culture (1% of the main culture volume) in 300 mL baffled shake flask and incubated at 37 °C and 160 rpm in a rotary shaker until an OD₅₇₈ of 0.5 was reached. At this time point, the expression of CYP109E1 was induced by adding 5 g/L xylose. After 24 h expression at 30 °C, the cultures were harvested by centrifugation (4500×g, 4 °C), washed, and resuspended in 50 mM potassium phosphate buffer (pH 7.4) with 2% glycerol. Whole-cell conversions of 100 μM of statins **1–3** and 200 μM of terpenes **4–10** were carried out in 25 mL volume in a rotary shaker at 30 °C and 150 rpm. The conversions of nootkatone **6**, isolongifolen-9-one **7**, α -ionone **4**, β -ionone **5**, α -damascone **8**, β -damascone **9**, and β -damascenone **10** were performed in sealed baffled shake flasks. Substrate stock solutions were prepared by dissolving them in DMSO or ethanol. The biotransformation of each substrate was monitored within 2 h by taking 500- μL culture samples. The samples were extracted with double volume of ethyl acetate, dried, and stored at –20 °C until HPLC analysis. To obtain sufficient amounts (2–10 mg) of conversion products for the structure elucidation via NMR, the whole-cell reactions were scaled up to 0.5–1 L culture volume. The reactions were stopped after 2 or 4 h and extracted with double volume of ethyl acetate. The organic phases were dried over anhydrous MgSO₄, concentrated to dryness using a rotivapor (Büchi R-114), and stored at –20 °C until purification via HPLC.

Conversion analysis and product isolation via HPLC

The conversion analysis was performed via reversed phase HPLC technique using a Jasco system (a Pu-980 HPLC pump, an AS-950 sampler, an UV-975 UV/Vis detector, a LG-980–02 gradient unit; Jasco, Gross-Umstadt, Germany) and an ec MN Nucleodur C18 (5 μm , 4.0 × 125 mm) column (Macherey-Nagel, Bethlehem, PA, USA). For the purification of conversion products, a preparative ec MN Nucleodur C18

VP (5 μm , 8.0 \times 250 mm) column (Macherey-Nagel, Bethlehem, PA, USA) was used. The mobile phase consisted of 10% acetonitrile in water (solvent A) and pure acetonitrile (solvent B). A gradient from 20 to 80% of solvent B was used for the separation of α -ionone **4**, β -ionone **5**, α -damascone **8**, β -damascone **9**, β -damascenone **10**, compactin **1**, and lovastatin **2** conversions, from 20 to 100% for the analysis of nootkatone **6** and isolongifolen-9-one **7** conversions and from 0 to 100% for simvastatin **3**, medroxyprogesterone acetate **11**, norethisterone **12**, and norethisterone acetate **13** conversions. A flow rate of either 1 mL/min (conversion measurements) or 3.5 mL/min (product isolation) and a temperature of 40 °C were set during the analysis of all compounds. The UV detection was accomplished at 236 (statins **1–3**), 240 (steroids **11–13**, nootkatone **6**, and isolongifolen-9-one **7**), 228 (α -ionone **4**, α -damascone **8**, and β -damascone **9**), 232 (β -damascenone **10**), or 296 nm (β -ionone **5**).

Conversion analysis via GC-MS and LC-MS

GC-MS measurements were performed with a system consisting of an AI/AS 3000 autosampler, a DSQ II quadrupole, a Focus GC column oven (Thermo Scientific, Waltham, USA), and a DB-5 column (Agilent) with a length of 25 m, 0.32 mm ID, and 0.52 μm film thickness. The conversions were analyzed as described elsewhere (Litzenburger and Bernhardt 2016).

Analytical HPLC-MS was performed on a Thermo Dionex UltiMate 3000 HPLC using NUCLEOSHELL RP 18plus (100 \times 4.6 mm, 2.7 μm) column (Macherey-Nagel, Bethlehem, PA, USA) coupled to a Bruker AmaZon SL ESI-MS system (Bruker, Billerica, MA, USA). The mobile phase consisted of water with 0.1% formic acid (solvent A) and pure acetonitrile with 0.1% formic acid (solvent B). A gradient from 5 to 95% of solvent B was used for the separation. Mass spectra were acquired in positive mode ranging from 100 to 600 m/z using UltraScan mode.

Structure elucidation by NMR spectroscopy

NMR spectra were recorded on a Bruker (Rheinstetten, Germany) DRX 500 NMR spectrometer. A combination of ^1H , ^{13}C , $^1\text{H}^1\text{H}$ -COSY, HSQC, and HMBC experiments was used for structure elucidation. All chemical shifts are relative to CHCl_3 (δ = 7.24) or CDCl_3 (δ = 77.00) using the standard δ notion in parts per million (ppm).

Molecular docking

For the docking experiments, the recently solved crystal structure of CYP109E1 was used (Józwik et al. 2016). Two structurally different substrates, the statin compactin **1** and the norisoprenoid compound α -ionone **4**, were docked into the

active site of CYP109E1 in its closed conformation (PDB: 5L94) using AutoDock 4.0 (Morris et al. 2009). The Windows version 1.5.6 of AutoDock Tools was used to compute Kollman charges for the enzyme and Gasteiger-Marsili charges for the ligands (Sanner 1999). A partial charge of +0.400e was assigned manually to the heme iron, which corresponds to Fe(II) that was compensated by adjusting the partial charges of the ligating nitrogen atoms to -0.348e. While the protein was kept as rigid, the flexible bonds of the ligands were assigned automatically and verified by manual inspection. A cubic grid box with a size of 52 Å \times 50 Å \times 48 Å was fixed above the heme moiety to cover the whole active site of the enzyme. The spacing between grid points was 0.375 Å. Two hundred docking runs (for each substrate) were carried out applying the Lamarckian genetic algorithm using default parameter settings. The binding conformations were analyzed according to estimated binding energies and distances of the target carbon atom to the heme iron.

Results

Substrate binding to CYP109E1

To screen CYP109E1 for potential new substrates, a library of 13 compounds was used. The library contained the steroids norethisterone **12** and medroxyprogesterone acetate **11**, compactin **1**, and the terpenes α -ionone **4**, β -ionone **5**, and nootkatone **6**, which previously have been identified as substrates of the CYP109 family (Furuya et al. 2009; Girhard et al. 2010), as well as related compounds with biotechnological or pharmaceutical impact (Scheme 1). First, the potential substrates were investigated for their ability to bind to CYP109E1. This was done by monitoring the high-spin shift induction using difference spectroscopy. When a P450 substrate displaces the axial water ligand, it changes the spin-state of the iron atom from low-spin to high-spin (Schenkman and Jansson 1998). Spectroscopically, this transition is reflected by a shift in the absorption maximum from around 420 to 390 nm (type I difference spectrum). Previously, it has been reported that the spin-shift is not necessary for the catalytic activity of a P450 (Girhard et al. 2010; Simgen et al. 2000). On the other hand, a very large type I spin-shift observed for many bacterial P450s (Bell and Wong 2007) indicating the ability of its substrates to displace almost all water molecules in the active site results in an effective electron transfer and high catalytic activities by substrate-gating mechanism (Sligar and Gunsalus 1976; Fisher and Sligar 1985; Honeychurch et al. 1999; Poulos and Raag 1992). Therefore, this spectroscopic method remains to be well suitable for screening of potential P450 substrates as well as inhibitors (Khatri et al. 2016; Schmitz et al. 2012). All here tested compounds, except for steroids **11–13**, were able to induce a type I spin-shift of

CYP109E1, which allowed us to investigate the substrate binding spectroscopically (Fig. 1 and S1) and to determine dissociation constants (K_d). Statin compounds **1–3** showed tighter binding to P450 than terpene substrates **4–10** (Table 1). Our results indicate that simvastatin **3** binds tighter to CYP109E1 than the other statins. The K_d of simvastatin **3** [$K_d = 4.7 \mu\text{M}$] was shown to be approximately 18 times lower than that of compactin **1** [$K_d = 84 \mu\text{M}$] and two times lower than that of lovastatin **2** [$K_d = 9.6 \mu\text{M}$] (Fig. 1 and S1). The strongest binding to CYP109E1 among terpenes **4–10** was observed for β -ionone **5** [$K_d = 91 \mu\text{M}$] and the weakest for isolongifolen-9-one **7** [$K_d = 216 \mu\text{M}$] (Fig. S1). Interestingly, α -ionone **4** (51%) and simvastatin **3** (43%) were able to induce the highest spin-state shifts among the investigated substrates, whereas lovastatin **2** shifted the state to a lesser extent (11%).

Biotransformation of medroxyprogesterone acetate, norethisterone, and norethisterone acetate

Although the tested steroids **11–13** did not show any spectral shift when incubated with CYP109E1, their potential biotransformation was investigated in vitro. As observed previously with deoxycorticosterone and testosterone as substrates of CYP106A2 and CYP109B1, respectively, a type I spectral shift is not a necessary prerequisite for bioconversion (Girhard et al. 2010; Simgen et al. 2000). The steroidal substrates medroxyprogesterone acetate **11**, norethisterone **12**, and norethisterone acetate **13** were thus investigated using a reconstituted P450 system with AdR and Adx_{4–108} as redox partners. CYP109E1 did not show any activity towards these compounds (data not shown), and they were, therefore, not further tested with the CYP109E1 based whole-cell system in vivo.

Biotransformation of statin substrates

The three statins, compactin **1**, lovastatin **2**, and simvastatin **3**, identified as CYP109E1 ligands by difference spectroscopy, were further tested as potential substrates for CYP109E1 in vitro. The activity of CYP109E1 was reconstituted with bovine AdR and truncated Adx_{4–108} as described in the “Material and methods” section. CYP109E1 was found to convert all three statin compounds **1–3** resulting in one major reaction product **14, 15** for compactin **1** and lovastatin **2**, respectively (Fig. 2a, c) and two products **16, 17** for simvastatin **3** conversion (Fig. 2e). The selectivity of compactin and lovastatin conversions (77 and 94%) was found to be remarkably higher compared to that of simvastatin (Table S1). Interestingly, the conversion ratio of CYP109E1 towards compactin **1** was much lower compared with the other statins resulting in only 11% conversion after 15 min compared with lovastatin **2** (63%) and simvastatin **3** (72%) (Fig. 2a, c, e and S2).

To prepare and isolate higher amounts of compactin **1**, lovastatin **2**, and simvastatin **3** conversion products for the analysis via NMR spectroscopy, *B. megaterium* MS941 whole cells transformed with pSMF2.1.CYP109E1 were used. After in vivo conversion of statins, the main products of the compactin **1** and lovastatin **2** conversion (**14** and **15**, Fig. 2b, d) as well as two products of simvastatin **3** conversion (**16** and **17**, Fig. 2f) have been purified in sufficient amounts. NMR analysis (data S7) revealed that CYP109E1 is able to hydroxylate compactin **1** and lovastatin **2** at position C6'β resulting in the formation of pravastatin **14** and 6'β-hydroxy-lovastatin **15**, respectively (Scheme 2). The simvastatin **3** metabolites were identified as 3'α-hydroxy-simvastatin **16** and 4"-hydroxy-simvastatin **17**. The *B. megaterium* MS941 strain containing the pSMF2.1 vector, which was used as a negative

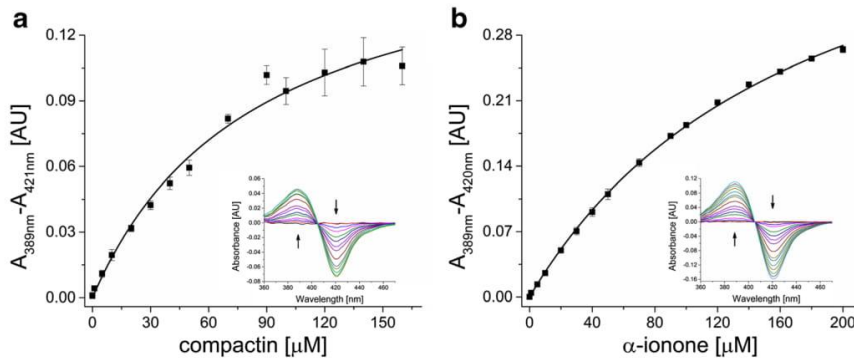


Fig. 1 The absorbance changes plotted against the corresponding concentrations of compactin **1** (a) and α -ionone **4** (b) titrated to CYP109E1 as described in the “Material and methods” section. The mean values were fitted by hyperbolic regression, and the K_d value was

calculated. The inset shows type I spectral shifts induced by the binding of the increasing amount of the substrate to CYP109E1. Arrows show the direction of spectral changes at increasing substrate concentrations

Table 1 Binding of different compounds to CYP109E1

Compound	Spin-state shift [%] ^a	<i>K_d</i> [μM] ^b
Compactin	17	84 ± 13
Lovastatin	11	9.6 ± 3.5
Simvastatin	43	4.7 ± 1.8
α-Ionone	51	178 ± 6
β-Ionone	23	91 ± 9
Nootkatone	22	129 ± 8
Isolongifolen-9-one	24	216 ± 18
α-Damascone	27	161 ± 8
β-Damascone	20	167 ± 7
β-Damascenone	17	154 ± 7
Medroxyprogesterone acetate	—	—
Norethisterone	—	—
Norethisterone acetate	—	—

K_d dissociation constant, — no spin-state shift observed

^a Estimated to approximately ± 5%

^b Estimated with a coefficient of determination (*R*²) ≥ 0.99

control for the CYP109E1-dependent conversions, showed no activity towards the investigated substrates (data not shown).

Biotransformation of terpene substrates

All tested terpenes **4–10** showed type I binding spectra, and the reactions of CYP109E1 with these compounds were further characterized. Similar to statins **1–3**, the activity of CYP109E1 towards the potential terpene substrates α-ionone **4**, β-ionone **5**, nootkatone **6**, isolongifolen-9-one **7**, α-damascone **8**, β-damascone **9**, and β-damascenone **10** was initially tested using the reconstituted system. CYP109E1 showed high conversion within 15 min under in vitro conditions (95% of α-ionone **4**, 96% of β-ionone **5**, 70% of nootkatone **6**, 91% of isolongifolen-9-one **7**, 72% of α-damascone **8**, 70% of β-damascone **9** and β-damascenone **10**) (Fig. S2). The reaction selectivity except for β-damascenone conversion was high (77–93%) yielding one main product (Table S1). All these substrates were also successfully converted by *B. megaterium* cells overexpressing CYP109E1, and the product patterns and selectivities were similar compared to those in vitro. The main products of α-ionone **4**, β-ionone **5**, α-damascone **8**, and β-damascone **9** were compared with authentic standards by GC-MS (Litzenburger and Bernhardt 2016) and identified as 3-hydroxy-α-ionone **18**, 4-hydroxy-β-ionone **19**, 3-hydroxy-α-damascone **23**, and 4-hydroxy-β-damascone **24**, respectively (Fig. 3a, b, e, f and S3–S6). Moreover, 3-hydroxy-α-ionone **18** and 3-hydroxy-α-damascone **23** were found to be 3,6-trans-products. The conversion products of nootkatone **6**, isolongifolen-9-one **7**, and β-damascenone **10** were isolated via HPLC and elucidated by NMR

spectroscopy. The products of nootkatone **6** and isolongifolen-9-one **7** conversion were identified as 11(*R*),12-epoxy-nootkatone **20**, 11(*S*),12-epoxy-nootkatone **21**, and 4(*R*)-hydroxy-isolongifolen-9-one **22**, respectively (Fig. 3c, d). Products of in vivo conversion of β-damascenone **10** were found to be 3,4-dihydroxy-β-damascone **27**, 2-hydroxy-β-damascone **25**, and 3,4-epoxy-β-damascone **26** (Fig. 4a). The control strain *B. megaterium* MS941 containing only the pSMF2.1 vector showed low conversion of the investigated terpene substrates **4–10** after 2 h (data not shown), most probably due to the activity of CYP109E1 encoded in the bacterial genome.

Interestingly, the formation of 3,4-dihydroxy-β-damascone **27** was observed in vivo (Fig. 4a), whereas no corresponding peak (Fig. 4a, *t_R* = 2.8 min) was detectable in vitro using the reconstituted CYP109E1-based system (data not shown). For further characterization, the in vivo conversion was monitored over time. The HPLC results showed significant changes in product distribution within 4 h. After 1 h of conversion, 3,4-epoxy-β-damascone **26** and 3,4-dihydroxy-β-damascone **27** were found to be the major and minor products with 34 and 8% of total shares, respectively. The amount of 3,4-dihydroxy-β-damascone **27** increased up to 45% after 4 h of conversion, and the increase was correlated with a decrease of 3,4-epoxy-β-damascone **26** (Fig. 4b). Thus, the time-dependent data suggested that the double hydroxylated product is formed from 3,4-epoxy-β-damascone **26** by a CYP109E1-independent reaction.

Molecular docking

The crystal structure of CYP109E1 in its closed form was used to investigate the enzyme-substrate interaction and observed regioselectivity of hydroxylation for two of the novel substrates, compactin **1** and α-ionone **4**, by docking of these structurally different substances into the active site of CYP109E1. Both substrates appeared in docking positions allowing hydroxylation at experimentally identified positions, C6' (distance ~ 4.4 Å) for compactin **1** and C3 (distance ~ 4 Å) for α-ionone **4**, respectively. Eight amino acid residues including Ile85, Leu238, Ile241, Ala242, Thr246, Ala291, Leu292, and His293 were found to form the binding pocket of CYP109E1 with compactin **1** whereas only six (Arg69, Ile85, Ala242, Val289, Leu292, His293) were predicted to interact with the smaller substrate α-ionone **4** (Fig. 5). The results predicted that both substrates were bound by van der Waals forces and hydrophobic interactions. Active site residues with predicted hydrophobic interactions with both substrates are Ile85 (BC-loop, SRS1), Ala242 (I-helix, SRS4), and Leu292 (K-β5-loop, SRS5). Considering the electrostatic interactions with the substrates, only His293 was predicted to form a hydrogen bond with compactin **1** and α-ionone **4** (Fig. 5).

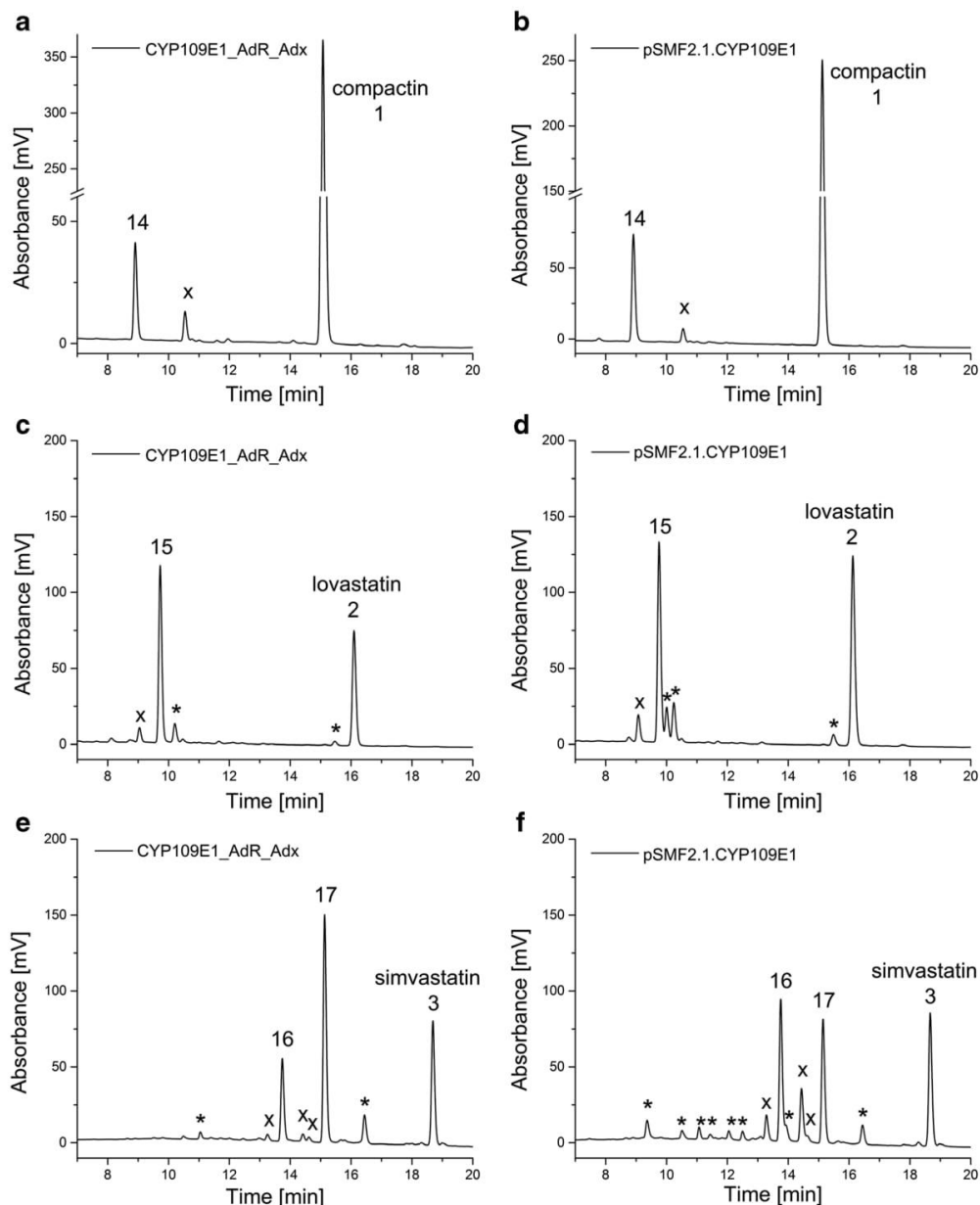


Fig. 2 HPLC chromatograms of in vitro (**a, c, e**) and in vivo (**b, d, f**) conversion of statins **1–3**. **14, 15, 16**, and **17** represent products of compactin **1**, lovastatin **2**, and simvastatin **3** conversion by CYP109E1, respectively, which have been isolated and characterized. The minor products are labeled with “x” (masses are provided in Table S1) and impurities with asterisk

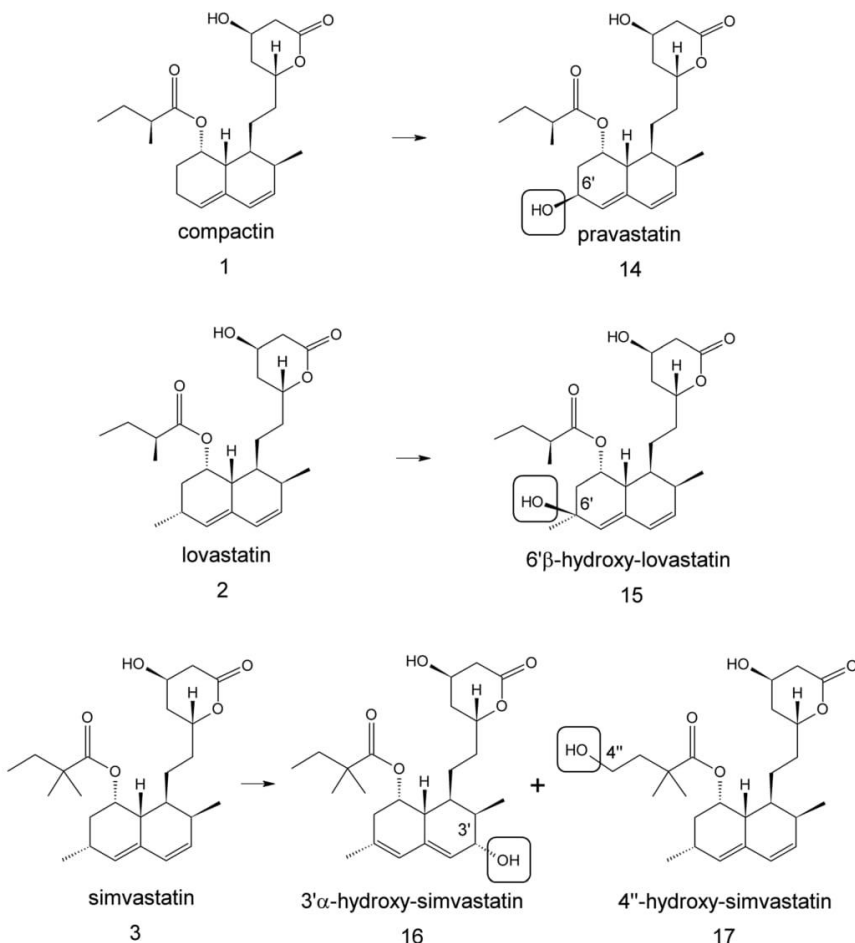
respectively, which have been isolated and characterized. The minor products are labeled with “x” (masses are provided in Table S1) and impurities with asterisk

Schmitz et al. 2014), as well as sesquiterpenes (Sowden et al. 2005), fatty acids, amides, and alcohols (Miura and Fulco 1975). CYP109E1 is a newly identified member of this group, and therefore, elucidation of its substrate range is of great interest. During the initial study on CYP109E1, the crystal structure was solved revealing a highly dynamic active site (Józwik et al. 2016). Phylogenetically, CYP109E1 was found to be related to

Discussion

Various P450s from *B. megaterium* attract interest due to their ability to perform the biotransformation of a broad spectrum of highly interesting compounds such as steroids (Berg and Rafter 1981; Kiss et al. 2015; Putkaradze et al. 2017; Rauschenbach et al. 1993), di- and triterpenes (Bleif et al. 2011; Brill et al. 2014;

Scheme 2 Chemical structures of the statin conversion products **14–17** identified via NMR



the steroid hydroxylase CYP106A1 and, therefore, a focused library of important steroids was tested as its potential substrates. The study revealed that among the 13 tested steroidal compounds, only testosterone was converted by CYP109E1 resulting in the corresponding 16 β -hydroxy product (Józwik et al. 2016). Another important compound which was recently identified as substrate of CYP109E1 is the secosteroid vitamin D3 (Abdulgughni et al. 2017). The enzyme showed 25- and 24-hydroxylase activities towards vitamin D3 generating the valuable compound 25-hydroxy vitamin D3 and two new metabolites hydroxylated at position C24(S) and C25 (Abdulgughni et al. 2017).

In order to further characterize CYP109E1, we aimed to extend the substrate spectrum by investigating its activity towards a focused library of biotechnologically valuable compounds. The enzyme showed no activity for the three tested steroidal compounds **11–13**, whereas several statins **1–3** and terpenes **4–10** were successfully converted (Scheme 1). Compactin **1**, lovastatin **2**, and simvastatin **3**, identified as novel substrates of CYP109E1.

during our study, belong to the group of statins, effective pharmaceutical agents widely used against lipid disorders. In several studies, a broad range of pleiotropic effects of statins was also described proposing their application for the treatment of inflammatory and neurological diseases as well as tumors (Gazzero et al. 2012). All three compounds were able to shift the heme iron of CYP109E1 into the high-spin state. Dissociation constants determined by substrate titrations showed strongest binding for simvastatin **3** to CYP109E1, with a K_d of $4.7 \pm 1.8 \mu\text{M}$ compared to $9.6 \pm 3.5 \mu\text{M}$ and $84 \pm 13 \mu\text{M}$ for lovastatin **2** and compactin **1**, respectively. Investigated statin compounds **1–3** were successfully converted by CYP109E1 into one main product, and the activity of the P450 towards lovastatin **2** and simvastatin **3** was higher than that towards compactin **1** using the heterologous redox partners AdR and Adx_{4–108} (Fig. 2a, c, e). The CYP109E1-based reactions were further investigated *in vivo* in a mutant of *B. megaterium* DSM319, MS941, extensively investigated by our group to generate pharmaceutically important metabolites (Abdulgughni et al. 2017; Kiss et al.

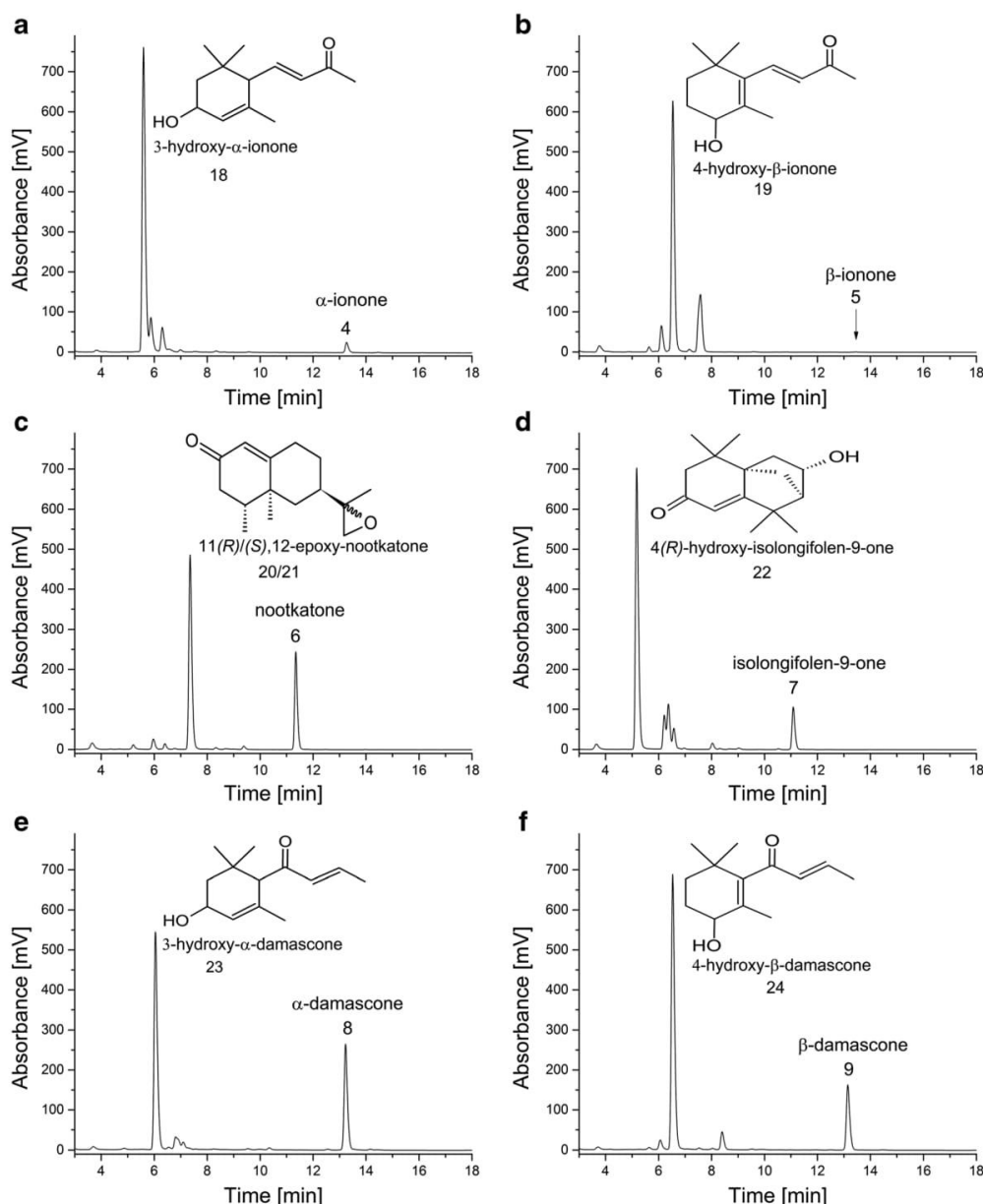


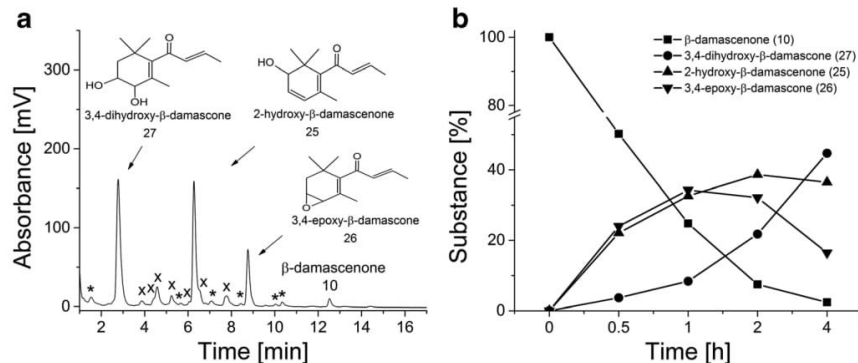
Fig. 3 HPLC chromatograms of in vivo conversions of α -ionone **4** (**a**), β -ionone **5** (**b**), nootkatone **6** (**c**), isolongifolen-9-one **7** (**d**), α -damascone **8**, and β -damascone **9** (**e**) with the identified products shown close to

the peaks. Masses of the minor products detected in vitro as well as in vivo are provided in Table S1

2015; Putkaradze et al. 2017). The observed product patterns of statins in vitro and in vivo (Fig. 2) were very similar and allowed us to scale up the whole-cell reactions to isolate sufficient amounts of the main products for structure identification via NMR spectroscopy. The data revealed that CYP109E1 hydroxylates compactin **1** with a high stereoselectivity at the C6' position forming the biologically active form of the widely used

pharmaceutical pravastatin **14** and this way characterizing CYP109E1 as a novel pravastatin synthase. To the best of our knowledge, so far only two other non-mutated P450 monooxygenases are known being able to convert compactin **1** to active pravastatin variant. The CYP109E1-based whole-cell system produced up to 14 mg/L pravastatin **14** after 4 h of biotransformation which is comparable to the previously described

Fig. 4 HPLC chromatogram of β -damascenone **10** conversion by the *B. megaterium* MS941 cells overexpressing CYP109E1 (**a**) and time-dependent in vivo conversion within 4 h (**b**). The minor products are labeled with “x” (masses are provided in Table S1) and impurities with asterisk

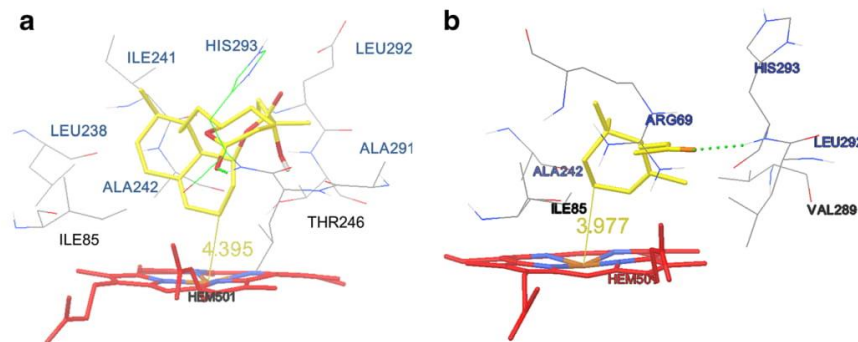


E. coli systems with P450sca-2 (12.9 mg/L within 21 h) (Ba et al. 2013) and CYP107DY1 (13.2 mg/L within 20 h) (Milhim et al. 2016) but provides much higher space-time yield. The activity of this industrially relevant P450 system for pravastatin **14** production might be further optimized by identification of a more effective redox chain, by more suitable production hosts, and by a rational or semi-rational design of the enzyme (Ba et al. 2013; McLean et al. 2015; Milhim et al. 2016). Moreover, to overcome known limitations of cytochrome P450 whole-cell systems on industrial scale, such as substrate solubility, toxicity, and uptake from the cells, expression of CYP109E1 by compactin-producing *Penicillium chrysogenum* similar to the expression of P450_{Prava} (McLean et al. 2015) might be promising. Besides compactin **1**, lovastatin **2** was also converted into the C6'- β -hydroxylated product by CYP109E1 while simvastatin **3** was found to be hydroxylated at the C3' α and C4'' positions (Scheme 2). 6'- β -Hydroxy-lovastatin **15** and 3' α -hydroxy-simvastatin **16** are human liver metabolites of the statin drugs formed by P450 enzymes, whereas 4''-hydroxy-simvastatin **17** is a synthetic drug derivative. None of these compounds are commercially available although they are highly required in larger quantities for activity and safety studies, particularly due to the reported improved pharmacokinetic properties of some statin metabolites (Kandel et al. 2014) and the known drug-drug interactions of statin pharmaceuticals (Kellick et al. 2014). There are few reports describing the generation of these metabolites, such as chemical

synthesis of 3' α -hydroxy-simvastatin **16**, electrochemical oxidation, and biotransformation of lovastatin **2** and simvastatin **3** with CYP3A4 or CYP102A1 mutants (Khera and Hu 2013; Kim et al. 2011; Stokker 1994). However, CYP109E1 seems to be a perfect candidate for the production of these metabolites through mild and cost-effective biocatalysis with much higher selectivities and higher product yields compared to previously established methods. Moreover, CYP109E1 represents the first enzyme that is able to introduce a hydroxyl group at the C4'' position into the simvastatin molecule.

In addition to statins **1–3**, seven terpene compounds **4–10** were identified as novel substrates of CYP109E1 and their biotransformation was further investigated. Terpene and terpenoid hydroxylation and epoxidation by microbial P450 enzymes have been reported in the literature (Çelik et al. 2005; Hall and Bell 2014; Litzenburger and Bernhardt 2016; Schifrin et al. 2015). However, the high demand of valuable terpene derivatives and their mostly unselective and low-yield production via chemical synthesis makes exploration of new effective biocatalysts for terpene oxyfunctionalization highly important. Here, α -ionone **4**, β -ionone **5**, α -damascone **8**, β -damascone **9**, β -damascenone **10**, nootkatone **6**, and isolongifolen-9-one **7** were found to serve as substrates for CYP109E1 identifying this P450 as a novel terpene hydroxylase and epoxidase. All compounds were able to bind to the enzyme and induce a type I difference spectrum of CYP109E1. Concerning dissociation constants, terpenes **4–10**

Fig. 5 Docking orientations of compactin **1** (**a**) and α -ionone **4** (**b**) shown in yellow in the active site of CYP109E1 capable of hydroxylation at C6' and C3, respectively. The distance of the corresponding carbon atom from the heme iron is given in angstrom. Amino acids forming the active site in the presence of each substrate are shown and named



showed weaker binding to the active site of CYP109E1 than statin substrates **1–3**. However, they have been converted by CYP109E1 with high efficiencies and regioselectivities in vitro as well as in vivo. The reaction products of α -ionone **4**, β -ionone **5**, α -damascone **8**, and β -damascone **9** were identified as 3-hydroxy- α -ionone **18**, 4-hydroxy- β -ionone **19**, 3-hydroxy- α -damascone **23**, and 4-hydroxy- β -damascone **24**, respectively. Thus, CYP109E1 hydroxylates preferably at allylic positions which are energetically favorable and also preferred by other P450s converting these compounds (Çelik et al. 2005; Hall and Bell 2014; Khatri et al. 2010; Litzenburger and Bernhardt 2016). The resulting hydroxylated ionones and damascones are important compounds which might be used as precursors or building blocks in chemical synthesis of fragrance constituents due to their floral and fruity scents as well as in bioassays due to their bioactive properties. For example, the 4-hydroxy derivative of β -ionone **5** has been reported to be a versatile synthon (More and Bhat 2013) whereas 4-hydroxy- β -damascone **24** was found to possess very strong antifeedant properties against lesser mealworm *Alphitobius diaperinus* (Gliszczynska et al. 2016). The CYP109E1-based *B. megaterium* system used in our study is very suitable for the production of these metabolites. To compare it with the previously established P450-based production systems, whole-cell experiments using higher substrate concentrations and longer incubation times are necessary. However, based on the observed fast conversion of up to 200 μ M substrate within 2 h under non-optimized conditions, the whole-cell system used in our study seems to be efficient for the production of these valuable metabolites. The NMR data of nootkatone **6** and β -damascenone **10** conversion products revealed for the first time the epoxidation activity of CYP109E1 resulting in the formation of 11(*R*),12-epoxy-nootkatone **20**, 11(*S*),12-epoxy-nootkatone **21**, and 3,4-epoxy- β -damascone **26**, respectively. 3,4-Epoxy- β -damascone **26** has been previously reported to be a conversion product of β -damascone **9** by CYP101C1 from *N. aromaticivorans* DSM12444 (Ma et al. 2011), whereas 11,12-epoxy-nootkatone has been described to be produced by CYP102A1 mutants as well as unknown fungal proteins. It showed antiproliferative activity against leukemia cell line HL-60 (Gliszczynska et al. 2011; Sowden et al. 2005). In our studies, 3,4-epoxy- β -damascone **26** was further metabolized in vivo to 3,4-dihydroxy- β -damascone **27** by a CYP109E1-independent reaction proposed to be catalyzed by an unknown epoxide hydrolase from the DSM319 as described for other *B. megaterium* strains (Michaels et al. 1980; Tang et al. 2001; Zhang et al. 2010). Besides 3,4-epoxy- β -damascone **26**, a novel compound, 2-hydroxy- β -damascenone **25**, was identified as conversion product of CYP109E1. Its properties are unknown and need to be investigated. Isolongifolen-9-one **7** was hydroxylated regio- and stereoselectively at C4 by CYP109E1 yielding 4(*R*)-hydroxy-isolongifolen-9-one **22**. This compound has been described in the literature as conversion product of isolongifolen-9-one **7** by four fungal cultures, and it has been shown to have an

inhibitory activity on tyrosinase, the key enzyme for melanin biosynthesis (Choudhary et al. 2003). In another study, the suppressive effect of 4(*R*)-hydroxy-isolongifolen-9-one **22** against chemical mutagen-induced SOS response in *Salmonella typhimurium* TA1535/pSK1002 has been reported (Sakata et al. 2010).

In addition to the in vitro and in vivo characterization of CYP109E1, in silico experiments were performed using the crystal structure of this enzyme in order to predict residues responsible for substrate binding and to understand the structural basis of the observed hydroxylation regioselectivity. The molecular docking of the two selected structurally different novel substrates, compactin **1** and α -ionone **4**, into CYP109E1 indicated the presence of common as well as specific residues interacting with each substrate. The obtained docking orientations of these substrates in the active site supported experimental results, 6' β -hydroxylation of compactin **1** and 3-hydroxylation in the cyclohexene ring of α -ionone **4** (Fig. 5).

Taken together, we were able to characterize CYP109E1 from *B. megaterium* for the first time as a novel and highly regioselective statin and terpene hydroxylase as well as terpene epoxidase. Thus, CYP109E1 might be used to generate pharmaceutically and biotechnologically interesting compounds, such as the drug pravastatin **14** and the human statin drug metabolites 6' β -hydroxy-lovastatin **15** and 3' α -hydroxy-simvastatin **16** as well as several valuable terpene derivatives. Besides that, 4"-hydroxy-simvastatin **17** and a novel compound, 2-hydroxy- β -damascenone **25**, were obtained using CYP109E1 as biocatalyst, and are now available for further investigations. Finally, our *B. megaterium* whole-cell system was successfully utilized for the production of the statin and terpene metabolites in milligram scale. The established CYP109E1 system is a good candidate for improvement towards industrial scale.

Acknowledgements The authors thank Birgit Heider-Lips for the purification of AdR and Adx₄₋₁₀₈, Dr. Josef Zapp for the NMR measurements, and Ghadban Beshr from the Helmholtz Institute for Pharmaceutical Research Saarland (HIPS) for LC-MS measurements.

Conflict of interest The authors declare that they have no competing interests.

Compliance with ethical standards The article does not contain any studies with human participants or animals performed by any of the authors.

References

- Abdulgughni A, Józwik IK, Putkaradze N, Brill E, Zapp J, Thunnissen AMWH, Hannemann F, Bernhardt R (2017) Characterization of cytochrome P450 CYP109E1 from *Bacillus megaterium* as a novel vitamin D₃ hydroxylase. *J Biotechnol* 243:38–47. <https://doi.org/10.1016/j.biote.2016.12.023>

- Ba L, Li P, Zhang H, Duan Y, Lin Z (2013) Semi-rational engineering of cytochrome P450sca-2 in a hybrid system for enhanced catalytic activity: insights into the important role of electron transfer. *Biotechnol Bioeng* 110:2815–2825. <https://doi.org/10.1002/bit.24960>
- Barg H, Malten M, Jahn M, Jahn D (2005) Protein and vitamin production in *Bacillus megaterium*. In: Barredo JL (ed) *Microbial processes and products*. Humana Press, New York, pp 205–223
- Bell SG, Wong LL (2007) P450 enzymes from the bacterium *Novosphingobium aromaticivorans*. *Biochem Biophys Res Commun* 360(3):666–672. <https://doi.org/10.1016/j.bbrc.2007.06.119>
- Berg A, Rafter JJ (1981) Studies on the substrate specificity and inducibility of cytochrome P-450meg. *Biochem J* 196:781–786
- Bernhardt R (2006) Cytochromes P450 as versatile biocatalysts. *J Biotechnol* 124:128–145. <https://doi.org/10.1016/j.jbiotec.2006.01.026>
- Bernhardt R, Urlacher VB (2014) Cytochromes P450 as promising catalysts for biotechnological application: chances and limitations. *Appl Microbiol Biotechnol* 98:6185–6203. <https://doi.org/10.1007/s00253-014-5767-7>
- Biedendieck R, Malten M, Barg H, Bunk B, Martens JH, Deery E, Leech H, Warren MJ, Jahn D (2010) Metabolic engineering of cobalamin (vitamin B12) production in *Bacillus megaterium*. *Microb Biotechnol* 3:24–37. <https://doi.org/10.1111/j.1751-7915.2009.00125.x>
- Bleif S, Hannemann F, Zapp J, Hartmann D, Jauch J, Bernhardt R (2011) A new *Bacillus megaterium* whole-cell catalyst for the hydroxylation of the pentacyclic triterpene 11-keto- β -boswellic acid (KBA) based on a recombinant cytochrome P450 system. *Appl Microbiol Biotechnol* 93:1135–1146. <https://doi.org/10.1007/s00253-011-3467-0>
- Brill E, Hannemann F, Zapp J, Brüning G, Jauch J, Bernhardt R (2014) A new cytochrome P450 system from *Bacillus megaterium* DSM319 for the hydroxylation of 11-keto- β -boswellic acid (KBA). *Appl Microbiol Biotechnol* 98:1701–1717. <https://doi.org/10.1007/s00253-013-5029-0>
- Brown AJ (2007) Cholesterol, statins and cancer. *Clin Exp Pharmacol Physiol* 34:135–141. <https://doi.org/10.1111/j.1440-1681.2007.04565.x>
- Celik A, Flitsch SL, Turner NJ (2005) Efficient terpene hydroxylation catalysts based upon P450 enzymes derived from *Actinomycetes*. *Org Biomol Chem* 3:2930–2934. <https://doi.org/10.1039/b506159h>
- Choudhary MI, Musharraf SG, Khan MTH, Abdelrahman D, Parvez M, Shaheen F, Rahman A-u (2003) Microbial transformation of isolongifolen-4-one. *Helv Chim Acta* 86:3450–3460. <https://doi.org/10.1002/hlca.200390289>
- Endo A, Hasumi K (1993) HMG-CoA reductase inhibitors. *Nat Prod Rep* 10:541–550. <https://doi.org/10.1039/NP9931000541>
- Eppinger M, Bunk B, Johns MA, Edirisinghe JN, Kutumbaka KK, Koenig SSK, Creasy HH, Rosovitz MJ, Riley DR, Daugherty S, Martin M, Elbourne LD, Paulsen I, Biedendieck R, Braun C, Grayburn S, Dhingra S, Lukyanchuk V, Ball B, Ul-Qamar R, Seibel J, Bremer E, Jahn D, Ravel J, Vary PS (2011) Genome sequences of the biotechnologically important *Bacillus megaterium* strains QM B1551 and DSM319. *J Bacteriol* 193:4199–4213. <https://doi.org/10.1128/JB.00449-11>
- Fisher MT, Sligar SG (1985) Control of heme protein redox potential and reduction rate: linear free energy relation between potential and ferric spin state equilibrium. *J Am Chem Soc* 107(17):5018–5019
- Fulco AJ (1991) P450BM-3 and other inducible bacterial P450 cytochromes: biochemistry and regulation. *Annu Rev Pharmacol Toxicol* 31:177–203. <https://doi.org/10.1146/annurev.pa.31.040191.001141>
- Furuya T, Shibata D, Kino K (2009) Phylogenetic analysis of *Bacillus* P450 monooxygenases and evaluation of their activity towards steroids. *Steroids* 74:906–912. <https://doi.org/10.1016/j.steroids.2009.06.005>
- Gazzero P, Proto MC, Gangemi G, Malfitano AM, Ciaglia E, Pisanti S, Santoro A, Laenza C, Bifulco M (2012) Pharmacological actions of statins: a critical appraisal in the management of cancer. *Pharmacol Rev* 64:102–146. <https://doi.org/10.1124/pr.111.004994>
- Girhard M, Klaus T, Khatri Y, Bernhardt R, Urlacher VB (2010) Characterization of the versatile monooxygenase CYP109B1 from *Bacillus subtilis*. *Appl Microbiol Biotechnol* 87:595–607. <https://doi.org/10.1007/s00253-010-2472-z>
- Gliszczynska A, Łysek A, Janecka T, Świdławska M, Wietrzyk J, Wawrzęńczyk C (2011) Microbial transformation of (+)-nootkatone and the antiproliferative activity of its metabolites. *Bioorg Med Chem* 19:2464–2469. <https://doi.org/10.1016/j.bmc.2011.01.062>
- Gliszczynska A, Gladkowski W, Dancewicz K, Gabryś B, Szczepanik M (2016) Transformation of β -damascone to (+)-(S)-4-hydroxy- β -damascone by fungal strains and its evaluation as a potential insecticide against aphids *Myzus persicae* and lesser mealworm *Alphitobius diaperinus* Panzer. *Catal Commun* 80:39–43. <https://doi.org/10.1016/j.catcom.2016.03.018>
- Hall EA, Bell SG (2014) The efficient and selective biocatalytic oxidation of norisoprenoid and aromatic substrates by CYP101B1 from *Novosphingobium aromaticivorans* DSM12444. *RSC Adv* 5: 5762–5773. <https://doi.org/10.1039/c4ra14010a>
- Honeychurch MJ, Hill AO, Wong LL (1999) The thermodynamics and kinetics of electron transfer in the cytochrome P450cam enzyme system. *FEBS Lett* 451(3):351–353
- Janocha S, Schmitz D, Bernhardt R (2015) Terpene hydroxylation with microbial cytochrome P450 monooxygenases. *Adv Biochem Eng Biotechnol* 148:215–250. https://doi.org/10.1007/10_2014_296
- Janocha S, Carius Y, Hutter M, Lancaster CRD, Bernhardt R (2016) Crystal structure of CYP106A2 in substrate-free and substrate-bound form. *ChemBioChem* 17(9):852–860. <https://doi.org/10.1002/cbic.201500524>
- Józwik IK, Kiss FM, Gricman L, Abdulmughni A, Brill E, Zapp J, Pleiss J, Bernhardt R, Thunnissen AWH (2016) Structural basis of steroid binding and oxidation by the cytochrome P450 CYP109E1 from *Bacillus megaterium*. *FEBS J* 283:4128–4148. <https://doi.org/10.1111/febs.13911>
- Kandel SE, Wienkers LC, Lampe JN (2014) Cytochrome P450 enzyme metabolites in lead discovery and development. *Annu Rev Med Chem* 49:347–359. <https://doi.org/10.1016/B978-0-12-800167-7.00022-5>
- Katagiri M, Ganguli BN, Gunsalus IC (1968) A soluble cytochrome P-450 functional in methylene hydroxylation. *J Biol Chem* 243(12): 3543–3546
- Kellick KA, Bottorff M, Toth PP (2014) A clinician's guide to statin drug-drug interactions. *J Clin Lipidol* 8:30–46. <https://doi.org/10.1016/j.jacl.2014.02.010>
- Khatri Y, Girhard M, Romankiewicz A, Ringle M, Hannemann F, Urlacher VB, Hutter MC, Bernhardt R (2010) Regioselective hydroxylation of norisoprenoids by CYP109D1 from *Sorangium cellulosum* So ce56. *Appl Microbiol Biotechnol* 88:485–495. <https://doi.org/10.1007/s00253-010-2756-3>
- Khatri Y, Ringle M, Lisurek M, von Kries JP, Zapp J, Bernhardt R (2016) Substrate hunting for the myxobacterial CYP260A1 revealed new 1 α -hydroxylated products from C-19 steroids. *ChemBioChem* 17(1): 90–101. <https://doi.org/10.1002/cbic.201500420>
- Khera S, Hu N (2013) Generation of statin drug metabolites through electrochemical and enzymatic oxidations. *Anal Bioanal Chem* 405:6009–6018. <https://doi.org/10.1007/s00216-013-7021-z>
- Kim KH, Kang JY, Kim DH, Park SH, Park SH, Kim D, Park KD, Lee YJ, Jung HC, Pan JG, Ahn T, Yun CH (2011) Generation of human chiral metabolites of simvastatin and lovastatin by bacterial CYP102A1 mutants. *Drug Metab Dispos* 39(1):140–150. <https://doi.org/10.1124/dmd.110.036392>

- Kiss FM, Schmitz D, Zapp J, Dier TKF, Volmer DA, Bernhardt R (2015) Comparison of CYP106A1 and CYP106A2 from *Bacillus megaterium*—identification of a novel 11-oxidase activity. *Appl Microbiol Biotechnol* 99:8495–8514. <https://doi.org/10.1007/s00253-015-6563-8>
- Korneli C, Biedendieck R, David F, Jahn D, Wittmann C (2013) High yield production of extracellular recombinant levansucrase by *Bacillus megaterium*. *Appl Microbiol Biotechnol* 97:3343–3353. <https://doi.org/10.1007/s00253-012-4567-1>
- Kulpreecha S, Boonruangthavorn A, Meksiriporn B, Thongchul N (2009) Inexpensive fed-batch cultivation for high poly(3-hydroxybutyrate) production by a new isolate of *Bacillus megaterium*. *J Biosci Bioeng* 107:240–245. <https://doi.org/10.1016/j.jbbiose.2008.10.006>
- Lamon-Fava S (2013) Statins and lipid metabolism: an update. *Curr Opin Lipidol* 24:221–226. <https://doi.org/10.1097/MOL.0b013e3283613b8b>
- Lisurek M, Kang MJ, Hartmann RW, Bernhardt R (2004) Identification of monohydroxy progestones produced by CYP106A2 using comparative HPLC and electrospray ionisation collision-induced dissociation mass spectrometry. *Biochem Biophys Res Commun* 319:677–682
- Litzenburger M, Bernhardt R (2016) Selective oxidation of carotenoid-derived aroma compounds by CYP260B1 and CYP267B1 from *Sorangium cellulosum* So ce56. *Appl Microbiol Biotechnol* 100:4447–4457. <https://doi.org/10.1007/s00253-015-7269-7>
- Luthra A, Denisov IG, Sligar SG (2011) Spectroscopic features of cytochrome P450 reaction intermediates. *Arch Biochem Biophys* 507(1):26–35. <https://doi.org/10.1016/j.abb.2010.12.008>
- Ma M, Bell SG, Yang W, Hao Y, Rees NH, Bartlam M, Zhou W, Wong LL, Rao Z (2011) Structural analysis of CYP101C1 from *Novosphingobium aromaticivorans* DSM12444. *Chembiochem* 12:88–99
- Malten M, Hollmann R, Deckwer WD, Jahn D (2005) Production and secretion of recombinant *Leuconostoc mesenteroides* dextranucrase DsrS in *Bacillus megaterium*. *Biotechnol Bioeng* 89:206–218. <https://doi.org/10.1002/bit.20341>
- Matsuoka T, Miyakoshi S, Tanzawa K, Nakahara K, Hosobuchi M, Serizawa N (1989) Purification and characterization of cytochrome P-450sca from *Streptomyces carbophilus*. *Eur J Biochem* 184:707–713. <https://doi.org/10.1111/j.1432-1033.1989.tb15070.x>
- McLean KJ, Hans M, Meijrink B, van Scheppingen WB, Vollebregt A, Tee KL, van der Laan JM, Leys D, Munro AW, van den Berg MA (2015) Single-step fermentative production of the cholesterol-lowering drug pravastatin via reprogramming of *Penicillium chrysogenum*. *Proc Natl Acad Sci U S A* 112:2847–2852. <https://doi.org/10.1073/pnas.1419028112>
- Michaels BC, Ruettinger RT, Fulco AJ (1980) Hydration of 9,10-epoxypalmitic acid by a soluble Enzyme from *Bacillus megaterium*. *Biochem Biophys Res Commun* 92(4):1189–1195
- Milhim M, Putkaradze N, Abdulmughni A, Kern F, Hartz P, Bernhardt R (2016) Identification of a new plasmid-encoded cytochrome P450 CYP107DV1 from *Bacillus megaterium* with a catalytic activity towards mevastatin. *J Biotechnol* 240:68–75. <https://doi.org/10.1016/j.biote.2016.11.002>
- Miura Y, Fulco AJ (1975) ω -1, ω -2 and ω -3 hydroxylation of long-chain fatty acids, amides and alcohols by a soluble enzyme system from *Bacillus megaterium*. *Biochim Biophys Acta* 388:305–317
- More GP, Bhat SV (2013) Facile lipase catalysed syntheses of (S)-(+)-4-hydroxy- β -ionone and (S)-(+) -4-hydroxy- β -damascone: chiral flavorants and synthons. *Tetrahedron Lett* 54:4148–4149. <https://doi.org/10.1016/j.tetlet.2013.05.089>
- Morris GM, Huey R, Lindstrom W, Sanner MF, Belew RK, Goodsell DS, Olson AJ (2009) AutoDock4 and AutoDockTools4: automated docking with selective receptor flexibility. *J Comput Chem* 30(16):2785–2791. <https://doi.org/10.1002/jcc.21256>
- Narhi LO, Fulco AJ (1987) Identification and characterization of two functional domains in cytochrome P-450BM-3, a catalytically self-sufficient monooxygenase induced by barbiturates in *Bacillus megaterium*. *J Biol Chem* 262:6683–6690
- Omura T, Sato R (1964) The carbon monoxide-binding pigment of liver microsomes. I. Evidence for its hemoprotein nature. *J Biol Chem* 239:2370–2378
- Peterson JA, Lu JY, Geisselsoeder J, Graham-Lorence S, Carmona C, Witney F, Lorence MC (1992) Cytochrome P-450terp. Isolation and purification of the protein and cloning and sequencing of its operon. *J Biol Chem* 267(20):14193–14203
- Poulos TL, Raag R (1992) Cytochrome P450cam: crystallography, oxygen activation, and electron transfer. *FASEB J* 6(2):674–679
- Putkaradze N, Kiss FM, Schmitz D, Zapp J, Hutter MC, Bernhardt R (2017) Biotransformation of prednisone and dexamethasone by cytochrome P450 based systems—identification of new potential drug candidates. *J Biotechnol* 242:101–110. <https://doi.org/10.1016/j.jbiotec.2016.12.011>
- Rauschenbach B, Isenringen M, Noeske-Jungblut C, Boidol W, Siewert G (1993) Cloning sequencing and expression of the gene for cytochrome P450meg, the steroid-15 β -monooxygenase from *Bacillus megaterium* ATCC 13368. *Mol Gen Genet* 241:170–176
- Rygus T, Hillen W (1992) Catabolite repression of the xyl operon in *Bacillus megaterium*. *J Bacteriol* 174:3049–3055
- Sagara Y, Wada A, Takata Y, Waterman MR, Sekimizu K, Horiuchi T (1993) Direct expression of adrenodoxin reductase in *Escherichia coli* and the functional characterization. *Biol Pharm Bull* 16:627–630
- Sakaki T (2012) Practical application of cytochrome P450. *Biol Pharm Bull* 35:844–849
- Sakata K, Oda Y, Miyazawa M (2010) Suppression of SOS-inducing activity of chemical mutagens by metabolites from microbial transformation of (-)-isolongifolene. *J Agric Food Chem* 58:2164–2167. <https://doi.org/10.1021/jf903651c>
- Sanner MF (1999) Python: a programming language for software integration and development. *J Mol Graph Modell* 17(1):57–61
- Schenkman JB, Jansson I (1998) Spectral analyses of cytochromes P450. In: Phillips I, Shephard EA (eds) Cytochrome P450 protocols. Humana Press, New York, pp 25–34
- Schifrin A, Litzenburger M, Ringle M, Ly TTB, Bernhardt R (2015) New sesquiterpene oxidations with CYP260A1 and CYP264B1 from *Sorangium cellulosum* So ce56. *Chembiochem* 16:2624–2632. <https://doi.org/10.1002/cbic.201500417>
- Schmitz D, Zapp J, Bernhardt R (2012) Hydroxylation of the triterpenoid diterpocarpol with CYP106A2 from *Bacillus megaterium*. *FEBS J* 279:1663–1674. <https://doi.org/10.1111/j.1742-4658.2012.08503.x>
- Schmitz D, Zapp J, Bernhardt R (2014) Steroid conversion with CYP106A2—production of pharmaceutically interesting DHEA metabolites. *Microp Cell Factories* 13:81. <https://doi.org/10.1186/1475-2859-13-81>
- Simgen B, Contzen J, Schwarzer R, Bernhardt R, Jung C (2000) Substrate binding to 15 β -hydroxylase (CYP106A2) probed by FT infrared spectroscopic studies of the iron ligand CO stretch vibration. *Biochem Biophys Res Commun* 269:737–742. <https://doi.org/10.1006/bbrc.2000.2348>
- Sligar SG, Gunsalus IC (1976) A thermodynamic model of regulation: modulation of redox equilibria in camphor monooxygenase. *Proc Natl Acad Sci* 73(4):1078–1082
- Sono M, Roach MP, Coulter ED, Dawson JH (1996) Heme-containing oxygenases. *Chem Rev* 96:2841–2888
- Sowden RJ, Yasmin S, Rees NH, Bell SG, Wong LL (2005) Biotransformation of the sesquiterpene (+)-valencene by cytochrome P450cam and P450BM-3. *Org Biomol Chem* 3:57–64. <https://doi.org/10.1039/b413068e>
- Stammen S, Müller BK, Korneli C, Biedendieck R, Gamer M, Franco-Lara E, Jahn D (2010) High-yield intra- and extracellular protein

- production using *Bacillus megaterium*. *Appl Environ Microbiol* 76: 4037–4046. <https://doi.org/10.1128/AEM.00431-10>
- Stokker GE (1994) Synthesis of the 3'(S)-hydroxy derivative of simvastatin. *Bioorg Med Chem Lett* 4:1767–1770. [https://doi.org/10.1016/S0960-894X\(00\)80377-7](https://doi.org/10.1016/S0960-894X(00)80377-7)
- Tang YF, Xu JH, Ye Q, Schulze B (2001) Biocatalytic preparation of (S)-phenyl glycidyl ether using newly isolated *Bacillus megaterium* ECU1001. *J Mol Catal B Enzym* 13:61–68. [https://doi.org/10.1016/S1381-1177\(00\)00230-7](https://doi.org/10.1016/S1381-1177(00)00230-7)
- Uhlmann H, Beckert V, Schwarz D, Bernhardt R (1992) Expression of bovine adrenodoxin in *E. coli* and site-directed mutagenesis of 2FE-2S/cluster ligands. *Biochem Biophys Res Commun* 188:1131–1138
- Ullah AJ, Murray RI, Bhattacharyya PK, Wagner GC, Gunsalus IC (1990) Protein components of a cytochrome P-450 linalool 8-methyl hydroxylase. *J Biol Chem* 265(3):1345–1351
- Urlacher VB, Lutz-Wahl S, Schmid RD (2004) Microbial P450 enzymes in biotechnology. *Appl Microbiol Biotechnol* 64:317–325. <https://doi.org/10.1007/s00253-003-1514-1>
- Urlacher VB, Makhsumkhanov A, Schmid RD (2006) Biotransformation of beta-ionone by engineered cytochrome P450 BM-3. *Appl Microbiol Biotechnol* 70:53–59. <https://doi.org/10.1007/s00253-005-0028-4>
- Vary PS, Biedendieck R, Fuerch T, Meinhardt F, Rohde M, Deckwer WD, Jahn D (2007) *Bacillus megaterium*—from simple soil bacterium to industrial protein production host. *Appl Microbiol Biotechnol* 76: 957–967. <https://doi.org/10.1007/s00253-007-1089-3>
- Virus C, Lisurek M, Simgen B, Hannemann F, Bernhardt R (2006) Function and engineering of the 15β-hydroxylase CYP106A2. *Biochem Soc Trans* 34:1215–1218. <https://doi.org/10.1042/BST0341215>
- Williams JW, Morrison JF (1979) The kinetics of reversible tight-binding inhibition. *Methods Enzymol* 63:437–467
- Wittchen KD, Meinhardt F (1995) Inactivation of the major extracellular protease from *Bacillus megaterium* DSM319 by gene replacement. *Appl Microbiol Biotechnol* 42:871–877. <https://doi.org/10.1007/BF00191184>
- Zhang Z, Sheng Y, Jiang K, Wang Z, Zheng Y, Zhu Q (2010) Bioresolution of glycidyl (o, m, p)-methylphenyl ethers by *Bacillus megaterium*. *Biotechnol Lett* 32:513–516. <https://doi.org/10.1007/s10529-009-0181-4>

Supplementary material

Applied Microbiology and Biotechnology

CYP109E1 is a novel versatile statin and terpene oxidase from *Bacillus megaterium*

Natalia Putkaradze^a, Martin Litzenburger^a, Ammar Abdulkhader^a, Mohammed Milhim^a, Elisa Brill^a, Frank Hannemann^a, Rita Bernhardt^a

^a Institute of Biochemistry, Saarland University, D-66123 Saarbruecken, Germany

Corresponding author:

Prof. Dr. Rita Bernhardt

Department of Biochemistry, Saarland University, Campus, B 2.2

D-66123 Saarbruecken, Germany

Tel.: +49 (0)681 302 4241

Fax: +49 (0)681 302 4739

E-Mail: ritabern@mx.uni-saarland.de

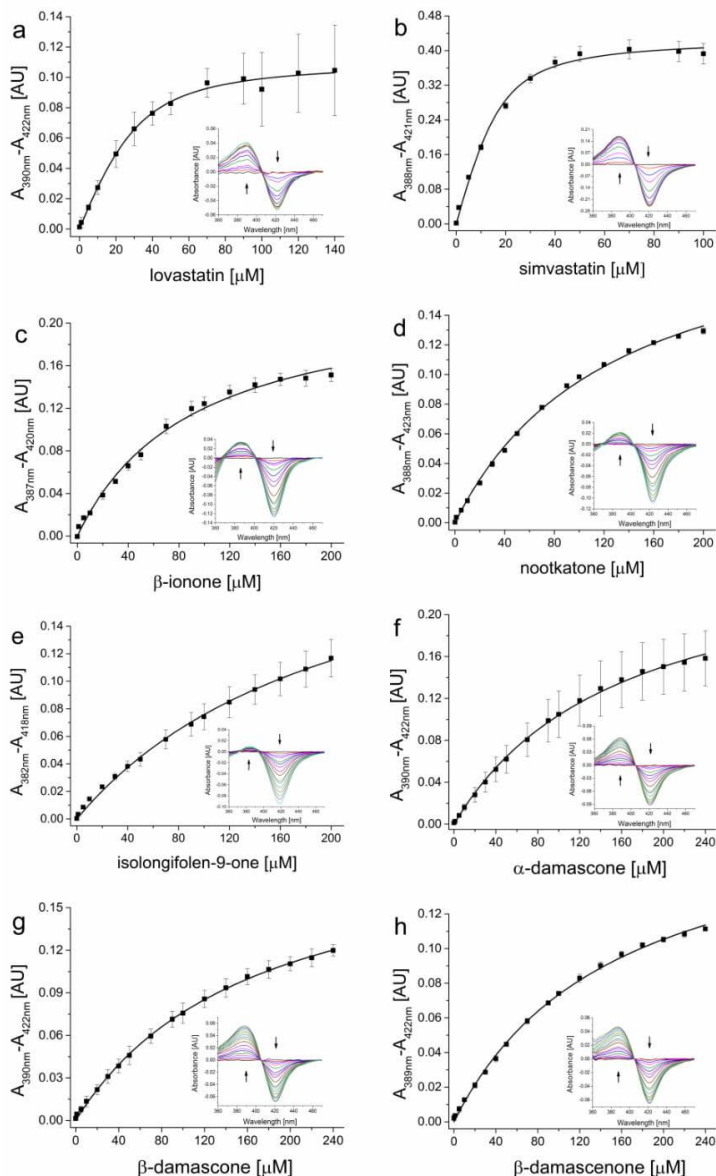


Fig. S1 The absorbance changes plotted against the corresponding concentrations of lovastatin **2** (a), simvastatin **3** (b), β -ionone **5** (c), nootkatone **6** (d), isolongifolen-9-one **7** (e), α -damascone **8** (f), β -damascone **9** (g) and β -damascenone **10** (h) titrated to CYP109E1 as described in "Material and methods". The mean values were fitted by either tight binding equation or hyperbolic regression and the K_d value was calculated. The *inset* shows type I spectral shifts induced by the binding of the increasing

amount of the substrate to CYP109E1. Arrows show the direction of spectral changes at increasing substrate concentrations

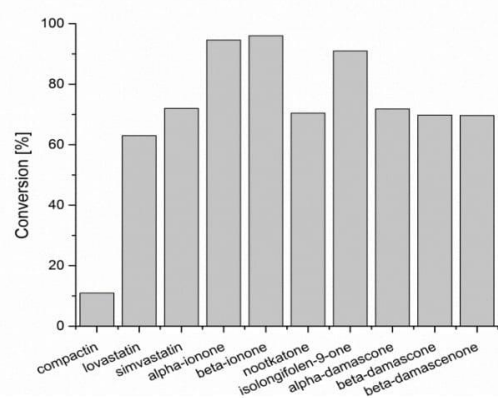


Fig. S2 Conversion ratio of 100 μ M compactin **1**, lovastatin **2** and simvastatin **3** and 200 μ M of other substrates **4-10** after 15 min *in vitro* in the presence of CYP109E1 using AdR and Adx₄₋₁₀₈ as redox partners

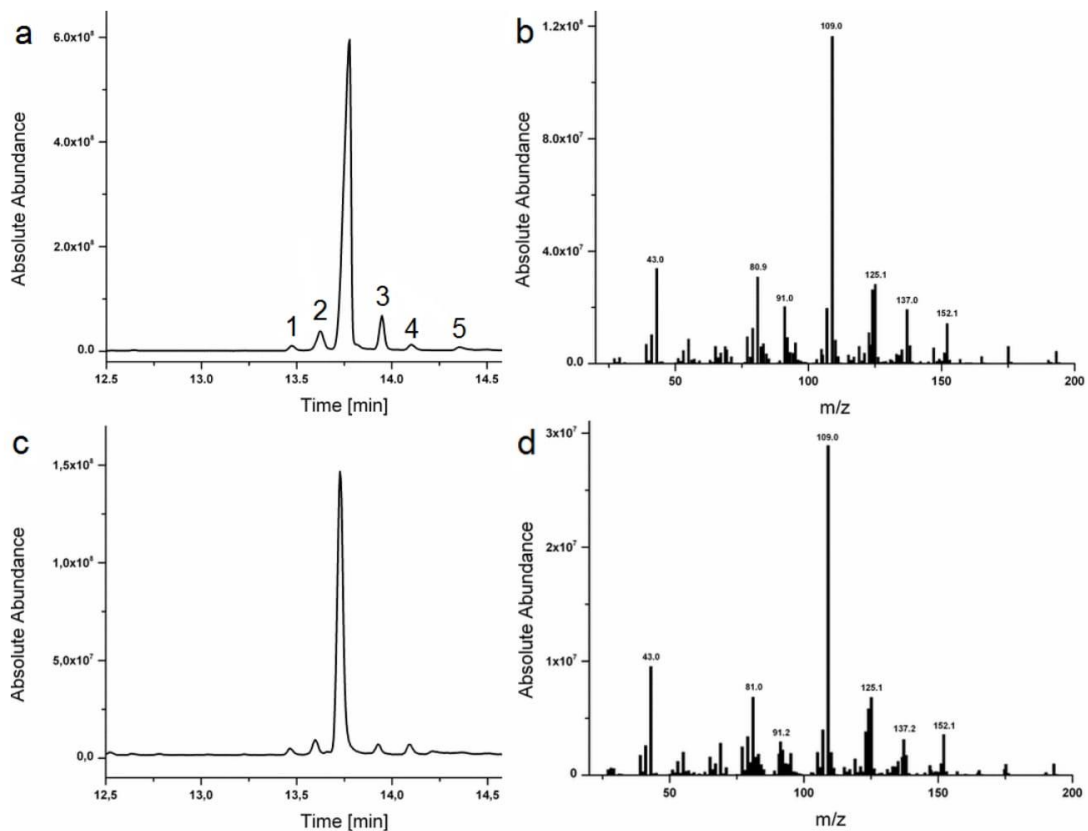


Fig. S3 GC-MS data of the α -ionone **4** conversion product by CYP109E1 (a and b) and by CYP267B1 (c and d) identified as 3-hydroxy- α -ionone **18** (Litzenburger et al. 2016). 1-5 are the minor products with known masses (Table S1)

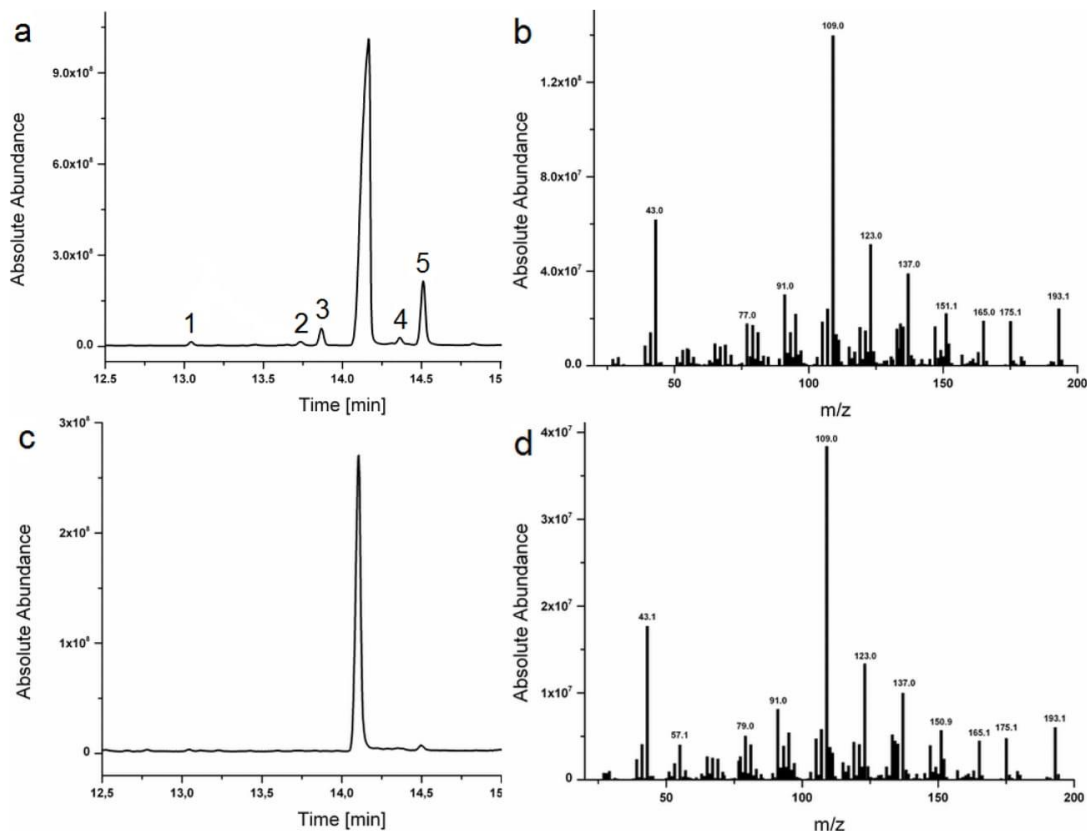


Fig. S4 GC-MS data of the β -ionone **5** conversion product by CYP109E1 (a and b) and by CYP267B1 (c and d) identified as 4-hydroxy- β -ionone **19** (Litzenburger et al. 2016). 1-5 are the minor products with known masses (Table S1)

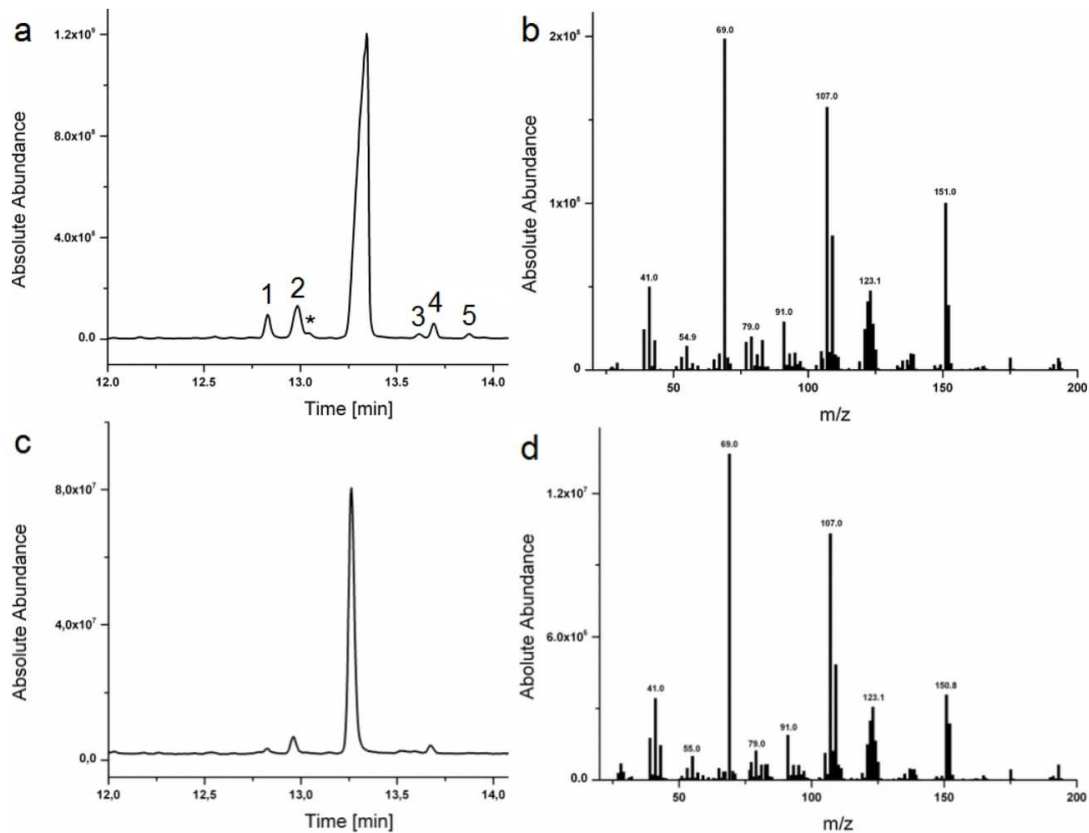


Fig. S5 GC-MS data of the α -damascone **8** conversion product by CYP109E1 (a and b) and by CYP267B1 (c and d) identified as 3-hydroxy- α -damascone **23** (Litzenburger et al. 2016). 1-5 are the minor products with known masses (Table S1). Impurity is labelled with “*”

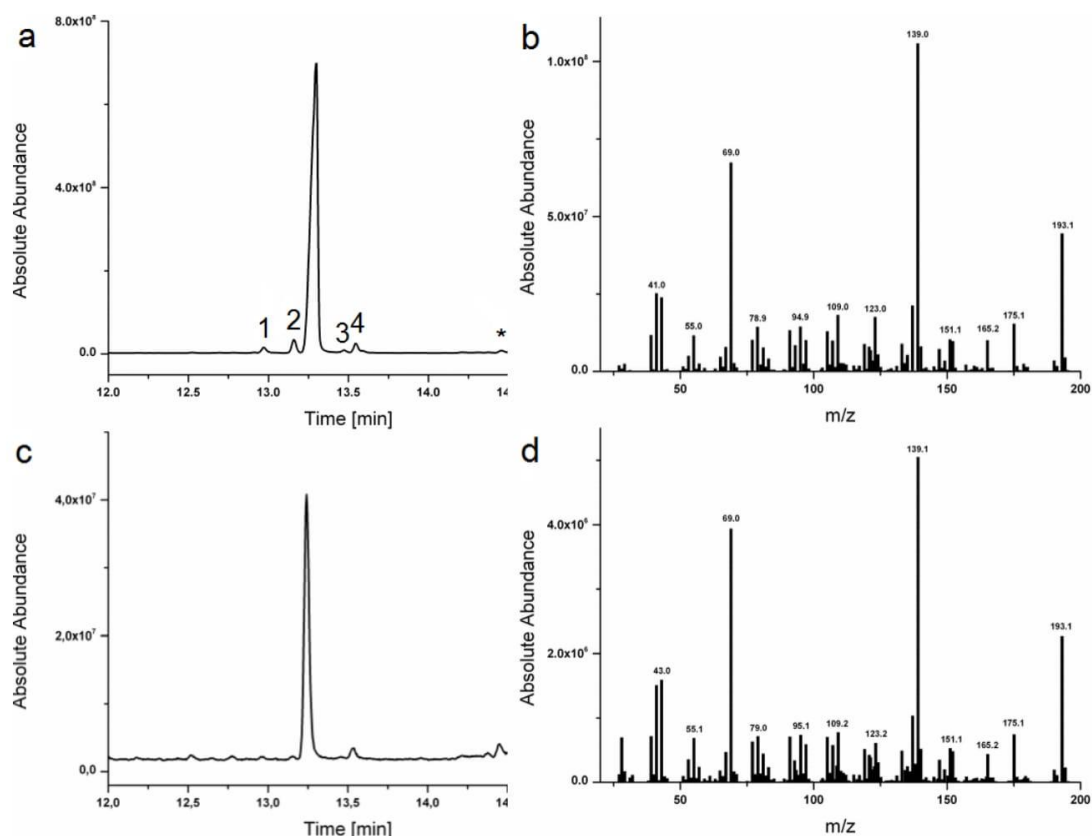
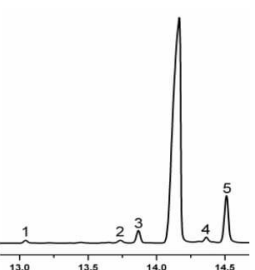
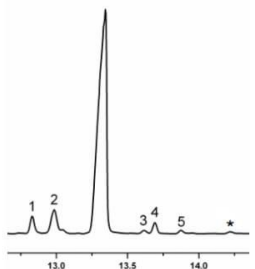
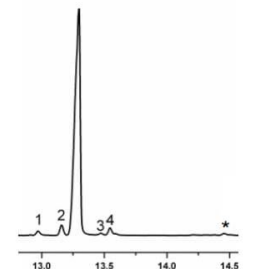
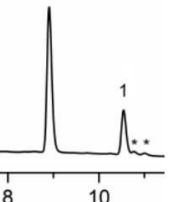
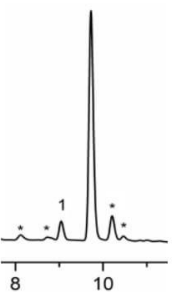
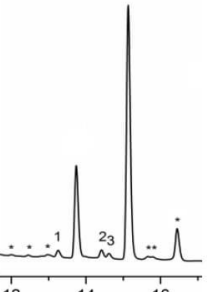
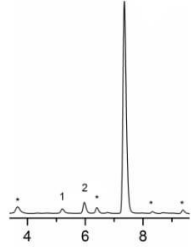
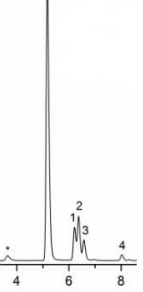


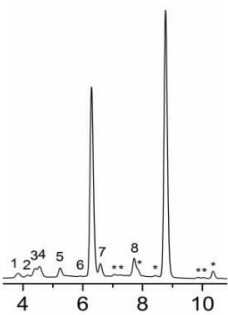
Fig. S6 GC-MS data of the β -damascone **9** conversion product by CYP109E1 (a and b) and by CYP267B1 (c and d) identified as 4-hydroxy- β -damascone **24** (Litzenburger et al. 2016). 1-4 are the minor products with known masses (Table S1). Impurity is labelled with “*”

Table S1 Selectivity of the CYP109E1-catalyzed reactions *in vitro* and masses of the reaction products. Minor products are numbered and labelled. “*” indicates impurities

Compound		product	t_R [min]	$\Delta m/z$	Selectivity [%]
α -ionone		1	13.5	+16	1.1
		2	13.6	+16	5.2
		3	13.9	+14	6.2
		4	14.1	+16	1.4
		5	14.4	+16	1.1
		3-hydroxy- α -ionone	13.7	+16	85

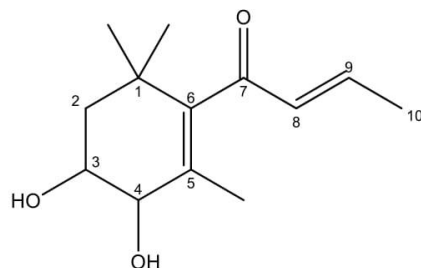
β -ionone		<table border="1"> <tbody> <tr><td>1</td><td>13.0</td><td>+16</td><td>0.6</td></tr> <tr><td>2</td><td>13.7</td><td>+16</td><td>0.7</td></tr> <tr><td>3</td><td>13.9</td><td>+16</td><td>2.6</td></tr> <tr><td>4</td><td>14.4</td><td>+16</td><td>1.3</td></tr> <tr><td>5</td><td>14.5</td><td>+16</td><td>10.2</td></tr> <tr><td>4-hydroxy-β-ionone</td><td>14.2</td><td>+16</td><td>84.5</td></tr> </tbody> </table>				1	13.0	+16	0.6	2	13.7	+16	0.7	3	13.9	+16	2.6	4	14.4	+16	1.3	5	14.5	+16	10.2	4-hydroxy- β -ionone	14.2	+16	84.5
1	13.0	+16	0.6																										
2	13.7	+16	0.7																										
3	13.9	+16	2.6																										
4	14.4	+16	1.3																										
5	14.5	+16	10.2																										
4-hydroxy- β -ionone	14.2	+16	84.5																										
α -damascone		<table border="1"> <tbody> <tr><td>1</td><td>12.8</td><td>+16</td><td>3.6</td></tr> <tr><td>2</td><td>13.0</td><td>+16</td><td>7.4</td></tr> <tr><td>3</td><td>13.6</td><td>+16</td><td>0.6</td></tr> <tr><td>4</td><td>13.7</td><td>+14</td><td>2.1</td></tr> <tr><td>5</td><td>13.9</td><td>+16</td><td>0.8</td></tr> <tr><td>3-hydroxy-α-damascone</td><td>13.3</td><td>+16</td><td>85.4</td></tr> </tbody> </table>				1	12.8	+16	3.6	2	13.0	+16	7.4	3	13.6	+16	0.6	4	13.7	+14	2.1	5	13.9	+16	0.8	3-hydroxy- α -damascone	13.3	+16	85.4
1	12.8	+16	3.6																										
2	13.0	+16	7.4																										
3	13.6	+16	0.6																										
4	13.7	+14	2.1																										
5	13.9	+16	0.8																										
3-hydroxy- α -damascone	13.3	+16	85.4																										
β -damascone		<table border="1"> <tbody> <tr><td>1</td><td>13.0</td><td>+16</td><td>1.6</td></tr> <tr><td>2</td><td>13.2</td><td>+14</td><td>2.7</td></tr> <tr><td>3</td><td>13.5</td><td>+16</td><td>0.4</td></tr> <tr><td>4</td><td>13.6</td><td>+16</td><td>2.4</td></tr> <tr><td>4-hydroxy-β-damascone</td><td>13.3</td><td>+16</td><td>92.8</td></tr> </tbody> </table>				1	13.0	+16	1.6	2	13.2	+14	2.7	3	13.5	+16	0.4	4	13.6	+16	2.4	4-hydroxy- β -damascone	13.3	+16	92.8				
1	13.0	+16	1.6																										
2	13.2	+14	2.7																										
3	13.5	+16	0.4																										
4	13.6	+16	2.4																										
4-hydroxy- β -damascone	13.3	+16	92.8																										
compactin		<table border="1"> <tbody> <tr><td>1</td><td>10.6</td><td>+16</td><td>23</td></tr> <tr><td>pravastatin</td><td>8.9</td><td>+16</td><td>77</td></tr> </tbody> </table>				1	10.6	+16	23	pravastatin	8.9	+16	77																
1	10.6	+16	23																										
pravastatin	8.9	+16	77																										

lovastatin		1 6'β-hydroxy-lovastatin	9.1 9.8	+16 +16	6 94
simvastatin		1 2 3 3'α-hydroxy-simvastatin 4''-hydroxy-simvastatin	13.3 14.4 14.6 13.8 15.2	+16 +16 +14 +16 +16	4.7 5 3 23 64
nootkatone		1 2 11,12-epoxy-nootkatone	5.2 5.9 7.4	+16 +16 +16	1.2 6.2 92.6
isolongifolen-9-one		1 2 3 4 4(R)-hydroxy-isolongifolen-9-one	6.3 6.4 6.6 8.1 5.3	+16 +16 +16 +14 +16	6.5 10.6 4.4 1.3 77.2

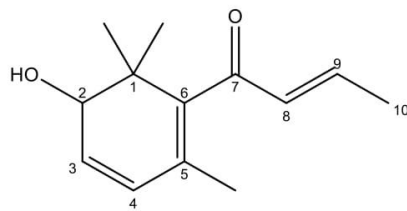
β -damascenone		1	3.8	+32	1.6
		2	4.1	+32	0.8
		3	4.4	+32	2
		4	4.5	+32	3
		5	5.3	+18	1.6
		6	5.9	+14	0.5
		7	6.6	+16	3
		8	7.7	+16	3.6
		2-hydroxy- β -damascenone	6.4	+16	35.3
		3,4-epoxy β -damascone	8.7	+16	48.7

Data S7: NMR data of investigated compounds

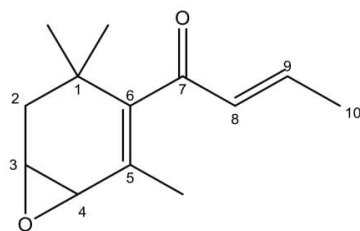
3,4-dihydroxy- β -damascone 27: ^1H NMR (CDCl_3 , 500 MHz): 6.74 (dq, 1H, $J=15.8, 6.9$ Hz, H9), 6.13 (dq, 1H, $J=15.8, 1.6$ Hz, H8), 3.94 (d, 1H, $J=7.9$ Hz, H4), 3.87 (ddd, 1H, $J=12.2, 8.1, 3.8$ Hz, H3), 1.91 (dd, 3H, $J=6.9, 1.6$ Hz, H10), 1.74-1.63 (m, 2H, H2a and H2b), 1.60 (d, 3H, $J=1.0$ Hz, C5-Me), 1.17 (s, 3H, C1-Me), 0.96 (s, 3H, C1-Me); ^{13}C NMR (CDCl_3 , 125 MHz): 200.23 (C7), 146.77 (C9), 142.14 (C6), 133.81 (C8), 129.89 (C5), 76.88 (C4), 71.08 (C3), 44.88 (C2), 36.15 (C1), 29.85 (C1-Me), 28.70 (C1-Me), 18.46 (C10), 15.88 (C5-Me).



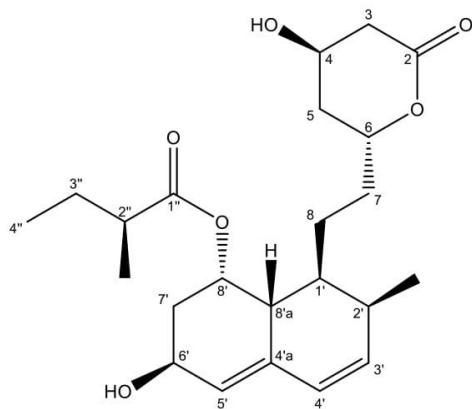
2-hydroxy- β -damascenone 25: ^1H NMR (CDCl_3 , 500 MHz): 6.81 (dq, 1H, $J=15.7, 6.9$ Hz, H9), 6.17 (dq, 1H, $J=15.7, 1.6$ Hz, H8), 5.97 (dd, 1H, $J=9.5$ Hz, 4.7 Hz, H3), 5.87 (d, 1H, $J=9.5$ Hz, H4), 3.80 (d, 1H, $J=4.8$ Hz, H2), 1.92 (dd, 3H, $J=6.9$ Hz, 1.6 Hz, H10), 1.65 (s, 3H, C5-Me), 1.08 (s, 6H, C1-Me (2x)); ^{13}C NMR (CDCl_3 , 125 MHz): 200.34 (C7), 146.98 (C9), 140.05 (C6), 134.28 (C8), 129.15 (C3), 129.06 (C4), 126.80 (C5), 73.79 (H2), 39.21 (C1), 24.69 (C1-Me), 19.37 (C1-Me), 19.24 (C5-Me), 18.93 (C10).



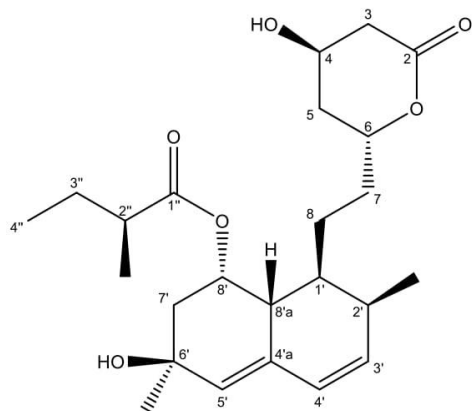
3,4-epoxy β-damascone 26: ¹H NMR (CDCl₃, 500 MHz): 6.73 (dq, 1H, J= 15.7, 6.9 Hz, H9), 6.13 (dq, 1H, J= 15.7, 1.6 Hz, H8), 3.50 (ddd, J=6.6, 4.3, 2.3 Hz, H3), 3.13 (d, 1H, J= 4.3 Hz, H4), 1.98 (dd, J= 14.6, 2.5 Hz, 1H, H2a), 1.91 (dd, 3H, J= 7.0, 1.5 Hz, H10), 1.74-1.63 (m, 1H, H2b), 1.61 (d, 3H, J= 1.0 Hz, C5-Me), 1.16 (s, 3H, C1-Me), 0.96 (s, 3H, C1-Me); ¹³C NMR (CDCl₃, 125 MHz): 200.14 (C7), 147.59 (C9), 144.74 (C6), 133.89 (C8), 127.03 (C5), 54.24 (C4), 51.20 (C3), 37.90 (C2), 33.95 (C1), 32.12 (C1-Me), 29.55 (C1-Me), 19.83 (C10), 18.50 (C5-Me).



Pravastatin 14: ¹H NMR (500 MHz, CDCl₃): 5.98 (d, 1H, J=9.7 Hz, H4'), 5.87 (dd, 1H, J= 9.7, 5.9 Hz, H3'), 5.55 (br s, 1H, H5'), 5.39 (br s, 1H, H8'), 4.62-4.56 (m, 1H, H6), 4.42-4.34 (m, 2H, H6', H4), 2.72 (dd, 1H, J= 17.6, 5.1 Hz, H3a), 2.60 (ddd, J= 17.6, 3.7, 1.6 Hz, H3b), 2.55 (m, 1H, H7), 2.40-2.30 (m, 3H, H2', H8'a, H2''), 1.93-1.90 (m, 1H, H5a), 1.85 (m, 1H, H7a), 1.70-1.62 (m, 3H, H1', H5b, H3''a), 1.44-1.37 (m, 3H, H8, H3''b), 1.28-1.24 (m, 1H, H7b), 1.09 (d, 3H, J=7.0 Hz, C2''-Me), 0.88 (d, 3H, J= 7.0 Hz, C2'-Me), 0.87 (t, 3H, J=7.4 Hz, H4''); ¹³C NMR (125 MHz, CDCl₃): 176.29 (C1''), 169.94 (C2), 135.79 (C3'), 135.29 (C4'a), 127.39 (C4'), 126.12 (C5'), 75.93 (C6), 69.04 (C8'), 65.04 (C6'), 62.75 (C4), 41.58 (C2''), 38.59 (C3), 37.60 (C8'a), 36.69 (C7'), 36.60 (C1'), 36.18 (C5), 32.75 (C7), 30.95 (C2''), 26.64 (C3''), 23.76 (C8), 16.80 (C2''-Me), 13.56 (C2'-Me), 11.76 (C4'').

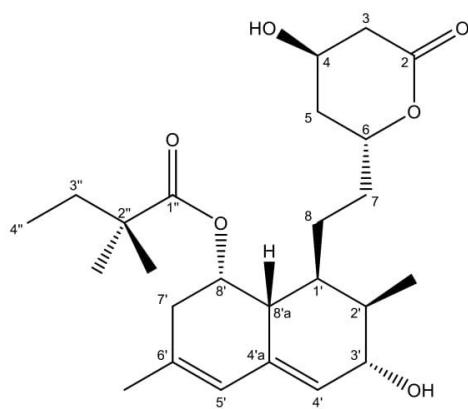


6'β-hydroxy-lovastatin 15: ^1H NMR (500 MHz, CDCl_3): 5.96 (d, 1H, $J=10.0$ Hz, H4'), 5.89 (dd, 1H, $J=10.0, 6.1$ Hz, H3'), 5.43 (br s, 1H, H5'), 5.39 (m, 1H, H8'), 4.62-4.55 (m, 1H, H6'), 4.37-4.32 (m, 1H, H4), 2.70 (dd, 1H, $J=17.6, 5.1$ Hz, H3a), 2.60 (ddd, 1H, $J=17.6, 3.8, 1.7$ Hz, H3b), 2.42-2.29 (m, 5H, H7', H2', H8'a, H2''), 1.96-1.80 (m, 2H, H5a, H7a), 1.70-1.60 (m, 3H, H1', H5b, H3''a), 1.44-1.38 (m, 3H, H8, H3''b), 1.32 (s, 3H, C6'-Me), 1.29-1.24 (m, 1H, H7b), 1.10 (d, 3H, $J=6.9$ Hz, C2''-Me), 0.87 (d, 3H, $J=7.2$ Hz, C2'-Me), 0.86 (t, 3H, $J=7.4$ Hz, H4''); ^{13}C NMR (125 MHz, CDCl_3): 176.41 (C1''), 170.12 (C2), 135.88 (C3'), 133.48 (C4'a), 129.64 (C5'), 127.58 (C4'), 76.05 (C6), 68.92 (C8'a), 68.77 (C6'), 62.71 (C4), 42.18 (C7'), 41.41 (C2''), 38.54 (C3), 37.41 (C8'a), 36.34 (C5), 36.17 (C6), 32.69 (C7), 30.75 (C6'-Me), 30.55 (C2''), 26.82 (C3''), 24.00 (C8), 16.25 (C2''-Me), 13.55 (C2'-Me), 11.71 (C4'').

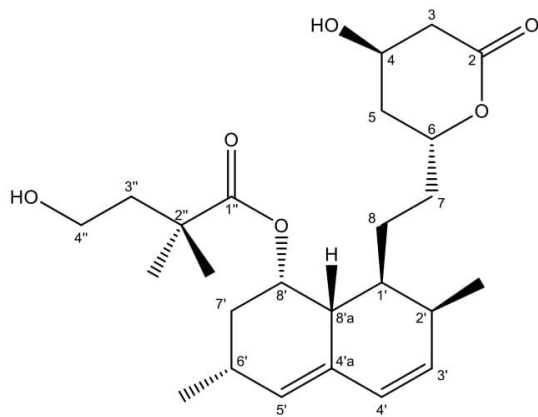


3'α-hydroxy-simvastatin 16: ^1H NMR (500 MHz, CDCl_3): 5.87 (s, 1H, H5'), 5.60 (d, 1H, $J=4.7$ Hz, H4'), 5.37 (d, 1H, $J=2.6$ Hz, H8'), 4.67-4.60 (m, 1H, H6), 4.38-4.34 (m, 1H, H4), 3.92 (d, 1H, $J=4.7$ Hz, H3'), 2.72 (dd, 1H, $J=17.6, 5.1$ Hz, H3a), 2.60 (ddd, 1H, $J=17.6, 3.8, 1.6$ Hz, H3b), 2.38 (d, 1H, $J=17.1$

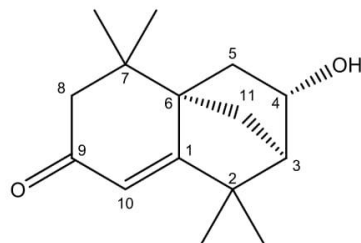
Hz, H7'a), 2.21 (dd, 1H, J= 18.9, 1.9 Hz, H7'b), 2.02-1.91 (m, 3H, H5a, H2' H8'a), 1.80-1.65 (m, 4H, H5b, H1', H8a, H7a), 1.71 (s, 3H, C6'-Me), 1.54-1.44 (m, 4H, H7b, H8b, H3''), 1.07 (s, 3H, C2''-Me), 1.06 (s, 3H, C2''-Me), 0.76 (t, 3H, J=7.5 Hz, C4''), 0.74 (d, 3H, J=7.2 Hz, C2'-Me); ^{13}C NMR (125 MHz, CDCl_3): 177.75 (C1''), 170.24 (C2), 137.52 (C6'), 134.06 (C4'a), 124.24 (C5'), 122.38 (C4'), 76.12 (C6), 70.11 (C3'), 67.46 (C8'), 62.76 (C4), 42.93 (C2''), 39.69 (C8'a), 38.58 (C3), 36.37 (C5), 36.33 (C7'), 35.48 (C2'), 33.23 (C7), 33.19 (C3''), 31.33 (C1'), 24.93 (C2''-Me), 24.93 (C8) 24.38 (C2''-Me), 23.29 (C6'-Me), 10.57 (C2'-Me), 9.26 (C4'').



4''-hydroxy-simvastatin 17: ^1H NMR (500 MHz, CDCl_3): 5.97 (d, 1H, J= 9.7 Hz, H4'), 5.76 (dd, 1H, J= 9.6, 6.1 Hz, H3'), 5.49 (br s, 1H, H5'), 5.33 (q, 1H, J= 3.3, 2.9 Hz, H8'), 4.65-4.59 (m, 1H, H6), 4.33-4.30 (m, 1H, H4), 3.70-3.65 (m, 1H, H4''), 3.64- 3.59 (m, 1H, H4''), 2.74 (dd, 1H, J= 17.7, 5.4 Hz, H3a), 2.58 (ddd, 1H, J=17.7, 4.1, 1.5 Hz, H3b), 2.43-2.39 (m, 1H, H6'), 2.37-2.32 (m, 1H, H2'), 2.25 (dd, 1H, J= 11.8, 2.6 Hz, H8'a), 1.98-1.89 (m, 4H, H7', H5a, H3''a), 1.96-1.89 (m, 1H, H7a), 1.79-1.66 (m, 3H, H5b , H1', H3''b), 1.48 -1.39 (m, 1H, H8a), 1.38-1.34 (m, 2 H, H8b, H7b), 1.18 (s, 3H, C2''-Me), 1.16 (s, 3H, C2''-Me), 1.06 (d, 3H, J= 7.4 Hz, C6'-Me), 0.86 (d, 3H, J= 7.0, C2'-Me); ^{13}C NMR (125 MHz, CDCl_3): 178.58 (C1''), 170.64 (C2), 132.93 (C3'), 131.39 (C4'a), 129.62 (C5'), 128.32 (C4'), 76.29 (C6), 68.87 (C8'), 62.44 (C4), 59.42 (C4''), 42.54 (C3''), 41.53 (C2''), 38.46 (C3), 37.39 (C8'a), 36.88 (C1'), 35.88 (C5), 32.59 (C7'), 32.56 (C7), 30.61 (C2'), 27.23 (C6'), 26.23 (C2''-Me), 24.93 (C2''-Me), 24.19 (C8), 23.08 (C6'-Me), 13.81 (C2'-Me).



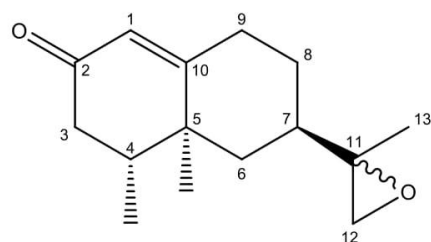
4(R)-hydroxy-isolongifolen-9-one 22: ^1H NMR (CDCl_3 , 500 MHz): 5.70 (s, 1H, H10), 4.31 (brd, 1H, J=6.6 Hz, H4), 2.31 (d, 1H, J= 16.2 Hz, H8a), 2.06 (dd, 1H, J= 16.2, 0.8 Hz, H8b), 1.95 (brs, 1H, H3), 1.80 (ddd, 1H, J= 13.0, 6.6, 2.6 Hz, H5a), 1.73 (ddd, 1H, J= 13.0, 2.1, 1.0 Hz, H5b), 1.59 (m, 2H, H11), 1.11 (s, 3H, C2-Me), 1.09 (s, 3H, C2-Me), 1.06 (s, 3H, C7-Me), 0.97 (s, 3H, C7-Me); ^{13}C NMR (CDCl_3 , 125 MHz): 199.81 (C9), 181.71 (C1), 117.58 (C10), 70.30 (C4), 57.96 (C6), 54.42 (C3), 49.81 (C8), 42.10 (C2), 40.16 (C5), 34.10 (C7), 32.82 (C11), 27.20 (C2-Me), 25.90 (C7-Me), 25.28 (C7-Me), 24.25 (C2-Me).



11(R), 12-epoxy-nootkatone 20: ^1H NMR (CDCl_3 , 500 MHz): 5.73 (brs, 1H, H1), 2.62 (m, 1H, H12a), 2.56 (m, 1H, H12b), 2.42 (m, 1H, H9a), 2.35 (m, 1H, H9b), 2.23 (m, 2H, H3), 2.02 (m, 1H, H6a), 1.99 (m, 1H, H7), 1.88 (m, 1H, H8a), 1.60 (m, 1H, H4), 1.22 (m, 1H, H8b), 1.22 (s, 3H, H13), 1.10 (m, 1H, H6b), 1.04 (s, 3H, C5-Me), 0.96 (d, 3H, J=6.7 Hz, C4-Me); ^{13}C NMR (CDCl_3 , 125 MHz): 199.50 (C2), 168.80 (C10), 124.87 (C1), 58.91 (C11), 53.33 (C12), 42.01 (C3), 40.50 (C7), 40.43 (C6), 39.60 (C4) 39.01 (C5), 32.43 (C9), 28.79 (C8), 17.73 (C13), 16.74 (C5-Me), 14.89 (C4-Me).

11(S), 12-epoxy-nootkatone 21: ^1H NMR (CDCl_3 , 500 MHz): 5.73 (brs, 1H, H1), 2.63 (m, 1H, H12a), 2.57 (m, 1H, H12b), 2.42 (m, 1H, H9a), 2.35 (m, 1H, H9b), 2.23 (m, 2H, H3), 1.99 (m, 1H, H7), 1.97 (m, 1H, H8a), 1.90 (m, 1H, H6a), 1.58 (m, 1H, H4), 1.29 (m, 1H, H8b), 1.24 (s, 3H, H13), 1.04 (s, 3H, C5-

Me), 1.00 (m, 1H, H6b), 0.94 (d, 3H, J=6.7 Hz, C4-Me); ^{13}C NMR (CDCl_3 , 125 MHz): 199.40 (C2), 168.87 (C10), 124.87 (C1), 59.13 (C11), 53.65 (C12), 42.01 (C3), 40.74 (C6), 40.44 (C7), 39.42 (C4) 38.97 (C5), 32.38 (C9), 28.37 (C8), 18.04 (C13), 16.74 (C5-Me), 14.89 (C4-Me).



2.4 Milhim et al. 2016

Identification of a new plasmid-encoded cytochrome P450 CYP107DY1 from *Bacillus megaterium* with a catalytic activity towards mevastatin

Mohammed Milhim, Natalia Putkaradze, Ammar Abdulkhugni, Fredy Kern, Philip Hartz, Rita Bernhardt

2016, Journal of Biotechnology. 240:68-75

DOI: 10.1016/j.biote.2016.11.002

Reprinted with the permission of Elsevier.



Identification of a new plasmid-encoded cytochrome P450 CYP107DY1 from *Bacillus megaterium* with a catalytic activity towards mevastatin

Mohammed Milhim, Natalia Putkaradze, Ammar Abdulkhugni, Fredy Kern, Philip Hartz, Rita Bernhardt*

Institute of Biochemistry, Saarland University, 66123 Saarbrücken, Germany



ARTICLE INFO

Article history:

Received 2 September 2016

Received in revised form 28 October 2016

Accepted 1 November 2016

Available online 2 November 2016

Keywords:

Bacillus megaterium

CYP107 family

Bacterial cytochrome P450

Mevastatin

Pravastatin

BmCPR

Fdx2

ABSTRACT

In the current work, we describe the identification and characterization of the first plasmid-encoded P450 (CYP107DY1) from a *Bacillus* species. The recombinant CYP107DY1 exhibits characteristic P450 absolute and reduced CO-bound difference spectra. Reconstitution with different redox systems revealed the autologous one, consisting of BmCPR and Fdx2, as the most effective one. Screening of a library of 18 pharmaceutically relevant compounds displayed activity towards mevastatin to produce pravastatin. Pravastatin is an important therapeutic drug to treat hypercholesterolemia, which was described to be produced by oxyfunctionalization of mevastatin (compactin) by members of CYP105 family. The hydroxylation at C6 of mevastatin was also suggested by docking this compound into a computer model created for CYP107DY1. Moreover, in view of the biotechnological application, CYP107DY1 as well as its redox partners (BmCPR and Fdx2) were successfully utilized to establish an *E. coli* based whole-cell system for an efficient biotransformation of mevastatin. The *in vitro* and *in vivo* application of the CYP107DY1 also offers the possibility for the screening of more substrates, which could open up further biotechnological usage of this enzyme.

© 2016 Elsevier B.V. All rights reserved.

1. Introduction

Selective oxyfunctionalization of nonactivated carbon-hydrogen bonds represents a challenge in the industrial field. In general, the use of chemical methods has many disadvantages such as hazardous conditions, cost-efficiency and the lack of chemo-, stereo-, and regioselectivity. Therefore, in the last years many efforts have been carried out in the search for selective and efficient enzymatic systems that are able to incorporate oxygen into nonactivated carbon-hydrogen bonds. Cytochromes P450 (P450s) [E.C.1.14.-] are heme-iron containing enzymes that catalyze the monooxygenation of various nonactivated hydrocarbons with high regio-, stereo- and enantioselectivity including the biosynthesis of hormones, signal molecules, defense-related chemicals and secondary metabolites in addition to their central role in the metabolism of endogenous (steroids and fatty acids) and exogenous (drugs and toxins) substances (Bernhardt, 2006;

Bernhardt and Urlacher, 2014). They are found in all kingdoms of life including mammals, plants, insects, fungi, archaea, and bacteria (except *E. coli*) as well as in viruses. In eukaryotes, they are mostly integral membrane-bound proteins, whereas prokaryotic P450 systems are more likely soluble and located in the cytoplasm. P450s rely for their activities on redox partners. Based on the composition of the redox partner involved in the transfer of electrons, the P450 systems can be categorized into different classes (Hannemann et al., 2007) of which the most researched ones are the classes I and II. Class I contains the bacterial and the eukaryotic mitochondrial P450s, which obtain electrons from NADPH using two proteins, a flavin adenine dinucleotide (FAD)-containing ferredoxin reductase and an iron-sulfur containing ferredoxin. Class II comprises the eukaryotic microsomal P450s, which obtain electrons from NADPH via a FAD and FMN-containing P450 reductase.

The numbers of the newly identified P450s increased drastically over the past few years (Nelson, 2009), but there is nevertheless a still growing demand to exploit novel P450s as a valuable biocatalyst in the industrial field.

Bacillus megaterium is a nonpathogenic, aerobic, Gram-positive rod-shaped bacterium. Due to its high protein production capacity, plasmid stability and the ability to take up a variety of hydrophobic

* Corresponding author at: Institute of Biochemistry, Campus B2.2, Saarland University, D-66123 Saarbrücken, Germany.

E-mail address: ritabern@mx.uni-saarland.de (R. Bernhardt).

substrates, *B. megaterium* gained throughout the last decades a lot of interest in the industrial field for the production of biotechnologically relevant substances (Bunk et al., 2010). The publication of the complete genome sequence of the *B. megaterium* strains QM B1551 and DSM319 in 2011 (Eppinger et al., 2011) enabled the identification of new proteins. Among them are cytochromes P450 and a NADPH dependent diflavin reductase, which have been shown to be very important for biotechnological and pharmaceutical applications (Brill et al., 2013; Milhim et al., 2016). *B. megaterium* encodes for several P450s. The self-sufficient CYP102A1 (also known as BM3) is the most investigated bacterial P450 so far, which has been used and redesigned to catalyze the oxidation of a variety of biotechnologically interesting substances (Whitehouse et al., 2012). In addition, the biotechnologically valuable CYP106 family, CYP106A1 from *B. megaterium* strain DSM319 (Brill et al., 2013) and CYP106A2 from *B. megaterium* strain ATCC 13368 (Berg et al., 1976, 1979), was characterized to be associated with the biotransformation of a diverse array of substrates such as steroids and terpenoid substances (Brill et al., 2013; Schmitz et al., 2012). Furthermore, CYP109E1 was recently identified from *B. megaterium* strain DSM319 as steroid hydroxylase (Józwik et al., 2016).

In this study, we report the identification and characterization of a new plasmid-encoded P450 from the *B. megaterium* QM B1551. The bioinformatic analysis of the new P450 showed that it belongs to the CYP107 family. It was successfully cloned and expressed in *E. coli*. Screening of a potential substrates showed that CYP107DY1 possesses hydroxylation activity towards mevastatin.

2. Materials and methods

2.1. Strains, expression vectors, enzymes, and chemicals

E. coli TOP10 from Invitrogen (Karlsruhe, Germany) was used for cloning experiments. *E. coli* C43 (DE3) and the expression vector pET17b, both from Novagen (Darmstadt, Germany), were used for recombinant gene expression. Substrates were obtained from TCI (Eschborn, Germany). Pravastatin lactone was from Santa Cruz Biotechnology (Heidelberg, Germany). All other chemicals were purchased from Sigma-Aldrich (Schnelldorf, Germany).

2.2. Cloning of the gene encoding CYP107DY1

For protein purification purposes, the DNA fragment encoding the full length CYP107DY1 (Supplementary Fig. S1) was synthesized (Genart, Regensburg, Germany) and cloned into the expression vector pET17b with the *Nde*I/*Kpn*I restriction sites. For purification with IMAC, the 3'end of the gene was extended with a sequence coding for six histidines. Plasmid was verified by sequencing.

2.3. Heterologous gene expression and purification of CYP107DY1, reductases and ferredoxins

For heterologous gene expression, *E. coli* C43 (DE3) cells were co-transformed with the expression vector pET17b congaing the sequence for CYP107DY1 and the chaperone GroEL/GroES-encoding plasmid pGro12, which has a kanamycin resistance gene (Brixius-Anderko et al., 2015; Nishihara et al., 1998). Cultures were grown at 37 °C to an optical density of 0.6 in 200 ml TB medium containing the suitable antibiotics. The expression of the protein was induced by adding 1 mM IPTG, the synthesis of heme was enhanced by addition of 1 mM heme precursor δ-ALA. The cells were grown at 28 °C and 180 rpm for 24 h.

For purification, cell pellets were sonicated in 50 ml lysis buffer (50 mM potassium phosphate pH 7.4, 20% glycerol, 0.1 mM DTE, 500 mM sodium acetate, and 0.1 mM PMSF). After centrifugation

at 30,000g for 30 min at 4 °C, the supernatant was applied on a Ni-NTA agarose column equilibrated with lysis buffer. The column was washed with 100 ml equilibration buffer supplemented with 40 mM imidazole followed by 20 ml elution buffer supplemented with 200 mM imidazole (50 mM potassium phosphate pH 7.4, 20% glycerol, 0.1 mM DTE, and 0.1 mM PMSF). The eluted protein was dialyzed against elution buffer without imidazole, concentrated and stored at -80 °C.

The *B. megaterium* redox system BmCPR and Fdx2 were purified as reported previously (Brill et al., 2013; Milhim et al., 2016). The purification of the redox system from the fission yeast *Schizosaccharomyces pombe* Arh1 and Etp1^{fd} was carried out as described before (Bureik et al., 2002; Ewen et al., 2008). Recombinant bovine AdR and the Adx₄₋₁₀₈ (truncated form of Adx comprising amino acids 4-108) were purified as mentioned elsewhere (Sagara et al., 1993; Uhlmann et al., 1992).

The concentration of recombinant P450 was estimated using the CO-difference spectral assay as described previously with $\epsilon_{450-490} = 91 \text{ mM}^{-1} \text{ cm}^{-1}$ (Omura and Sato, 1964). The concentration of BmCPR was quantified by measuring the flavin absorbance at 456 nm with $\epsilon_{456} = 21 \text{ mM}^{-1} \text{ cm}^{-1}$ for the oxidized enzyme (Milhim et al., 2016). The concentrations of the AdR and Arh1 were measured using the extinction coefficient $\epsilon_{450} = 11.3 \text{ mM}^{-1} \text{ cm}^{-1}$ (Ewen et al., 2008; Hiwatashi et al., 1976). The concentrations of Fdx2 and Etp1^{fd} were measured using the extinction coefficient $\epsilon_{390} = 6.671 \text{ mM}^{-1} \text{ cm}^{-1}$ and $\epsilon_{414} = 9.8 \text{ mM}^{-1} \text{ cm}^{-1}$, respectively (Brill et al., 2013; Schiffler et al., 2004).

2.4. Investigation of electron transfer partners

The functional interaction of the electron transfer partners for a particular P450 can be determined by recording the NADPH reduced CO-complex peak at 450 nm when P450 was coupled with the different ferredoxins/ferredoxin reductases in the absence of substrate. For this, CYP107DY1 was mixed with ferredoxins (Fdx2, Etp1^{fd} or Adx₄₋₁₀₈) and ferredoxin reductases (BmCPR, Arh1 or AdR) with ratios of 1:40:5 μM [CYP107DY1:ferredoxin:ferredoxin reductase] in 50 mM HEPES buffer pH 7.4 and NADPH was added to a final concentration of 1 mM. The spectrum of NADPH-reduced samples was recorded after bubbling the sample with carbon monoxide (CO) gas. The reduction efficiency of the redox partners was then evaluated by comparing the peak at 450 nm of the CO-complexed CYP107DY1 reduced with the different redox systems and the peak at 450 nm of the CO-complexed CYP107DY1 reduced with sodium-dithionite.

2.5. In vitro conversion and HPLC analysis

The in vitro conversion of the substrates was carried out with a reconstituted system at 30 °C in conversion buffer (50 mM HEPES, pH 7.4, 20% glycerol). The reconstituted system contained 0.5 μM CYP107DY1, 2.5 μM BmCPR, 20 μM Fdx2, 1 mM MgCl₂, 5 mM glucose-6-phosphate, 1 U glucose-6-phosphate dehydrogenase for NADPH regeneration and 100 μM substrate. The reaction was started by adding NADPH (200 μM) and stopped after 15 min by the addition of 1 vol ethyl acetate and extracted twice. The organic phase was evaporated under vacuum. Residuum was dissolved in 20% acetonitrile/water mixture and subjected to HPLC analysis. HPLC analysis was performed using a Jasco system. A reversed-phase ec MN Nucleodur C18 (4.0 × 125 mm) column (Macherey-Nagel) was used for all experiments at an oven temperature of 40 °C. Mevastatin and its metabolite pravastatin were eluted from the column using a gradient of acetonitrile from 20 to 100% in water over 20 min. The detection wavelength of mevastatin and its metabolite pravastatin was 236 nm.

2.6. Circular dichroism (CD) spectroscopy

Circular dichroism (CD) spectra were recorded at 30 °C using a JASCO J-715 spectropolarimeter over the wavelength range 190–260 nm for the far-UV region and 300–500 nm for the near-UV/Vis region at a protein concentration of 2 μM (~0.1 mg/ml) and 20 (~1 mg/ml), respectively, dissolved in 10 mM potassium phosphate buffer pH 7.4 with the following parameters: path-length of 0.1 cm for the far-UV region and 1 cm for the near-UV/Vis region measurement, data pitch of 0.1 nm, band width of 5 nm, accumulation 3 times. Spectra were recorded in triplicate and averaged.

2.7. Homology modeling of CYP107DY1 and molecular docking with mevastatin

Using the homology modeling program Modeller 9.14 (University of California San Francisco, USA), a model of CYP107DY1 was calculated using CYP107RB1 (Vdh) (PDB accession code: 3A4G) as template. The coordinates of the heme-porphyrin atoms from the template structure were added subsequently to the obtained homology model. No further structural refinement of the model was performed.

The three dimensional structure of the mevastatin molecule was obtained from PubChem (Kim et al., 2016). The docking simulations of the homology model of CYP107DY1 with the mevastatin molecule were carried out using Autodock 4.0 (Morris et al., 2009). The Windows version 1.5.6 of Autodock Tools was used to compute Kollman charges for the enzyme and Gasteiger-Marsili charges for the ligand (Sanner, 1999). 200 docking runs were carried out applying the Lamarckian genetic algorithm using default parameter settings.

2.8. In vivo whole-cell biotransformation

For the establishment of a CYP107DY1-dependent whole-cell system, a tricistronic pET17b-based vector, encoding the CYP107DY1-BmCPR-Fdx2 genes, was constructed. CYP107DY1 coding sequence was amplified and cloned via the restriction sites *Nde*I/*Hind*III. The resulting vector (pET17b-CYP107DY1) served then as a backbone for the cloning of BmCPR, which was amplified via PCR and cloned with the restriction sites *Bam*HI/*Not*I. Fdx2 coding region was PCR amplified and cloned downstream CYP107DY1-BmCPR using the restriction sites *Not*I/*Xba*I. All resulting vectors were verified by sequencing.

E. coli C43 (DE3) cells were co-transformed with the suitable expression vector based on pET17b, coding for CYP107DY1-BmCPR-Fdx2, and the chaperone GroEL/GroES-coding plasmid pGro12, which has a kanamycin resistance gene (Brixius-Anderko et al., 2015; Nishihara et al., 1998). Transformed cells were grown overnight in 50 ml LB broth medium supplemented with 100 μg/ml ampicillin and 50 μg/ml kanamycin at 37 °C and shaking at 180 rpm. For the expression of proteins, 50 ml TB medium containing 100 μg/ml ampicillin and 50 μg/ml kanamycin were inoculated (1:100) with the transformed cells and cultivated at 37 °C with rotary shaking at 140 rpm. Protein expression was induced at OD₆₀₀ = 0.6–0.8 with 1 mM IPTG, 4 mg/ml arabinose (for induction of GroES/GroEL expression) and 1 mM δ-ALA as heme precursor. The temperature was then reduced to 28 °C. After incubation for 24 h, cells were harvested by centrifugation (4000 g) for 20 min at 4 °C and washed once with 1 vol of conversion buffer (50 mM potassium phosphate buffer (pH 7.4) supplemented with 2% glycerol). After a second centrifugation, the cell pellets were resuspended in conversion buffer to an end cell-suspension concentration of 60 g wet cell weight (wcw)/L buffer. The substrate mevastatin was added to a final concentration of 100 μM and the culture was incubated for the indicated time at 30 °C and 140 rpm

for 20 h. To enable higher substrate conversion, EDTA (20 mM) or polymyxin B (32 μg/ml) was added to increase permeability and substrate uptake of the *E. coli* cells (Janocha and Bernhardt, 2013; Kern et al., 2016). Substrate was extracted twice with the same volume of ethyl acetate and the organic phase was evaporated using a rotary evaporator. After that, the residues were dissolved in the high performance liquid chromatography (HPLC) mobile phase (20% ACN) and subjected to HPLC analysis using the same method mentioned in Section 2.5.

3. Results and discussion

3.1. Bioinformatic analysis

The publication of the complete genome sequence of the *B. megaterium* strains QM B1551 and DSM319 in 2011 (Eppinger et al., 2011) enabled the characterization of new proteins. Recently, we were able to identify and characterize different P450s and related proteins from the strain DSM319 (Brill et al., 2013; Gerber et al., 2015; Milhim et al., 2016). In contrast to the DSM319 strain, strain QM B1551 harbors seven indigenous plasmids (Eppinger et al., 2011). Sequence analysis of the indigenous plasmids showed that plasmid number 5 (pBM500) has an open reading frame (BMQ_pBM50008) containing 1233 base pairs, which encodes for a protein comprising 410 amino acids with a predicted molecular weight of about 46.742 kDa. The analysis of the BMQ_pBM50008 domains using the Pfam Database (Finn et al., 2016) for highly conserved motifs of the P450 family proved the presence of the heme-binding motif (F-x-x-G-x-x-C-x-G), the (A/G-G-x-E/D-T-T/S) motif in the I-helix and the (E-x-x-R) motif in the K-helix (Supplementary Fig. S1), suggesting its identification as a cytochrome P450.

Multiple sequence alignment showed that the protein sequence of BMQ_pBM50008 belongs to the CYP107 family. After submission of the protein sequence of BMQ_pBM50008 to the P450 nomenclature committee (Prof. Dr. David Nelson), it was found to match best to CYP107DA1 with 49% sequence identity and, therefore, was assigned as a new subfamily with the name CYP107DY1. CYP107 is the largest family among bacterial P450s comprising more than 2500 subfamily members (<https://cyped.biocatnet.de/sFam/107>). Besides the CYP105 family, members of the CYP107 family are shown to be the most studied bacterial P450s that participate in the degradation and biotransformation of a broad spectrum of xenobiotics as well as in secondary metabolite biosynthesis, and, therefore, are considered to be important for industrial biotechnology; for example CYP107BR1 from *Pseudomonas autotrophica* for the activation of Vitamin D₃ (Sakaki et al., 2011), CYP107E from *Micromonospora griseorubida* for mycinamicin biosynthesis (Inouye et al., 1994), and P450_{terf} (CYP107L) from *Streptomyces platensis* for the hydroxylation of terfenadine (Lombard et al., 2011).

CYP107DY1 is the first P450 found to be encoded on a bacillus sp. plasmid. There are only few examples of plasmid-encoded P450s described so far in the literature, such as the CYP107A2 (LkmF) and CYP107AP1 (LkmK) from *Streptomyces rochei*, which participate in the biosynthesis of the macrolide antibiotic lankomycin (Arakawa et al., 2006) and CYP102H1 from *Nocardia farcinica* that catalyzes the hydroxylation of linoleic acid (Chung et al., 2012).

The plasmid-encoded nature of the identified P450 is very interesting since the absence of CYP107 members in the genome of *B. megaterium* indicates that the presence of the corresponding gene of the CYP107DY1 on the plasmid may be due to horizontal gene transfer displacement rather than intragenic transfer from the chromosome to the plasmid. This suggests that the P450s can play an important role in adaptation and evolution in prokaryotes.

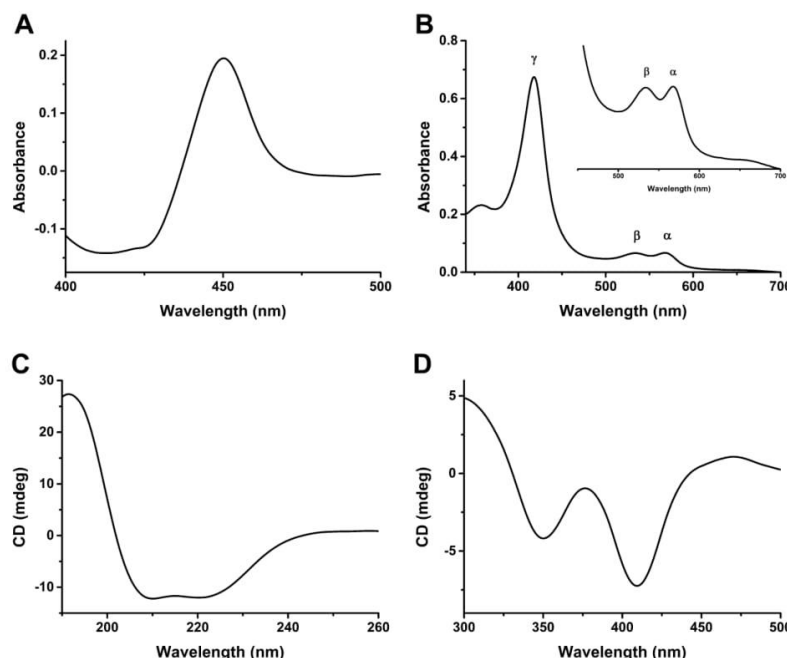


Fig. 1. Spectral characteristics of CYP107DY1. (A) The CO difference spectrum of CYP107DY1. (B) The UV-vis spectral characteristics of the purified CYP107DY1. The inset shows the magnification of the spectrum in the α and β band region. Circular dichroism (CD) spectra in the far-UV (C) and in the near-UV/visible (D) region at a CYP107DY1 concentration of 2 μ M and 20 μ M, respectively, resuspended in 10 mM potassium phosphate buffer pH 7.4. The CD spectrum was recorded using the following parameters: path length 1 mm (for far-UV) and 5 mm (near-UV/visible); time constant 2 s; band pass 5 nm; number of scans 3.

3.2. Expression, purification and spectrophotometric characterization

The DNA fragment encoding the full length CYP107DY1 was cloned into the expression vector pET17b and expressed in *E. coli* C43 (DE3). The expression levels were calculated by measuring reduced CO difference spectrum in the cell lysate (Omura and Sato, 1964). The carbon monoxide bound form gave a typical peak maximum at 450 nm (Fig. 1A). The full-length CYP107DY1 was purified in a soluble form with an expression level of 20 nmol/L. It was previously shown that the co-expression of some P450s with chaperones leads to an improvement of protein folding and thus increases of the expression level (Arase et al., 2006; Brixius-Anderko et al., 2015; Nishihara et al., 1998). The co-expression with the chaperones GroES and GroEL also improved the expression of CYP107DY1 more than 10 times, yielding 210 nmol/L.

Besides the CO-difference spectrum, the UV-vis absorption spectrum provides a simple technique for the characterization of P450 enzymes. The oxidized form of substrate free CYP107DY1 exhibited a major (γ) Soret peak at 417 and the smaller α and β bands at 567 and 535 nm, respectively (Fig. 1B), indicating a low spin state of the heme iron in the P450. In addition, the CD spectra of the oxidized CYP107DY1 were measured in the far-UV- and near UV-vis region. The far-UV CD spectrum showed a negative dichroic double band with minima at 208 and 222 nm (Fig. 1C), an indication of predominantly α -helical secondary structure (Poulos et al., 1986, 1987; Ravichandran et al., 1993). In the near UV-vis region, CYP107DY1 displayed two large negative signals at 350 nm and at 408 nm (Fig. 1D). These are in correspondence with the characteristic peaks for other bacterial P450s (Lepesheva et al., 2001; Munro et al., 1994).

Taken together, the spectrophotometric properties of the purified CYP107DY1 indicate that the enzyme is produced in the active form with proper heme incorporation.

3.3. Searching for a suitable redox partner

The availability of a redox partner/s is essential for studying the functionality of CYP107DY1. By searching the ORFs around the CYP107DY1 coding region as well as the ORFs on the seven indigenous plasmids of the QM B1551 strain, no redox partner (reductase and/or ferredoxin) was identified. Therefore, we tested herein different autologous and heterologous redox systems. As autologous electron transfer partners, the diflavins reductase BmCPR and the ferredoxin Fdx2 of *B. megaterium* DSM319 were selected. The BmCPR-Fdx2 system has been shown to support efficiently the activity of CYP106A1 (Milhim et al., 2016). As heterologous redox partners, the soluble *Schizosaccharomyces pombe* redox system adrenodoxin reductase homologue 1 (Arh1) and its ferredoxin (Etp1^{fd}) as well as the bovine adrenodoxin reductase (AdR) and adrenodoxin (Adx4-108) were used. The redox systems Arh1-Etp1^{fd} and AdR-Adx4-108 are described to transfer electrons to different classes of P450s (Brixius-Anderko et al., 2015; Ly et al., 2012).

Based on the measurement of the reduced CO-bound spectrum of CYP107DY1, the redox partners were tested and compared. Using the heterologous redox partners Arh1-Etp1^{fd} and AdR-Adx4-108 very low peaks (<5%) compared with the dithionite reduced CO difference peak at 450 nm were recovered within 5 min. In contrast, the autologous redox partners BmCPR-Fdx2 were very efficient and able to recover ~99.5% of the peak (Fig. 2). Therefore, the BmCPR-Fdx2 redox system was selected for further investigations with CYP107DY1.

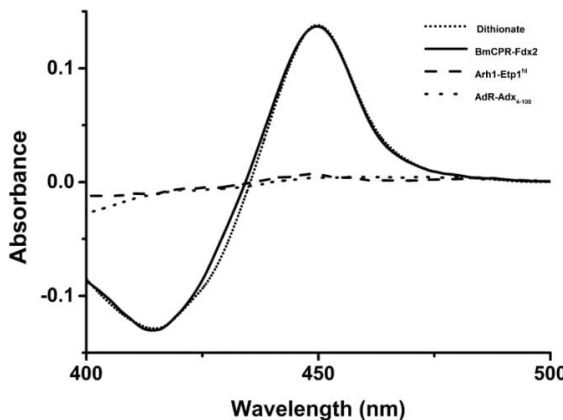


Fig. 2. Determination of CYP107DY1 reduction using autologous and heterologous electron transfer partners. The dithionite reduced CO-difference spectrum (short dot line) of CYP107DY1 was compared with the NADPH reduced BmCPR-Fdx2 (solid line), Arh1-Etp1^{fd} (dash line) and AdR-Adx₄₋₁₀₈ (dot line) CO-complexed spectrum. The NADPH (1 mM) reduced CO-difference spectra were recorded in a 200 μ l mixture of CYP/ferredoxin/reductase with a 1:40:5 molar ratio in 50 mM HEPES buffer pH 7.4 containing 20% glycerol (see Materials and methods).

3.4. In vitro conversion of mevastatin

The identification of suitable substrates and the characterization of the catalytic activity of a new enzyme are significant challenges. Therefore, at first a phylogenetic based approach was used in this study to predict a functional homolog of the new P450. The deduced amino acid sequence of CYP107DY1 was aligned with some related bacterial P450s with known function or substrate/s. The aligned sequences were then used for the construction of a neighbor-joining phylogenetic tree, which shows that CYP107DY1 is clustered with CYP267B1 from *Sorangium cellulosum* So ce56 (Fig. 3). CYP267B1 belongs to the CYP107 family (<http://drnelson.uthsc.edu/Bacteria.html>) and was previously characterized as a versatile drug metabolizer (Kern et al., 2016). Therefore, using an in vitro reconstituted assay we screened the activity of CYP107DY1 towards various pharmaceutical substrates (Supplementary Table 1). Among the 18 tested drugs, CYP107DY1 was found to metabolize mevastatin producing one product at a retention time of 9 min (Fig. 4B) compared with the negative control (Fig. 4A). The conversion ratio of 100 μ M mevastatin within 15 min was ~30%. The product retention time was identical to that of a pravastatin authentic standard (Fig. 4C). The results presented in Fig. 5 showed that CYP107DY1 activity can be supported by all tested redox systems, with an obvious higher efficiency using BmCPR-Fdx2. The conversion ratio of the 100 μ M mevastatin using Arh1-Etp1^{fd} and AdR-Adx₄₋₁₀₈ as redox partners was ~5% and ~3%, respectively, compared with when using of the BmCPR-Fdx2.

The regioselective oxyfunctionalization of the precursor mevastatin is crucial for the production of pravastatin, the widely used therapeutic agent for hypercholesterolemia (Lamon-Fava, 2013). This was described previously using CYP105A3 (P450sca2) from *Streptomyces carbophilus* (Matsuoka et al., 1989) and mutant CYP105AS1 from *Amycolatopsis orientalis* (McLean et al., 2015). However, CYP107DY1 is the first reported P450 of the CYP107 family, which can highly selectively hydroxylate such statin drugs.

3.5. Homology modeling and docking of CYP107DY1 with mevastatin

For the prediction of the three dimensional structure of CYP107DY1, homology modeling was performed. In order to select

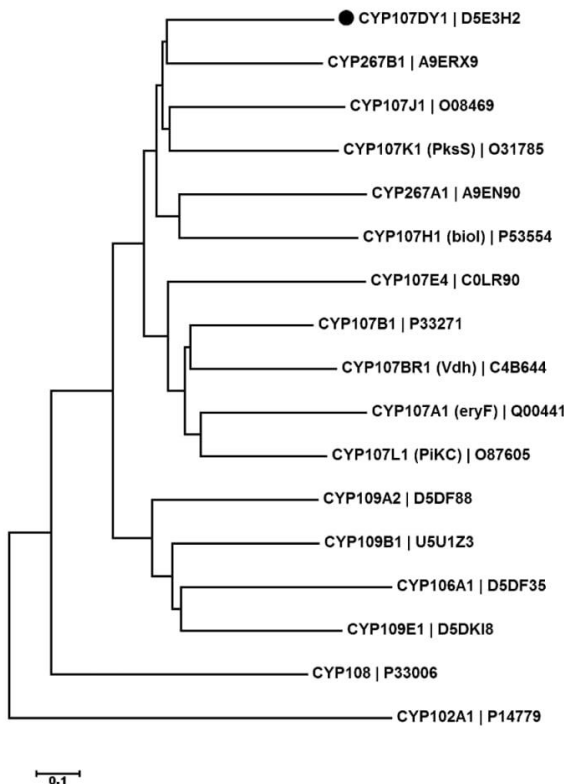


Fig. 3. Evolutionary relationships of CYP107DY1. The alignment was done with 10-gap setting and 0.1-gap extension, with slow alignment input in ClustalW2 server. The tree was constructed by neighbor joining algorithm with bootstrap analysis of 1000 replicates. The scale bar represents 0.1 amino acid substitution per amino acid. The CYP107DY1 is indicated with the closed circle (●). The number next to the gene name represents the UniProtKB accession number.

a suitable template, the amino acid sequence of the CYP107DY1 was submitted to the RCSB protein data bank BLAST server (<http://www.rcsb.org/pdb/search/advSearch.do?search=new>). The CYP107BR1 (Vdh) from *Pseudonocardia autotrophica* (UniProt acc. no.: C4B644) showed a sequence identity of 40% to CYP107DY1. The corresponding crystal structure of CYP107BR1 (Vdh) (PDB acc. code: 3A4G) was, therefore, chosen as a structural template. The CYP107DY1 homology model (Supplementary Fig. S2) has a typical three-dimensional P450 structure consisting of a C-terminus relatively rich in α -helices and an N-terminus relatively rich in β -sheets. Overall, it comprises 13 α -helices designated A, B₁ and C-L and 12 β -sheets grouped into 5 regions. The prosthetic heme group is embedded in the active site and surrounded by the L-helix from the proximal side and the L-helix from the distal side. The conserved cysteine residue (Cys360) is located in the loop region preceding the L-helix. The key structural features of the CYP107DY1 suggest that its overall topology correlates with the general folding properties of P450s (Supplementary Fig. S2).

Three-dimensional structures of P450s are very helpful to understand the enzyme-substrate interaction. Therefore, mevastatin was docked into CYP107DY1. In the docking simulation the target protein was kept as rigid body. The flexible bonds of the ligands were assigned automatically and verified by manual inspection. A cubic grid box with a size of 52 Å \times 52 Å \times 52 Å was fixed above the heme moiety to cover the whole active site of the enzyme. As illustrated in Fig. 6, the substrate molecule is located over the

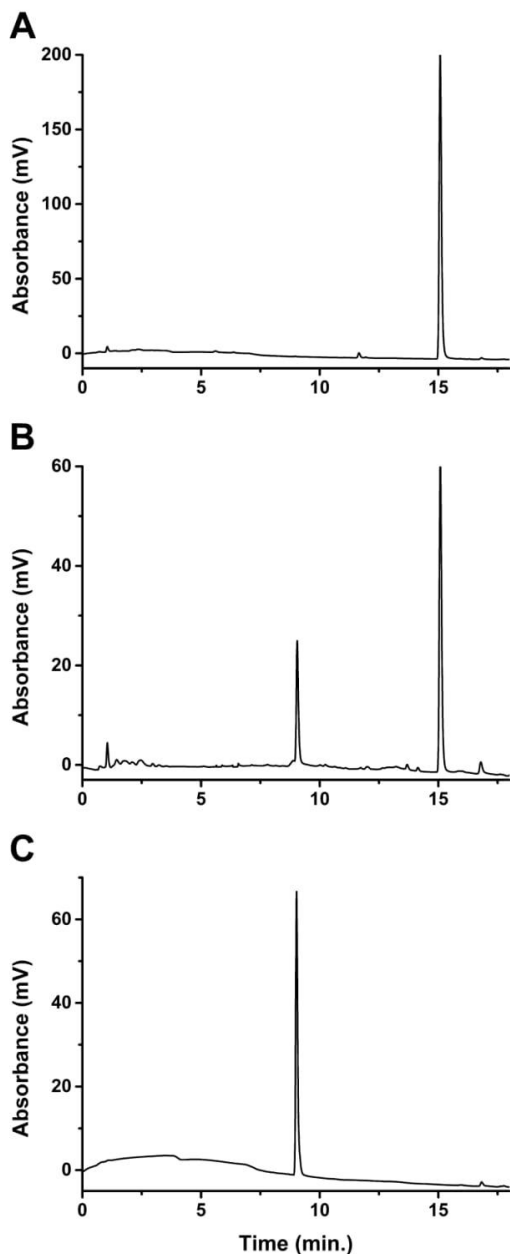


Fig. 4. HPLC analysis of the conversion of mevastatin with CYP107DY1. In vitro conversion of 100 μ M mevastatin in the (A) absence of CYP107DY1 or (B) presence of CYP107DY1. The reaction was carried out in 50 mM HEPES buffer pH 7.4 with 20% glycerol. The reconstituted system contained 0.5 μ M CYP107DY1, 2.5 μ M BmCPR, 20 μ M Fdx2 and the NADPH regeneration system. The conversion was carried out for 15 min at 30 °C. (C) Pravastatin authentic standard.

heme. In addition, the side chains of seven amino acid residues (including Leu99, Leu245, Thr249, Ala250, Glu253, Thr254 and Gly300) were found to define a cavity with mevastatin. The keto group of the 2-methylbutanoate side chain and the hydroxyl group on the lactone ring of the mevastatin molecule formed two hydrogen bonds with Thr249 and Glu253, respectively. These interactions enable the orientation of the molecule in a position that allows

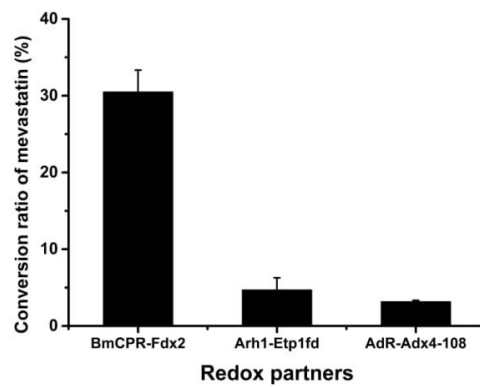


Fig. 5. Effect of the different redox partners on the in vitro conversion of mevastatin by CYP107DY1. In vitro conversion of 100 μ M mevastatin by CYP107DY1 using the redox system BmCPR-Fdx2 of, Arh1-Etp1^{fd} and AdR-Adx4-108. The reaction was carried out in 50 mM HEPES buffer pH 7.4 with 20% glycerol. The reconstituted system contained 0.5 μ M CYP107DY1, 2.5 μ M reductase (BmCPR, AdR or Arh1), and 20 μ M ferredoxin (Fdx2, Etp1^{fd} or Adx4-108) and the NADPH regeneration system. The reaction was carried out for 15 min at 30 °C. The data is represented as mean \pm SD of three separate measurements.

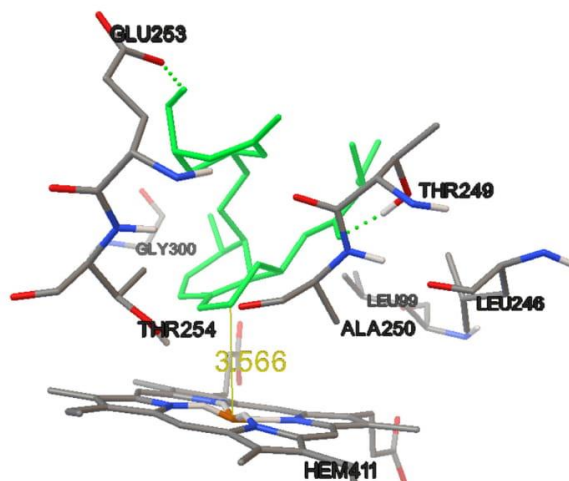
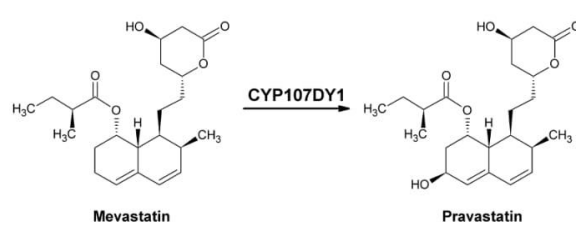


Fig. 6. Docking conformation of mevastatin. The ligand mevastatin is shown in green. The distance of the C-6 atom from the heme iron is shown in yellow in Å. Some of the amino acids that form the active site of the CYP107DY1 in the presence of mevastatin are shown and named. (For interpretation of the references to colour in this figure legend, the reader is referred to the web version of this article.)



Scheme 1. Conversion of mevastatin to pravastatin by CYP107DY1.

atom C-6 to face the heme iron (distance \sim 3.5 Å) (Fig. 6), favorable for a hydroxylation at this position to produce the pravastatin (Scheme 1), supporting our experimental data shown in Fig. 4.

Table 1

CYP107DY1-based (a) *Escherichia coli* Whole-cell biotransformation yield of mevastatin.

Additives (b)	Pravastatin yield (mg/L)
Without additives	13.2 ± 2.5
Polymyxin B	17.9 ± 2.1
EDTA	28.5 ± 3.1

^a *E. coli* C43 (DE3) cells were co-transformed with the expression vector based on pET17b, coding for CYP107DY1-BmCPR-Fdx2, and the chaperone GroEL/GroES-coding plasmid pGro12.

^b Polymyxin B and EDTA were added to a final concentration of 32 µg/ml and 20 mM, respectively.

3.6. Biotransformation of mevastatin using a whole-cell based system

The in vitro activity of CYP107DY1 towards mevastatin was very encouraging to address the question whether it is applicable for the in vivo production of pravastatin. Therefore, and as a proof of concept, a CYP107DY1 based *E. coli* whole-cell biotransformation system, utilizing BmCPR and Fdx2 as redox partners, was established. We chose *E. coli* as host, because, in contrast to *B. megaterium*, it has the advantage that no endogenous P450 can interfere with the desired reaction. For this purpose, a tricistronic pET17b-based vector, expressing CYP107DY1, BmCPR and Fdx2, was constructed. The whole-cell biotransformation was performed with resting cells in potassium phosphate buffer instead of the terrific broth complex medium, since indole, which results from the tryptophan metabolism by *E. coli*, may have an inhibitory effect on the activity of P450s (Brixius-Anderko et al., 2016; Ringle et al., 2013).

As shown in Table 1, the whole-cell biotransformation system yielded about 13.2 mg/L pravastatin. This amount is comparable to the previously reported WT CYP105A3 (P450sca2) *E. coli*-based whole-cell system, which yielded 12.8 mg/L pravastatin (Ba et al., 2013a, 2013b). It was shown previously that the hindered transport of the substrate into the *E. coli* cells is most likely responsible for the low biotransformation ratio (Janocha and Bernhardt, 2013). Therefore, we used the peptide antibiotic polymyxin B and the chelating agent EDTA, which are reported to exhibit permeabilization activity towards the outer membrane of the Gram-negative bacteria. Concerning this, *E. coli*-based whole cell systems were also designed for other P450s in our laboratory, in which optimal concentrations of polymyxin B (32 µg/ml) and EDTA (20 mM) were employed to achieve the highest conversion of substrates (Janocha and Bernhardt, 2013; Kern et al., 2016; Litzenburger et al., 2015). The use of polymyxin B lead to an 1.3 fold increase in the pravastatin production, yielding 17.9 mg/L, while the highest yield was achieved using EDTA with a 2.2 fold increase yielding 28.5 mg/L (Table 1), which suggests the potential of the constructed whole-cell system in the production of pravastatin.

Novel P450s are increasingly emerging because of the availability of many genome sequences. However, the multi-component nature of the P450s and other factors (Bernhardt and Urlacher, 2014) limit their biotechnological use. The characterization of CYP107DY1 and its successful employment in the in vivo pravastatin production is the first step in the industrialization of this interesting P450. The application of this novel pravastatin-producing P450 in an industrially optimized host as recently shown for the mutant CYP105AS1 (McLean et al., 2015) will certainly pave the way for a successful use in a biotechnological process.

4. Conclusion

Regio- and stereoselective oxidation of non-activated carbon atoms using P450s is of great interest for synthetic biology. The

robustness of the bacterial P450s is attractive for the industrial production of different valuable products (Bernhardt and Urlacher, 2014). However, despite the high potential and the recent development with respect to exploiting the P450s in biotechnological applications, there are various challenges limiting their use in industrial processes, for instance their dependency on electron transfer proteins. In the recent study, we have identified, cloned and expressed a new plasmid-encoded cytochrome P450 from *B. megaterium* QM B1551, which was categorized into a new subfamily (CYP107DY1). In addition, we were able to find a redox system (BmCPR-Fdx2) that can efficiently support the activity of the CYP107DY1, which enabled the identification of mevastatin as a substrate. The successful construction of *E. coli*-based whole cell system utilizing CYP107DY1 is of great importance not only for efficient production of pravastatin but also for future characterization of new substrates, functionalization of drugs and the production of new metabolites. Further improvements, either at the cellular level by expressing CYP107DY1 in other microorganisms (McLean et al., 2015), or at the molecular level by rational design to improve the activity of this P450 (Ba et al., 2013b) will contribute to the set-up of efficient industrial processes using this novel P450.

Author contributions

M.M. carried out all experiments, analyzed and interpreted the data and drafted the manuscript. N.P. and F.K. participated in the establishment of the experiments. A.A. participated in the substrate docking. P.H. and R.B. participated in the interpretation and discussion of experimental results and writing of the manuscript.

Conflict of interest

The authors declare that they have no competing interest.

Acknowledgments

The authors would like to thank Birgit Heider-Lips for the purification of AdR and Adx, Dr. Elisa Brill for cloning of Fdx2 and Tanja Sagadin for the purification of Arh1 and Etp1^{fd}. The authors also gratefully acknowledge Prof. Dr. David Nelson (The University of Tennessee Health Science Center) for helping in the CYP107DY1 classification.

Appendix A. Supplementary data

Supplementary data associated with this article can be found, in the online version, at <http://dx.doi.org/10.1016/j.biote.2016.11.002>.

References

- Arakawa, K., Kodama, K., Tatsuno, S., Ide, S., Kinashi, H., 2006. Analysis of the loading and hydroxylation steps in lankamycin biosynthesis in *Streptomyces rochei*. *Antimicrob. Agents Chemother.* 50, 1946–1952.
- Arase, M., Waterman, M.R., Kagawa, N., 2006. Purification and characterization of bovine steroid 21-hydroxylase (P450c21) efficiently expressed in *Escherichia coli*. *Biochem. Biophys. Res. Commun.* 344, 400–405.
- Ba, L., Li, P., Zhang, H., Duan, Y., Lin, Z., 2013a. Engineering of a hybrid biotransformation system for cytochrome P450sca-2 in *Escherichia coli*. *Biotechnol. J.* 8, 785–793.
- Ba, L., Li, P., Zhang, H., Duan, Y., Lin, Z., 2013b. Semi-rational engineering of cytochrome P450sca-2 in a hybrid system for enhanced catalytic activity: insights into the important role of electron transfer. *Biotechnol. Bioeng.* 110, 2815–2825.
- Berg, A., Gustafsson, J.A., Ingelman-Sundberg, M., 1976. Characterization of a cytochrome P450-dependent steroid hydroxylase system present in *Bacillus megaterium*. *J. Biol. Chem.* 251, 2831–2838.
- Berg, A., Ingelman-Sundberg, M., Gustafsson, J.A., 1979. Isolation and characterization of cytochrome P450meg. *Acta Biol. Med. Ger.* 38, 333–344.

- Bernhardt, R., Urlacher, V.B., 2014. Cytochromes P450 as promising catalysts for biotechnological application: chances and limitations. *Appl. Microbiol. Biotechnol.* 98, 6185–6203.
- Bernhardt, R., 2006. Cytochromes P450 as versatile biocatalysts. *J. Biotechnol.* 124, 128–145.
- Brill, E., Hannemann, F., Zapp, J., Brüning, G., Jauch, J., Bernhardt, R., 2013. A new cytochrome P450 system from *Bacillus megaterium* DSM319 for the hydroxylation of 11-keto- β -boswellic acid (KBA). *Appl. Microbiol. Biotechnol.* 98, 1703–1717.
- Brixius-Anderko, S., Schiffer, L., Hannemann, F., Janocha, B., Bernhardt, R., 2015. A CYP21A2 based whole-cell system in *Escherichia coli* for the biotechnological production of prednisol. *Microb. Cell Fact.* 14, <http://dx.doi.org/10.1186/s12934-015-0332-2>.
- Brixius-Anderko, S., Hannemann, F., Ringle, M., Khatri, Y., Bernhardt, R., 2016. An indole deficient *Escherichia coli* strain improves screening of cytochromes P450 for biotechnological applications. *Biotechnol. Appl. Biochem.*, <http://dx.doi.org/10.1002/bab.1488>.
- Bunk, B., Schulz, A., Stammen, S., Münch, R., Warren, M.J., Rohde, M., Jahn, D., Biedendieck, R., 2010. A short story about a big magic bug. *Bioeng. Bugs* 1, 85–91.
- Bureik, M., Schiffler, B., Hiraoka, Y., Vogel, F., Bernhardt, R., 2002. Functional expression of human mitochondrial CYP1B2 in fission yeast and identification of a new internal electron transfer protein, etp1. *Biochemistry (Mosc.)* 41, 2311–2321.
- Chung, Y.-H., Song, J.-W., Choi, K.-Y., Yoon, J.W., Yang, K.-M., Park, J.-B., 2012. Cloning, expression, and characterization of P450 monooxygenase CYP102H1 from *Nocardia farcinica*. *J. Korean Soc. Appl. Biol. Chem.* 55, 259–264.
- Eppinger, M., Bunk, B., Johns, M.A., Edirisinghe, J.N., Kutumbakar, K.K., Koenig, S.S.K., Creasy, H.H., Rosovitz, M.J., Riley, D.R., Daugherty, S., Martin, M., Elbourne, L.D.H., Paulsen, I., Biedendieck, R., Braun, C., Grayburn, S., Dhingra, S., Lukyanchuk, V., Ball, B., Ul-Qamar, R., Seibel, J., Bremer, E., Jahn, D., Ravel, J., Vary, P.S., 2011. Genome sequences of the biotechnologically important *Bacillus megaterium* strains QM B1551 and DSM319. *J. Bacteriol.* 193, 4199–4213.
- Ewen, K.M., Schiffler, B., Uhlmann-Schiffler, H., Bernhardt, R., Hannemann, F., 2008. The endogenous adrenodoxin reductase-like flavoprotein arh1 supports heterologous cytochrome P450-dependent substrate conversions in *Schizosaccharomyces pombe*. *FEMS Yeast Res.* 8, 432–441.
- Finn, R.D., Coggill, P., Eberhardt, R.Y., Eddy, S.R., Mistry, J., Mitchell, A.L., Potter, S.C., Punta, M., Qureshi, M., Sangrador-Vegas, A., Salazar, G.A., Tate, J., Bateman, A., 2016. The Pfam protein families database: towards a more sustainable future. *Nucleic Acids Res.* 44, D279–D285.
- Gerber, A., Kleser, M., Biedendieck, R., Bernhardt, R., Hannemann, F., 2015. Functionalized PHB granules provide the basis for the efficient side-chain cleavage of cholesterol and analogs in recombinant *Bacillus megaterium*. *Microb. Cell Fact.* 14, 107, <http://dx.doi.org/10.1186/s12934-015-0300-y>.
- Hannemann, F., Bichet, A., Ewen, K.M., Bernhardt, R., 2007. Cytochrome P450 systems—biological variations of electron transport chains. *Biochim. Biophys. Acta BBA Gen. Subj.* 1770 (P450), 330–344.
- Hiwatashi, A., Ichikawa, Y., Maruya, N., Yamano, T., Aki, K., 1976. Properties of crystalline reduced nicotinamide adenine-dinucleotide phosphate-adrenodoxin reductase from bovine adrenocortical mitochondria. 1. Physicochemical properties of holo-NADPH-adrenodoxin and apo-NADPH-adrenodoxin reductase and interaction between non-heme iron proteins and reductase. *Biochemistry (Mosc.)* 15, 3082–3090.
- Inouye, M., Takada, Y., Muto, N., Beppu, T., Horinouchi, S., 1994. Characterization and expression of a P450-like mycacinamicin biosynthesis gene using a novel *Micromonospora*–*Escherichia coli* shuttle cosmid vector. *Mol. Gen. Genet. MGG* 245, 456–464.
- Józwik, I.K., Kiss, F.M., Gricman, L., Abdulmughni, A., Brill, E., Zapp, J., Pleiss, J., Bernhardt, R., Thunnissen, A.-M.W.H., 2016. Structural basis of steroid binding and oxidation by the cytochrome P450 CYP109E1 from *Bacillus megaterium*. *FEBS J.*, <http://dx.doi.org/10.1111/febs.13911>.
- Janocha, S., Bernhardt, R., 2013. Design and characterization of an efficient CYP105A1-based whole-cell biocatalyst for the conversion of resin acid diterpenoids in permeabilized *Escherichia coli*. *Appl. Microbiol. Biotechnol.* 97, 7639–7649.
- Kern, F., Khatri, Y., Litzenburger, M., Bernhardt, R., 2016. CYP267A1 and CYP267B1 from *Sorangium cellulosum* So ce56 are highly versatile drug metabolizers. *Drug Metab. Dispos.* 44, 495–504.
- Kim, S., Thiessen, P.A., Bolton, E.E., Chen, J., Fu, G., Gindulyte, A., Han, L., He, J., He, S., Shoemaker, B.A., Wang, J., Yu, B., Zhang, J., Bryant, S.H., 2016. PubChem substance and compound databases. *Nucleic Acids Res.* 44, D1202–D1213.
- Lamon-Fava, S., 2013. Statins and lipid metabolism: an update. *Curr. Opin. Lipidol.* 24, 221–226.
- Lepesheva, G.I., Podust, L.M., Bellamine, A., Waterman, M.R., 2001. Folding requirements are different between sterol 14 α -demethylase (CYP51) from *Mycobacterium tuberculosis* and human or fungal orthologs. *J. Biol. Chem.* 276, 28413–28420.
- Litzenburger, M., Kern, F., Khatri, Y., Bernhardt, R., 2015. Conversions of tricyclic antidepressants and antipsychotics with selected P450s from *Sorangium cellulosum* So ce56. *Drug Metab. Dispos.* 43, 392–399.
- Lombard, M., Salard, I., Sari, M.-A., Mansuy, D., Buisson, D., 2011. A new cytochrome P450 belonging to the 107L subfamily is responsible for the efficient hydroxylation of the drug terfenadine by *Streptomyces platensis*. *Arch. Biochem. Biophys.* 508, 54–63.
- Ly, T.T.B., Khatri, Y., Zapp, J., Hutter, M.C., Bernhardt, R., 2012. CYP264B1 from *Sorangium cellulosum* So ce56: A fascinating norisoprenoid and sesquiterpene hydroxylase. *Appl. Microbiol. Biotechnol.* 95, 123–133.
- Matsuoka, T., Miyakoshi, S., Tanzawa, K., Nakahara, K., Hosobuchi, M., Serizawa, N., 1989. Purification and characterization of cytochrome P450ca from *Streptomyces carbophilus*. ML-236B (compactin) induces a cytochrome P450ca from *Streptomyces carbophilus* that hydroxylates ML-236B to pravastatin sodium (CS-514), a tissue-selective inhibitor of 3-hydroxy-3-methylglutaryl-coenzyme-A reductase. *Eur. J. Biochem. FEBS* 184, 707–713.
- McLean, K.J., Hans, M., Meijrink, B., van Scheppingen, W.B., Vollebregt, A., Tee, K.L., van der Laan, J.-M., Leys, D., Munro, A.W., van den Berg, M.A., 2015. Single-step fermentative production of the cholesterol-lowering drug pravastatin via reprogramming of *Penicillium chrysogenum*. *Proc. Natl. Acad. Sci. U. S. A.* 112, 2847–2852.
- Milhim, M., Gerber, A., Neunzig, J., Hannemann, F., Bernhardt, R., 2016. A Novel NADPH-dependent flavoprotein reductase from *Bacillus megaterium* acts as an efficient cytochrome P450 reductase. *J. Biotechnol.* 231, 83–94.
- Morris, G.M., Huey, R., Lindstrom, W., Sanner, M.F., Belew, R.K., Goodsell, D.S., Olson, A.J., 2009. AutoDock4 and AutoDockTools4: automated docking with selective receptor flexibility. *J. Comput. Chem.* 30, 2785–2791.
- Munro, A.W., Lindsay, J.G., Coggins, J.R., Kelly, S.M., Price, N.C., 1994. Structural and enzymological analysis of the interaction of isolated domains of cytochrome P450 BM3. *FEBS Lett.* 343, 70–74.
- Nelson, D.R., 2009. The cytochrome P450 homepage. *Hum. Genomics* 4, 59–65.
- Nishihara, K., Kanemori, M., Kitagawa, M., Yanagi, H., Yura, T., 1998. Chaperone coexpression plasmids: differential and synergistic roles of DnaK-DnaJ-GrpE and GroEL-GroES in assisting folding of an allergen of Japanese cedar pollen, Cry2, in *Escherichia coli*. *J. Appl. Environ. Microbiol.* 64, 1694–1699.
- Omura, T., Sato, R., 1964. The carbon monoxide-binding pigment of liver microsomes. II. Solubilization purification, and properties. *J. Biol. Chem.* 239, 2379–2385.
- Poulos, T.L., Finzel, B.C., Howard, A.J., 1986. Crystal structure of substrate-free *Pseudomonas putida* cytochrome P450. *Biochemistry (Mosc.)* 25, 5314–5322.
- Poulos, T.L., Finzel, B.C., Howard, A.J., 1987. High-resolution crystal structure of cytochrome P450cam. *J. Mol. Biol.* 195, 687–700.
- Ravichandran, K.C., Boddupalli, S.S., Hasermann, C.A., Peterson, J.A., Deisenhofer, J., 1993. Crystal structure of hemoprotein domain of P450 BM3, a prototype for microsomal P450. *Science* 261, 731–736.
- Ringle, M., Khatri, Y., Zapp, J., Hannemann, F., Bernhardt, R., 2013. Application of a new versatile electron transfer system for cytochrome P450-based *Escherichia coli* whole-cell bioconversions. *Appl. Microbiol. Biotechnol.* 97, 7741–7754.
- Sagara, Y., Wada, A., Takata, Y., Waterman, M.R., Sekimizu, K., Horiuchi, T., 1993. Direct expression of adrenodoxin reductase in *Escherichia coli* and the functional characterization. *Biol. Pharm. Bull.* 16, 627–630.
- Sakaki, T., Sugimoto, H., Hayashi, K., Yasuda, K., Munetsuna, E., Kamakura, M., Ikushiro, S., Shiro, Y., 2011. Bioconversion of vitamin D to its active form by bacterial or mammalian cytochrome P450: *Biochim. Biophys. Acta Proteins Proteomics* 1814, 249–256.
- Sanner, M.F., 1999. Python: a programming language for software integration and development. *J. Mol. Graph. Model.* 17, 57–61.
- Schiffler, B., Bureik, M., Reinle, W., Müller, E.-C., Hannemann, F., Bernhardt, R., 2004. The adrenodoxin-like ferredoxin of *Schizosaccharomyces pombe* mitochondria. *J. Inorg. Biochem.* 98, 1229–1237.
- Schmitz, D., Zapp, J., Bernhardt, R., 2012. Hydroxylation of the triterpenoid dipterocarpol with CYP106A2 from *Bacillus megaterium*. *FEBS J.* 279, 1663–1674.
- Uhlmann, H., Beckert, V., Schwarz, D., Bernhardt, R., 1992. Expression of bovine adrenodoxin in *Escherichia coli* and site-directed mutagenesis of (2-Fe-2s) cluster ligands. *Biochem. Biophys. Res. Commun.* 188, 1131–1138.
- Whitehouse, C.J.C., Bell, S.G., Wong, L.-L., 2012. P450 BM3 (CYP102A1): connecting the dots. *Chem. Soc. Rev.* 41, 1218–1260.

Supplementary material

Identification of a new plasmid-encoded cytochrome P450 CYP107DY1 from *Bacillus megaterium* with a catalytic activity towards mevastatin

**Mohammed Milhim, Natalia Putkaradze, Ammar Abdulkughni, Fredy Kern, Philip Hartz and
Rita Bernhardt***

Institute of Biochemistry, Saarland University, 66123 Saarbrücken, Germany

*Address correspondence to:

Prof. Dr. Rita Bernhardt, Institute of Biochemistry, Campus B 2.2, Saarland University, 66123
Saarbrücken (Germany)

E-mail: ritabern@mx.uni-saarland.de

Phone: +49 681 302 4241

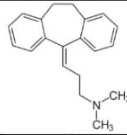
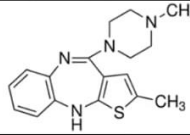
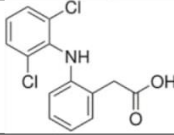
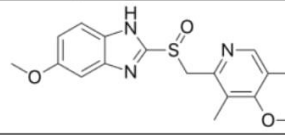
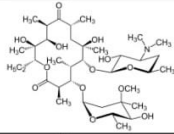
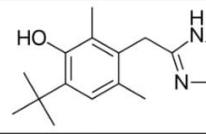
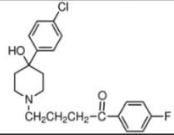
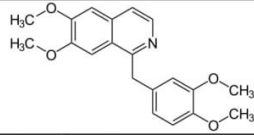
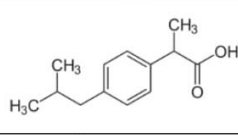
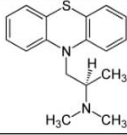
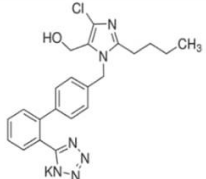
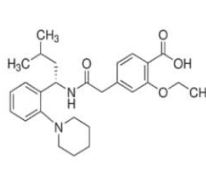
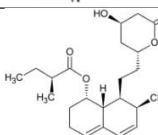
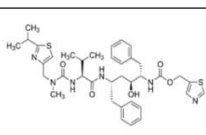
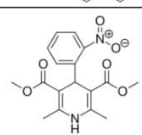
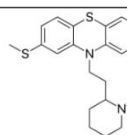
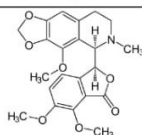
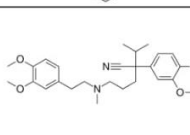
Fax: +49 681 302 4739

Supplementary Table 1. Protein sequence identity values of CYP107DY1 with different cytochrome P450s.

Closest match with different CYP107					
Protein Abb.	Natural function or substrate/s	No. of aa	Species	Identity % ^(a)	UniProtKB accession numbers ^(b)
CYP107DY1	---	410	<i>B. megaterium</i> QM B1551	100	D5E3H2
CYP267B1	Drug metabolism	405	<i>Sorangium cellulosum</i> So ce5	43.5	A9ERX9
CYP107B1	7-ethoxycoumarin	405	<i>Saccharopoly sporaerythraea</i>	41.9	P33271
CYP107K1 (PksS)	Polyketide biosynthesis (bacillaene biosynthesis)	405	<i>Bacillus subtilis</i> (Strain 168)	41.8	O31785
CYP107H1 (bioI)	Biotin biosynthesis	395	<i>Bacillus subtilis</i> (Strain 168)	40.8	P53554
CYP107J1	Testosterone enanthate	410	<i>Bacillus subtilis</i> (Strain 168)	40.7	O08469
CYP107BR1 (Vdh)	Vitamin D3	403	<i>Pseudonocardia autotrophica</i>	40	C4B644
CYP107L1 (PiKC)	Pikromycin biosynthesis	416	<i>Streptomyces venezuelae</i>	39.2	O87605
CYP107A1 (eryF)	Erythromycin biosynthesis	404	<i>Saccharopolyspora erythraea</i>	36.2	Q00441
CYP107E4	Diclofenac	396	<i>Actinoplanes sp.</i> ATCC 53771	36	C0LR90
CYP109B1	Various substrates (e.g. (+)-valencene)	396	<i>Bacillus subtilis</i>	35.4	U5U1Z3
CYP267A1	Drugs metabolism	429	<i>Sorangium cellulosum</i> So ce5	35.3	A9EN90
CYP109A2	Steroids	403	<i>B. megaterium</i> DSM319	34.6	D5DF88
CYP109E1	Steroids	404	<i>B. megaterium</i> DSM319	32.7	D5DK18
CYP106A1	Steroids and terpenoids	410	<i>B. megaterium</i> DSM319	29.1	D5DF35
CYP108	α -terpinol	428	<i>Pseudomonas sp.</i>	28	P33006
CYP102A1	Fatty acids	1,049	<i>B. megaterium</i> DSM319	18.4	P14779

(a) Based on Clustal Omega Multiple Sequence Alignment (MSA) (<http://www.ebi.ac.uk/Tools/msa/>)(b) <http://www.uniprot.org/>

Supplementary Table 2. List of tested substrates with CYP107DY1

Name	Structure	Name	Structure
Amitriptyline		Olanzapine	
Diclofenac		Omeprazole	
Erythromycin		Oxymetazoline	
Haloperidol		Papaverine	
Ibuprofen		Promethazine	
Losartan		Repaglinide	
Mevastatin		Ritonavir	
Nifedipine		Thioridazine	
Noscapine		Verapamil	

```

1 ATGAAAAAGGTTACAGTTGATGATTAGCTCTCCAGAAAATATGCACGATGTCATCGGATTTATAAAAAACTCACTGAACATCAAGAACCTCTTATTCGTTG
1 M K K V T V D D F S S P E N M H D V I G F Y K K L T E H Q E P L I R L

106 GATGATTATTACGGGTTGGGACCGGCATGGGTCGCATTACGTGATGACGATGTTGTTACGATACTAAAGAACCCCGTTCTCAAAGATGTAACGGAGATTCA
36 D D Y Y G L G P A W V A L R H D D V V T I L K N P R F L K D V R K F T

211 CCATTGCAAGATAAAAAGGATTCTATAGATGATGACACATCTGCGAGCAAACCTGTTGAATGGATGATGAATATGCCGAATATGCTTACGGTCGATCCACCGA
71 P L Q D K K D S I D D S T S A S K L F E W M M N M P N M L T V D P P D

316 CACACTCGTTGCGCAGGTTGGCCTAAAGCCTTACGCCACGTATGATCGAGAACCTTCGACCTCGTACAGCAGATTACCAATGAGCTATTGGATTCA
106 H T R L R R L A S K A F T P R M I E N L R P R I Q Q I T N E L L D D S V

421 GAAGGAAAAGGAATATGGATCTTGCAGGATTTCTCTGCCCATTATTGTCATTTCAGAGATGCTAGGGATTCCACCTTATGATCAGAACAGATT
141 E G K R N M D L V A D F S F P L P I I V I S E M L G I P P L D Q K R F

526 CGCGACTGGACAGATAAAACTCATCAAAGCACGATGGATCTAGCCAAAGGGCTGTAGTTATGAAACACTCAAGGAGTTATTGATTACATCAAAAAATGCTG
176 R D W T D K L I K A A M D P S Q G A V V M E T L K E F I D Y I K K M L

631 GTCGAAAAGCGCAACATCCAGACGATGATGATGAGTGGCTTGTGCAAGCACATGAGCAAGAAGATAAGTTGAGCGAGAACGAGCTTCCACGATTGG
211 V E K R N H P D D D V M S A L L Q A H E Q E D K L S E N E L L S T I W

736 CTACTCAATTACAGCGGACATGAGACGACGCCCATCTAACGCAACGCCGTACTGGCGCTATTGAAGCATCCGAACAAATGGCCTGCTCGGGATAAT CCT
246 L L I T A G H E T T A H L I S N G V L A L L K H P E Q M R L L R D N P

841 TCTTTACTCCCCCTCTGCCGTTGAAGAGCTGCTACGCTATGCCGGACCGGTATGATTGGTGGCGTTTGCGGGTGAAGATATCATCATGCATGGAAAATGATT
281 S L L P S A V E E L L R Y A G P V M I G G R F A G E D I I M H G K M I

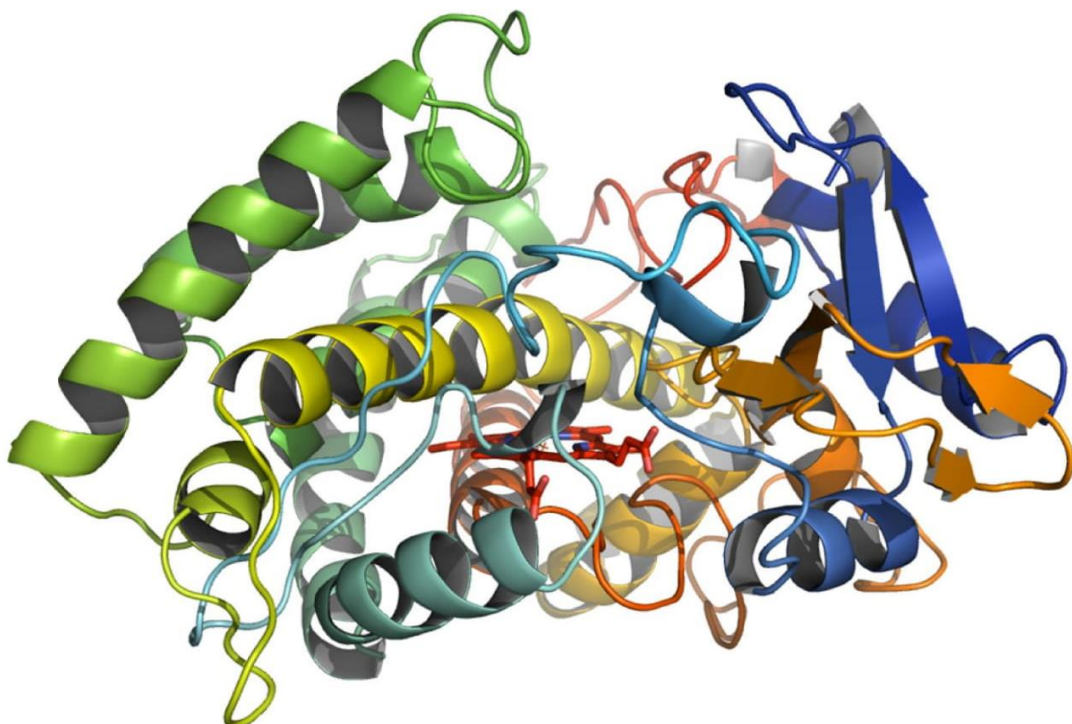
946 CCCAAAGGTGAAATGGTGTGTTCTCGCTGGCCCAATATTGATTACAGAAAATTCTCTATCCGTAGGGATTGGATATTACACGGCAGGAGATGAGCAT
316 P K G E M V L F S L V A A N I D S Q K F P S Y P E G L D I T R E E N E H

1051 CTCACCTTCGGAAAAGGTATCCATATTGTTGGGAGCGCTTGGCGCGCATGGAAAGCACATATCGCTTCGGCACATTGCTTCAACGGTTCTGATTTACGA
351 L T F G K G I H H C L G A P L A R M E A H I A F G T L L Q R F P D L R

1156 TTGGCAATCGAATCGGAGCAACTGGTTTATAACACACAGCACATTGGCTCTCTTAAAGCTTGCAGTTATTTCCTAA
386 L A I E S E Q L V Y N N S T L R S L K S L P V I F * *

```

Supplementary Fig. S1. The open reading frame sequence of the CYP107DY1. The upper and the lower lines represent the nucleotide and deduced amino acid sequences, respectively. The one-letter code for each amino acid is aligned with the first nucleotide of each codon. Several conserved motifs used for the identification of cytochrome P450s are underlined. I- helix (A/G-G-x-E/D-T-T/S), K-helix (E-x-x-R), and the heme pocket (F-x-x-G-x-x-x-C-x-G).



Supplementary Fig. S2. Homology model of CYP107DY1. A model of CYP107DY1 was calculated using CYP107RB1 (Vdh) (PDB accession code: 3A4G) as template. The coordinates of the heme-porphyrin atoms from the template structure were added subsequently to the obtained homology model. Program Modeller 9.14 (University of California San Francisco, USA) was used.

3. Discussion and outlook

Cytochrome P450s represent a very important and diverse enzyme superfamily. They are widespread in nature and are able to metabolize structurally as well as functionally different compounds from the small aroma terpenoid camphor (MW ~ 150) to much bigger molecules such as the anti-tumor agent epothilone D (MW ~ 500) or the drug cyclosporine A (MW ~ 1200) (Combalbert et al., 1989; Katagiri et al., 1968; Ogura et al., 2004). Despite their huge number and sequence variety, P450s can be divided into the following groups: (i) xenobiotic-metabolizing P450s involved in degradation of drugs, insecticides, herbicides and other xenobiotics, (ii) P450s playing key roles in anabolic metabolic transformations such as the biosynthesis of hormones and active signaling agents, and (iii) extremely diverse microbial P450s performing oxidative tailoring of a wide array of chemical structures. The latter group is pharmaceutically and biotechnologically highly interesting since its members can be used as model systems for studying human P450s associated with various diseases (Kelly and Kelly, 2013) and as biotechnological tools for low-cost production of valuable compounds. In contrast to mammalian or plant P450s, microbial P450s have several advantages: they are cytosolic soluble proteins, thus easier to overproduce and handle, and they exhibit higher catalytic activities (Bernhardt, 2006; Bernhardt and Urlacher, 2014). Thanks to sequencing projects of microbial genomes and metagenomes, the number of microbial P450s continues increasing constantly. Despite being a challenging task, identifying the function of these novel proteins is highly desirable due to their potential for synthetic applications as well as in drug discovery (Kandel et al., 2014). From a biotechnological perspective, the establishment of novel P450-based microbial whole-cell biocatalysts is more desirable than using purified or immobilized enzymes. The main reasons are the multi-enzyme nature of P450 systems and their continuous requirement of reducing equivalents. In whole-cell systems, functional P450 and electron mediator proteins can be overproduced and exploited *in vivo* for biotransformation without the need of cost- and time-consuming purification procedures of component proteins. At the same time, the primary electron donor, NAD(P)H, can be provided through the central metabolism of the organism and, in case of its limitation, can be restored by introducing an enzymatic regenerating system (Bernhardt and Urlacher, 2014). In this context, *B. megaterium* is a highly interesting bacterium. On the one hand, several strains of this microorganism encode important well-known and novel poorly-characterized P450s as well as their redox proteins (Berg and Rafter, 1981; Brill et al., 2014; Milhim et al., 2016b; Narhi and Fulco, 1987). Examples of P450s originating from *B. megaterium* are a fatty acid hydroxylase CYP102A1, a steroid hydroxylase CYP106A2 as well as a newly identified vitamin D3 hydroxylase CYP109E1 and a compactin hydroxylase CYP107DY1 (Brill, 2013; Fulco, 1991; Milhim et al., 2016a; Whitehouse et al., 2012). Besides that, the bacterium has been shown to be a useful host, overexpressing various P450 systems

even from mammals (Brill et al., 2014; Bleif et al., 2012; Kiss et al., 2015a; Gerber et al., 2015). Furthermore, human CYP11A1- and CYP27A1-based systems in combination with bovine redox partners, established recently in *B. megaterium* MS941 strain, showed higher product yields in comparison to similar recombinant systems in *Saccharomyces cerevisiae* and *Escherichia coli* (Duport et al., 1998; Ehrhardt et al., 2016a; Gerber et al., 2015; Salamanca-Pinzón and Guengerich, 2011). It is not surprising that *B. megaterium* systems based on endogenous soluble P450s are also effective. For example, ATCC13368 strain, the native host of CYP106A2 was successfully applied for the preparative conversion of dehydroepiandrosterone into its pharmaceutically important 7 β -hydroxymetabolite (Schmitz et al., 2014). In other studies, MS941 strains, overexpressing only P450s, or P450 with semi-homologous (endogenous Fdx, Arh1 from *S. pombe*) or heterologous (bovine AdR, Adx) redox chains, were applied for regio-selective hydroxylations of various steroids, di- and triterpenes (Bleif et al., 2011, 2012; Brill et al., 2014; Kiss et al., 2015a).

CYP106A2 and CYP109E1 are interesting and functionally different P450 monooxygenases from *B. megaterium*. CYP106A2 is a versatile steroid hydroxylase, whereas CYP109E1 is a vitamin D3 hydroxylase with limited catalytic activity towards common steroidal compounds. Both enzymes are soluble, belong to the class I P450 systems, and have been shown to be successfully overexpressed in *B. megaterium* as well as heterologously in *E. coli* (Bleif et al., 2012; Józwik et al., 2016; Schmitz et al., 2012). Since their physiological role and substrates remain unknown, it is attractive to further characterize these P450s to explore biotechnologically desirable reactions and establish novel P450-based effective, eco-friendly and low-cost whole-cell systems for the production of valuable products in reasonable amounts. CYP106A2- and CYP109E1-based biotransformations of structurally diverse compounds are studied in this work. Due to the fact that CYP106A2 is being investigated since many years, several studies have been conducted to identify its substrate range and, consequently, a number of various compounds has been screened and reported as substrates (Schmitz et al., 2018). This work aimed for a detailed characterization of biotransformation of the pharmaceutically highly important steroids prednisone and dexamethasone in order to produce hydroxylated products using several CYP106A2-based whole-cell systems. In contrast to CYP106A2, CYP109E1 has been investigated for only a few years, resulting in the identification of four substrates so far (Brill, 2013). Therefore, this work aimed to further characterize CYP109E1 by exploring novel potential substrates and to establish whole-cell systems for the production of important oxygenated products.

3.1 Production of glucocorticoid drug derivatives

Prednisone and dexamethasone are synthetic steroidal (glucocorticoid) drugs (Scheme 1 in **Chapter 2.1**), identified as substrates of CYP106A2 that show a type I spectral shift and *in vitro* conversion in

previous study (Schmitz et al., 2014). However, the reaction products have not been identified. Due to the fact that CYP106A2 is a versatile steroid hydroxylase, and hydroxysteroids are important for drug design and development approaches, the conversion of both drugs was characterized in detail in this study (**Chapter 2.1**).

Investigating binding titrations with difference spectroscopy (Figure 1 in **Chapter 2.1**) and *in vitro* kinetics (Figure 3 in **Chapter 2.1**) showed tighter binding affinity of dexamethasone ($K_d=189\text{ }\mu\text{M}$, $K_M=115\text{ }\mu\text{M}$) to CYP106A2 compared with that of prednisone ($K_d=434\text{ }\mu\text{M}$, $K_M=185\text{ }\mu\text{M}$). Despite the stronger binding, the catalytic activity of CYP106A2 towards dexamethasone was found to be remarkably lower ($k_{cat}=8\text{ min}^{-1}$) than towards prednisone ($k_{cat}=116\text{ min}^{-1}$). It was shown that CYP106A2 hydroxylates both glucocorticoids in a highly regio- and stereo-selective manner, yielding exclusively one product using bovine AdR and Adx₄₋₁₀₈ as redox partners (Figure 2 in **Chapter 2.1**). The CYP106A2-mediated conversions were further investigated by *B. megaterium* whole-cell systems in order to reproduce the *in vitro* activity and isolate the products for the structure identification via NMR. Significant differences have been observed between prednisone and dexamethasone conversions using several CYP106A2-based *B. megaterium* systems. In case of dexamethasone, the product pattern *in vivo* was similar to *in vitro*, whereas for prednisone, one product was identified *in vitro* and up to four *in vivo* using the different strains (Figures 2 and 5 in **Chapter 2.1**). The natural host strain of CYP106A2, ATCC13368 (ATCC_wt), showed higher selectivity and activity towards prednisone than the MS941 strains that overexpressed either CYP106A2 (MS941_C) or CYP106A2 with adrenal redox partners (MS941_CAA) (Figure 6 in **Chapter 2.1**). The NMR analysis of the obtained prednisone products revealed already reported as well as new derivatives that were modified at four sites in the steroid structure: 15 β -hydroxyprednisone, 15 β , 17, 21-trihydroxy-preg-4-en-3,11,20-trione, 20 β -dihydrocortisone, cortisone, 15 β ,17,20 β ,21-tetrahydroxy-preg-4-en-3,11-dione and 15 β ,17,20 β ,21-tetrahydroxy-preg-1,4-dien-3,11-dione (Figure 6). In addition, prednisone was found to be converted to 20 β -dihydrocortisone via the intermediate cortisone also with MS941_wt control strain that does not encode CYP106A2. This result indicated that the structural modifications at positions C20 and C1-C2 are carried out by endogenous enzymes of *B. megaterium* strains such as FabG (Gerber et al., 2016). In contrast to prednisone, dexamethasone was not converted by MS941_wt (CYP106A2-independent) strain and its conversion by different CYP106A2-based whole-cells yielded one product, 15 β -hydroxydexamethasone. Thus, the obtained results identified the 15 β -hydroxylase activity of CYP106A2 towards both investigated substrates. *In silico* studies using the crystal structure of CYP106A2 (Janocha et al., 2016) provided an explanation of the aforementioned lower activity of CYP106A2 towards dexamethasone. It was suggested that the radical formed after hydrogen abstraction at C15 can migrate to the energetically more favorable position 16 (Figure 4 in

Chapter 2.1), causing the radical depletion and, therefore, lowering the 15β -hydroxylation activity of P450 towards this substrate.

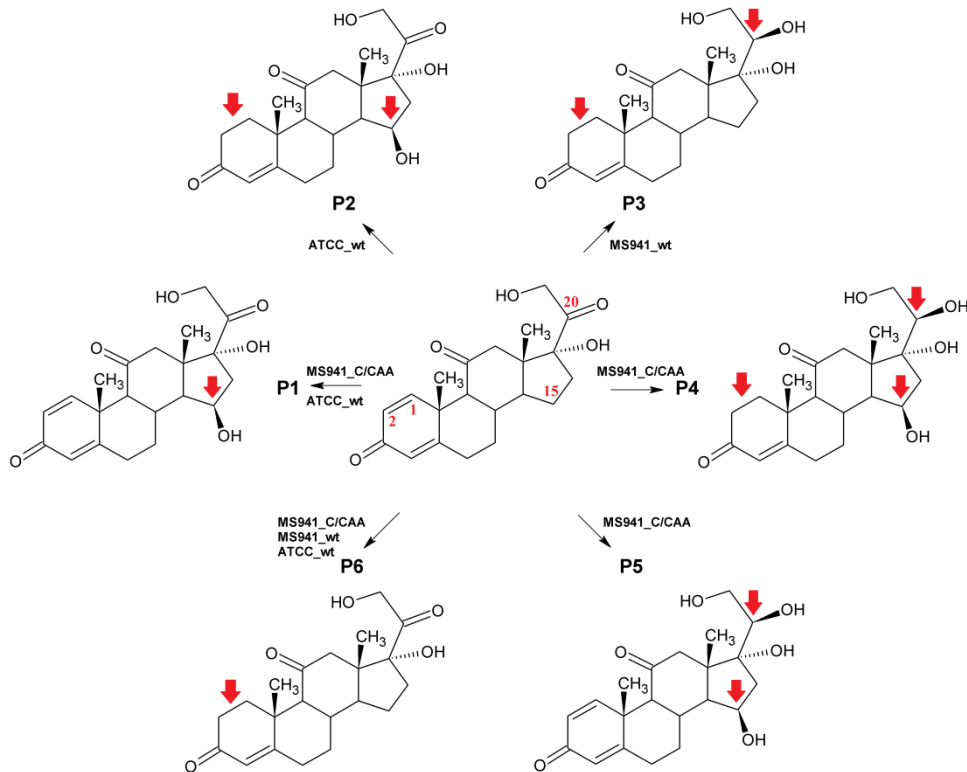


Figure 6. Chemical structures of prednisone derivatives produced by different *B. megaterium* strains. Prednisone is depicted in the middle (positions modified in its structure are numbered). Site of modification for a particular product is shown with a red arrow. P1: 15β -hydroxyprednisone, P2: 15β , 17, 21-trihydroxy-preg-4-en-3,11,20-trione, P3: 20 β -dihydrocortisone, P4: 15β ,17,20 β ,21-tetrahydroxy-preg-4-en-3,11-dione, P5: 15β ,17,20 β ,21-tetrahydroxy-preg-1,4-dien-3,11-dione, P6:cortisone. Figure adapted from Putkaradze et al. (2017a)

To sum up, CYP106A2 was identified as a highly selective prednisone and dexamethasone 15β -hydroxylase. This enzyme provides a possibility to generate 15β -hydroxyprednisone and 15β -hydroxydexamethasone using a reconstituted *in vitro* system as well as *B. megaterium* whole-cell biocatalysts. Due to the high selectivity of dexamethasone conversion *in vivo*, the investigated CYP106A2-based strains can be applied for milligram-scale production of 15β -hydroxydexamethasone and can be further studied to optimize the productivity. In contrast to dexamethasone, low selectivity was observed for prednisone conversion *in vivo*, yielding two new prednisone metabolites, 15β ,17,20 β ,21-tetrahydroxy-preg-4-en-3,11-dione and 15β ,17,20 β ,21-tetrahydroxy-preg-1,4-dien-3,11-dione, in addition to the 15β -hydroxylated product. Therefore, for the highly selective and low-cost production of 15β -hydroxyprednisone, a CYP106A2-based system in other microorganisms such as *E. coli* should be established. 15β -hydroxydexamethasone and prednisone derivatives (15β -hydroxyprednisone, 15β ,17,20 β ,21-tetrahydroxy-preg-4-en-3,11-dione

and $15\beta,17,20\beta,21$ -tetrahydroxy-preg-1,4-dien-3,11-dione), generated in this study, are pharmaceutically interesting uncharacterized compounds. They can be used for biological activity studies and as lead steroidal compounds for further modification. To shift the hydroxylation activity of CYP106A2 from 15β to pharmaceutically important positions such as 9α (for prednisone) or 6β (for both substrates) protein engineering strategies can be applied (Nikolaus et al., 2017; Nguyen et al., 2012).

3.2 CYP109E1 as versatile biocatalyst

A novel P450 from *B. megaterium*, CYP109E1, has been identified as testosterone and vitamin D₃ hydroxylase in previous and our parallel studies (Abdulmughni et al., 2017; Józwik et al., 2016). Interestingly, CYP109E1 is phylogenetically related to the steroid hydroxylase CYP106A1; however, in contrast to CYP106A1, of the tested 3-oxo- Δ^4 -steroids it converts only testosterone efficiently (Table 3). Some steroids, such as corticosterone and dexamethasone, bind to the enzyme and induce a high-spin shift, nevertheless they are not metabolized. Considering the steroid structures and experimental data, it can be assumed that the hydroxyl group at position C17 (present in cortisone, cortisol, RSS, prednisone, dexamethasone and prednisolone) restricts the binding to the heme when there is no methyl group at position C16 (present in dexamethasone). In addition, the methyl group at position C10 in testosterone (not present in 19-nortestosterone) seems crucial for binding and catalytic activity of CYP109E1. The structural (crystallographic), computational (MD simulations) and experimental (site-directed mutagenesis) results for corticosterone and testosterone binding and conversion provided important insights on the interactions of CYP109E1 with these steroids. In the active site, the steroid compounds are proposed to be orientated in two positions perpendicular to the heme plane so that in the first case the 3-keto group of steroids (A ring) is the closest to the heme and the C17 position is far away (unproductive binding mode) and *vice versa* (productive binding mode) (Józwik et al., 2016). The experimental data for another steroid-related substrate of CYP109E1, vitamin D₃, suggests similar binding orientations showing either 1-hydroxylation (analogously to the A ring of steroids) or predominant 24/25-hydroxylations (side chain) (Abdulmughni et al., 2017). Interestingly, vitamin D₃ is not able to displace the water ligand of the heme; however, it can be converted by CYP109E1. Additionally, two smaller molecules, nootkatone and isolongifolen-9-one, showed type I difference spectrum and were converted by CYP109E1 (Brill, 2013).

With the goal to provide further insights concerning the substrate range and biotechnological potential of this important P450, several compounds have been tested as potential substrates. They have been selected based on two principles: 1) known substrates of CYP109 family enzymes and related

compounds (Furuya et al., 2009) (Scheme 1 in **Chapter 2.3**), and 2) compounds with methyl-branched hydrocarbon chains such as that of vitamin D₃ (Figure S1). As a result, the substrate range of CYP109E1 was expanded with many compounds that are significant for the biotechnological and pharmaceutical as well as fragrance industries (Table 3). Most of them showed a type I spin shift of CYP109E1 upon binding (Figures 1 and S1 in **Chapter 2.3**) and were successfully converted with high selectivities *in vitro* as well as *in vivo* (Figures 2 and 3 in **Chapter 2.3**). A *B. megaterium* CYP109E1-based system has been successfully utilized for the biotransformations of the novel compounds and for the isolation of the reaction products on milligram-scale for the structure identification via NMR spectrometry. An important statin drug (pravastatin), hydroxylated drug metabolites (6'β-hydroxy-lovastatin, 3'α-hydroxy-simvastatin and 4"-hydroxy-simvastatin) and several terpene derivatives (3-hydroxy-α-ionone, 4-hydroxy-β-ionone, 11,12-epoxy-nootkatone, 4(*R*)-hydroxy-isolongifolen-9-one, 3-hydroxy-α-damascone, 4-hydroxy-β-damascone, 3,4-epoxy-β-damascone and 2-hydroxy-β-damascenone) have been produced using a CYP109E1-based whole-cell biocatalyst (Putkaradze et al., 2017b). It is important to note, that CYP109E1 is the first enzyme to be identified as being capable of converting simvastatin to 4"-hydroxy-simvastatin as well as β-damascenone to 2-hydroxy-β-damascenone, a novel compound, providing the possibility to easily synthesize and functionally characterize these molecules. Furthermore, this enzyme is able to perform one of the most important P450-based reactions on industrial scale, the conversion of a natural product, compactin, to pravastatin. Due to its observed wide substrate specificity, screening of a natural product library seems highly promising to identify new reactions of CYP109E1 as described for CYP106A2 in previous study (Schmitz et al., 2014). In addition, the CYP109E1-based system found to be effective *in vivo*, especially in producing the ionone derivatives, converting up to 200 μM α- and β-ionone almost completely within 2 h (Figure 3a and b in **Chapter 2.3**). Each conversion needs to be further investigated in order to identify suitable optimization strategies and enhance the productivity. It is noteworthy that *B. megaterium* cells, used in this study, are overexpressing CYP109E1 without redox partners and the activity of P450 is supported by endogenously synthesized unknown proteins. Therefore, the identification of the cognate redox partners and their coexpression together with CYP109E1 seems to be a very promising strategy to increase the productivity of the *in vivo* system.

Five more compounds, cholesterol, 7-ketcholesterol, ergosterol, stigmasterol and vitamin D₂ (ergocalciferol), were selectively converted by CYP109E1 *in vitro* and were identified as its novel substrates (Figures S2a and S3). As previously mentioned, their structures are similar to vitamin D₃ having a steroidal or seco-steroidal core and a hydrocarbon side chain. Because of the reported narrow cavity of the active site with almost exclusively hydrophobic architecture near to heme and predominant 24(*S*)/25-hydroxylation activity towards vitamin D₃ (Figure 3 in **Chapter 2.2**),

modifications at side-chain positions are also expected for other similar substrates. To prove this, the biotransformation of cholesterol by CYP109E1 has been further investigated. The *in vitro* experiment showed that cholesterol was converted by CYP109E1 to two main products with comparable selectivities (Figure S2a and b). The conversion was successfully reproduced *in vivo* (Figure S2c) and the reaction products have been isolated for structure elucidation by NMR (NMR data in **Chapter 5.1**).

Table 3. Overview of tested compounds for *in vitro* assays with CYP109E1 and all identified substrates. “n.d” not determined

Compound	Spin shift	<i>In vitro</i> conversion	Reference
Testosterone	yes	yes	(Brill, 2013)
Vitamin D3	no	yes	(Brill, 2013)
Nootkatone	yes	yes	(Brill, 2013)
Isolongifolen-9-one	yes	yes	(Brill, 2013)
Androstenedione	yes	low (<10%)	(Józwik et al., 2016)
Cortisol	no	no	(Józwik et al., 2016)
Cortisone	no	no	(Józwik et al., 2016)
Corticosterone	yes	no	(Józwik et al., 2016)
DOC	yes	low (<7%)	(Józwik et al., 2016)
RSS	no	no	(Józwik et al., 2016)
Prednisone	no	no	(Józwik et al., 2016)
Dexamethasone	yes	no	(Józwik et al., 2016)
Prednisolone	no	no	(Józwik et al., 2016)
Progesterone	no	no	(Józwik et al., 2016)
Testosterone acetate	yes	low (<10%)	(Józwik et al., 2016)
19-nortestosterone	no	no	(Józwik et al., 2016)
Compactin	yes	yes	this work
Lovastatin	yes	yes	this work
Simvastatin	yes	yes	this work
Medroxyprogesterone acetate	no	no	this work
Norethisterone	no	no	this work
Norethisterone acetate	no	no	this work
α -ionone	yes	yes	this work
β -ionone	yes	yes	this work
α -damascone	yes	yes	this work
β -damascone	yes	yes	this work
β -damascenone	yes	yes	this work
Cholesterol	n.d.	yes	this work
7-ketocholesterol	n.d.	yes	this work
Ergosterol	n.d.	yes	this work
Stigmasterol	n.d.	yes	this work
Vitamin D ₂	n.d.	yes	this work

As expected, it was found that CYP109E1 is able to catalyze 24(S)- and 25-hydroxylations of cholesterol, similar to vitamin D₃ (Figure 7). 24(S)- and 25-hydroxycholesterols are highly important

physiological oxysterols. They act as agonists of liver receptors LXR α and LXR β (Berrodin et al., 2010; Janowski et al., 1999) as well as ligands of the RAR-related orphan receptors ROR α and ROR γ (Mutemberezi et al., 2016). 24(S)-hydroxycholesterol is formed by CYP46A1 in the brain and it has also been suggested as a biomarker for neurodegenerative diseases (Leoni and Caccia, 2013), whereas 25-hydroxycholesterol is synthesized by the enzyme cholesterol 25-hydroxylase and has been reported to have potent effects on the immune system (McDonald and Russell, 2010). The intensive research on the wide-ranging effects of the oxysterols demands their availability in sufficient amounts and makes systems producing these metabolites biotechnologically highly attractive. To date, the obtained oxysterols are highly expensive compounds: 24(S)-hydroxycholesterol is about 3300-fold and 25-hydroxycholesterol up to 500-fold more expensive than their precursor, cholesterol.

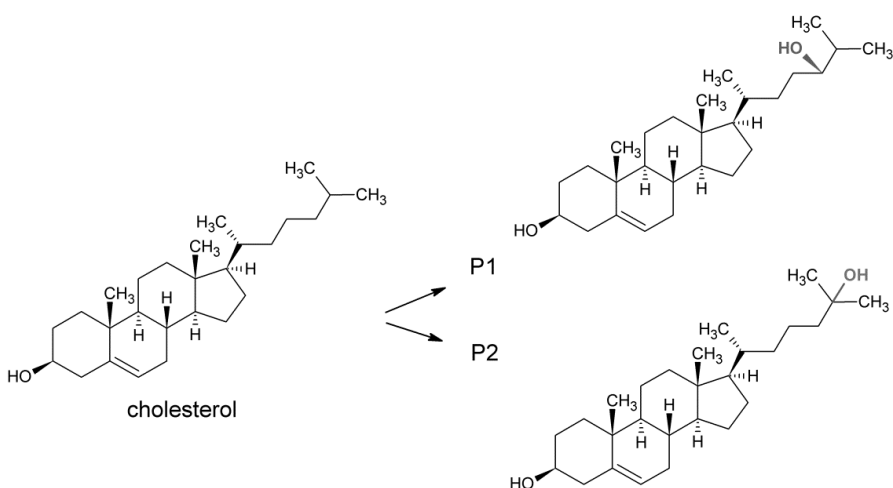


Figure 7. Chemical structures of cholesterol and its metabolites produced by CYP109E1, elucidated by NMR spectrometry. P1: 24(S)-hydroxycholesterol, P2: 25-hydroxycholesterol

Interestingly, the CYP109E1-based *B. megaterium* system used in our studies (Abdulmughni et al., 2017; Putkaradze et al., 2017b) showed remarkably low activity towards cholesterol, yielding about 20% conversion of 200 μ M substrate after 48 h, which was not the case for other substrates such as vitamin D₃. The reason of this can be a partial availability of cholesterol for CYP109E1 due to their different cellular localizations. As reported in previous study, cholesterol accumulates in poly-3-hydroxybutyrate (PHB) bodies of *B. megaterium* (Gerber et al., 2015), whereas CYP109E1 is a soluble protein localized in the cytoplasm. Therefore, application of a *B. megaterium* strain, that lacks the ability to synthesize PHB bodies for CYP109E1-based whole-cell conversion of cholesterol, seems very promising to analyse this. As an alternative, a novel CYP109E1-based *E. coli* system was successfully established in this study showing 3.3-fold higher conversion of cholesterol compared with *B. megaterium* system (Figure S2d) and representing also even more promising basis for further improvement.

In summary, the substrate range of CYP109E1 was extended with 13 new compounds including statins (compactin, lovastatin and simvastatin), norisoprenoids (ionones, damascones and β -damascenone), sterols (cholesterol, 7-ketocholesterol, ergosterol and stigmasterol) and a seco-steroid (vitamin D₂). Most of the novel CYP109E1-dependent biotransformations were characterized *in vitro* as well as *in vivo*. This lead to identification of several biotechnologically interesting reactions (and two whole-cell systems), producing statin drug metabolites, terpene derivatives and important oxysterols. Apart from them, CYP109E1 was found to be able to catalyze a novel enzymatic reaction, 4"-hydroxylation of simvastatin, and an industrially relevant transformation producing pravastatin.

3.3 Towards engineering of CYP109E1 for pravastatin production

Regio- and stereo-selective 6' β -hydroxylation of compactin to the drug pravastatin is a highly important reaction (Sakaki, 2012). As mentioned before, CYP109E1 has been identified as one of a few P450s capable of carrying out this biotransformation. It is important to note that this wild type enzyme can produce the pharmacologically active pravastatin in a highly stereo-selective manner (Scheme 2 in **Chapter 2.3**). Moreover, the CYP109E1-based whole-cell system, applied in this study, produced up to 14 mg/L pravastatin within 4 h, showing comparable productivity to other wild type systems, CYP105A3 (12.9 mg/L within 21 h) and CYP107DY1 (13.2 mg/L within 20 h), while increasing the space-time yield 5 times (Milhim et al., 2016a; Putkaradze et al., 2017b). This makes the CYP109E1-based system a good candidate for optimization in order to improve the pravastatin production. Despite showing high selectivity (82 \pm 5%), CYP109E1 activity towards compactin, both *in vitro* and *in vivo*, was shown to be remarkably lower in comparison with other statin substrates, e.g. lovastatin and simvastatin (Figures 2 and S2 in **Chapter 2.3**). Moreover, the determined dissociation constants showed about 18- and 9-fold weaker binding for compactin ($K_d=84\text{ }\mu\text{M}$) to CYP109E1 compared to simvastatin ($K_d=4.7\text{ }\mu\text{M}$) and lovastatin ($K_d=9.6\text{ }\mu\text{M}$), respectively (Table 1 in **Chapter 2.3**). Therefore, CYP109E1 is an attractive target for further improvement via mutagenesis. In general, active site engineering is an effective strategy to enhance the catalytic activity or especially the selectivity of P450s (Wong, 1998). There are few factors that control the selectivity of P450: (i) the affinity of a compound to the binding pocket that is determined by hydrophobicity of the molecule and the active site architecture, (ii) the reactivity of a particular C-H bond in the molecule determined by the bond energy, and (iii) the limitations determined by the active site adapting the ligand relative to oxidizing species and hindering its mobility (Ortiz de Montellano, 2010). The change in the selectivity of P450 towards its substrate through active site engineering is promising due to the fact that it depends mostly on the distance between the oxidation site of the substrate and the ferryl oxygen (Wong, 1998). The identification of the key residues involved in the substrate recognition is fundamental for successful active site re-design, which can be accomplished by site-directed

mutagenesis studies. It is important to note, that mutations in the active site can also have negative effects on heme redox potential causing limitation of electron transfer, on oxygen activation and proton delivery as well as on productive substrate binding (Makris et al., 2007). On the other hand, mutations away from the active site, in the substrate entrance channel or on the protein surface, such as the region interacting with redox partners, can improve the activity of a P450. In order to enhance the 6'β-hydroxylation activity of CYP109E1 towards compactin, several single alanine mutants, I85A, V169A, K187A and E245A, have been tested *in vitro* (Figure S4a). These mutants were created in previous and parallel studies, showing higher catalytic activities for the formation of either 16β-hydroxytestosterone or 25-hydroxyvitamin D₃ (Abdulmughni et al., 2017; Józwik et al., 2016). Among the screened mutants the I85A variant showed higher selectivity for the formation of pravastatin (>99%) and a 2.5-fold increase in catalytic activity in comparison with the wild type (Figure S4b). Thus, the position 85 was found to be important for compactin conversion by CYP109E1 and was further investigated in *B. megaterium* using position-85 single mutants substituted to several hydrophobic and polar charged residues: I85A, I85V, I85M, I85F, I85W, I85D and I85R (kindly provided by Ammar Abdulmughni). As shown in Figure 8a, the valine substitution slightly increased the activity, albeit decreased the selectivity. Substitutions by hydrophobic residues bigger than isoleucine (methionine, phenylalanine and tryptophan) drastically decreased the activity (Figure 8a), whereas substitution by the charged amino acids arginine and aspartic acid completely abolished it (data not shown). Similar to *in vitro* result, substitution of isoleucine with alanine significantly increased the activity as well as selectivity compared with the wild type *in vivo* (Figure 8b, c and d). The isoleucine residue at position 85 is located in the active site pocket on the BC loop (SRS1) near to the heme. This and analogous positions, such as F87 of CYP102A1, have been reported to be crucial for determining P450 selectivity towards its substrates and catalytic activity (Gricman et al., 2015). For example, the I85A mutant of CYP109E1 improved the selectivity of CYP109E1 towards vitamin D₃ yielding an about 2-fold increase of 25-hydroxyvitamin D₃ production, whereas the F87A mutant of CYP102A1 enhanced a NADPH-supported hydroxylation activity towards p-nitrophenoxydodecanoic acid 2.5 times and an H₂O₂-supported activity even further (Abdulmughni et al., 2017; Li et al., 2001). In contrast to vitamin D₃ conversion, the replacement of isoleucine 85 with alanine of CYP109E1 increased not only the selectivity but also the catalytic activity about 3-fold (Figure 8). Thus, the I85A variant was identified as very promising for further optimization. This CYP109E1 single mutant, on the one hand, has the potential to be applied for establishing a high-yield pravastatin-producing whole-cell system such as *Penicillium chrysogenum* (McLean et al., 2015). On the other hand, it is also interesting as a basis for further improvement of the CYP109E1 activity through mutagenesis. The I85 residue was predicted to involve in hydrophobic interactions of CYP109E1 with compactin by molecular docking (Figure 5a in

Chapter 2.3). Other putative compactin binding residues identified by docking calculations, L238 (SRS4), L292 and H293 (SRS5), might be also highly interesting for further investigation.

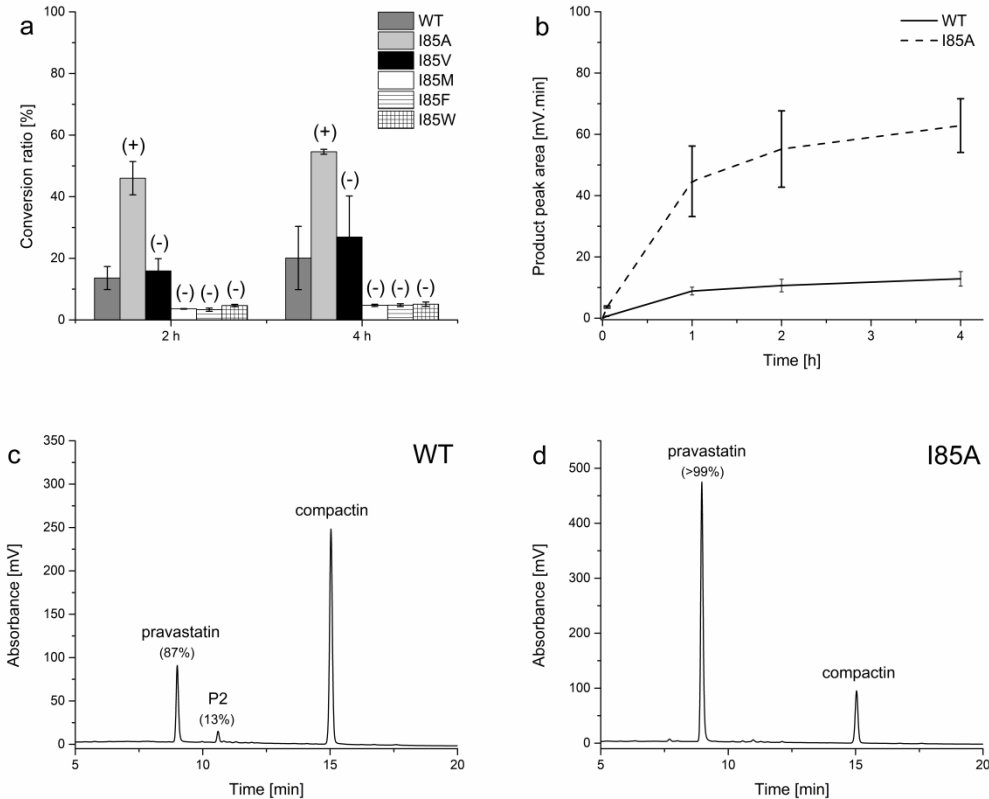


Figure 8. *In vivo* conversion of compactin by selected I85 mutants (a). "(-)" selectivity similar or lower than of WT, "(+)" selectivity higher than of WT. Comparison of wild type (WT) and I85A in *B. megaterium* MS941 (b). Conversion of WT (solid), of I85A (dashed). The data represents the mean of three independent measurements with the corresponding standard deviations. HPLC chromatograms of compactin conversion by WT (c) and I85A mutant (d)

Moreover, it seems promising to re-design CYP109E1 according to the best pravastatin-producing mutant of CYP105AS1 from *A. orientalis*, P450_{prava}, due to the similarity of mutated residues to CYP109E1. P450_{prava} is a quintuple mutant of CYP105AS1 with enhanced stereo-selectivity and 21-fold improved affinity for compactin compared to the wild type (McLean et al., 2015; Yasuda et al., 2018). The sequence alignment of P450_{prava} (I95T/Q127R/A180V/L236I/A265N) and CYP109E1 indicated that two mutated residues, arginine at position 127 and valine at position 180, already exist in the wild type of CYP109E1 (R117 and V169) (Figure 9). Two residues, I95 and L236, substituted with threonine and isoleucine in P450_{prava}, respectively, are present in CYP109E1 in their original forms (I85 and L238). Their structural localizations in the active site are also very similar (Figure 10). Therefore, substitution of these residues in CYP109E1 with the amino acids similar to P450_{prava} seems

to be promising. Furthermore, the fifth mutated residue 265 is distant from the active site and is proposed to be important for the activity and/or stability of CYP105AS1 (Yasuda et al., 2018). Therefore, it would also be interesting to investigate the corresponding residue in CYP109E1 (residue 267).

CYP109E1	60 E-----QKNIFSSDRRPPQNQRQTALGTSI
P450prava	61 IDPRFSNRPEHKHPVFSVIPRPGG-ATKAPAPGWFTNMDAPEHTRYRRMLISQFTVRRIK
	: : ** * * : : : * : * : * : * : . ** : : *
CYP109E1	AWEPKIAIRITNELLQEVEH-LEDIDIVEHLSYPLPVMVIADILGVPIEDQRQFKDWSDII
P450prava	ELEPRIVRITEDHLDAMAKAGPPVDLVQAFALPVPSLVICELLGVSYADHAFFQEQTTIM
	;*.**: * : : : : * : * : * : ***:*** * : * : : * :
CYP109E1	VAGPSNNERETLEKLQQEKMKANDELEYFYRIIEEKRTRPGDDIISVLLQAKEEGKQLT
P450prava	VSVD-----KTQDEVTTALGKLTRYIAELVATKRLSPKDDLLGSLIT---DTDILT
	*: * * ; * . * . : * : . : : * * * * : * : . : * :
CYP109E1	DEEIVGFSILLLIAGNETTNLNISNTIYCLMEDKASFERLKREKELLPSGIEEVLRYRSP 288
P450prava	DEELTNIALILLVAGHETTANMLGLGTFALLQHPEQIANLD----SPDAVEELLRYLSI 281
	:..:..::***:..: ..*:.. . : . * . * ..:***:*** *

Figure 9. Part of the sequence alignment of CYP109E1 and the quintuple mutant of CYP105AS1, P450_{prava}, showing the mutated residues (in red). Substitutions of P450_{prava} present also in CYP109E1 are shown in blue. The alignment was generated with Clustal Omega (Goujon et al., 2010; Sievers et al., 2011)

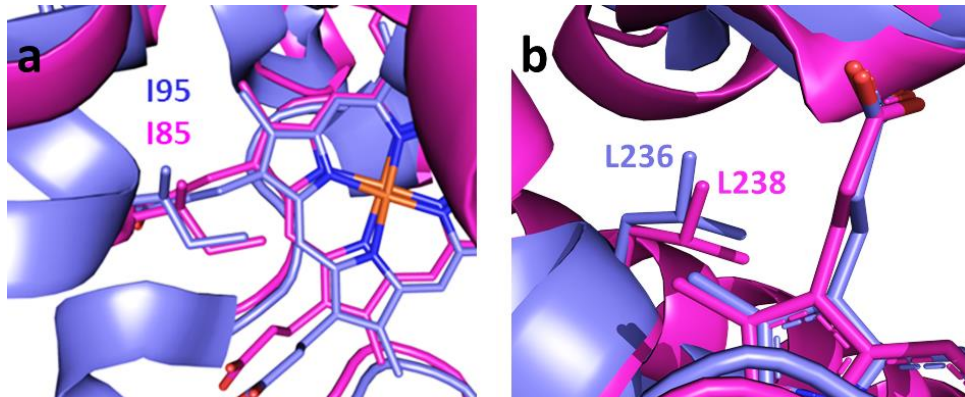


Figure 10. Structural similarity of the two active site residues of CYP109E1 (magenta) and CYP105AS1 (purpleblue): I85, I95 (a) and L238, L236 (b). For the alignment substrate-free crystal structures of CYP109E1 (PDB ID: 5L90) (Józwik et al., 2016) and CYP105AS1 (PDB ID: 4OQS) (McLean et al., 2013), and PyMOL (DeLano Scientific, CA, USA) were used. The root mean square deviation (RMSD) is 1.29 Å

3.4 Conclusions

Taken together, this work provides novel insights into *in vitro* and *in vivo* catalysis of CYP106A2 and CYP109E1 enzymes from *B. megaterium*. The well-studied CYP106A2 was further characterized as a highly regio- and stereo-selective 15 β -hydroxylase of prednisone and dexamethasone. The newly

DISCUSSION AND OUTLOOK

identified CYP109E1 was found to act as a versatile statin, norisoprenoid and sterol oxidase performing, among others, the industrially important $6'\beta$ -hydroxylation of compactin to the drug pravastatin. This enzyme has been characterized as one of a few highly stereo-selective compactin hydroxylases, showing higher pravastatin yield within 4 h *in vivo* compared to other wild type P450 systems. Furthermore, this study has shown the ability of CYP106A2 and CYP109E1 whole-cell biocatalysts to produce diverse biotechnologically and pharmaceutically interesting compounds, such as drug derivatives (15β -hydroxyprednisone, 15β -hydroxydexamethasone, $6'\beta$ -hydroxy-lovastatin, $3'\alpha$ -hydroxy-simvastatin and $4''$ -hydroxy-simvastatin), valuable oxysterols ($24(S)$ -hydroxycholesterol and 25 -hydroxycholesterol) and several terpenoids (3-hydroxy- α -ionone, 4-hydroxy- β -ionone, $11,12$ -epoxy-nootkatone, $4(R)$ -hydroxy-isolongifolen-9-one, 3-hydroxy- α -damascone, 4-hydroxy- β -damascone and $3,4$ -epoxy- β -damascone). The investigated systems were found to be suitable for generating these complex organic molecules on milligram-scale. Moreover, they have demonstrated unique yet simple ways to produce new compounds, such as 2-hydroxy- β -damascenone, $15\beta,17,20\beta,21$ -tetrahydroxy-preg-1,4-dien-3,11-dione and $15\beta,17,20\beta,21$ -tetrahydroxy-preg-4-en-3,11-dione, and, by doing so, make the functional investigation of these substances possible. The obtained results provide an important basis for further improvements of CYP106A2 and CYP109E1 as well as their whole-cell systems towards industrial scale.

4. References

- Abdulgughni, A., Józwik, I.K., Putkaradze, N., Brill, E., Zapp, J., Thunnissen, A.-M.W.H., Hannemann, F., and Bernhardt, R. (2017). Characterization of cytochrome P450 CYP109E1 from *Bacillus megaterium* as a novel vitamin D₃ hydroxylase. *J. Biotechnol.* 243, 38–47.
- Agematu, H., Matsumoto, N., Fujii, Y., Kabumoto, H., Doi, S., Machida, K., Ishikawa, J., and Arisawa, A. (2006). Hydroxylation of testosterone by bacterial cytochromes P450 using the *Escherichia coli* expression system. *Biosci. Biotechnol. Biochem.* 70, 307–311.
- Barriuso, J., Nguyen, D.T., Li, J.W.-H., Roberts, J.N., MacNevin, G., Chaytor, J.L., Marcus, S.L., Vederas, J.C., and Ro, D.-K. (2011). Double oxidation of the cyclic nonaketide dihydromonacolin L to monacolin J by a single cytochrome P450 monooxygenase, LovA. *J. Am. Chem. Soc.* 133, 8078–8081.
- Basch, J., and Chiang, S.-J. (2007). Cloning and expression of a cytochrome P450 hydroxylase gene from *Amycolatopsis orientalis*: hydroxylation of epothilone B for the production of epothilone F. *J. Ind. Microbiol. Biotechnol.* 34, 171–176.
- Belin, P., Le Du, M.H., Fielding, A., Lequin, O., Jacquet, M., Charbonnier, J.-B., Lecoq, A., Thai, R., Courçon, M., and Masson, C. (2009). Identification and structural basis of the reaction catalyzed by CYP121, an essential cytochrome P450 in *Mycobacterium tuberculosis*. *Proc. Natl. Acad. Sci.* 106, 7426–7431.
- Bell, S.G., and Wong, L.-L. (2007). P450 enzymes from the bacterium *Novosphingobium aromaticivorans*. *Biochem. Biophys. Res. Commun.* 360, 666–672.
- Bell, S.G., Yang, W., Yorke, J.A., Zhou, W., Wang, H., Harmer, J., Copley, R., Zhang, A., Zhou, R., Bartlam, M., et al. (2012). Structure and function of CYP108D1 from *Novosphingobium aromaticivorans* DSM12444: an aromatic hydrocarbon-binding P450 enzyme. *Acta Crystallogr. D. Biol. Crystallogr.* 68, 277–291.
- Berg, A., and Rafter, J.J. (1981). Studies on the substrate specificity and inducibility of cytochrome P-450meg. *Biochem. J.* 196, 781–786.
- Berg, A., Carlstrom, K., Gustafsson, J.A., and Ingelman-Sundberg, M. (1975). Demonstration of a cytochrome P-450-dependent steroid 15beta-hydroxylase in *Bacillus megaterium*. *Biochem. Biophys. Res. Commun.* 66, 1414–1423.

- Berg, A., Gustafsson, J.A., and Ingelman-Sundberg, M. (1976). Characterization of a cytochrome P-450-dependent steroid hydroxylase system present in *Bacillus megaterium*. *J. Biol. Chem.* 251, 2831–2838.
- Berg, A., Ingelman-Sundberg, M., and Gustafsson, J.A. (1979). Purification and characterization of cytochrome P-450meg. *J. Biol. Chem.* 254, 5264–5271.
- Bernhardt, R. (2006). Cytochromes P450 as versatile biocatalysts. *J. Biotechnol.* 124, 128–145.
- Bernhardt, R., and Urlacher, V.B. (2014). Cytochromes P450 as promising catalysts for biotechnological application: chances and limitations. *Appl. Microbiol. Biotechnol.* 98, 6185–6203.
- Berrodin, T.J., Shen, Q., Quinet, E.M., Yudt, M.R., Freedman, L.P., and Nagpal, S. (2010). Identification of 5 α , 6 α -epoxycholesterol as a novel modulator of liver X receptor activity. *Mol. Pharmacol.* 78, 1046–1058.
- Bischoff, D., Bister, B., Bertazzo, M., Pfeifer, V., Stegmann, E., Nicholson, G.J., Keller, S., Pelzer, S., Wohlleben, W., and Süßmuth, R.D. (2005). The biosynthesis of vancomycin-type glycopeptide antibiotics—a model for oxidative side-chain cross-linking by oxygenases coupled to the action of peptide synthetases. *ChemBioChem.* 6, 267–272.
- Bleif, S., Hannemann, F., Lisurek, M., von Kries, J.P., Zapp, J., Dietzen, M., Antes, I., and Bernhardt, R. (2011). Identification of CYP106A2 as a regioselective allylic bacterial diterpene hydroxylase. *ChemBioChem.* 12, 576–582.
- Bleif, S., Hannemann, F., Zapp, J., Hartmann, D., Jauch, J., and Bernhardt, R. (2012). A new *Bacillus megaterium* whole-cell catalyst for the hydroxylation of the pentacyclic triterpene 11-keto- β -boswellic acid (KBA) based on a recombinant cytochrome P450 system. *Appl. Microbiol. Biotechnol.* 93, 1135–1146.
- Brill, E. (2013). Identifizierung und Charakterisierung neuer Cytochrom P450 Systeme aus *Bacillus megaterium* DSM319. Dissertation. Universität des Saarlandes.
- Brill, E., Hannemann, F., Zapp, J., Brüning, G., Jauch, J., and Bernhardt, R. (2014). A new cytochrome P450 system from *Bacillus megaterium* DSM319 for the hydroxylation of 11-keto- β -boswellic acid (KBA). *Appl. Microbiol. Biotechnol.* 98, 1701–1717.
- Bunk, B., Schulz, A., Stammen, S., Münch, R., Warren, M.J., Rohde, M., Jahn, D., and Biedendieck, R. (2010). A short story about a big magic bug. *Bioeng. Bugs.* 1, 85–91.

- Bureik, M., and Bernhardt, R. (2007). Steroid hydroxylation: microbial steroid biotransformations using cytochrome P450 enzymes. *Modern Biooxidation*. Wiley-VCH publishing. 155–176.
- Bureik, M., Schiffler, B., Hiraoka, Y., Vogel, F., and Bernhardt, R. (2002). Functional expression of human mitochondrial CYP11B2 in fission yeast and identification of a new internal electron transfer protein, etp1. *Biochemistry*. 41, 2311–2321.
- Cali, J.J., and Russell, D.W. (1991). Characterization of human sterol 27-hydroxylase. A mitochondrial cytochrome P-450 that catalyzes multiple oxidation reaction in bile acid biosynthesis. *J. Biol. Chem.* 266, 7774–7778.
- Cardini, G., and Jurtschuk, P. (1968). Cytochrome P-450 involvement in the oxidation of n-octane by cell-free extracts of *Corynebacterium sp.* strain 7E1C. *J. Biol. Chem.* 243, 6070–6072.
- Combalbert, J., Fabre, I., Fabre, G., Dalet, I., Derancourt, J., Cano, J.P., and Maurel, P. (1989). Metabolism of cyclosporin A. IV. Purification and identification of the rifampicin-inducible human liver cytochrome P-450 (cyclosporin A oxidase) as a product of P450IIIA gene subfamily. *Drug Metab. Dispos.* 17, 197–207.
- Correia, M.A., and Mannering, G.J. (1973). Reduced diphosphopyridine nucleotide synergism of the reduced triphosphopyridine nucleotide-dependent mixed-function oxidase System of hepatic microsomes: I. Effects of activation and inhibition of the fatty acyl coenzyme A desaturation system. *Mol. Pharmacol.* 9, 455–469.
- Denisov, I.G., and Sligar, S.G. (2015). Activation of molecular oxygen in cytochromes P450. *Cytochrome P450*. 4th ed. Springer International Publishing, 69–109.
- Denisov, I.G., Makris, T.M., Sligar, S.G., and Schlichting, I. (2005). Structure and chemistry of cytochrome P450. *Chem. Rev.* 105, 2253–2278.
- Donova, M.V., and Egorova, O.V. (2012). Microbial steroid transformations: current state and prospects. *Appl. Microbiol. Biotechnol.* 94, 1423–1447.
- Duport, C., Spagnoli, R., Degryse, E., and Pompon, D. (1998). Self-sufficient biosynthesis of pregnenolone and progesterone in engineered yeast. *Nat. Biotechnol.* 16, 186–189.
- Durairaj, P., Hur, J.-S., and Yun, H. (2016). Versatile biocatalysis of fungal cytochrome P450 monooxygenases. *Microb. Cell Factories*. 15, 125.

- Ehrhardt, M., Gerber, A., Hannemann, F., and Bernhardt, R. (2016a). Expression of human CYP27A1 in *B. megaterium* for the efficient hydroxylation of cholesterol, vitamin D3 and 7-dehydrocholesterol. *J. Biotechnol.* 218, 34–40.
- Ehrhardt, M., Gerber, A., Zapp, J., Hannemann, F., and Bernhardt, R. (2016b). Human CYP27A1 catalyzes hydroxylation of β-sitosterol and ergosterol. *Biol. Chem.* 397, 513–518.
- England, P.A., Harford-Cross, C.F., Stevenson, J.-A., Rouch, D.A., and Wong, L.-L. (1998). The oxidation of naphthalene and pyrene by cytochrome P450cam. *FEBS Lett.* 424, 271–274.
- Eppinger, M., Bunk, B., Johns, M.A., Edirisinghe, J.N., Kutumbaka, K.K., Koenig, S.S.K., Creasy, H.H., Rosovitz, M.J., Riley, D.R., Daugherty, S., et al. (2011). Genome sequences of the biotechnologically important *Bacillus megaterium* strains QM B1551 and DSM319. *J. Bacteriol.* 193, 4199–4213.
- Estabrook, R.W., Cooper, D.Y., and Rosenthal, O. (1963). The light reversible carbon monoxide inhibition of the steroid c21-hydroxylase system of the adrenal cortex. *Biochem. Z.* 338, 741–755.
- Estabrook, R.W., Shet, M.S., Faulkner, K., and Fisher, C.W. (1996). The use of electrochemistry for the synthesis of 17α-hydroxyprogesterone by a fusion protein containing P450c17. *Endocr. Res.* 22, 665–671.
- Ewen, K.M., Ringle, M., and Bernhardt, R. (2012). Adrenodoxin—a versatile ferredoxin. *IUBMB Life.* 64, 506–512.
- Fasan, R. (2012). Tuning P450 enzymes as oxidation catalysts. *ACS Catal.* 2, 647–666.
- Fulco, A.J. (1991). P450BM-3 and other inducible bacterial P450 cytochromes: biochemistry and regulation. *Annu. Rev. Pharmacol. Toxicol.* 31, 177–203.
- Furuya, T., and Kino, K. (2010). Genome mining approach for the discovery of novel cytochrome P450 biocatalysts. *Appl. Microbiol. Biotechnol.* 86, 991–1002.
- Furuya, T., Shibata, D., and Kino, K. (2009). Phylogenetic analysis of *Bacillus* P450 monooxygenases and evaluation of their activity towards steroids. *Steroids.* 74, 906–912.
- Garfinkel, D. (1958). Studies on pig liver microsomes. I. Enzymic and pigment composition of different microsomal fractions. *Arch. Biochem. Biophys.* 77, 493–509.

- Gerber, A., Kleser, M., Biedendieck, R., Bernhardt, R., and Hannemann, F. (2015). Functionalized PHB granules provide the basis for the efficient side-chain cleavage of cholesterol and analogs in recombinant *Bacillus megaterium*. *Microb. Cell Factories.* 14, 107
- Gerber, A., Milhim, M., Hartz, P., Zapp, J., and Bernhardt, R. (2016). Genetic engineering of *Bacillus megaterium* for high-yield production of the major teleost progestogens $17\alpha,20\beta$ -di- and $17\alpha,20\beta,21\alpha$ -trihydroxy-4-pregnene-3-one. *Metab. Eng.* 36, 19–27.
- Girhard, M., Klaus, T., Khatri, Y., Bernhardt, R., and Urlacher, V.B. (2010). Characterization of the versatile monooxygenase CYP109B1 from *Bacillus subtilis*. *Appl. Microbiol. Biotechnol.* 87, 595–607.
- Girhard, M., Bakkes, P.J., Mahmoud, O., and Urlacher, V.B. (2015). P450 Biotechnology. Cytochrome P450. 4th ed. Springer International Publishing. 451–520.
- Gotoh, O. (1992). Substrate recognition sites in cytochrome P450 family 2 (CYP2) proteins inferred from comparative analyses of amino acid and coding nucleotide sequences. *J. Biol. Chem.* 267, 83–90.
- Goujon, M., McWilliam, H., Li, W., Valentin, F., Squizzato, S., Paern, J., and Lopez, R. (2010). A new bioinformatics analysis tools framework at EMBL–EBI. *Nucleic Acids Res.* 38, W695–699.
- Green, A.J., Rivers, S.L., Cheesman, M., Reid, G.A., Quaroni, L.G., Macdonald, I.D., Chapman, S.K., and Munro, A.W. (2001). Expression, purification and characterization of cytochrome P450 Biol: a novel P450 involved in biotin synthesis in *Bacillus subtilis*. *J. Biol. Inorg. Chem.* 6, 523–533.
- Gricman, Ł., Vogel, C., and Pleiss, J. (2015). Identification of universal selectivity-determining positions in cytochrome P450 monooxygenases by systematic sequence-based literature mining. *Proteins.* 83, 1593–1603.
- Groves, J.T., McClusky, G.A., White, R.E., and Coon, M.J. (1978). Aliphatic hydroxylation by highly purified liver microsomal cytochrome P-450. Evidence for a carbon radical intermediate. *Biochem. Biophys. Res. Commun.* 81, 154–160.
- Guengerich, F.P. (1999). Cytochrome P-450 3A4: regulation and role in drug metabolism. *Annu. Rev. Pharmacol. Toxicol.* 39, 1–17.
- Guengerich, F.P. (2001). Common and Uncommon Cytochrome P450 Reactions Related to Metabolism and Chemical Toxicity. *Chem. Res. Toxicol.* 14, 611–650.

- Gustafsson, M.C., Roitel, O., Marshall, K.R., Noble, M.A., Chapman, S.K., Pessegueiro, A., Fulco, A.J., Cheesman, M.R., von Wachenfeldt, C., and Munro, A.W. (2004). Expression, purification, and characterization of *Bacillus subtilis* cytochromes P450 CYP102A2 and CYP102A3: flavocytochrome homologues of P450 BM3 from *Bacillus megaterium*. *Biochemistry*. 43, 5474–5487.
- Hall, E.A., and Bell, S.G. (2014). The efficient and selective biocatalytic oxidation of norisoprenoid and aromatic substrates by CYP101B1 from *Novosphingobium aromaticivorans* DSM12444. *RSC Adv.* 5, 5762–5773.
- Hannemann, F., Bichet, A., Ewen, K.M., and Bernhardt, R. (2007). Cytochrome P450 systems—biological variations of electron transport chains. *Biochim. Biophys. Acta*. 1770, 330–344.
- Hawkes, D.B., Adams, G.W., Burlingame, A.L., de Montellano, P.R.O., and De Voss, J.J. (2002). Cytochrome P450cin (CYP176A), isolation, expression, and characterization. *J. Biol. Chem.* 277, 27725–27732.
- He, K., Iyer, K.R., Hayes, R.N., Sinz, M.W., Woolf, T.F., and Hollenberg, P.F. (1998). Inactivation of cytochrome P450 3A4 by bergamottin, a component of grapefruit juice. *Chem. Res. Toxicol.* 11, 252–259.
- Hefner, J., Rubenstein, S.M., Ketchum, R.E., Gibson, D.M., Williams, R.M., and Croteau, R. (1996). Cytochrome P450-catalyzed hydroxylation of taxa-4(5),11(12)-diene to taxa-4(20),11(12)-dien-5alpha-ol: the first oxygenation step in taxol biosynthesis. *Chem. Biol.* 3, 479–489.
- Hlavica, P. (1984). On the function of cytochrome *b*5 in the cytochrome P-450-dependent oxygenase system. *Arch. Biochem. Biophys.* 228, 600–608.
- Hodek, P., Trefil, P., and Stiborová, M. (2002). Flavonoids—potent and versatile biologically active compounds interacting with cytochromes P450. *Chem. Biol. Interact.* 139, 1–21.
- Horiuchi, T., Gotoh, O., Noshiro, M., and Yoshida, Y. (1998). CYP51-like gene of *Mycobacterium tuberculosis* actually encodes a P450 similar to eukaryotic CYP51. *J. Biochem.* 124, 694–696.
- Huang, X., and Groves, J.T. (2017). Beyond ferryl-mediated hydroxylation: 40 years of the rebound mechanism and C–H activation. *J. Biol. Inorg. Chem.* 22, 185–207.
- Janocha, S., and Bernhardt, R. (2013). Design and characterization of an efficient CYP105A1-based whole-cell biocatalyst for the conversion of resin acid diterpenoids in permeabilized *Escherichia coli*. *Appl. Microbiol. Biotechnol.* 97, 7639–7649.

- Janocha, S., Carius, Y., Hutter, M., Lancaster, C.R.D., and Bernhardt, R. (2016). Crystal structure of CYP106A2 in substrate-free and substrate-bound form. *ChemBioChem.* 17, 852–860.
- Janowski, B.A., Grogan, M.J., Jones, S.A., Wisely, G.B., Kliewer, S.A., Corey, E.J., and Mangelsdorf, D.J. (1999). Structural requirements of ligands for the oxysterol liver X receptors LXR α and LXR β . *Proc. Natl. Acad. Sci.* 96, 266–271.
- Jefcoate, C.R. (1978). Measurement of substrate and inhibitor binding to microsomal cytochrome P-450 by optical-difference spectroscopy. *Methods Enzym.* 52, 258–279.
- Jo, H.-Y., Park, S.-H., Le, T.-K., Ma, S.H., Kim, D., Ahn, T., Joung, Y.H., and Yun, C.-H. (2017). Peroxide-dependent oxidation reactions catalyzed by CYP191A1 from *Mycobacterium smegmatis*. *Biotechnol. Lett.* 39, 1245–1252.
- Johnston, J.B., Ouellet, H., and de Montellano, P.R.O. (2010). Functional redundancy of steroid C26-monooxygenase activity in *Mycobacterium tuberculosis* revealed by biochemical and genetic analyses. *J. Biol. Chem.* 285, 36352–36360.
- Józwik, I.K., Kiss, F.M., Gricman, Ł., Abdulkugnhi, A., Brill, E., Zapp, J., Pleiss, J., Bernhardt, R., and Thunnissen, A.-M.W.H. (2016). Structural basis of steroid binding and oxidation by the cytochrome P450 CYP109E1 from *Bacillus megaterium*. *FEBS J.* 283, 4128–4148.
- Kandel, S.E., Wienkers, L.C., and Lampe, J.N. (2014). Cytochrome P450 enzyme metabolites in lead discovery and development. *Annu. Rep. Med. Chem.* 49, 347–359.
- Katagiri, M., Ganguli, B.N., and Gunsalus, I.C. (1968). A soluble cytochrome P-450 functional in methylene hydroxylation. *J. Biol. Chem.* 243, 3543–3546.
- Kellis, J.T., and Vickery, L.E. (1987). Purification and characterization of human placental aromatase cytochrome P-450. *J. Biol. Chem.* 262, 4413–4420.
- Kelly, S.L., and Kelly, D.E. (2013). Microbial cytochromes P450: biodiversity and biotechnology. Where do cytochromes P450 come from, what do they do and what can they do for us? *Philos. Trans. R. Soc. Lond. B. Biol. Sci.* 368, 20120476.
- Kern, F., Dier, T.K.F., Khatri, Y., Ewen, K.M., Jacquot, J.-P., Volmer, D.A., and Bernhardt, R. (2015). Highly efficient CYP167A1 (EpoK) dependent epothilone B formation and production of 7-ketone epothilone D as a new epothilone derivative. *Sci. Rep.* 5, 14881.

- Kern, F., Khatri, Y., Litzenburger, M., and Bernhardt, R. (2016). CYP267A1 and CYP267B1 from *Sorangium cellulosum* So ce56 are highly versatile drug metabolizers. *Drug Metab. Dispos.* 44, 495–504.
- Khatri, Y., Hannemann, F., Ewen, K.M., Pistorius, D., Perlova, O., Kagawa, N., Brachmann, A.O., Müller, R., and Bernhardt, R. (2010). The CYPome of *Sorangium cellulosum* So ce56 and identification of CYP109D1 as a new fatty acid hydroxylase. *Chem. Biol.* 17, 1295–1305.
- Khatri, Y., Hannemann, F., Girhard, M., Kappl, R., Même, A., Ringle, M., Janocha, S., Leize-Wagner, E., Urlacher, V.B., and Bernhardt, R. (2013). Novel family members of CYP109 from *Sorangium cellulosum* So ce56 exhibit characteristic biochemical and biophysical properties. *Biotechnol. Appl. Biochem.* 60, 18–29.
- Khatri, Y., Ringle, M., Lisurek, M., von Kries, J.P., Zapp, J., and Bernhardt, R. (2016). Substrate hunting for the myxobacterial CYP260A1 revealed new 1 α -hydroxylated products from C-19 steroids. *ChemBioChem.* 17, 90–101.
- Kim, T.-W., Hwang, J.-Y., Kim, Y.-S., Joo, S.-H., Chang, S.C., Lee, J.S., Takatsuto, S., and Kim, S.-K. (2005). *Arabidopsis* CYP85A2, a cytochrome P450, mediates the Baeyer-Villiger oxidation of castasterone to brassinolide in brassinosteroid biosynthesis. *Plant Cell.* 17, 2397–2412.
- Kiss, F.M., Schmitz, D., Zapp, J., Dier, T.K.F., Volmer, D.A., and Bernhardt, R. (2015a). Comparison of CYP106A1 and CYP106A2 from *Bacillus megaterium* – identification of a novel 11-oxidase activity. *Appl. Microbiol. Biotechnol.* 99, 8495–8514.
- Kiss, F.M., Lundemo, M.T., Zapp, J., Woodley, J.M., and Bernhardt, R. (2015b). Process development for the production of 15 β -hydroxycyproterone acetate using *Bacillus megaterium* expressing CYP106A2 as whole-cell biocatalyst. *Microb. Cell Factories.* 14, 28.
- Klingenbergs, M. (1958). Pigments of rat liver microsomes. *Arch. Biochem. Biophys.* 75, 376–386.
- Lambeth, J.D., Seybert, D.W., and Kamin, H. (1979). Ionic effects on adrenal steroidogenic electron transport. The role of adrenodoxin as an electron shuttle. *J. Biol. Chem.* 254, 7255–7264.
- Lebeault, J.M., Lode, E.T., and Coon, M.J. (1971). Fatty acid and hydrocarbon hydroxylation in yeast: role of cytochrome P-450 in *Candida tropicalis*. *Biochem. Biophys. Res. Commun.* 42, 413–419.

- Leoni, V., and Caccia, C. (2013). 24S-hydroxycholesterol in plasma: a marker of cholesterol turnover in neurodegenerative diseases. *Biochimie.* 95, 595–612.
- Lepesheva, G.I., and Waterman, M.R. (2004). CYP51—the omnipotent P450. *Mol. Cell. Endocrinol.* 215, 165–170.
- Lewis, J.C., Coelho, P.S., and Arnold, F.H. (2011). Enzymatic functionalization of carbon–hydrogen bonds. *Chem. Soc. Rev.* 40, 2003–2021.
- Li, Q.-S., Ogawa, J., and Shimizu, S. (2001). Critical role of the residue Size at position 87 in H₂O₂-dependent substrate hydroxylation activity and H₂O₂ inactivation of cytochrome P450BM-3. *Biochem. Biophys. Res. Commun.* 280, 1258–1261.
- Lisurek, M., Simgen, B., Antes, I., and Bernhardt, R. (2008). Theoretical and experimental evaluation of a CYP106A2 low homology model and production of mutants with changed activity and selectivity of hydroxylation. *ChemBioChem.* 9, 1439–1449.
- Litzenburger, M., and Bernhardt, R. (2016). Selective oxidation of carotenoid-derived aroma compounds by CYP260B1 and CYP267B1 from *Sorangium cellulosum* So ce56. *Appl. Microbiol. Biotechnol.* 100, 4447–4457.
- Lu, W.J., Xu, C., Pei, Z., Mayhoub, A.S., Cushman, M., and Flockhart, D.A. (2012). The tamoxifen metabolite norendoxifen is a potent and selective inhibitor of aromatase (CYP19) and a potential lead compound for novel therapeutic agents. *Breast Cancer Res. Treat.* 133, 99–109.
- Makris, T.M., von Koenig, K., Schlichting, I., and Sligar, S.G. (2007). Alteration of P450 distal pocket solvent leads to impaired proton delivery and changes in heme geometry. *Biochemistry.* 46, 14129–14140.
- Matsubara, H., and Saeki, K. (1992). Structural and functional diversity of ferredoxins and related proteins. *Adv. Inorg. Chem.* 38, 223–280.
- Matsunaga, I., Yamada, A., Lee, D.-S., Obayashi, E., Fujiwara, N., Kobayashi, K., Ogura, H., and Shiro, Y. (2002). Enzymatic reaction of hydrogen peroxide-dependent peroxygenase cytochrome P450s: kinetic deuterium isotope effects and analyses by resonance Raman spectroscopy. *Biochemistry.* 41, 1886–1892.
- Matteson, K.J., Chung, B., and Miller, W.L. (1984). Molecular cloning of DNA complementary to bovine adrenal P450scc mRNA. *Biochem. Biophys. Res. Commun.* 120, 264–270.

- McDonald, J.G., and Russell, D.W. (2010). Editorial: 25-Hydroxycholesterol: a new life in immunology. *J. Leukoc. Biol.* 88, 1071–1072.
- McLean, K.J., Lafite, P., Levy, C., Cheesman, M.R., Mast, N., Pikuleva, I.A., Leys, D., and Munro, A.W. (2009). The structure of *Mycobacterium tuberculosis* CYP125 molecular basis for cholesterol binding in a P450 needed for host infection. *J. Biol. Chem.* 284, 35524–35533.
- McLean, K.J., Hans, M., Meijrink, B., van Scheppingen, W.B., Vollebregt, A., Tee, K.L., van der Laan, J.-M., Leys, D., Munro, A.W., and van den Berg, M.A. (2015). Single-step fermentative production of the cholesterol-lowering drug pravastatin via reprogramming of *Penicillium chrysogenum*. *Proc. Natl. Acad. Sci.* 112, 2847–2852.
- Milhim, M., Putkaradze, N., Abdulkughni, A., Kern, F., Hartz, P., and Bernhardt, R. (2016a). Identification of a new plasmid-encoded cytochrome P450 CYP107DY1 from *Bacillus megaterium* with a catalytic activity towards mevastatin. *J. Biotechnol.* 240, 68–75.
- Milhim, M., Gerber, A., Neunzig, J., Hannemann, F., and Bernhardt, R. (2016b). A Novel NADPH-dependent flavoprotein reductase from *Bacillus megaterium* acts as an efficient cytochrome P450 reductase. *J. Biotechnol.* 231, 83–94.
- Moorthy, B., Chu, C., and Carlin, D.J. (2015). Polycyclic aromatic hydrocarbons: from metabolism to lung cancer. *Toxicol. Sci.* 145, 5–15.
- Müller, H.G., Schunck, W.H., Riege, P., and Honeck, H. (1984). Cytochrome P-450 of microorganisms. *Cytochrome P-450*. Akademie-Verlag Berlin. 337–369.
- Munro, A.W., Leys, D.G., McLean, K.J., Marshall, K.R., Ost, T.W.B., Daff, S., Miles, C.S., Chapman, S.K., Lysek, D.A., Moser, C.C., et al. (2002). P450 BM3: the very model of a modern flavocytochrome. *Trends Biochem. Sci.* 27, 250–257.
- Mutemberezi, V., Guillemot-Legrif, O., and Muccioli, G.G. (2016). Oxysterols: From cholesterol metabolites to key mediators. *Prog. Lipid Res.* 64, 152–169.
- Narhi, L.O., and Fulco, A.J. (1982). Phenobarbital induction of a soluble cytochrome P-450-dependent fatty acid monooxygenase in *Bacillus megaterium*. *J. Biol. Chem.* 257, 2147–2150.
- Narhi, L.O., and Fulco, A.J. (1987). Identification and characterization of two functional domains in cytochrome P-450BM-3, a catalytically self-sufficient monooxygenase induced by barbiturates in *Bacillus megaterium*. *J. Biol. Chem.* 262, 6683–6690.

- Nebert, D.W., Adesnik, M., Coon, M.J., Estabrook, R.W., Gonzalez, F.J., Guengerich, F.P., Gunsalus, I.C., Johnson, E.F., Kemper, B., and Levin, W. (1987). The P450 gene superfamily: recommended nomenclature. *DNA*. 6, 1–11.
- Nebert, D.W., Wikvall, K., and Miller, W.L. (2013). Human cytochromes P450 in health and disease. *Phil Trans R. Soc. B. Biol. Sci.* 368, 20120431.
- Nelson, D.R. (2018). Cytochrome P450 diversity in the tree of life. *Biochim. Biophys. Acta*. 1866, 141–154.
- Nguyen, K.T., Virus, C., Günnewich, N., Hannemann, F., and Bernhardt, R. (2012). Changing the regioselectivity of a P450 from C15 to C11 hydroxylation of progesterone. *ChemBioChem*. 13, 1161–1166.
- Nikolaus, J., Nguyen, K.T., Virus, C., Riehm, J.L., Hutter, M., and Bernhardt, R. (2017). Engineering of CYP106A2 for steroid 9 α - and 6 β -hydroxylation. *Steroids*. 120, 41–48.
- Nishihara, K., Kanemori, M., Kitagawa, M., Yanagi, H., and Yura, T. (1998). Chaperone coexpression plasmids: differential and synergistic roles of DnaK-DnaJ-GrpE and GroEL-GroES in assisting folding of an allergen of Japanese cedar pollen, Cryj2, in *Escherichia coli*. *Appl. Environ. Microbiol.* 64, 1694–1699.
- Ogura, H., Nishida, C.R., Hoch, U.R., Perera, R., Dawson, J.H., and Ortiz de Montellano, P.R. (2004). EpoK, a cytochrome P450 involved in biosynthesis of the anticancer agents epothilones A and B. Substrate-mediated rescue of a P450 enzyme. *Biochemistry*. 43, 14712–14721.
- Omura, T., and Sato, R. (1962). A new cytochrome in liver microsomes. *J. Biol. Chem.* 237, 1375–1376.
- Omura, T., and Sato, R. (1964). The carbon monoxide-binding pigment of liver microsomes. i. evidence for its hemoprotein nature. *J. Biol. Chem.* 239, 2370–2378.
- Ortiz de Montellano, P.R. (2010). Hydrocarbon hydroxylation by cytochrome P450 enzymes. *Chem. Rev.* 110, 932–948.
- Ortiz de Montellano, P.R. (2018). Potential drug targets in the *Mycobacterium tuberculosis* cytochrome P450 system. *J. Inorg. Biochem.* 180, 235–245.

- Ouellet, H., Guan, S., Johnston, J.B., Chow, E.D., Kells, P.M., Burlingame, A.L., Cox, J.S., Podust, L.M., and De Montellano, P.R.O. (2010). *Mycobacterium tuberculosis* CYP125A1, a steroid C27 monooxygenase that detoxifies intracellularly generated cholest-4-en-3-one. *Mol. Microbiol.* **77**, 730–742.
- Peterson, J.A., and Graham, S.E. (1998). A close family resemblance: the importance of structure in understanding cytochromes P450. *Structure.* **6**, 1079–1085.
- Pikuleva, I.A. (2006). Cholesterol-metabolizing cytochromes P450. *Drug Metab. Dispos.* **34**, 513–520.
- Pikuleva, I.A., and Waterman, M.R. (2013). Cytochromes P450: roles in diseases. *J. Biol. Chem.* **288**, 17091–17098.
- Poulos, T.L., and Johnson, E.F. (2015). Structures of cytochrome P450 enzymes. *Cytochrome P450.* 4th ed. Springer International Publishing. 3–32.
- Poulos, T.L., Finzel, B.C., Gunsalus, I.C., Wagner, G.C., and Kraut, J. (1985). The 2.6-A crystal structure of *Pseudomonas putida* cytochrome P-450. *J. Biol. Chem.* **260**, 16122–16130.
- Poulos, T.L., Finzel, B.C., and Howard, A.J. (1987). High-resolution crystal structure of cytochrome P450cam. *J. Mol. Biol.* **195**, 687–700.
- Putkaradze, N., Kiss, F.M., Schmitz, D., Zapp, J., Hutter, M.C., and Bernhardt, R. (2017a). Biotransformation of prednisone and dexamethasone by cytochrome P450 based systems - Identification of new potential drug candidates. *J. Biotechnol.* **242**, 101–110.
- Putkaradze, N., Litzenburger, M., Abdulmughni, A., Milhim, M., Brill, E., Hannemann, F., and Bernhardt, R. (2017b). CYP109E1 is a novel versatile statin and terpene oxidase from *Bacillus megaterium*. *Appl. Microbiol. Biotechnol.* **101**, 8379–8393.
- Rauschenbach, R., Isernhagen, M., Noeske-Jungblut, C., Boidol, W., and Siewert, G. (1993). Cloning sequencing and expression of the gene for cytochrome P450meg, the steroid-15β-monooxygenase from *Bacillus megaterium* ATCC 13368. *Mol. Gen. Genet. MGG.* **241**, 170–176.
- Ravichandran, K.G., Boddupalli, S.S., Hasermann, C.A., Peterson, J.A., and Deisenhofer, J. (1993). Crystal structure of hemoprotein domain of P450BM-3, a prototype for microsomal P450's. *Science.* **261**, 731–736.

- Ringle, M. (2013). Charakterisierung ausgewählter Cytochrome P450 aus *Sorangium cellulosum* So ce56: neue potentielle Biokatalysatoren. Dissertation. Universität des Saarlandes.
- Rittle, J., and Green, M.T. (2010). Cytochrome P450 compound I: capture, characterization, and CH bond activation kinetics. *Science*. 330, 933–937.
- Ruckpaul, K., and Bernhardt, R. (1984). Biochemical aspects of the monooxygenase system in the endoplasmic reticulum of mammalian liver. *Cytochrome P-450*. Akademie-Verlag Berlin. 9–57.
- Ruhmann-Wennhold, A., Johnson, L.R., and Nelson, D.H. (1970). Cytochrome P-450 in adrenal mitochondria of male and female rats. *Biochim. Biophys. Acta*. 223, 206–209.
- Rygus, T., and Hillen, W. (1992). Catabolite repression of the xyl operon in *Bacillus megaterium*. *J. Bacteriol.* 174, 3049–3055.
- Sadeghi, S.J., Fantuzzi, A., and Gilardi, G. (2011). Breakthrough in P450 bioelectrochemistry and future perspectives. *Biochim. Biophys. Acta*. 1814, 237–248.
- Sakaki, T. (2012). Practical application of cytochrome P450. *Biol. Pharm. Bull.* 35, 844–849.
- Sakaki, T., Sugimoto, H., Hayashi, K., Yasuda, K., Munetsuna, E., Kamakura, M., Ikushiro, S., and Shiro, Y. (2011). Bioconversion of vitamin D to its active form by bacterial or mammalian cytochrome P450. *Biochim. Biophys. Acta*. 1814, 249–256.
- Salamanca-Pinzón, S.G., and Guengerich, F.P. (2011). A tricistronic human adrenodoxin reductase-adrenodoxin-cytochrome P450 27A1 vector system for substrate hydroxylation in *Escherichia coli*. *Protein Expr. Purif.* 79, 231–236.
- Schiffer, L., Müller, A.-R., Hobler, A., Brixius-Anderko, S., Zapp, J., Hannemann, F., and Bernhardt, R. (2016a). Biotransformation of the mineralocorticoid receptor antagonists spironolactone and canrenone by human CYP11B1 and CYP11B2: characterization of the products and their influence on mineralocorticoid receptor transactivation. *J. Steroid Biochem. Mol. Biol.* 163, 68–76.
- Schiffer, L., Brixius-Anderko, S., Hannemann, F., Zapp, J., Neunzig, J., Thevis, M., and Bernhardt, R. (2016b). Metabolism of oral turinabol by human steroid hormone-synthesizing cytochrome P450 enzymes. *Drug Metab. Dispos.* 44, 227–237.
- Schifrin, A., Litzenburger, M., Ringle, M., Ly, T.T.B., and Bernhardt, R. (2015). New sesquiterpene oxidations with CYP260A1 and CYP264B1 from *Sorangium cellulosum* So ce56. *ChemBioChem*. 16, 2624–2632.

- Schmitz, D., Zapp, J., and Bernhardt, R. (2012). Hydroxylation of the triterpenoid dipterocarpol with CYP106A2 from *Bacillus megaterium*. *FEBS J.* 279, 1663–1674.
- Schmitz, D., Zapp, J., and Bernhardt, R. (2014). Steroid conversion with CYP106A2 – production of pharmaceutically interesting DHEA metabolites. *Microb. Cell Factories.* 13, 81.
- Schmitz, D., Janocha, S., Kiss, F.M., and Bernhardt, R. (2018). CYP106A2—A versatile biocatalyst with high potential for biotechnological production of selectively hydroxylated steroid and terpenoid compounds. *Biochim. Biophys. Acta.* 1866, 11–22.
- Schuster, I. (2011). Cytochromes P450 are essential players in the vitamin D signaling system. *Biochim. Biophys. Acta.* 1814, 186–199.
- Shumyantseva, V.V., Bulko, T.V., and Archakov, A.I. (2005). Electrochemical reduction of cytochrome P450 as an approach to the construction of biosensors and bioreactors. *J. Inorg. Biochem.* 99, 1051–1063.
- Sievers, F., Wilm, A., Dineen, D., Gibson, T.J., Karplus, K., Li, W., Lopez, R., McWilliam, H., Remmert, M., Söding, J., et al. (2011). Fast, scalable generation of high-quality protein multiple sequence alignments using Clustal Omega. *Mol. Syst. Biol.* 7, 539.
- Simgen, B., Contzen, J., Schwarzer, R., Bernhardt, R., and Jung, C. (2000). Substrate binding to 15 β -hydroxylase (CYP106A2) probed by FT Infrared spectroscopic studies of the iron Ligand CO stretch vibration. *Biochem. Biophys. Res. Commun.* 269, 737–742.
- Sligar, S.G. (1999). Nature's universal oxygenases: the cytochromes P450. *Essays Biochem.* 34, 71–84.
- Sono, M., Roach, M.P., Coulter, E.D., and Dawson, J.H. (1996). Heme-containing oxygenases. *Chem. Rev.* 96, 2841–2888.
- Souter, A., McLean, K.J., Smith, W.E., and Munro, A.W. (2000). The genome sequence of *Mycobacterium tuberculosis* reveals cytochromes P450 as novel anti-TB drug targets. *J. Chem. Technol. Biotechnol.* 75, 933–941.
- Straathof, A.J., Panke, S., and Schmid, A. (2002). The production of fine chemicals by biotransformations. *Curr. Opin. Biotechnol.* 13, 548–556.

- Sugimoto, H., Shinkyo, R., Hayashi, K., Yoneda, S., Yamada, M., Kamakura, M., Ikushiro, S., Shiro, Y., and Sakaki, T. (2008). Crystal structure of CYP105A1 (P450SU-1) in complex with 1 α , 25-dihydroxyvitamin D3. *Biochemistry*. 47, 4017–4027.
- Tang, E.K., Chen, J., Janjetovic, Z., Tieu, E.W., Slominski, A.T., Li, W., and Tuckey, R.C. (2013). Hydroxylation of CYP11A1-derived products of vitamin D3 metabolism by human and mouse CYP27B1. *Drug Metab. Dispos.* 41, 1112–1124.
- Teoh, K.H., Polichuk, D.R., Reed, D.W., Nowak, G., and Covello, P.S. (2006). *Artemisia annua* L. (Asteraceae) trichome-specific cDNAs reveal CYP71AV1, a cytochrome P450 with a key role in the biosynthesis of the antimalarial sesquiterpene lactone artemisinin. *FEBS Lett.* 580, 1411–1416.
- Ullah, A.J., Murray, R.I., Bhattacharyya, P.K., Wagner, G.C., and Gunsalus, I.C. (1990). Protein components of a cytochrome P-450 linalool 8-methyl hydroxylase. *J. Biol. Chem.* 265, 1345–1351.
- Urlacher, V.B. (2010). Catalysis with cytochrome P450 monooxygenases. *Handbook of green chemistry*. Wiley-VCH publishing. 1–25.
- Urlacher, V.B., and Eiben, S. (2006). Cytochrome P450 monooxygenases: perspectives for synthetic application. *Trends Biotechnol.* 24, 324–330.
- Vary, P.S., Biedendieck, R., Fuerch, T., Meinhardt, F., Rohde, M., Deckwer, W.-D., and Jahn, D. (2007). *Bacillus megaterium*--from simple soil bacterium to industrial protein production host. *Appl. Microbiol. Biotechnol.* 76, 957–967.
- Viruš, C., and Bernhardt, R. (2008). Molecular evolution of a steroid hydroxylating cytochrome P450 using a versatile steroid detection system for screening. *Lipids*. 43, 1133–1141.
- Watanabe, I., Nara, F., and Serizawa, N. (1995). Cloning, characterization and expression of the gene encoding cytochrome P-450 sca-in2 from *Streptomyces carbophilus* involved in production of pravastatin, a specific HMG-CoA reductase inhibitor. *Gene*. 163, 81–85.
- Werck-Reichhart, D., and Feyereisen, R. (2000). Cytochromes P450: a success story. *Genome Biol.* 1, 3003.1–3003.9.
- Whitehouse, C.J.C., Bell, S.G., and Wong, L.-L. (2012). P450BM3 (CYP102A1): connecting the dots. *Chem. Soc. Rev.* 41, 1218–1260.
- Wong, L.L. (1998). Cytochrome P450 monooxygenases. *Curr. Opin. Chem. Biol.* 2, 263–268.

REFERENCES

- Yasuda, K., Sugimoto, H., Hayashi, K., Takita, T., Yasukawa, K., Ohta, M., Kamakura, M., Ikushiro, S., Shiro, Y., and Sakaki, T. (2018). Protein engineering of CYP105s for their industrial uses. *Biochim. Biophys. Acta.* 1866, 23–31.
- Yoshimoto, F.K., and Auchus, R.J. (2016). Rapid kinetic methods to dissect steroidogenic cytochrome P450 reaction mechanisms. *J. Steroid Biochem. Mol. Biol.* 161, 13–23.
- Zehentgruber, D., Hannemann, F., Bleif, S., Bernhardt, R., and Lütz, S. (2010). Towards preparative scale steroid hydroxylation with cytochrome P450 monooxygenase CYP106A2. *ChemBioChem.* 11, 713–721.
- Zhai, S., Dai, R., Friedman, F.K., and Vestal, R.E. (1998). Comparative inhibition of human cytochromes P450 1A1 and 1A2 by flavonoids. *Drug Metab. Dispos.* 26, 989–992.

5. Appendix

5.1 Supplemental methods

CYP109E1-based system in *E. coli* and cholesterol conversion: the gene encoding CYP109E1 was amplified by PCR and cloned into the pSMF2.1CAA vector (Bleif et al., 2012) via SpeI and KpnI restriction sites replacing CYP106A2 with CYP109E1. The resulting vector, pSMF2.1E1AA, was cotransformed with the chaperone (GroEL-GroES)-coding plasmid pGro12 (Nishihara et al., 1998) in *E. coli* BL21 cells (Novagen). The control strain was created by cotransforming the backbone pSMF2.1 vector (Bleif et al., 2012) with pGro12. *E. coli* cells were cultured at 37 °C in Luria-Bertani (pre-culture) and Terrific Broth (main culture) media supplemented with 100 µg/mL ampicillin and 50 µg/mL kanamycin. At OD₆₀₀ of 0.5 1 mM δ-aminolevulinic acid and 4 mg/mL arabinose were added. The culture were incubated at 30 °C in a rotary shaker and harvested after 22 h. The *in vivo* conversion was performed similar to *B. megaterium* cells as described previously (Putkaradze et al., 2017b). Cholesterol was dissolved in 45% 2-hydroxypropyl-β-cyclodextrin solution. Preparative whole-cell conversion of cholesterol was carried out in baffled shake flasks using 600 mL *E. coli* culture. UV/Vis detection of cholesterol and its metabolites via HPLC was performed after cholesterol oxidase treatment at 240 nm as described elsewhere (Gerber et al., 2015). The conversion products were purified via silica gel chromatography and a mixture of hexane and ethyl acetate (7:3) was used as a mobile phase.

NMR data of 25-OH cholesterol: ¹H NMR (CDCl₃, 500 MHz): 0.66 (s, 3H, H18), 0.91 (d, 3H, J= 6.6 Hz, H21), 0.98 (s, 3H, H19), 1.19 (s, 6H, H26, H27), 3.51 (m, 1H, H3), 5.33 (m, 1H, H6); ¹³C NMR (CDCl₃, 125 MHz): 11.85 (C18), 18.67 (C21), 19.31 (C19), 20.75 (C23), 21.06 (C11), 24.27 (C15), 28.23 (C16), 29.66 (C26, C27), 31.63 (C2), 31.89 (C7, C8), 35.73 (C20), 36.43 (C22), 36.49 (C10), 37.23 (C1), 39.76 (C12), 42.27 (C4), 42.32 (C13), 44.39 (C24), 50.10 (C9), 56.05 (C17), 56.74 (C14), 71.16 (C25), 71.81 (C3), 121.71 (C6), 140.74 (C5).

NMR data of 24(S)-OH cholesterol: ¹H NMR (CDCl₃, 500 MHz): 0.66 (s, 3H, H18), 0.90 (m, 9H, H21, H26, H27), 0.98 (s, 3H, H19), 3.29 (m, 1H, H24), 3.51 (m, 1H, H3), 5.33 (m, 1H, H6); ¹³C NMR (CDCl₃, 125 MHz): 11.85 (C18), 16.67 (C26), 18.80 (C27), 19.05 (C21), 19.38 (C19), 21.06 (C11), 24.26 (C15), 28.19 (C16), 30.68 (C23), 31.63 (C2), 31.91 (C8), 31.94 (C7), 32.17 (C22), 33.11 (C25), 35.92 (C20), 36.48 (C10), 37.22 (C1), 39.74 (C12), 42.27 (C4), 42.31 (C13), 50.08 (C9), 55.90 (C17), 56.71 (C14), 71.80 (C3), 77.42 (C24), 121.70 (C6), 140.73 (C5).

5.2 Supplemental data

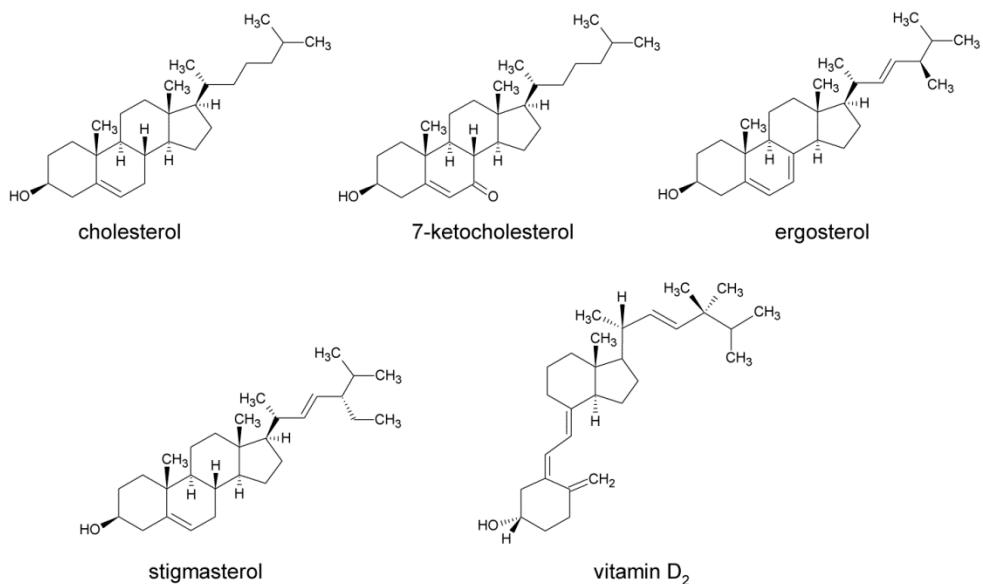


Figure S1. Chemical structures of novel CYP109E1 substrates with hydrocarbon side chain

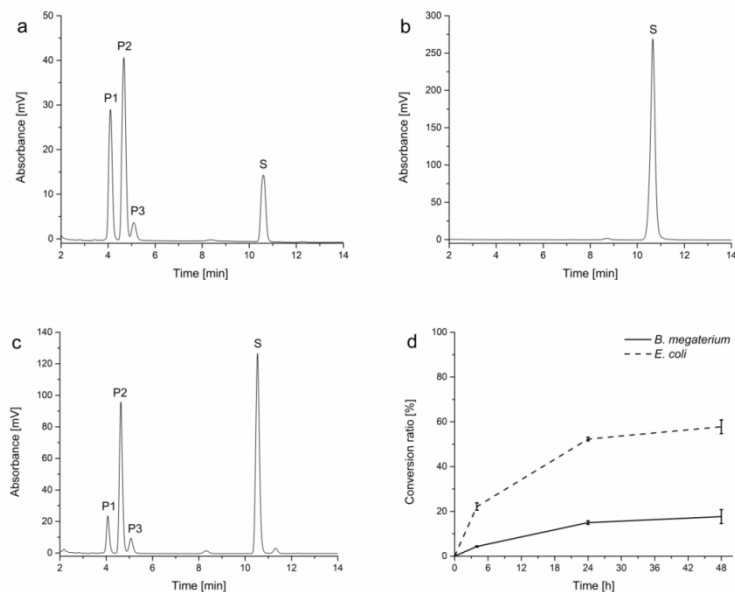


Figure S2. HPLC chromatograms of biotransformation of cholesterol by CYP109E1: *in vitro* conversion of 100 µM substrate (a), *in vitro* control reaction without CYP109E1 (b), whole-cell conversion of 200 µM substrate with *E. coli* BL21 strain transformed with pSMF2.1E1AA and pGro12 (c), comparison of cholesterol conversion with *B. megaterium* and *E. coli* cells (d).

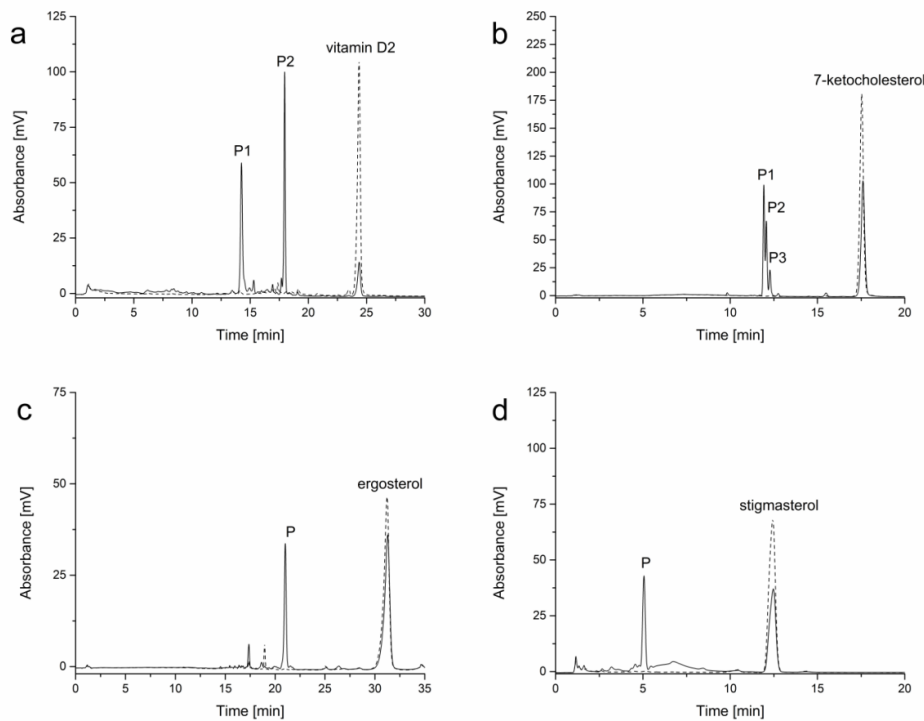


Figure S3. HPLC chromatograms of *in vitro* conversion by CYP109E1 of vitamin D₂ (a), 7-ketocholesterol (b), ergosterol (c) and stigmasterol (d). Conversions were performed using a reconstituted CYP109E1 system as described elsewhere (Putkaradze et al., 2017b). Each substrate, dissolved in 45% 2-hydroxypropyl-β-cyclodextrin solution, was added to a final concentration of 100 μM and the samples were incubated for 1 (7-ketocholesterol and ergosterol) or 2 h (vitamin D₂ and stigmasterol). Conversion of vitamin D₂ was detected at 265 nm, of ergosterol at 280 nm, other conversions were detected at 240 nm as described elsewhere (Gerber et al., 2015)

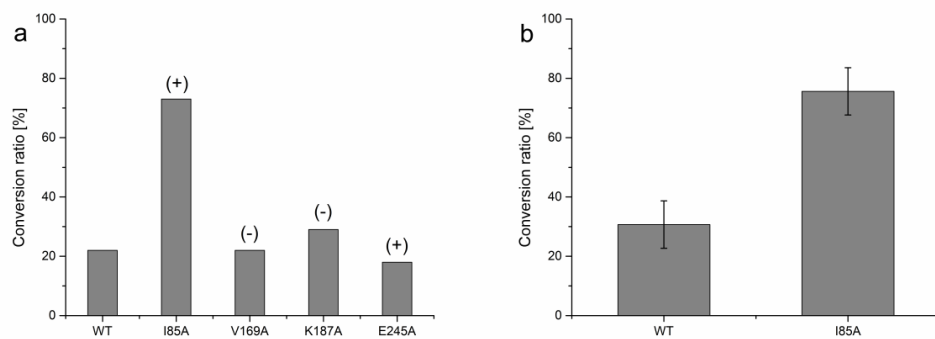


Figure S4. CYP109E1 mutant screening for compactin conversion *in vitro* (a). Comparison of compactin conversion by WT and I85A performed in triplicate (b). "(-)" selectivity lower than of WT, "(+)" selectivity higher than of WT